Generation and Characterisation of anti-C6 monoclonal antibodies in C6 deficient mice: The search for an anti-C6 therapy.

Lisa Victoria Jane Eynstone Clayton, BSc (Hons), MPhil.

Thesis presented for the degree of Doctor of Philosophy
University of Wales 2005.

Department of Medical Biochemistry and Immunology,
School of Medicine,
Cardiff University,
United Kingdom.

ProQuest LLC
789 East Eisenhower Parkway
P.O. Box 1346
Ann Arbor, MI 48106-1346

This thesis is dedicted to my family.

Acknowledgements

I would like to thank my supervisor, Professor B. Paul Morgan for his advice and guidance during the course of this study and for enabling me to continue to work in the department whilst writing up. I would also like to thank Dr Claire Harris for her valued advice and comments, especially regarding my work conducted on the BIAcore. I am also grateful to Dr Edward Laverty for initiating me in the ways of phage display.

I would like to express my gratitude to the three companies who I have been funded by, working on their projects whilst in the department; Adprotech (now Inflazyme Pharmaceuticals Ltd.); Identigen^{oyf} and The Binding Site.

I would also like to thank Professor Reinhardt Würzner, University of Innsbruck, Austria for the gift of an anti-C6 antibody, WÜ 6.4, and Dr Ann Orren for providing access to samples of human C6 deficient serum.

In addition, I would like to thank all the members of the Complement Biology Group, both past and present who have helped out in many ways at a practical level during this project. In particular, Fiona, for helping me to become comfortable with protein purification and Brad, for patiently teaching me to collect macrophages.

Finally, I would like to thank my husband Aled for his support, advice and encouragement.

Abbreviations

ADEAE	antibody-mediated demyelinating EAE
AP	alternative pathway
BSA	bovine serum albumin
C	complement component
C1 inh	C1 inhibitor
C4bp	C4 binding protein
C6D	C6 deficient
CFD	complement fixation diluent
CP	classical pathway
CPB	cardiopulmonary bypass
CVF	cobra venom factor
DAF	decay accelerating factor
DMSO	dimethylsulphoxide
DNA	deoxyribonucleic acid
DTT	dithiothreitol
E	erythrocytes
EA	antibody-sensitised erythrocytes
EAE	experimental allergic encephalomyelitis
ECL	enhanced chemiluminescence
EDTA	ethylene diamine tetra-acetic acid
ELISA	enzyme linked immunosorbent assay
Fc	fraction crystallisable of immunoglobulin
FCS	foetal calf serum
fB	factor B
fD	factor D
fH	factor H
fI	factor I
FIMs	Factor I modules
GPI	glycosyl-phosphatidylinositol
HAT supplement	hypoxanthine, aminopterin and thymidine
HBS	HEPES buffered saline
HEPES	N-(2-hydroxyethyl)piperazine-N'-2-ethanesulfonic acid
HRPO	horseradish peroxidase

HT supplement	hypoxanthine and thymidine
IFN-β	interferon-β
Ig	immunoglobulin
IL	interleukin
kDa	kilo Daltons
mAb	monoclonal antibody
MAC	membrane attack complex
MASP	MBL associated serine protease
MBL	mannose binding lectin
MCP	membrane cofactor protein
MS	multiple sclerosis
NF-κB	nuclear factor – kappa B
OD	optical density
PBS	phosphate buffered saline
PCR	polymerase chain reaction
PEG	polyethylene glycol
R	receptor
RA	rheumatoid arthritis
RCA	regulators of complement activation
RU	response units
scFv	single chain antibody
SC5b-9	soluble C5b-9
SCR	short consensus repeat
sCR1	soluble complement receptor 1
SDS-PAGE	sodium dodecyl sulphate-polyacrylamide gel electrophoresis
SLE	systemic lupus erythematosus
SMAP	small MBL-associated protein
SPR	surface plasmon resonance
TCC	terminal complement complex
TEMED	NNN'N'-tetramethylethylenediamine
TNF-α	tumour necrosis factor-α
UV	ultraviolet

Suppliers and Company Addresses

Amicon Bioseparations	Millipore, Bedford, Massachusetts, USA
BD Biosciences Pharmingen	San Diego, California, USA
BIAcore AB	Uppsala, Sweden
Bioprocessing	Consett, UK
BioRad	Hercules, California, USA
Boehringer-Mannheim	Roche Applied Science, Indianapolis, USA
Dade-Behring	Marburg, Germany
Dako Ltd.	Ely, UK
Difco, Becton Dickinson	Oxford, UK
European Collection of Animal Cell Cultures (ECACC)	Porton Down, UK
Fisher Scientific	Loughborough, UK
GE Healthcare	Chalfont St. Giles, Buckinghamshire, UK
Gibco, Invitrogen Corporation	Paisley, UK
Greiner	Dursley, UK
Hybaid	Middlesex, UK
Invitrogen	Paisley, UK
Jackson ImmunoResearch Laboratories, Inc.	West Grove, Pennsylvania, USA
Kodak	Rochester, New York, USA
Medicell International Ltd.	London, UK
Nalgene	via Fisher Scientific, Loughborough, UK
New England Biolabs	Hitchin, UK
Nunc	via Fisher Scientific, Loughborough, UK
Oxoid Ltd.	Basingstoke, UK
Perkin-Elmer	Beaconsfield, UK
Pierce	Rockford, Illinois, USA
Promega	Southampton, UK
Quidel Corporation	San Diego, USA
Sartorius AG	Gottingen, Germany
Severn Biotech Ltd.	Kidderminster, UK
Sigma	Poole, UK
TCS Biosciences Ltd.	Claydon, Buckingham, UK
X-Ograph Ltd.	Malmesbury, UK

Table of Contents

Summary

The membrane attack complex (MAC) has been implicated in the pathology associated with several immune-mediated diseases and clinical interventions. However, there are currently no drugs available that specifically inhibit MAC assembly. The aim of this thesis was to generate and characterise agents that inhibit the activity of C6, a component of the MAC, with a view to testing them in models in which the development of pathology is mediated by MAC formation.
Two approaches were taken in generating agents that recognise C6: firstly, phage display was used to identify C6 inhibitory peptides. Several C6 inhibitory phage-peptides were identified and, whilst the synthetic peptide analogues bound C6, their inhibitory properties were not retained. However, motifs within each identified peptide had sequence homology with either C5b or C7, two other components of the MAC that bind to C6. This technique may be more useful in determining the domains of C5b and C7 that interact with C6 to form the MAC.
For the second approach, monoclonal antibodies were raised against rabbit, rat, mouse and human C6. The two most interesting antibodies were raised against human C6 and inhibited complement-mediated haemolysis in a cell-based assay. Both of these antibodies were species specific, excluding the possibility of testing their therapeutic properties in animal models of complement-mediated disease. Instead, an ex vivo model of cardiopulmonary bypass was established and used to test the ability of these antibodies to block soluble C5b-9 formation. Neither antibody inhibited soluble C5b-9 formation, suggesting that they might be interfering with the insertion of C6 into the cell membrane during MAC assembly. Nevertheless, the agents described in this thesis demonstrate that it is possible to specifically inhibit MAC formation and the reagents are now in place to test the proof-of-concept for therapeutic targeting of C6 in complement mediated disease.

Chapter 1: General Introduction

1.1. The Complement System

Complement (C) is so-called as it was originally discovered as a heat-labile component of normal plasma that was able to augment the opsonization of bacteria by antibodies [1]. Thus it was said to 'complement' the adaptive immune system [2].

C plays a central role in innate immune defence against invading pathogens through C fixation and opsonization, and by triggering local acute inflammation. It is involved in the induction of antibody responses [3-5], linking innate and adaptive immunity and also in the clearance of immune complexes and inflammatory products [6]. This suggests that aspects of the C system pre-date the adaptive immune system in evolutionary terms, although it is likely that both systems have evolved together.

The effects of C are mediated through three activating enzymatic cascades: the classical, alternative and mannose-binding lectin (MBL) pathways. All of these cascades activate a common non-enzymatic cascade, the terminal pathway, which results in the assembly of the membrane attack complex (MAC), the insertion of which into the cell membrane leads to the formation of a transmembrane pore [7-15]. If sufficient numbers of MAC are present in the cell membrane, then cell death occurs due to lysis [16]. In order to prevent inappropriate C activation, the C cascade is highly regulated by a number of regulatory proteins (C regulators), acting at multiple levels of the system.

If C activation occurs over a sustained period of time and the C regulators fail to adequately control this, then C-mediated damage can occur to tissues and organs. Examples of the development of such pathologies include rheumatoid arthritis (RA), multiple sclerosis (MS) and glomerulonephritis. In these situations, intervention with therapies that specifically inhibit C activity and thus subsequent C-mediated damage are clinically beneficial. Although anti-C therapies are in development, these tend to target the activating pathways, even though it is likely that the activity of the MAC is responsible for most of the tissue damage. The purpose of this thesis is to investigate strategies for inhibiting the activity of one of the MAC components, C6, thereby preventing MAC formation. To help with understanding the rationale behind this approach, this chapter describes the C system and the various attempts to make C inhibitors so far.

1.1.1. The C Activating Pathways

Although the activating pathways of C are triggered by different stimuli, the consequences of them are all the same. That is, to enzymatically activate C3 to C3b, which then binds to the surface membranes of microorganisms so that they are targeted to cells expressing C3 receptors (C3R), such as

phagocytic cells [17]. In addition, the activation pathways cleave C5, releasing a soluble peptide, C5a and creating C5b. C5a activates phagocytic cells, mast cells and basophils, resulting in the recruitment of more plasma proteins and phagocytic cells to the site of C activation [18]. C5b is the first component of the terminal pathway, which results in MAC formation and consequently, cell lysis [19]. Further information about the characteristics of the C proteins is presented in Table 1.1.

1.1.1.1. The Classical Pathway

The Classical pathway is triggered by the binding of C1, a multimolecular complex, to the F_c (constant fragment) regions of IgG or IgM antibodies that are complexed with antigen (immune complex) [20-22]. C1 comprises the recognition protein C1q and a catalytic subunit, $C1r_2C1s_2$ that is a calcium-dependent tetramer containing two molecules each of the serine proteinase proenzymes C1r and C1s [23,24]. C1q is a member of the collectin family (collagenous lectins) and is a large protein (460 kDa), comprising a bundle of six collagen-like triple helices, each ending in a C-terminal globular domain, so that the complex resembles a bunch of six tulips [25-27]. It is these globular domains that recognise the F_c regions of IgM and IgG and bind to the antigen-antibody complex. The catalytic subunit $C1r_2C1s_2$ spatially traverses the tulip structure of C1q [28,29] and the binding of a minimum of two of the globular domains of C1q to F_c domains is required to bring about the conformational change of C1q so that it binds $C1r_2C1s_2$ more tightly, resulting in the autoactivation of C1r, which in turn enzymatically activates C1s [28]. Activation requires the participation of at least two IgG molecules, or one pentameric IgM molecule [30]. Therefore, IgM molecules are more effective in activating the C system than are IgG molecules; further, the human IgG subclasses differ in their efficiency for binding and activating C1q, such that they can be ranked in the order IgG3>IgG1>IgG2; IgG4 has no activating ability [31]. Various substances, such as bacterial lipopolysaccharide, viral membranes, man-made liposomes, nucleic acids and components of damaged cells are also capable of activating C1 in an antibody –independent manner. Such activators may also be of physiological and pathological significance [32].

Activated C1s catalyses cleavage of C4 at a single site in the α chain, resulting in the release of C4a (a small soluble peptide with no defined function) and C4b, within which a labile intramolecular thioester bond becomes exposed. The thioester bond enables C4b to covalently bind to a hydroxyl or amino group on the cell surface [33] in close proximity to C1q. The membrane bound C4b, in the presence of Mg^{2+} ions, binds C2 near its amino terminus and presents it for cleavage by C1s, yielding C2a and C2b [34-36]. C2a remains bound to C4b, forming C4b2a, a complex with proteolytic activity for C3 and known as C3 convertase [36]. The C3 convertase cleaves C3 into two fragments: a small soluble peptide, C3a, that is an anaphylatoxin and C3b. A labile thioester bond becomes exposed in C3b [42], through which it

Table 1.1 The component proteins of the complement system

Component	Structure	Plasma concentration mg/l	Molecular weight (kDa)	Gene location Chromosome (Chr)
Classical pathway:				
C1 $C1qr_2s_2$	3 subunits:C1q C1r C1s	180	460 80 80	C1q A, B and C chains; Chr 1p34-36: C1r, C1s; Chr 12p13
C4	3 chains:α β γ	600	97 75 33	2 genes (C4A and C4B) in Major Histocompatability Complex (MHC) Chr 6
C2	Single chain	20	102	MHC Chr 6
Alternative pathway:				
Factor B	Single chain	210	93	MHC Chr 6
Factor D	Single chain	2	24	Chr 19
Properdin	Oligomers of identical chains	5	53 (each chain)	X chromosome
Mannose Binding Lectin pathway				
MBL	Oligomers (1-6) of trimers of identical chains	150 (varies)	75 (each trimer)	Chr 10
MASP-1	2 chains: A, B	6	91	Chr 3q27
MASP-2	2 chains: A, B	?	78	Chr 1p36.23-31
MASP-3	2 chains: A, B		101.5	Chr 3q27
Common				
C3	2 chains: α β	1300	110 75	Chr 19
Terminal pathway				
C5	2 chains	70	115 75	Chr 9
C6	Single chain	65	120	Chr 5
C7	Single chain	55	110	Chr 5
C8	3 chains:α β γ	55	65 65 22	α,β; Chr 1: γ; Chr 9
C9	Single chain	60	69	Chr 5

Table adapted from Complement Regulatory Proteins, Morgan BP and Harris CL, page 3 [37]; additional information from Contemporary Immunology: Therapeutic Interventions in the Complement System, Chapter 1: Complement as a regulatory and effector pathway in human diseases, page 3 [38], Stover *et al* [39], Presanis *et al* [40] and Mullighan *et al* [41].

can bind covalently either to cell membranes in the same way as C4, or to the activating C4b2a complex to form the C5 convertase (C4b2a3b) [43-46]. C5 can then bind non-covalently to a site on C3b in the C5 convertase and be cleaved by C2a within the convertase complex. This results in the release of C5a, a soluble molecule with potent chemoattractant and anaphylatoxic properties. C5b, the first component of the terminal pathway, is also generated, but remains attached to C3b on the cell surface during the early stages of MAC assembly. This is shown in Figure 1.1.
Although C3, C4 and C5 share structural similarities and are likely to have evolved from a common ancestor [33,42,47,48], C5b does not contain a labile thioester bond [47], but instead contains a labile hydrophobic surface binding site and a site for binding C6 that become exposed following the cleavage of C5 [21].

1.1.1.2. The Mannose-Binding Lectin (MBL) Pathway

The MBL pathway is the most recently discovered activation pathway [49-52]. MBL is a member of the collectin family; its structure is homologous to C1q – multimeric molecules with globular binding regions and collagenous stalks. MBL acts in the same way as C1q, but instead of binding antibodies, it binds to arrays of terminal mannose groups [53,54] and N-acetyl glucosamine residues, which are present in large quantities on viral surfaces and bacterial cell walls. MBL is an oligomer of structural subunits, each of which comprises three identical 32 kDa polypeptides [55,56]. Several sizes of MBL oligomer have been identified [57]. Like C1q, MBL is associated with serine protease proenzymes: MBL-associated serine proteases (MASPs) and the overall structure of these resemble those of C1r and C1s [58-60]. Two have been described, designated MASP-1 and -2 [58,61]. MASP-1 can be alternatively spliced, resulting in MASP-3 [57] and a truncated form of MASP-2 has been identified - a non-protease, small MBL-associated protein (sMAP or Map19) [62,63]. Two MASPs will associate with MBL in a similar manner to the interaction between C1q, C1r and C1s. The association of the MASPs with MBL is dependent on the MBL oligomer size [57]. The detailed molecular events of this activation pathway are yet to be elucidated, although it is known that the binding of MBL to microbial carbohydrates activates the MASPs [64,65]. MASP-2, like C1s, cleaves and activates C4 and C2 to form the classical pathway C3 convertase, C4b2a [58,66-69], whilst MASP-1 directly cleaves C3 [57,66,70,71], resulting in the activation of the alternative pathway [70]. This is shown in Figure 1.1.

1.1.1.3. The Alternative Pathway

The alternative pathway is another antibody-independent C activating pathway, but distinct from both the classical and MBL-activating pathways. It is initiated by C3b, which can either be present in the fluid or bound through its thioester bond to an activating surface. Factor B (fB), which is functionally analogous to C2 and shares a 40% sequence homology, binds C3b in a Mg2+-dependent manner. fB

Figure 1.1 The Activation pathways of the Complement system

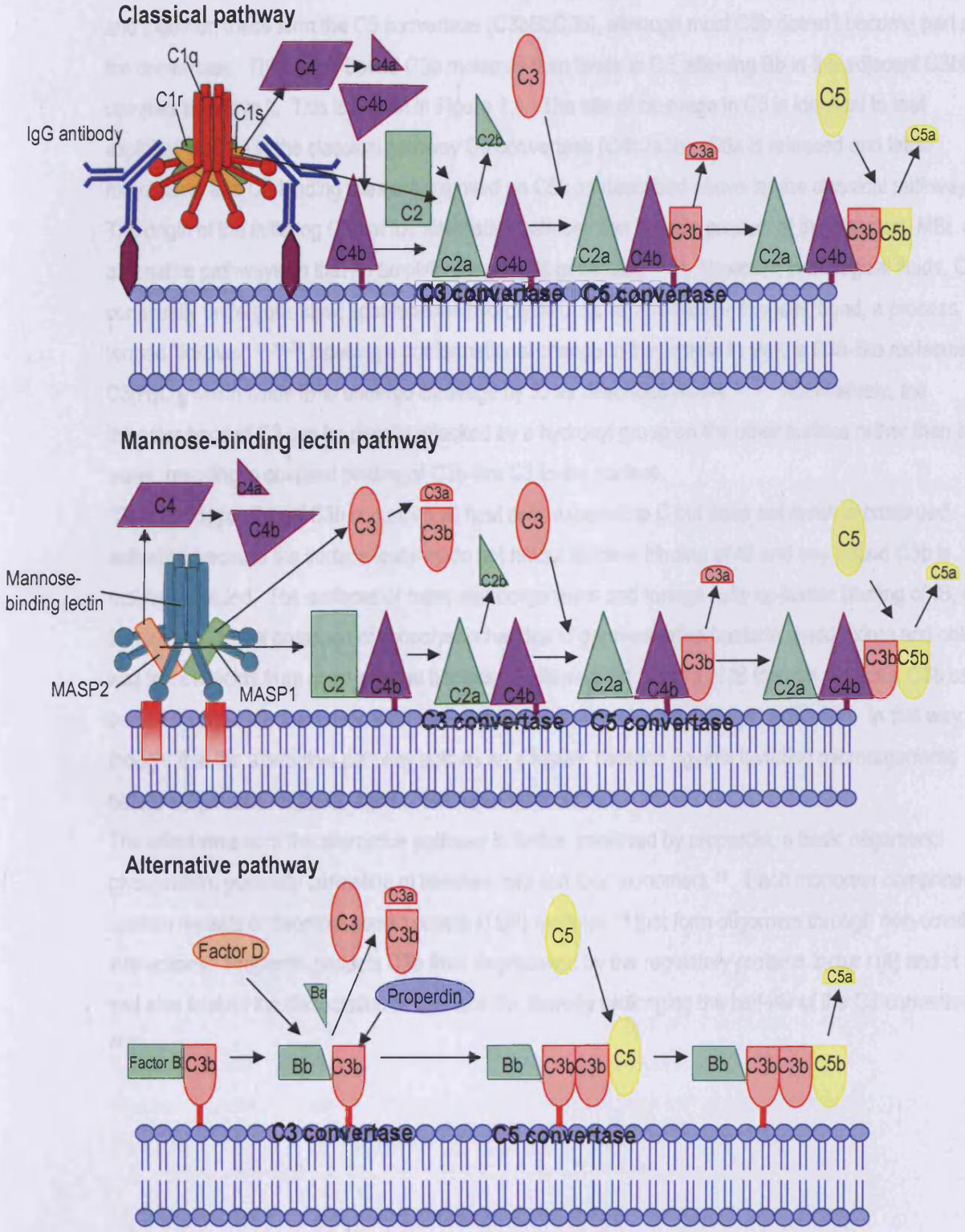

Adapted from Walport, 2001[6].

is then cleaved by the serine protease, factor D (fD), yielding C3bBb, where Bb now has an exposed serine protease domain and a smaller fragment, Ba, is released [72]. C3bBb is also a C3 convertase, which is equivalent to, but distinct from, that of the classical pathway, although they both cleave C3 at the same site, producing C3b. This C3b molecule can bind in close proximity to the C3bBb complex and together, these form the C5 convertase (C3bBbC3b), although most C3b doesn't become part of the convertase. This newly bound C3b molecule then binds to C5, allowing Bb in the adjacent C3bBb complex to cleave it. This is shown in Figure 1.1. The site of cleavage in C5 is identical to that exploited by C2a in the classical pathway C5 convertase (C4b2a3b). C5a is released and labile membrane- and C6-binding sites are exposed on C5b as described above for the classical pathway. The origin of the initiating C3b of the alternative pathway can be as a product of the classical, MBL or alternative pathways so that an amplification loop is generated [73,74]. However, in biological fluids, C3 continually undergoes slow, spontaneous hydrolysis of its intramolecular thioester bond, a process termed 'tickover' [47,74-76] inducing a conformational change in the protein to yield a C3b-like molecule, $C3(H_2O)$, which binds fB to undergo cleavage by fD as described above [73,74]. Alternatively, the thioester bond of C3 can be directly attacked by a hydroxyl group on the other surface rather than by water, resulting in covalent binding of C3b-like C3 to the surface.

'Tickover' deposition of C3b occurs on all host cells exposed to C but does not result in continued activation because the surface features do not favour efficient binding of fB and any bound C3b is rapidly degraded. The surfaces of many microorganisms and foreign cells do favour binding of fB, due, for example, to the presence of lipopolysaccharides of gram-negative bacteria (endotoxins) and cell wall techoic acids from gram-positive bacteria. Following the binding of fB to such surfaces, C3b can be rapidly generated and deposited on these surfaces, thereby amplifying C activation. In this way, it is thought that the alternative pathway acts as an effective defence against invading microorganisms before an immune response against them can be mounted.

The effectiveness of the alternative pathway is further improved by properdin, a basic oligomeric glycoprotein, generally consisting of between two and four monomers [77]. Each monomer comprises six tandem repeats of thrombospondin repeat (TSR) modules [78] that form oligomers through non-covalent interactions. Properdin protects C3b from degradation by the regulatory proteins factor I (fI) and H (fH), and also inhibits the dissociation of C3b and Bb, thereby prolonging the half-life of the C3 convertase [79,80].

1.1.2. The Terminal Pathway

All the terminal complex components; C6, C7, C8 and C9 are hydrophilic plasma proteins and comprise a single chain, apart from C8, which is composed of three chains, designated α, β and γ. C6, C7, the α and β chains of C8, as well as C9, share a structural homology [81]. C8γ is covalently linked with C8α, but is not homologous with any other C components [82]. The modular structures of these proteins are depicted in Figure 1.2, along with the C5α'-chain, the region of C5b that interacts with C6 and C7. Whilst still attached to C3b in the C5 convertase, C5b binds to circulating C6 at the cell surface through a 'metastable' binding site that is not accessible in intact C5 [21]. However, the precise sites of C5b, C6 and C7 that interact with each other are not yet fully characterised. The FIMs (factor I module) domains of C6 and C7 can bind to the C345C domain of C5b reversibly [83,84], although the FIMs domains enhance, but are not essential for the activity of C6 [84]. This has lead to the suggestion that during MAC formation the FIMs in C6 form an important but not crucial bond with C5b, and another domain of C6 binds to a metastable binding site within C5b. The FIMs domains of C7 then displace the FIMs domains of C6, so that C7 is incorporated into the complex [83,85]. When circulating C7 binds to C5b-6, two changes occur simultaneously. The C5b-7 complex is released from the C5 convertase to the fluid phase and a further conformational change in the complex is induced, exposing an unstable membrane binding site in the C5b-7 intermediate [86]. The membrane-binding site is prone to rapid decay, either by hydrolysis or through the interaction with a C regulatory protein, unless it binds to a membrane. In addition to the target cell membrane, it is possible for the C5b-7 complex to bind to an adjacent host cell membrane, which can result in the damage or lysis of the cell if the MAC forms; this is referred to as 'bystander lysis' [10,87,88]. Studies show that MAC formation is very inefficient in comparison to the formation of other C products [89]. C8 then binds to C7 in the C5b-7 complex through its β chain. This results in the complex C5b-8 embedding further into the membrane to form small pores, causing the cell to become 'slightly leaky' [90]. Finally, a molecule of C9 enters the C5b-8 complex and binds to the α chain of C8. Binding occurs via the MAC/perforin (MACPF) domain, together with the N-terminal thrombospondin-1 (TSP-1) and low-density lipoprotein receptor class A (LDLRA) domains of C9 [91]. The C9 molecule then unfolds, elongating from a globular, hydrophilic form to an amphipathic form that traverses the cell membrane, causing the membrane to leak even more. At the same time, multiple binding sites for C9 become exposed within the molecule, enabling further C9 molecules to bind, unfold and insert into the membrane. As more C9 molecules insert into the C5b-8 complex, the lesion becomes larger and a transmembrane pore forms, known as the membrane attack complex (MAC) [11,12,19,88]. This is shown in Figure 1.3.

Figure 1.2 Schematic modular structures of C5α'-chain, C6, C7, C8 and C9

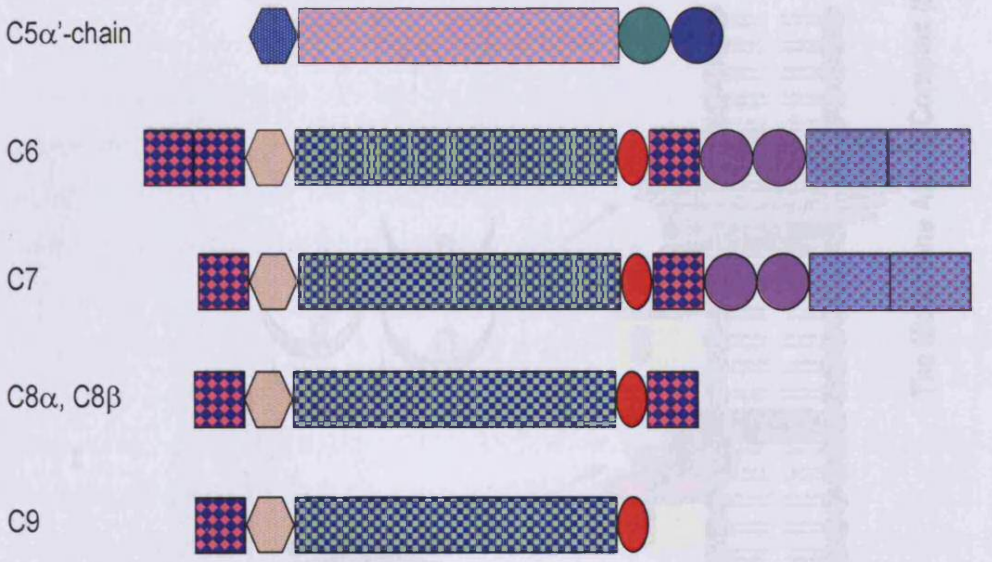

Key:

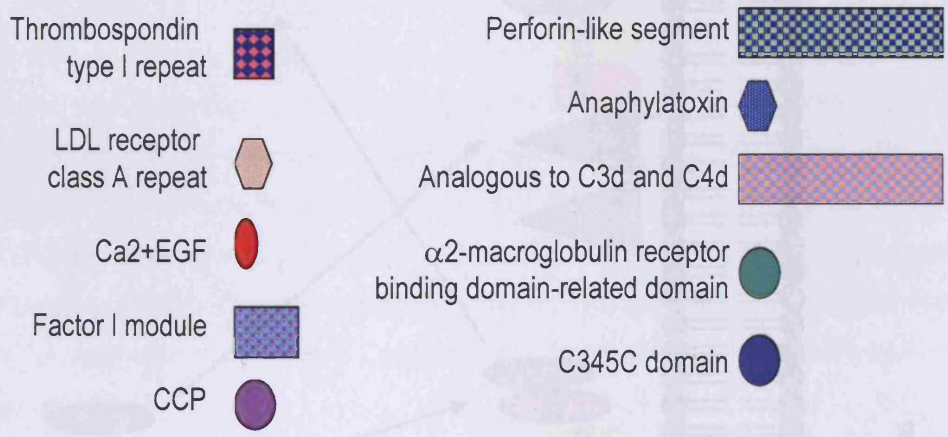

Adapted from Thai and Ogata[83] and 'The Complement Factsbook', edited by Morley, BJ and Walport, MJ.

Figure 1.3 The Terminal Pathway of the Complement System

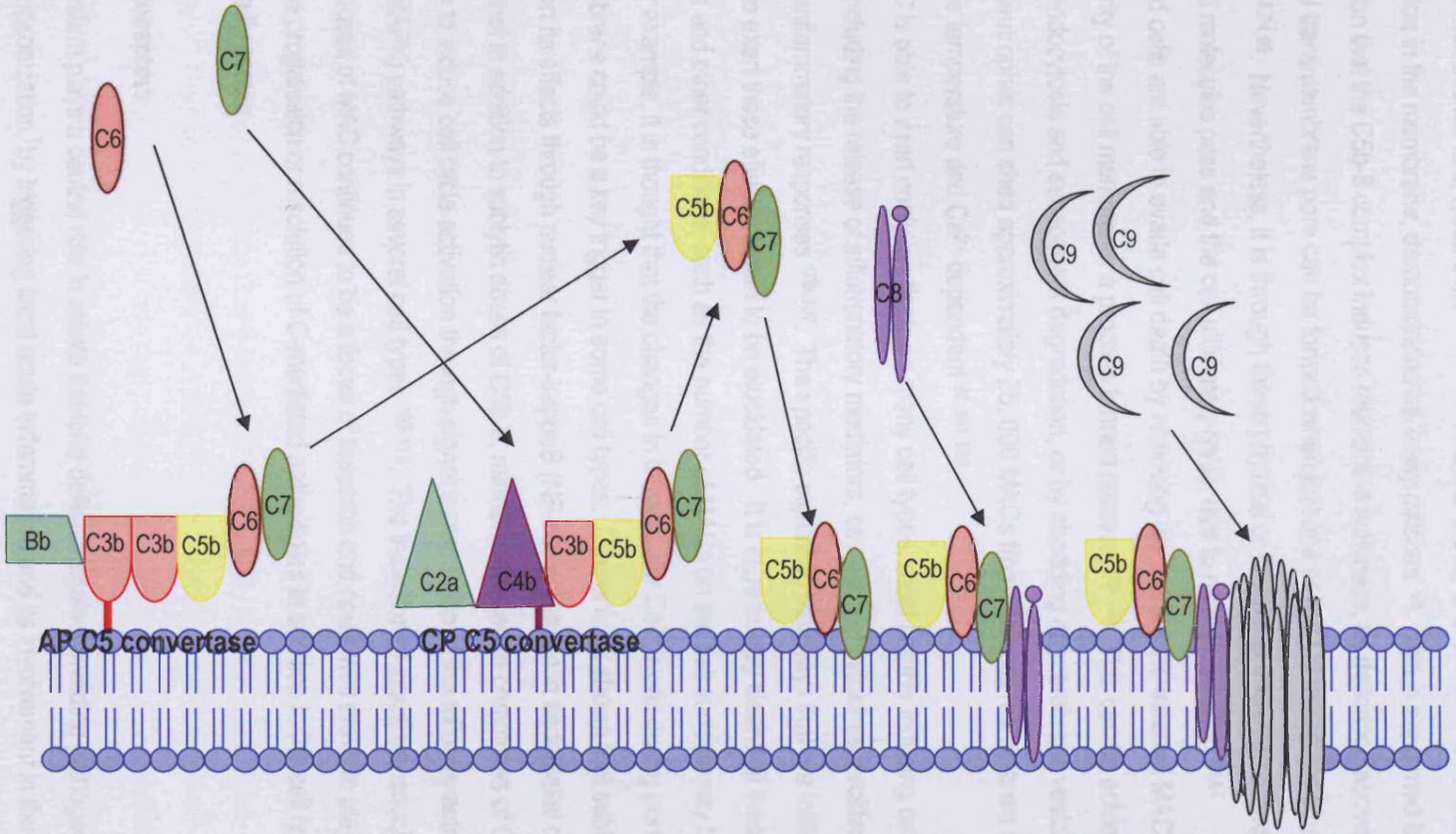

Adapted from Walport[83].

There is debate over the mechanism by which the MAC causes cell lysis. One theory is that the MAC forms a rigid ring around a stable transmembrane pore and this in some way is borne out by *in vitro* studies; when C9 molecules were incubated in the presence of Zn^{2+} ions, detergent-resistant aggregates of 12 or more C9 molecules formed in ring-like structures resembling the MAC lesion seen in the cell membranes of C lysed cells [11,12,88,92]. Another theory is that the MAC induces areas of lipid perturbation in the membrane, demonstrated as 'leaky patches' [93]. This is supported by the observation that the C5b-8 complex induces membrane leakiness, as described above, and also that a functional transmembrane pore can be formed when just one or two C9 molecules bind to the C5b-8 complex [8,94,95]. Nevertheless, it is through these physical or functional transmembrane pores that ions and small molecules pass and the cell ultimately lyses, due to osmotic swelling [96,97].

Nucleated cells are able to evade cell death by removing the membrane-inserted MAC and restoring the integrity of the cell membrane, a process termed recovery [98-100]. This can be achieved either through endocytosis and subsequent degradation, or by shedding on membrane vesicles [101-103]. Human neutrophils can shed approximately 25, 000 MACs from their cell membranes without lysing, and this is temperature and Ca^{2+}-dependent [98,104,105].

The MAC is able to exert nonlytic effects on many cell types, most notably inducing cell activation events, including the release of inflammatory mediators, secretion of cytokines, proliferation and many other proinflammatory responses [106,107]. The specific signalling pathways that are initiated by the MAC in order to exert these effects remain to be elucidated. It is increasingly clear that these vary between cell types and other conditions, such as the number of MACs on the cell surface may be important as well. For example, it is thought that the changes in intracellular Ca^{2+} levels during pore formation in the cell membrane could be a key trigger in some cell types. Others have shown that sublytic doses of the MAC exert its effects through nuclear factor-kappaB (NF-κB) activation in endothelial cells [108]. Studies indicate that in addition to sublytic doses of C5b-9, membrane-inserted complexes of C5b-7, C5b-8 are also able to induce cell cycle activation through signal transduction of the mitogen-activation protein kinase (MAPK) pathways in several cell types [109-113]. The induction of signal transduction pathways by sublytic doses of MAC continues to be a focus of research and could well prove to play an important role in the progression or resolution of C-mediated pathologies in addition to the cell lysis that undoubtedly occurs.

1.2. C Receptors

The C system plays a central role in innate immune defence against invading pathogens through C fixation, opsonization, by triggering local acute inflammation and its involvement in the induction of

antibody responses [3-5]. These effects are mediated by the products of C activation through their interaction with C receptors, which are expressed on a variety of cells. These include several receptors for C1q, and receptors for the large and small fragments of cleaved C3, C4 and C5 (Table 1.2).

1.2.1. C1q receptors

There are four putative receptors for C1q [114]: calreticulin (CRT; formerly known as collagenous C1q receptor (cC1qR) [115-121], C1q receptor for phagocytosis enhancement (C1qRp; formerly known as cC1qR100) [122], binding protein for the globular head of C1q (gC1q-R) [123,124] and C Receptor 1 (CR1 or CD35) [125], a multifunctional receptor.

CRT and C1qRp bind C1q through the collagen tail, but will also bind other collectins (collagenous lectins) in this way [126], including MBL and pulmonary surfactant protein A (SPA), which are both involved in host defence [55]. CRT is a multifunctional protein and is primarily an intracellular protein that is involved in glycoprotein quality control in the endoplasmic reticulum. The expression of C1qRp is restricted to neutrophils and monocytes [127,128].

gC1q-R binds C1q through the globular head of C1q and is a highly charged, acidic glycoprotein expressed on leukocytes, platelets and endothelial cells with a putative molecular weight of 33 kDa [129-133]. Further studies demonstrated that gC1q-R was only detectable on healthy cultured cells following permeabilization of the cell membrane, indicating that it was an intracellular protein [134]. Subsequently, it was shown that the leader sequence of gC1q-R is a mitochondrial targeting sequence and that it is expressed in mitochondrial compartments [135]. However, confusion over the full *in vivo* functions of gC1q-R remain, as it has been shown that some C1q-mediated events, such as the enhanced expression of P-selectin by platelets, as well as chemotaxis by mast cells are inhibited by anti-gC1q-R antibodies [136].

1.2.2. C Receptor 1 (CR1, CD35), a receptor for C1q, C3b and C4b

CR1 is a membrane bound molecule, comprising three domains, a cytoplasmic domain, a transmembrane region and an extracellular domain and is expressed on B-lymphocytes, monocytes and neutrophils. It binds to the collagen tails of C1q via long homologous repeat (LHR-) D. It has also been shown to be a receptor for MBL [137] and acts as receptors for C3b and C4b, discussed below. Although these receptors for C1q have been identified, it is likely that there are further C1q receptors. Their roles in C1q-mediated cell activation and other events remain to be elucidated fully.

CR1 is also a receptor for both C3b and C4b, which bind at different sites of the molecule [138]. Its major function as a receptor is to enable the transportation of immune complexes (coated in C3b and C4b) on

Table 1.2 Receptors for C components, fragments and complexes

Receptor	Ligand	Characteristics	Distribution
Calreticulin	C1q, collagenous region	70 kDa	Broad
C1qRp	C1q, collagenous region	100kDa, acidic glycoprotein	Monocytes, neutrophils
gC1qbp	C1q, globular heads	33 kDa, 80 kDa	Leukocytes, platelets
FHR	factor H	Not determined	Broad
CR1 (CD35)	C1q, C3b, C4b	180-220 kDa, single chain, transmembrane, approximately 30 short consensus repeats (SCRs)	Erythrocytes, B cells, neutrophils, monocytes.
CR2 (CD21)	C3d (and EBV)	145 kDa, single chain, transmembrane, 15-16 SCRs	B cells, follicular dendritic cells, epithelia, glia.
CR3 (CD11b/18)	iC3b (and matrix)	Heterodimer	Myeloid and natural killer cells.
CR4 (CD11c/18)	iC3b, C3dg	Heterodimer	Myeloid, macrophages.
C5aR (CD88)	C5a	40 kDa, 7 transmembrane spanning	Neutrophils, macrophages, mast cells, muscle.
C3aR	C3a	Approximately 60 kDa, 7 transmembrane spanning	Neutrophils, macrophages, mast cells, muscle.

Taken from The Complement System: a brief overview from Complement Regulatory Proteins by Morgan and Harris, p19 [37].

erythrocytes through the circulation to the spleen and liver, where they are cleared by mononuclear cells [17]. CR1 is also a C regulator and this is discussed later.

1.2.3. C Receptor 2 (CR2, CD21)

CR2 is highly homologous to CR1, although it does not have any C regulatory activity. It is the receptor for C3d, produced when C3b is cleaved by fI and serum proteases [139]. Although the role of CR2 is unclear on most cell types, on B cells it is known to be involved in the induction of antibody responses [139,140].

1.2.4. C Receptors 3(CR3, CD11b/CD18) and 4(CR4, CD11c/CD18)

CR3 and CR 4 are both members of the β2 integrin family of cell adhesion molecules [141-144]. CR3 is the receptor for iC3b and various extracellular matrix proteins, enabling myeloid and natural killer cells to bind to matrix and to C-opsonized surfaces. CR4 is the receptor for iC3b and C3dg and is thought to function in a similar manner to CR3.

1.2.5. The C3a (C3aR) and C5a (C5aR, CD88) receptors

The C3aR [145] and C5aR [146] are receptors for C3a and C5a respectively. They are both members of the 7-transmembrane-spanning receptor family and are highly homologous with each other. It is through the C5aR that C5a exerts its powerful effects of inducing migration and chemotaxis of neutrophils [147]. C5a, acting via C5aR, can also upregulate neutrophil surface expression of CR1 and CR3 [148,149], resulting in the recruitment of phagocytic cells in inflammation and rendering them fully active in phagocytosis.

1.3. C Regulation

There is the potential for host cells to be attacked by C products that could lead to the C-mediated destruction of host tissues. Therefore, the C system is strictly regulated through the inactivation of its activated components by C regulatory (C reg) proteins. Some are bound to the cell membrane on which C is activated, whilst others are in the fluid phase. C regs can be further divided into two groups; those that are encoded within the Regulators of C Activation (RCA) gene cluster, on the short arm of chromosome 1, and those that are not [150].

Proteins of the RCA cluster share a structural homology with each other – they are either partly or entirely made up of repeating domains called short consensus repeats (SCRs). Each SCR has a loop structure held in place by disulfide bonds between the conserved cysteines-1 and –3, and –2 and –4 [151]. The SCR motif and variations of it are common to many C proteins as well as a large number of non-C proteins [28]. RCA cluster proteins all bind and/or regulate C3 and C4 activation products [152],

suggesting a common evolutionary ancestor [153]. All the C regulators are summarised in Table 1.3 and are described in the following discussion in the order in which they act on the C pathway.

1.3.1. Inhibitors of C Activating Pathways

1.3.1.1. C1-inhibitor

C1-inhibitor (C1inh) is a serine protease inhibitor (serpin) present in the plasma that inhibits the activated C1 complex [154,155]. It binds strongly to the activated C1s and C1r subunits of C1 [156,157], resulting in their dissociation from C1q, thereby inactivating C1 [158,159]. It also prevents the spontaneous autoactivation of the classical pathway by forming a stable complex with native C1 in plasma [160].

1.3.1.2. Factor I (fI)

fI is a plasma serine protease that is dependent on the presence of specific cofactors to catalyse its cleavage of C3b and C4b in the convertases of the classical and alternative pathways. It is not encoded for in the RCA cluster, but all of its four cofactors are. Two of these cofactors are present in plasma: factor H (fH) and C4b binding protein (C4bp); and two are membrane bound: membrane cofactor protein (MCP, CD46) and the C receptor, CR1.

1.3.1.3. fH, an alternative pathway fluid phase cofactor for fI

fH binds C3b in the C3 and C5 convertases of the alternative pathway and catalyses the cleavage of C3b by fI [161], resulting in the formation of inactive iC3b and the release of C3f [162].

1.3.1.4. C4bp, a classical pathway fluid phase cofactor for fI

C4bp binds C4b in the classical pathway C3 convertase and catalyses the cleavage of C4b by fI, which results in the release of inactive C4c [163]. Interestingly, the C and coagulation systems are linked through C4bp. The β chain of C4bp (sometimes present - see Table 1.3) enables it to bind protein S (not to be confused with S-protein!) a component of the coagulation system [164].

1.3.1.5. fH and C4bp are decay accelerators

fH and C4bp also inhibit the C activating pathways independently of fI, by accelerating the dissociation of the components of the convertases from each other and this is termed decay acceleration [28,165]. When the convertases form during C activation, the components they comprise spontaneously dissociate from each other over several minutes. By binding tightly to C3b [166] in the AP convertases, fH displaces the enzymatic component of the complex, Bb or fB. fH also binds C3b in the fluid phase, thereby preventing it binding to fB. Likewise, C4bp binds C4b in the fluid phase, preventing C3 convertase formation and also to C4b in the C3 convertase, displacing C2a.

Table 1.3 Complement regulatory proteins

Molecule	Structure	Serum concentration (mg/l)	Molecular Weight (kDa)	Gene Location	Target
Plasma					
C1 inhibitor (C1 inh)	Single chain	200	76	11	C1
Factor H	Single chain	450	150	1 (RCA)	C3/C5 convertase
Factor I	2 chains	35	50 38	4	C3/C5 convertase
C4bp	6 or 7 α chains 1 or 0 β chain	250	70 45	1 (RCA) 1 (RCA)	Classical pathway C3 convertase
S protein	Single chain	500	83	17q	C5b-7
Clusterin	2 chains: α β	50	 35 38	8p	C5b-7
Carboxypeptidase N (CPN)	Dimeric heterodimer	30	290	?	C3a, C4a, C5a
Membrane					
Membrane Cofactor Protein (MCP) CD46	Single chain TM	-	60	1 (RCA)	C3/C5 convertase
Decay Accelerating Factor (DAF) CD55	Single chain GPI	-	65	1 (RCA)	C3/C5 convertase
C Receptor 1 (CR1) CD35	Single chain TM	-	200	1 (RCA)	C3/C5 convertase
CD59	Single chain GPI	-	20	11	C5b-8/C5b-9

Table adapted from Complement Regulatory Proteins, Morgan BP and Harris CL, page 33 [37].
TM – transmembrane; GPI – glycosyl phosphatidylinositol; RCA – regulators of complement activation gene cluster

1.3.1.6. MCP, a membrane bound activation pathway cofactor for fI

MCP is a membrane bound regulator that binds to C3b and C4b deposited on host cell membranes, which can then be degraded by fI, producing iC3b, C4c and C4d [167,168]. Therefore, MCP regulates both the classical and alternative pathways. Unlike fH and C4bp, it does not have decay acceleration properties. In addition to four amino-terminal SCR domains, MCP comprises a heavily glycosylated Ser/Thr/Pro (STP) rich region, a transmembrane and a cytoplasmic domain [169]. Soluble forms of MCP, with C regulatory activity, have been detected in reproductive tract fluids, tears and plasma [170,171]. Studies suggest that MCP is also involved in events unrelated to C regulation, such as sperm-egg fusion [172-175].

1.3.1.7. CR1, a membrane bound activation pathway cofactor for Factor I

In addition to being a C receptor for C1q [125], C3b and C4b [138], CR1 is also a C regulator. It binds C3b and C4b within the C3 and C5 convertases from the classical and alternative pathway and acts as a cofactor for fI, resulting in the degradation of C3b to iC3b and C4b to C4c and C4d [176,177]. The iC3b can be further cleaved by fI, with CR1 acting as cofactor to C3c and C3dg [178-180].

1.3.1.8. CR1 is a decay accelerator

CR1 is able to accelerate the decay of the CP and AP convertases in the same way as fH and C4bp, by binding to C3b and C4b, thereby displacing C2a and Bb from the convertases. Once it has disrupted the convertase it is associated with, it is released from the complex, enabling it to bind and inhibit other convertases on the membrane.

1.3.1.9. Decay Accelerating Factor (DAF, CD55)

DAF is a member of the RCA cluster family of proteins. Like MCP, it is membrane bound, but is attached to the cell membrane through a glycosyl phosphatidylinositol (GPI) anchor near its C-terminus [181,182]. DAF is not a cofactor for fI, but accelerates the decay of the CP and AP convertases by binding C4b and C3b, thereby displacing C2a or Bb respectively [183-185].

1.3.1.10. Carboxypeptidase-N (CPN)

CPN is a plasma zinc metalloprotease comprising two small enzymatically active subunits (CPN1) and two large subunits (CPN2) that prevent the enzyme being degraded [186]. It is a member of a large family of carboxypeptidases, where the active site is highly conserved and many of these proteins, like CPN, cleave arginine and lysine residues from various peptides. In the case of CPN, it cleaves carboxy-terminal (C-terminal) argninine (Arg) and lysine (Lys) residues of peptides found in plasma, including inflammatory kinins, creatine kinase MM and the C anaphylatoxins, C3a and C5a [187]. CPN

cleaves Arg residues of C3a and C5a, yielding C3adesArg and C5adesArg [188,189], respectively. These molecules are largely inactive, although C5a desArg is able to stimulate neutrophils and basophils to some degree [190].

1.3.2. Inhibitors of the Terminal Pathway

There are fluid phase and membrane bound terminal pathway inhibitors.

1.3.2.1. Fluid-phase Inhibitors

1.3.2.1.1. Hydrolysis of the C5b-7 membrane binding site

In the first instance, the C5b-7 complex in the fluid phase is subject to spontaneous decay due to the unstable nature of its membrane binding site which is susceptible to hydrolysis [86]. This significantly decreases the amount of complex depositing on the cell surface that can go on and form MAC and therefore represents an important means of C regulation.

1.3.2.1.2. C8

Plasma C8 is able to bind the C5b-7 complex in the fluid phase. This blocks the membrane binding site in the C5b-7 complex, thus preventing it binding to the cell surface [191].

1.3.2.1.3. S-protein (vitronectin)

S-protein [192,193] and vitronectin [194,195] were discovered independently of each other, but it was subsequently shown that they were the same molecule [196,197]. S-protein has a molecular weight of approximately 80 kDa and is widely distributed in biological fluids and tissues [194,198]. It binds the fluid-phase C5b-7 complex [193,199] at or near the metastable membrane binding site in C5b-7, thereby preventing the association of the complex with the membrane [193,199,200]. The resulting SC5b-7 complex is still able to bind C8 and multiple copies of C9, forming SC5b-9, also known as the terminal C complex (TCC) [201-203]. Conformational changes in C9 occur exposing neoepitopes identical to those in the MAC, although the structure formed does not physically resemble the MAC. This has enabled the development of specific assays to monitor the level of C activation *in vivo* [204,205].

S-protein binds perforin, a T cell lytic protein and terminal C components, which all share structural homology, through its heparin binding domain [206]. However, S-protein is primarily an adhesion molecule [198,207] and interacts with integrin receptors through its RGD domain [207-209]. The multifunctional activities of this molecule, together with its high plasma concentration (up to 10 μM) [210], make it an unsuitable candidate for modification as a potential therapeutic.

1.3.2.1.4. Clusterin

Human clusterin is a heterodimeric serum glycoprotein comprising two subunits, designated α and β respectively, each with a molecular weight of approximately 40 kDa [211]. The two chains are linked by disulfide bonds and are heavily glycosylated. Clusterin binds the C5b-7 complex in the fluid phase, preventing it binding to the cell membrane [212,213]. C8, C9 and S-protein are then incorporated, generating an inactive fluid-phase SC5b-9 complex identical to that described in the previous section. However, there is little evidence that inhibition of C by clusterin is physiologically relevant.
Clusterin is widely expressed in tissues, plasma and seminal plasma and its expression is elevated after cell injury or death [214-217]. This and other evidence has led to suggestions of its involvement in lipid transport in the circulation [218], male reproduction [219,220], and the neutralization of toxic debris released by dead and dying cells [214,215]. For these reasons, clusterin is an unsuitable candidate for an anti-C therapy.

1.3.2.2. Membrane bound regulators

1.3.2.2.1. CD59 (Homologous Restriction Factor-20, HRF-20)

CD59 is a GPI-anchored protein, with a molecular weight of approximately 20 kDa and was originally isolated from human erythrocyte cell membranes and discovered independently by various groups [221-226]. As well as being expressed on erythrocytes, CD59 is present on other circulating cells, endothelia, epithelia and most organs [225-228]. CD59 inhibits MAC formation by binding to the C5b-8 complex through the C8α chain. One molecule of C9 can still bind the CD59/C5b-8 complex through the C-terminal β domain of C9, but the recruitment of further molecules of C9 to the complex is blocked [229-231]. CD59 has been isolated from rats [232], mice [233], pigs [234], sheep [235] and non-human primates [236,237].

The C system is subject to strict control by regulatory proteins. Potentially, these could be modified and administered for use as therapies in order to control C activation in disease. Several of these, such as C4bp, clusterin and S-protein have important functions outside of the C system and make unsuitable candidates. Others, such as CR1 and CD59 are only involved in the C system and are therefore much better candidates for modification for drug development.

1.4. Deficiencies in C Components

The study of C component deficiencies has provided many insights into the physiological function of C proteins and the roles of C pathways *in vivo*. This is particularly useful in drug design, when

considering which part of the C system to target in an attempt to reduce the pathology caused by inappropriate C activity.

Inherited deficiencies of all the C proteins and most of the C regulatory proteins have been described [238-240]. These provide information about the precise functions of particular C components, as their deficiency is often associated with the development of a specific pathology. These are summarised in Table 1.4.

1.4.1. Deficiencies in Classical Pathway Components

Patients deficient in classical pathway components, i.e. C1, C4 or C2, are predisposed to immune complex diseases [241], most commonly manifested as Systemic Lupus Erythematosus (SLE) and glomerulonephritis, as well as to severe and recurrent pyogenic infections, for example, with *Streptococcus* and *Staphylococcus*. This emphasises the central roles the classical pathway plays in mediating the killing of invading bacteria and in the solubilizing immune complexes [239,240]. This is probably because the main ways of combating infection by these organisms is by phagocytosis followed by intracellular killing. Therefore, any disruption in the pathways that lead to intracellular killing, i.e. antibody deficiency, C deficiency or phagocyte function will lead to an increased susceptibility to this type of infection [240].

1.4.2. Deficiencies in Alternative Pathway Components

Deficiencies in the alternative pathway components have been described, but until recently, were thought to be rare [242]. Homozygous deficiencies in fH are associated with renal disease, membranoproliferative glomerulonephritis and atypical haemolytic uraemic syndrome (HUS) [243]. Heterozygous fH deficiencies are also associated with renal disease, most frequently, atypical HUS [243]. The fact that alternative pathway deficiencies are rarely detected suggests either that these deficiencies are most often mild and hence go undetected, or else the consequences are fatal and therefore not detected, highlighting the importance of the alternative pathway.

1.4.3. Deficiencies in Terminal Pathway Components

Terminal C component deficient patients often present with recurrent Neisserial infections, most often meningococcal infections, but are usually otherwise healthy [147,244]. This observation has lead to the suggestion that extracellular cytolysis by MAC has evolved as a means of host defence specifically for this type of infection [240].

Table 1.4 Complement Component Deficiencies

Component	Incidence	Disease associations
Classical pathway:		
C1q	> 40 cases described	Majority have SLE, predisposition to pyogenic infections, e.g. meningitis
C1r/C1s	Rare: ≈ 10 cases described, deficiencies tend to occur together	Majority have SLE, predisposition to pyogenic infections, e.g. meningitis
C4	Homozygous (C4A + C4B) deficiency rare; ≈ 40% of the population have heterozygous (C4A or C4B) deficiency	Homozygous deficiency associated with SLE; C4A deficients have increased predisposition to SLE; tendency for pyogenic infections
C2	Most common homozygous C deficiency in Caucasoids; 1:10 000 - 1:30 000	Predisposition to SLE, susceptibility to pyogenic infections; at least 25% of C2 deficient patients apparently healthy
Alternative pathway:		
Factor D	Very rare	Neisserial infection
Properdin	Not uncommon; inheritance is X-linked	Neisserial infection
Activation pathways:		
C3	Rare	Severe recurrent pyogenic infections; glomerulonephritis; SLE
Factor I	Very rare – results in a severe acquired C3 deficiency	Severe recurrent pyogenic infections; glomerulonephritis; SLE
Factor H	Very rare – results in a severe acquired C3 deficiency	Severe recurrent pyogenic infections; glomerulonephritis; SLE; haemolytic uraemic syndrome
Terminal pathway:		
C5	Rare	Neisserial infections; rarely SLE
C6	Second most common complement deficiency; 1:60 000	Neisserial infections; rarely SLE; at least 25% of homozygous individuals healthy
C7	1:25 000 in Japanese	Neisserial infections; rarely SLE
C8	Less rare	Neisserial infections; rarely SLE
C9	Rare in Caucasians; 1:1000 in Japanese	Neisserial infections in Caucasians; weak association with neisserial infections in Japanese
C Reg Proteins		
C1 inhibitor	1:150 000; autosomal dominant inheritance	Hereditary angiodema (HAE)
CR3/CR4		Severe immunodeficiency
DAF		No associated disease
CD59	Very rare	Paroxysomal nocturnal haemoglobinuria (PNH)-like disease

Table adapted from Morgan and Walport in Immunology Today [240].

The study of C deficient individuals has demonstrated that whilst all deficiencies have important clinical consequences for the individual, some deficiencies result in more severe diseases or a greater susceptibility to certain types of infection than others. Therefore, this must be taken into account when designing therapies that inhibit C activity, so that the potential for causing more disease is minimised. For example, inhibiting the classical pathway could result in the patient developing immune complex disease or having an increased susceptibility to pyogenic infections. On the other hand, inhibiting a terminal pathway component might lead to an increased susceptibility to *Neisserial* infections, but is less likely to lead to the development of immune complex disease and allows opsonisation and the solubilisation of immune complexes to occur, so that many infections can be overcome.

1.5. Complement and disease

The main physiological role of the C system is to overcome infection by invading pathogens, through the mechanisms described above. Nevertheless, it is clear that many infectious agents are able to hijack the C system and use it to advantage, potentially leading to the development of C-mediated pathologies. For example, parasitic infections, such as Schistosomiasis, Leishmaniasis and Trypanosomiasis are often long lasting, leading to the development of equilibrium between parasite and host, ensuring the survival of both host and parasite. In order for this to be achieved, such parasites are resistant to C activation at some point during their lifecycle and often, this is during the adult morphological blood-borne form. However, parasites continually release foreign antigen into the host circulation, resulting in circulating immune complexes, so that C activation occurs, followed by pathology. Furthermore, because continual C activation is occurring, many infected individuals are C depleted, so that they are more susceptible to other infections [245].

In recent years it has become apparent that although viruses are eliminated or controlled by the C system, some viruses are able to manipulate the C system to their own advantage, leading to their enhanced ability to infect the host or evade elimination by the C system. Viruses have developed various C evasion mechanisms. For example, Human Immunodeficiency virus (HIV) and Human Cytomegalovirus (HCMV) are able to incorporate C regulatory proteins into their viral envelope as they bud from the cell surface [246,247]. Many of the larger DNA viruses, such as the herpesviruses and poxviruses encode their own C regulatory proteins. These can share homology with cellular C regulatory proteins, as in the case of Kaposi's sarcoma-associated virus (KSHV), which codes for a protein, KSHV C control protein (KCP) that exhibits homology to DAF [248,249]. Alternatively, they can have no homology at all to cellular proteins, such as the herpes simplex virus-1 (HSV-1) and HSV-2 glycoproteins. Both of these evasion mechanisms protect the viruses from C attack. Furthermore,

some viruses enter host cells via C receptors or C regulatory proteins. For example, Epstein-Barr virus (EBV) infects B cells and endothelial cells through interactions between viral gp350/220 proteins and CR2, whilst the measles virus infects cells via interactions with MCP [250].

The activating pathways of C have been shown to be critical in host defence against bacterial infections. Gram-negative bacteria possess an outer cell wall, a major component of which is lipopolysaccharide (LPS), that contains Lipid A and this binds and activates C1, thus activating the classical pathway. Gram-positive bacteria are unlikely to directly activate the classical pathway, as their cell walls are up to 150 nm thick and consist predominantly of peptidoglycan and techoic acid. Therefore, they are more likely to activate C via the alternative pathway. Due to the cell wall thickness, gram-positive bacteria are resistant to C-mediated lysis and so C activation serves only to enhance phagocytosis of these bacteria by phagocytes.

1.6. Complement and Autoimmune Diseases

Inappropriate C activation is the driving force behind the development of pathology in many diseases, including inflammatory conditions such as RA and MS, as a consequence of ischaemia – reperfusion injury, as well as due to therapeutic intervention, for instance, extracorporeal circulation [251]. In such situations, the same protective C components that defend the patient against invading pathogens become chronically activated, leading to the sustained production of C3a and C5a which drive inflammation by recruiting and activating neutrophils, and MAC which may kill or injure cells.

RA is an autoimmune disorder, affecting 1-2 % of the worlds' population. It is characterised by inflammation of the synovial tissues, joint swelling, stiffness and pain that can progress to joint erosion [252]. Excessive C activation has been implicated in the pathogenesis of RA [253], as demonstrated by the detection of soluble C activation products in inflammatory joint synovial fluid [254-257] and the deposition of MAC within rheumatoid synovium *in vivo* [258,259].

The precipitating factors that result in the development of MS are complex and remain to be fully elucidated, but the presence of CD8+ T cells and antibodies have been implicated in axonal damage. The presence of antibodies further implies a role for the C system in disease progression [260]. However, the involvement of C activation in the progression of MS is proving increasingly complicated to understand, as recent clinical trails with anti-inflammatory agents did not yield the expected results, suggesting the possibility that the inflammation observed in MS may be of benefit to the patient [261].

Extracorporeal circulation as happens in cardiopulmonary bypass (CPB) is a necessary part of most types of cardiac surgery, but postoperative complications may occur, including respiratory failure, renal dysfunction, bleeding disorders, neurologic dysfunction and altered liver function. In turn, these can

result in multiple organ failure (MOF) and ultimately the death of the patient [262-266]. These complications arise due to a complex inflammatory response, initiated by neutrophil and C activation [267], which leads to platelet and leukocyte activation, resulting in widespread inflammation throughout the body [268]. Elevated levels of C3a have been detected both during and following CPB [267,269-271] and raised levels of SC5b-9 [272,273] have also been recorded. The levels of C3a and SC5b-9 are not elevated in patients who have undergone cardiac or other major surgery not requiring CPB [267,272].

Targeting the terminal pathway as a potential therapy is becoming an increasingly attractive prospect, as it has been implicated in the development of various pathologies. In a rat model of glomerulonephritis, limited apoptosis was detected in rats deficient in C6, a component of MAC, whereas in C6-sufficient rats, a high degree of apoptosis was observed [274]. A similar degree of apoptosis to that detected in C-sufficient rats was observed in C6 deficient rats treated with human C6, to reconstitute the deficiency. This strongly emphasises the role of MAC in the early stages of this disease model [274]. Moreover, a major advantage of a terminal pathway inhibitor is that the functions of the activation cascades, such as immune complex opsonisation and clearance of C3b coated bacteria, remain intact. The sole deficit in patients deficient in terminal complex components is susceptibility to infections with organisms of the genus *Neisseria* [275], which, although a serious condition, is preventable with the prophylactic use of antibiotics. Therefore, inhibition of MAC may be safer to use as a long-term therapy compared to activation pathway inhibitors.
C activation is a common feature in the progression of all the pathologies discussed above, even though the factors causing the activation are diverse. Theoretically, these diseases could be resolved by the therapeutic inhibition of C.

1.7. Complement-mediated disease and treatments

The traditional treatment of RA is to manage the patients' symptoms with nonsteroidal anti-inflammatory drugs (NSAIDs), corticosteroids and disease-modifying antirheumatic drugs (DMARDs) for example, methotrexate. The effectiveness of these drugs varies from patient to patient and there is a significant risk of toxicity when these drugs are used over the long term [252,276]. New types of drugs, biological response modifiers (BRMs) are beginning to be used, generally in patients in whom the use of traditional drugs is ineffective or contra-indicated. BRMs block the biological effects of inflammatory cytokines [252,277]. These include monoclonal antibodies against TNF-α such as Infliximab™, soluble TNF receptors, for example Etanercept™, and receptor antagonists to interleukin (IL)-1, e.g. Anakinra™. These drugs are more effective than the traditional treatments, as they alter the progression of joint erosion and also attenuate many associated symptoms. However, they are

expensive and also have adverse effects, for example anti-TNF-α therapies may be associated with an increased risk of infections, sepsis and demyelination disorders [252].

Corticosteroids are also used for the symptomatic relief of conditions arising as a result of MS, such as true vertigo, which 20% of MS patients suffer from [278]. Interferon-β (IFN-β) is often used as a treatment for MS; unfortunately, up to 35% of these patients develop neutralizing anti-IFN-β antibodies within 2 years of starting this therapy. These antibodies reduce or abolish the biologic effects and limit the clinical efficacy of IFN-β [279]. Glatiramer acetate, a collection of immunomodulatory synthetic polypeptides is also used to treat MS and like IFN-β, the patients remain relapse-free and the development of new lesions is reduced. However, it is limited in its effectiveness and there have been reports of adverse effects and toxicity issues [280]. Therefore, investigations are continuing into developing more effective treatments, including T-cell vaccination [281], inhibitors of matrix metalloproteinase-9 (MMP-9), the upregulation of which has been implicated in MS [282], gene therapy [283], and other immune-based therapies [284].

1.8. The Development of anti-Complement therapeutics

As inappropriate C activation is the driving force behind the development of pathology in many diseases, a sensible approach is to develop C inhibitors for therapeutic use. This section examines the various approaches that have been adopted from a historical perspective through to current developments.

1.8.1. Cobra Venom Factor (CVF)

Investigations with cobra venom gave one of the earliest indications that manipulating the C system may be of therapeutic benefit. The first decomplementation studies with cobra venom on animal sera were performed 100 years ago [285], although the active component, cobra venom factor (CVF) was not isolated until nearly 70 years later [Cochrane, 1970 #19; Gewurz, 1967 #598; [286-290]. CVF is a form of Cobra C3b [Alper, 1976 #602] and depletes C via the alternative pathway. CVF binds plasma fB, the fB is cleaved by fD and a stable C3 convertase (CVFBb), with a half-life of several hours in plasma, is formed. CVFBb is also resistant to the fluid phase regulators [291], so that it is able to cleave C3 in an unregulated manner, leading to the release of large amounts of C3a and C3b. This results in the systemic depletion of C3 [292] and thus C activity, for between 24 and 72 hours in experimental animals. By administering CVF repeatedly, systemic decomplementation can be maintained for up to a week [251]; after this time it becomes ineffective, due to a strong immune response and the subsequent generation of neutralising antibodies by the recipient [285]. In addition, large amounts of active C fragments are produced, resulting in shock, including circulatory collapse, metabolic acidosis and hypotension [293].

For these reasons, the use of CVF in humans would not be beneficial. Cobra venom has been used to treat RA, with little success [294,295]. Nonetheless, CVF has been very successful in treating many animal models involving uncontrolled inflammation, including transplantation [296-299], ischemia-reperfusion injury [300] and various autoimmune diseases [301-307]. This set the precedents that (1) C is involved in the development of a wide range of pathologies and (2) the C system can be manipulated for therapeutic benefit.

1.8.2. Heparin and other polyionic molecules

Heparin is a polyanionic glycosaminoglycan routinely used as an anticoagulant, including in patients with shock syndromes [308]. Its beneficial effect in such patients may in part be due to its ability to inhibit C, which has been demonstrated *in vitro* [309]. Heparin acts on the classical, alternative and terminal pathways by binding and inactivating C1, inhibiting the assembly of the C3 convertases and disrupting MAC formation [310-313]. Little has been done to determine the efficacy of heparin as an anti-C agent *in vivo*, probably because of its lack of specificity. It is used extensively to coat extra-corporeal circuits in (CPB) and renal dialysis, to reduce coagulation and C activation within the circuit [314,315].
Many other polyanionic molecules also have C inhibitory properties *in vitro*, including dextran sulphate, polyvinyl sulphate, polylysine and suramin [316]. In animal models, it has been demonstrated that suramin inhibits C and suppresses some components of the Arthus reaction and xenotransplant rejection [317,318], whilst in man it has been used with limited success to treat attacks of hereditary angiodema [319].

1.8.3. Serine protease inhibitors

Aprotinin is a non-specific serine protease inhibitor that is extracted from bovine lung and has been used to treat a variety of conditions over the last fifty years, including acute pancreatitis, septic and haemorrhagic shock and adult respiratory distress syndrome (ARDS) [320]. In the early 1980s, it was administered to patients in conjunction with heparin during CPB. At high doses, this was successful, particularly in reducing neutrophil activation [321]. However, it emerged that aprotinin increased the risk of patients suffering myocardial infarction during cardiac surgery, as well as other complications, such as acute renal failure and anaphylactic shock [320].
Hereditary angioedema (HAE) is caused by a deficiency in C1-Inhibitor (C1-Inh) [322], the serine protease inhibitor and sole inhibitor of C1. Morbidity in C1-Inh deficient patients is high following surgical procedures. This condition became the first to be treated therapeutically using a C regulator in 1975, when patients with HAE were transfused with fresh frozen human plasma prior to dental surgery as a prophylactic measure [323]. This treatment decreased the severity of complications following surgery; more specifically the precipitation of an attack of HAE was avoided [323]. Subsequently, patients with

acute attacks of HAE have been successfully treated with purified C1-Inh [324]. Purified, pasteurised human C1-Inh has been used as a treatment for acute episodes of HAE and prophylatically for example, prior to surgery since the early 1980s with few adverse effects [325-330] and clinical trials have shown this is a safe and effective treatment in controlling HAE [331]. Surprisingly, C1-Inh is not widely used as a C inhibitor in other conditions. This may be due the fact that its activity is specific for the classical pathway, so that immune complex clearance and opsonisation may not occur. Nonetheless, the use of C1-Inh highlights the potential of native C regulators as therapeutics.

1.8.4. Small molecule inhibitors

There are many examples of synthetic and naturally occurring molecules that have C inhibitory activity *in vitro*. For example, K-76COOH, a xenobiotic isolated from the fungus *Stachybotrys complementi*, inhibits the cleavage of C5 in *in vitro* studies [332]. In several C-mediated models of disease in guinea pigs and mice, K-76COOH inhibited disease development [333]. Rosmarinic acid, a polyphenolic phytochemical with antioxidant activity is extracted from the herb Rosemary. It covalently binds activated C3b in the forming convertase [334,335]. An extract of the Chinese medicinal herb, Ephedra, inhibited C in the activation and terminal pathways but the active component was not well characterised [336].

Nafamastat mesilate (FUT-175) is a synthetic molecule and protease inhibitor that was originally developed as an anticoagulant and inhibits proteases from many systems [337]. FUT-175 affects the C system at many levels, inhibiting C1r, C1s, fD and the C3/C5 convertase, but it also interferes with many other plasma protease systems [338,339]. In animal models, FUT-175 has been shown to be effective against C-mediated disease when administered singularly [340] and in combination with K-76COOH [341,342]. In human patients, FUT-175 is an effective treatment for glomerulonephritis [343,344]. However, as FUT-175 is such a powerful non-specific protease inhibitor, its use in humans is potentially harmful and so more specific and efficient C inhibitors, based upon FUT-175 are being generated [345].

1.8.5. The Development of Peptide Inhibitors

Initially, small peptides were identified as being able to inhibit C activity *in vitro*, such as the commonly used serine protease inhibitor, leupeptin [245]. Peptide inhibitors of C activation were also designed, which mimicked the sequence around the sites at which components are cleaved during activation. For example, peptides derived from the sequences of C3 around the site of cleavage by C2 and also the sequence of Factor B around the site of cleavage by Factor D were shown to be potent competitive inhibitors of activation *in vitro* [245]. However, the development of bacteriophage display technology has enabled the rapid identification and development of peptides with therapeutic potential.

The surface (coat) of a bacteriophage (phage) comprises various proteins that are gene products of the phage genome. In phage display technology this is exploited by fusing a sequence coding a peptide or protein to a gene encoding a coat protein, so that the peptide is expressed (displayed) with the coat protein on the phage surface [346]. The advantage of this technique is that the phenotype of a bacteriophage surface-displayed peptide is linked with the genotype encoding that peptide, packaged within the same phage particle (virion) [346,347]. This enables a high number of peptides to be rapidly screened and to identify peptides that bind any given protein without needing to know the sequence of the protein [348-350]. A library of 10^7-10^9 random peptides is quickly generated from inserted sequences through site-directed mutagenesis using degenerate oligodeoxynucleotides [351,352]. Phage-plasmid derivatives of F-pilus dependent filamentous (Ff) *Escherichia coli* (*E. coli*) phage such as fd or M13 are most frequently used for phage display because these are able to accommodate quite large insertions of cDNA segments relative to the size of the phage genome [353,354].

Phage display libraries have been used to identify possible therapeutic candidates in a diverse range of fields for example neutrophil elastase inhibitors [355,356], inhibitors of anti-FVIII antibodies [357], potential candidates for tumour vaccination [358] and C inhibitors [359-363]. DX-890 (previously known as EPI-HNE-4) was originally discovered using a phage display library that displayed protease inhibitory domains because it was created from wild-type bovine pancreatic trypsin inhibitor [355]. It is a specific and potent inhibitor of human neutrophil elastase (NE). NE degrades many of the components of the pulmonary extracellular matrix; it may be involved in the induction of inflammation and when present in excess, actively participates in the destruction of lung structures [356]. Excessive accumulation of NE occurs in the pulmonary fluid and tissues of patients suffering from cystic fibrosis (CF) [364-366]. In *in vitro* studies DX-890 inhibited the high levels of active NE present in 60% of sputum samples collected from children with CF and almost completely blocked (91%) the N-formyl-methionine-leucine-phenylalanine-induced migration of purified human neutrophils across a Matrigel basement membrane. *In vivo*, DX-890 protected rat lungs dose-dependently from haemorrhage, serum albumin leakage, residual active NE and discrete neutrophil influx in air spaces for up to 4 hours [356]. DX-890 is currently in phase II clinical trials for the treatment of CF [367].

Twenty-five percent of haemophilia A patients develop functionally inhibitory anti-FVIII antibodies following the therapeutic administration of FVIII. Phage display has been used to identify peptides that neutralise the activities of these anti-FVIII antibodies. *In vitro*, one of the identified peptides, peptide 107, inhibited the activity of the human anti-FVIII monoclonal antibody, Bo2C11 and restored normal haemostasis in a mouse model of haemophilia [357].

Tumour antigens have been identified using phage display in patients with colorectal cancer (CRC) [358]. This is a relatively new approach [368,369] and is a less time-consuming process than the current standard method that uses recombinant cDNA expression cloning (SEREX) [370]. It has been difficult to detect tumour specific antigens for solid tumour types of epithelial origin, in particular CRC [370]. These identified antigens may be potential candidates for tumour vaccination or may have a use as markers, either for diagnosis or prognosis [358].

Phage display has also been used to identify C inhibitory peptides including 'peptide 2J' and compstatin. Peptide 2J was originally discovered along with 41 other peptides to bind C1q [359]. Further characterisation demonstrated that peptide 2J was the only one to bind to the globular head of C1q with high affinity and specifically inhibit C1q haemolytic activity [360]. It is cross-reactive with primate and rodent C1q and its activity is dependent on its cyclical structure. These results suggest that peptide 2J has therapeutic potential.

Compstatin is a cyclic 13-mer peptide that was originally screened against C3b [361]. Subsequent experiments demonstrated that it binds C3, C3b and C3c, but not C3d, suggesting that it binds to the C3c region of C3. The binding of compstatin to C3 is reversible and it inhibits both the classical and alternative pathways of C activation. It is only cross-reactive with primate C3 and its activity is dependent on its cyclic conformation. Experiments to determine the mechanism of inhibition by compstatin indicated that it interacts with C3 to inhibit its cleavage. Compstatin inhibited the generation of C3a, soluble C5b-9 and leukocyte activation in *in vitro* models of CPB [362]. Similar results were observed in an *ex vivo* xenograft model, in which pig kidneys were perfused with fresh human blood. Compstatin inhibited the generation of C3 activation products and soluble C5b-9 in a statistically significant manner and xenograft survival was prolonged by compstatin [363]. These results demonstrate that the inhibition of C3 cleavage by compstatin stops additional C activation and inflammation and highlights its potential as a therapeutic agent. However, a major drawback of compstatin is its very short half-life, which means that it needs to be continuously infused in order to work. In addition, it is not cross-reactive with rodent C3, so that its therapeutic potential cannot be determined using the common rodent models of C-mediated disease. For these reasons, the likelihood of compstatin being further developed is limited, even though it is a potent inhibitor of C3 cleavage.

An added disadvantage of both compstatin and peptide 2J is that they both act at early stages in the C pathway. This eliminates the important opsonisation and pro-inflammatory effects mediated by cascade products. Potentially, this might increase the predisposition to bacterial infections and immune complex disease, especially if used as a long-term therapy [82].

1.8.6. The Modification of Native C Regulators

Native C regulators (CReg) allow the host to discern self from foreign cells and tissue [371]. By modifying these C inhibitors it may be possible to develop a potential therapy for use in conditions where C activation is unwanted.

1.8.6.1. First generation inhibitors

The therapeutic potential of soluble forms of membrane bound C regulators was first demonstrated when a soluble recombinant version of human CR1 (sCR1), consisting of the extracellular domain only was produced. This retained all the known functions of native CR1 *in vitro* i.e. it inhibited the formation of the C3 and C5 convertases, preventing C3b opsonisation, C5a generation and MAC formation [372,373]. In a rat model of ischemia/reperfusion injury, sCR1 reduced myocardial size by 44%, minimised the accumulation of neutrophils within the infarcted area and attenuated MAC deposition [372,373]. The protective effects of sCR1 have been confirmed in other animal models of ischemia/reperfusion injury [374-377].

Soluble CR1 was also used to treat rat models of human RA [378,379], as excessive C activation has been implicated in the pathogenesis of RA [253-259]. Rats treated with sCR1 prior to disease induction had a delayed onset of disease and their disease was less severe. This suggested that the activating pathways were important in the development of disease in these models. However, the treatment of rats with sCR1 following disease onset failed to inhibit disease progression. This indicated that either the C activating pathways play a less important role in disease progression once it is established or that the sCR1 was not retained at the inflammatory site for long enough to have a therapeutic effect. This latter hypothesis was supported by the observation that sCR1 had no inhibitory effect in the Antigen Induce Arthritis (AIA) model when administered systemically [378], as it was free to travel in the circulation, but it was inhibitory when administered locally [378].

Clinical trials have been conducted in humans using sCR1 to treat adult respiratory distress syndrome and the side-effects of CPB [380,381]. These studies established that sCR1 is safe, but its efficacy was poor in terms of treating disease. For these reasons, it was not developed further [251].

Soluble recombinant forms of the membrane-bound C regulators MCP and DAF have also been made. These are effective in blocking C activation *in vitro* as well as in animal models of C-mediated pathologies [382-384]. In contrast, a recombinant soluble form of CD59 proved to be a poor C inhibitor in serum; this is perhaps not surprising, as it inhibits MAC formation that is occurring within the cell membrane. *In vivo* it was cleared from the circulation by filtration in the kidney [385], probably due to its small size.

1.8.6.2. Second generation inhibitors

Various approaches have been taken to alter or improve the therapeutic efficacy of sCR1 *in vivo*. For example, sCR1[desLHR-A] lacks the seven amino-terminal SCR of full-length sCR1 and this confers alternative pathway specific inhibitory activity upon the molecule [386]. The advantages of such a molecule are clear; immune complex clearance and classical pathway activation are allowed to occur, whilst amplification of C3b formation is not. sCR1 has also been modified by adding sialyl Lewis^x (sLe^x) tetrasaccharide groups at Asn residues of sCR1, referred to as sCR1sLe^x. This enables the molecule to bind P-, E- and L-selectins, thus targeting it to sites of inflammation [387]. In addition, it inhibits selectin-dependent leukocyte adhesion at these sites, making it a potent anti-inflammatory agent [388]. In a stroke model, sCR1sLe^x had greater neuroprotective effects than unmodified sCR1 [389].

One of the most successful examples of modifying sCR1 is that of the drug APT070. This comprises the first three SCRs of CR1 [390] attached to a membrane-targeting anchor consisting of two sequentially-linked outer cell membrane ligands ('addressins') to tether it at the site of injection [391]. The therapeutic efficacy of APT070 was demonstrated in an experimental arthritis model, Antigen Induced Arthritis (AIA) [392]. Animals treated with APT070 had a significantly milder clinical and histological disease in comparison to untreated controls or animals treated with full-length sCR1 and this effect was dose-dependent. Moreover, APT070 was retained on cell surface membranes within the normal joint up to 48 hours post intra-articular injection. Similar beneficial effects were observed in a model of renal transplantation [393]. These data demonstrate that by modifying sCR1 so that it could be retained at the inflammatory site for longer, the therapeutic benefits of administering a soluble C regulator were far greater. A phase I clinical trial established that the administration of APT070 was tolerated by healthy volunteers [394]. A phase IIA trial is currently being conducted to determine the effects of intra-articular APT070 upon clinical and biochemical markers in RA patients [395].

APT070 satisfies many of the requirements for a C inhibitory drug – the sCR1 component is bacterially expressed and then the addressin is added chemically, making it 'relatively' cheap to produce. It is a small molecule, with a molecular weight of approximately 23 kDa, thereby minimising the potential for it to be immunogenic, and gets around the problem of being cleared rapidly from the site of administration due to the presence of the adressin tag. However, CR1 has a dual role in the C system, as a C regulator and receptor, and is not expressed on normal synoviocytes [396,397]. Although it seems to stop C activation, in disease, MAC is deposited on the surface of the synovium, implicating it in the development of pathology. Therefore, it may be more appropriate to modify CD59, to inhibit MAC formation. To this end, a similar membrane-targeting moiety has been attached to soluble CD59, improving its activity *in vitro* [398,399].

1.8.7. The potential of antibody-CReg hybrid molecules as therapeutics

This is a new area of research and so far, two types of antibody-CReg hybrids have been described. In the first type, the CReg is attached to the antibody Fab arms, which targets the molecule to a specific site. Zhang *et al* [400,401] made fusion proteins of either CD59 or DAF attached to anti-dansyl antibody fragments. When exposed to dansylated target cells, the CReg hybrid conferred protection against lysis by C. This needs to be tested further *in vivo*. In the second type, the CReg replaces the Fab arm, so that it is directly attached to the Fc portion of the antibody, giving the hybrid molecule a long half-life [402]. This has been done with the murine homologue of human CR1, C receptor-1-related gene/protein y (Crry) [403] and rat DAF and CD59 [404]. In all cases, when tested *in vivo*, these agents had a prolonged half-life and made effective therapeutics [404,405]. During the development of these molecules, Harris *et al* [404] noted that some of these fusion proteins were significantly less active than the free CReg, but that cleaving the CReg from the Fc with papain restored this activity. Therefore, by introducing cleavage sequences that are recognised by matrix metalloproteinases and/or aggrecanases between the Fc region and the CReg, the molecule can be targeted to become active at sites of inflammation where such enzymes are in abundance. This would create a drug with little or no systemic anti-C activity, that would become active only when required, but that would have a long half-life *in vivo* [398].

1.8.8. The development of monoclonal antibodies against C components

Another strategy to inhibit the progression of C-mediated disease has been to develop function-blocking monoclonal antibodies (mAbs) against C components. There are four advantages to this approach. Firstly, the mAbs raised are highly specific for the antigen of interest only. This will increase the efficacy of the drug. Secondly, mAbs have a high affinity for the antigen in comparison to other agents such as peptides and it is possible to select mAbs that block antigen activity. Thirdly, mAbs have a long half-life in the circulation – approximately four weeks. Lastly, a mAb can be 'humanised' – i.e. it can be manipulated to be more human-like, decreasing its antigenic potential. Numerous monoclonal antibodies have been licensed for clinical use and have been shown to be both safe and effective.

Rituximab™ was the first monoclonal antibody to be approved for clinical use as an anti-cancer therapy, specifically in treating indolent B-cell non-Hodgkin's lymphoma (NHL). It binds CD20, a transmembrane marker protein present on the surface of maturing B cells [406] and also present on the surface of most B-cell NHL [407]. Although CD20 is a pan-B cell marker, it was deemed an appropriate therapeutic target because it is expressed at high levels on the NHL cell surface, is not down-regulated after antibody binding and is not shed or secreted into the circulation, thereby increasing its efficacy as a therapeutic target [408]. Rituximab™ is a chimeric 'humanised' antibody comprising the anti-human

CD20-binding Fab regions of the original murine antibody and a human IgG1 Fc portion [408]. The reasons for making a chimeric antibody are threefold. Firstly, the patient develops human anti-mouse antibodies (HAMA) to murine antibodies when they are repeatedly administered [409-411]. The likelihood of this is greatly reduced if the murine IgG1 Fc portion is replaced with the human homologue [412-414]. The human Fc region binds the neonatal Fc receptor (FcRn) and recycles the antibody thereby prolonging its half-life in the circulation [415,416]. Finally, whilst the murine mAb binds the antigen, it is through the Fc region that the effector aspects of the molecule are exerted. The human Fc is more effective in activating these effectors in patients than a murine Fc region would be. As CD20 is a pan-B-cell marker, treatment with Rituximab™ leads to the depletion of both normal B cells and lymphoma cells, resulting in the clearance of normal B cells for approximately 6 months. Surprisingly, there is neither an increased risk of infection nor decrease in IgG levels in the patient [417]. Rituximab™ is believed to deplete B cells in three ways: firstly, by antibody dependent cell mediated cytotoxicity (ADCC), in which natural killer cells, macrophages, and monocytes are recruited through their Fcγ receptors, to bind the Fcγ portion of Rituximab™ which is bound to surface CD20, inducing CD20+ B cell lysis [418,419]. Secondly, through C dependent cytotoxicity induced when circulating C1q binds to Rituximab™ that is bound to surface CD20. The C cascade becomes activated, ending in MAC formation in the cell membrane causing CD20+ B cell lysis [406]. Thirdly, Rituximab™ promotes CD20+ B cell apoptosis [420]. It is also thought to sensitise lymphoma cells to the cytotoxic activity of chemotherapy [421,422]. Rituximab™ has been tested for use in other haematological malignancies with varying degrees of success [422]. Studies show that Rituximab™ is well tolerated by patients [422] and that most adverse events are infusion-related reactions, consisting mainly of fever and chills, in more than 50% patients. These usually occur within 30-120 minutes of the first infusion and are milder with subsequent infusions [423]. Fatal infusion reactions have occurred, although these are rare and risk factors identified include a high tumour burden and cardiopulmonary disease [424]. Patients have been monitored for the development of HAMA and human anti-chimeric antibodies (HACA) [422]. No HAMA responses were observed and 1.1% of patients were positive for HACA, demonstrating that the rationale of humanising therapeutic antibodies works and that repeated Rituximab™ exposure does not lead to the development of immune resisitance in the majority of patients.

The therapeutic potential of Rituximab™ is now being tested in other conditions in which the involvement of B-cells is implicated [425], including RA [424,426-430], idiopathic thrombocytopenic purpura [431], type II mixed cryoglobulinaemia [432], IgM antibody associated neuropathies [433] and SLE [434-436]. In RA patients, interim results are encouraging, with significant clinical improvement and only mild to moderate adverse events reported [424].

Campath-1H™ (Alemtuzumab) was licensed for clinical use in the treatment of patients with B-cell chronic lymphocytic leukaemia (CLL) who had not responded to other therapies in July 2001. It is a humanized monoclonal antibody raised against CD52, a GPI-anchored protein that is expressed on all mature lymphocytes, and in particularly high levels on malignant B lymphocytes [437], but is not expressed on haematopoietic stem cells [438]. The function of CD52 remains unknown, although signal transduction, via the T cell receptor has been induced in cross-linking studies [439]. Like Rituximab™, Campath-1H™ is thought to act on target cells and cause cell death by C activation [440], ADCC [441,442] and apoptosis [443]. Campath-1H™ has also been approved by the FDA to treat MS [444,445].
Mylotarg™ (Gemtuzumab Ozogamicin (GO)) was given conditional approval by the FDA in May 2000 for use as a single-agent therapy for first recurrence of CD33 positive AML in patients over 60 years old who were not considered suitable for treatment with cytotoxic chemotherapy [446]. Mylotarg™ is a chemotherapeutic agent comprising a humanised anti-CD33 antibody covalently linked to a derivative of a potent cytotoxic enediyne antibiotic, calicheamicin [447]. CD33 is a 67 kDa glycosylated transmembrane protein of unknown function, is expressed on most haematopoietic stem cells; on both mature and immature myeloid cells, and on erythroid, megakaryocytic, and multipotent progenitors [448]. CD33 is also found on leukaemic blasts from most AML and myelodysplastic syndrome (MDS) patients. CD33 was considered an attractive target for a mAb-based therapy in AML patients as it has little expression outside the hematopoietic system. Mylotarg™ is rapidly internalised into the target cell following binding to CD33 [449]. This is an attractive therapeutic approach, as the chemotherapeutic agent is specifically targeted to the malignant cell, rather than to many different cell types. Once Mylotarg™ binds to CD33, it is endocytosed [450] and cleaved inside lysosomes by acid hydrolysis, releasing calicheamicin. This is further processed making a reactive intermediate [451-454] that cleaves DNA phosphodiester bonds [455,456]. In vitro studies demonstrate that cell lines that are not resistant to the active agent are induced into G_2 arrest and this can be followed by apoptosis [457].
Many groups have focussed on generating mAbs that bind to C5 in such a way that is unable to be cleaved into its active components, C5a and C5b. Würzner *et al* [458] generated the anti-human C5 monoclonal antibody, N19/8. It was shown to bind human C5 and prevent its cleavage by either the classical or alternative pathway C5 convertases [438,439], thereby inhibiting the generation of C5a and soluble C5b-9 and blocking serum C haemolytic activity. It also inhibited C-mediated damage in an *ex vivo* model of xenotransplantation [459] and blocked both leukocyte and platelet activation in an *ex vivo* model of CPB [460]. Experiments using the N19/8 Fab fragments alone demonstrated that the C inhibitory properties of the intact antibody were retained, indicating that the observed properties of the antibody were dependent on the variable regions of N19/8 and not on the intact N19/8 antibody structure [461]. To improve the therapeutic properties of this mAb, the

N19/8 antibody was used to make a recombinant single chain antibody (scFv) directed against human C5. Single chain antibodies comprise the light and heavy variable chain regions of an antibody fused together to make a single tandem polypeptide. The binding specificity [462,463] and affinities [464,465] of the scFv molecule are often similar to that of the parent mAb, as the folded structure of an scFV is virtually identical to the variable region structure of the parental antibody [466]. The scFv molecule does not possess any effector functions, which is ideal for an anti-C therapy, but may still retain the ability to block the function of its target protein. scFv antibodies have greater therapeutic potential than intact mAbs as the possibility of the patient developing a HAMA response is significantly reduced, they quickly penetrate tissues [467] and can be rapidly produced in large quantities using E.coli [464,465]. Although the scFv N19/8 antibody bound human C5 with a high affinity and was as potent as N19/8 at reducing MAC formation, its ability to inhibit C5a generation was not significantly reduced, suggesting that it bound to the C5b region of intact C5 [468]. Like the intact mAb, the N19/8 scFv provided protection against C-mediated damage in an *ex vivo* model of xenotransplantation [468]. The discrepancy between the activities of the original antibody and the scFv variant might be due to steric hindrance as the original mAb was much larger than the scFv variant and may have inhibited C5a generation due to its size. However, the N19/8 scFv antibody was not developed further.

A more successful example of making scFv antibodies is that of mAb 5G1.1, an antibody that also recognises human C5 and inhibits cleavage of C5, thereby preventing the generation of the pro-inflammatory products, C5a and MAC. mAb 5G1.1 was humanised and scFv molecules were also produced by grafting the complementarity determining regions of 5G1.1 onto human framework regions [469]. Further investigations demonstrated that the intact humanised h5G1.1 antibody had identical inhibitory activity to the original murine monoclonal antibody in C lysis assays. In addition, humanised Fab and scFv molecules blocked C-mediated haemolysis and the humanised h5G1.1 scFv was also able to block C5a generation [469].

As the humanised h5G1.1 scFv (from now on referred to as h5G1.1-scFv) inhibits C5a generation and C-mediated lysis, its activity was tested in Phase I and II clinical trials to determine whether h5G1.1-scFv could prevent C activation occurring as a result of CPB [470]. This demonstrated that at the highest dose administered, h5G1.1-scFv was able to inhibit C haemolytic activity for up to 14 hours. There was a 40% reduction in myocardial injury, as measured by creatine kinase-MB release and there was a reduction in new cognitive deficits post CPB. At the two highest doses administered, leukocyte activation, as measured by surface expression of CD11b was reduced and also, there was a reduction in post-operative blood loss. Moreover, the generation of SC5b-9 was inhibited in a dose-dependent manner. A phase III clinical trial is underway and phase II

trials for the treatment of acute myocardial infarction are also being conducted [471]. H5G1.1-scFv is now designated the name Pexelizumab™ and the developers, Alexion, were granted Fast Track status for Pexelizumab™ by the US FDA [471]. The humanised mAb 5G1.1 is known as Eculizumab™ and was recently used in a pilot study to treat patients suffering from paroxysmal nocturnal hemoglobinuria (PNH) [472]. Patients suffering from this condition make blood cells without GPI-linked proteins on the cell surface, including DAF and CD59, rendering them susceptible to lysis by the C system. Treatment with Eculizumab™ was safe and well tolerated and reduced the incidence of intravascular haemolysis and haemoglobinuria. Patients required fewer blood transfusions and their quality of life improved. The FDA granted Eculizumab™ orphan drug status for the treatment of idiopathic membranous nephritis in May 2001 and for the treatment of PNH in August 2003.

Phage display technology can also be used to develop human mAbs [473]. Antibody proteins are produced on the phage coat of phagemid vectors instead of random peptides. Phage antibody libraries are made by cloning variable regions of human antibody genes, derived from naïve, immunized or synthetic antibody repertoires, into the phage coat-protein genes of phagemid vectors. Libraries containing greater than 10^{11} different variants have been constructed [474]. Antibody variable regions can then be selected for by biopanning against the target molecule in exactly the same way as random peptides are. The gene of an antibody variable region of interest can subsequently be made into a single chain recombinant antibody by grafting it onto human antibody constant regions [475]. Cambridge Antibody Technology together with Abbott developed an anti-TNF-α antibody using this technology. HUMIRA™ was the first human mAb produced in this way to be licensed by the FDA for the treatment of RA in December 2002. Clinical trials showed that it was safe and well tolerated at the doses used [476]. HUMIRA™ is also being tested in phase II clinical trials for the treatment of juvenile RA and Crohn's disease.

Another way of reducing the potential for HAMA responses is to create transgenic mice that are able to make human antibodies [444,445]. The mice are engineered to suppress their own antibody production and regions of the human antibody heavy and light chain loci are then transferred into these animals. The human antibody genes are functional in the context of the mouse machinery for antibody recombination and expression. Following immunisation protocols, the B cells secreting human antibodies can be collected from these mice and used to generate human monoclonal hybridoma cell lines. Two antibody-based drugs are currently in phase II trials developed using this technology. One is HuMAX-CD4, an anti-CD4 antibody being used to treat psoriasis, developed by Genmab and EISAI. The other developed by Genmab and Medarex is

HuMax-IL15, an anti-IL-15 antibody being used to treat RA and psoriasis. To date, no significant allergic reactions have been observed [475].

1.9. Aims and Objectives: The generation of agents that inhibit MAC formation

Although great advances have been made in the development of agents that block C activation, much of the damage caused by unregulated C activation is mediated by MAC formation. Therefore, it makes sense to develop inhibitors of MAC formation that do not interfere with the early C activating pathways so that immune complex opsonisation, clearance and chemoattraction of inflammatory cells to sites of injury or infection are able to occur in an appropriate manner. Thus, the aim of this project is to develop agents capable of specifically inhibiting MAC formation. We have chosen to generate reagents that act on C6, a central component of the terminal pathway that forms an integral part of the C5b-8 complex, which binds multiple molecules of C9, to form the MAC. No other roles for C6 have been described and it therefore provides an ideal and highly specific means of preventing MAC formation.
Two approaches will be used to produce reagents that bind C6 and inhibit its activity in MAC formation. One will be to generate anti-C6 function blocking cross-species reactive mAbs and the other will be to identify peptide sequences that functionally block C6 activity. In the first instance, mAbs will be raised against rat, mouse and human C6 in strains of spontaneously C6 deficient rats and mice. These will be characterised for their C6 inhibitory activity and also for their activity against other species of C6. The desired mAb will have an IgG isotype and functionally block human C6 activity and additionally mouse C6 or rat C6 activity, making it possible to evaluate the efficacies of these mAbs as therapies in *in vivo* models of C-mediated disease. For the second approach, bacteriophage display technology (phage display) will be used. A complex library of phage-peptides expressing 7-mer peptide sequences will be 'panned' against purified human C6. Those that bind C6 will be selected and their functional blocking activity for C6 determined. Phage-peptides with the greatest C6 inhibitory activity will be sequenced. The peptide will be characterised for its ability to bind C6 and block its functional activity *in vitro* and *in vivo*.
Arresting the C cascade at an earlier stage may not be the most clinically useful point to prevent TCC formation because both activation pathways as well as cleavage of C5 by injured tissue-released enzymes [477] or C5 activation by oxygen radicals [478] would have to be blocked. Arresting the C cascade at a later stage, as shown with anti-C8 mAbs [479,480], will neither inhibit membrane insertion of the terminal complement complex nor C5a liberation.

Although C8, S-protein, SP40 and CD59 are all involved in regulating C5b-9 formation, they do not make good therapeutic candidates. Therefore, various groups have sought to inhibit C5b-9 formation by generating antibodies against components of the C5b-9 complex that block its formation. The biological functions of the TCC are controlled by C8 [481].

Chapter 2: Materials and Methods

Materials

All chemicals, except where stated, were obtained from either Fisher Scientific UK (Loughborough, Leicestershire, UK) or Sigma (Poole, Dorset, UK) and were of analytical grade.

Methods

2.1. General Protein Techniques

Table 2.1 General Antibodies Used

Name	Conjugate	Used in	Company	Catalogue Number
Goat anti-mouse IgG (heavy and light chain)	Horseradish peroxidase (HRPO)	ELISA, Western	Bio-Rad, Hercules, California, USA	172-1011
Goat anti-mouse IgG Fcγ fragment specific	HRPO	ELISA	Jackson ImmunoResearch Laboratories, West Grove, Pennsylvania, USA	115-035-008
Rabbit anti-rat IgG	HRPO	ELISA	Sigma, Poole, Dorset, UK	
Mouse anti-rat IgG1, Clone RG11/39.4	Biotin	ELISA	BD Biosciences Pharmingen, San Diego, California, USA	553890
Mouse anti-rat IgG2a, Clone RG7/1.3	Biotin	ELISA	BD Biosciences Pharmingen	553894
Mouse anti-rat IgG2b, Clone RG7/11.1	Biotin	ELISA	BD Biosciences Pharmingen	553898
ExtrAvidin	HRPO	Dot Blot, Wesetrn	Sigma, Poole, Dorset, UK	E2886
Goat anti-mouse IgM (μ-chain specific)	HRPO	Dot Blot, Western	Sigma, Poole, Dorset, UK	A8786

2.1.1. Dialysis of proteins to exchange buffers

Dialysis tubing (Medicell International Ltd., London, UK) with a 12-14 kDa molecular weight cut off was boiled in deionised water for 5 minutes. The tubing was then tied securely at one end and about half-filled with the protein-containing solution to be dialysed. Air was expelled from the tubing that was then tied at the other end. The tubing was placed in an appropriately sized beaker containing the buffer (dialysis buffer) to be exchanged and stirred overnight at 4°C. To ensure full buffer exchange, dialysis was against 1000-fold the sample volume of dialysis buffer. The dialysis buffer was changed during dialysis in order to achieve this as necessary.

2.1.2. Concentrating proteins using ultrafiltration

Proteins were concentrated using the Amicon stirred cell 8000 series protein concentration system (Millipore, Bedford, Massachusetts, USA). Filter discs of appropriate cut-off size (either 30 kDa or 100 kDa) were soaked in deionised water for 5 minutes and then assembled into the apparatus. The protein containing solution was placed in the apparatus and concentrated under pressure. This forced the fluid through the filter membrane while proteins of molecular mass greater than the cut-off were retained and concentrated. The filter discs were stored in PBS containing 0.1% NaN_3 and reused for the same proteins only.

2.1.3. Coomassie Assay

This assay was primarily used in a semi-quantitative manner to detect the presence of protein. Fifty microlitres of Coomassie Protein Assay Reagent (Ready-to-use Coomassie Blue G-250 based reagent; Pierce, Rockford, Illinois, USA) was added to 50 µl sample in a 96-well plate. The Coomassie reagent changed colour from brown to blue in the presence of protein. The intensity of the colour change was directly proportional to the amount of protein present. When the concentration of protein in the sample was being determined, a standard curve was generated (1 – 20 µg/ml) using stock bovine serum albumin (BSA) solution diluted in the same diluent as the test samples were in. The absorbance of the wells was determined at 595 nm on a BioRad Microplate Reader (Model 3550-UV). A standard curve was plotted and the concentrations of the test samples calculated. The test sample was diluted to obtain values on the standard curve and the concentration of protein in the original sample calculated.

2.1.4. Micro BCA Protein Assay

This assay was used to accurately determine the protein concentration of a sample. The assay was supplied as a kit and the manufacturer's protocol was followed. The BCA reagent was made up by mixing 50 parts Reagent MA, 48 parts Reagent MB together with 2 parts Reagent MC. This was stable for one day at room temperature. A set of protein standards (1 – 20 µg/ml) was prepared by diluting the stock BSA solution provided in the same diluent as the test samples were in. One hundred microlitre aliquots of each standard, blank (diluent only) or test sample were pipetted into the appropriate microtitre plate wells and 100 µl of BCA reagent was added to each well. The plate was covered, the samples mixed on a plate shaker for 30 seconds, and then incubated for 2 hours at 37°C. The absorbance of the wells was measured at 570 nm on a Bio-

Rad Microplate Reader. A standard curve was plotted and the concentrations of the test samples calculated. The sample was diluted to obtain values on the standard curve and the concentration of protein in the original sample calculated.

2.1.5. Determination of protein concentration by measuring A_{280}

The approximate concentration of purified protein samples was determined by measuring the absorbance of the solution at 280 nm (A_{280}) in a UV spectrophotometer (GeneQuant II, GE Healthcare). A blank reading was taken as a reference using the buffer that the sample was diluted in. The solution was then placed in the same quartz cuvette and the absorbance measured. If the sample absorbance was greater than 2.0 then the sample was diluted in the same buffer and the A_{280} measured again. The protein concentration of the sample was calculated according to Beer-Lambert's Law:

Protein Concentration (mg/ml) = ((A_{280} x dilution factor)/ protein extinction coefficient).

2.1.6. Biotin conjugation of antibodies

The antibody was taken into 0.1 M carbonate buffer (0.1 M sodium hydrogen carbonate, 0.1M sodium carbonate, pH 8.4) by dialysis overnight at 4°C. The protein concentration was adjusted to 1 mg/ml. One hundred and twenty microlitres of N-hydroxysuccinimidobiotin (Sigma H-1759) freshly dissolved in dimethylsulphoxide (DMSO) (1 mg/ml) per milligram of antibody to be biotinylated was added to the antibody and mixed. The mixture was incubated for 4 hours at room temperature. Unbound biotin was removed by dialysis of the mixture into phosphate buffered saline (PBS) (8.1 mM Na_2HPO_4, 1.5 mM KH_2PO_4, 137 mM NaCl, pH7.4) overnight. To determine whether biotinylation had been successful, the biotinylated antibody was tested in a dot blot.

2.1.7. Dot Blotting

Buffer	Composition
Blocking buffer	5% non-fat milk/0.1% Tween-20/PBS
Washing buffer	0.1% Tween-20/PBS

To test the successful biotinylation of an antibody, doubling dilutions of the antibody were made and 1 µl aliquots of each of these dilutions were spotted onto nitrocellulose and allowed to dry in

a 37°C oven. The nitrocellulose was blocked with blocking buffer for 30 minutes, washed once for 5 minutes with washing buffer and incubated for 1 hour at room temperature on a roller with HRPO-ExtrAvidin, diluted 1 in 1000 in washing buffer. The blot was washed five times by incubating in washing buffer for five minutes each and developed by incubation in SuperSignal® West Pico Chemiluminescent Substrate (Catalogue number 34080, Pierce, Rockford, Illinois, USA). This is a kit, comprising two solutions: SuperSignal® West Pico Luminol/Enhancer Solution and SuperSignal® West Pico Stable Peroxide Solution. Immediately prior to developing the blot, 1ml of the luminol/enhancer solution was mixed with 1ml of the stable peroxide solution, to make ECL substrate. The blot was then allowed to develop in this mixture for 1 minute. Excess moisture was removed, and the blot was placed in a plastic bag and exposed to autoradiograph X-OMAT UV film (Kodak, Rochester, New York, USA). The exposed film was developed in a Compact X2 developer (X-Ograph Ltd.).

Dot blotting was also used to detect a specific protein within a heterogeneous solution, for example, to screen fractions during protein purification. This was done in the same way as described above, except that after blocking and washing, the blot was incubated in antibody to the protein of interest (primary antibody) diluted in washing buffer for 1 hour at room temperature. After washing as described, HRPO-conjugated anti-immunoglobulins (raised against the species of animal the primary antibody was raised in)(secondary antibody), diluted in washing buffer, was incubated with the blot for 1 hour at room temperature, washed and developed as above.

2.1.8. Sodium Dodecyl Sulphate-Polyacrylamide Gel Electrophoresis (SDS-PAGE)

SDS – polyacrylamide gel electrophoresis (SDS-PAGE) was used to detect proteins of interest according to modifications of the method of Laemmli [482]. The BioRad Mini Protean II or Hoefer Mighty Small gel running apparatus were used. A 4% (v/v) acrylamide stacking gel was poured on top of a 7.5% acrylamide resolving gel to make discontinuous gels.

The following recipes were sufficient for four 0.75 mm thick gels:

	4% Stacking gel (ml)	7.5% Resolving gel (ml)
Stacking buffer (0.5 M Tris, 0.4% SDS, pH 6.8)	1.2	-
Resolving buffer (1.5 M Tris, 0.4% SDS, pH 8.8)	-	3.75
40% acrylamide	0.506	2.8
Deionised water (dH_2O)	3.2	8.2
10% ammonium persulphate	.05	.15
TEMED	.005	.015

Buffers	Composition
Non-reducing loading buffer	0.1 M Tris, 10% glycerol, 2% SDS, bromophenol blue, pH 6.8
Reducing loading buffer	Non-reducing loading buffer + 0.625% β-mercaptoethanol
Running buffer	25mM Tris, 191 mM glycine, 1% SDS

Proteins were prepared for loading by dilution 2:1 in either non-reducing loading buffer or reducing loading buffer and boiled for 5 minutes before loading. If complex mixtures of proteins such as serum were being run, then the incubation was for 30 minutes at room temperature, as the samples precipitated if boiled. Molecular weight markers were loaded onto each gel for accurate determination of protein size. Markers used included Gibco, SeeBlue +2, NBL markers and BioRad broad range markers. The gels were run in running buffer at 200 V for approximately 45 minutes, until the dye-front had reached the bottom of the gel. Electrophoresed proteins were then visualised by staining the gel with Coomassie Brilliant Blue R250, silver stain or subject to western blot.

2.1.9. Coomassie Blue Staining of Electrophoresed Gels

The detection limit of this technique was 2 µg of protein in a band on an SDS gel.

Solution	Composition
Coomassie Blue stain	0.2% w/v Coomassie Brilliant Blue R250 in 45% v/v methanol, 10 % v/v acetic acid in dH_2O
Destain solution	45% v/v methanol, 10% v/v acetic acid in dH_2O
Gel drying buffer	4% v/v glycerol, 20% v/v methanol in dH_20

Following electrophoresis, the gels were immediately immersed in Coomassie Blue stain for between 1 hour to overnight on a rocker-table at room temperature. When the gels were stained, the staining buffer was removed; the gels rinsed in dH_2O and placed in destain solution until the protein bands were clearly visible and the background reduced. Following the transfer of proteins from gels to nitrocellulose (section 2.1.12), these gels were also stained and destained, to confirm the transfer had been successful.

For a permanent record, the stained gels were equilibrated for 5 minutes in gel drying buffer and sandwiched between two sheets of acetate gel drying film (Promega) pre-soaked in gel drying buffer and stretched within a gel drying frame overnight at room temperature.

2.1.10. Silver Staining of Electrophoresed Gels

The detection limit of this technique was 200 ng (0.2 µg) of protein in a band on an SDS gel [483]. The following incubation steps were for 20 minutes (unless stated) and were performed on a rocker-table at room temperature.

Solution	Composition
Silver stain solution 1	50% v/v methanol, 10% v/v acetic acid in dH_2O
Silver stain solution 2	5% v/v methanol, 7% v/v acetic acid in dH_2O
Glutaraldehyde solution	5% v/v glutaraldehyde in dH_2O
Oxidising solution	5 µg/ml DTT(dithiothretol) in dH_2O
Silver stain	0.1% w/v $AgNO_3$ in dH_2O
Developing solution	0.002% v/v formaldehyde, 3% w/v Na_2CO_3 in dH_2O

Following electrophoresis, the gels were sequentially incubated in silver stain solution 1, silver stain solution 2, briefly rinsed with dH_2O and incubated in glutaraldehyde solution. The gels were washed three times in dH_2O, for 15 minutes each and then incubated in oxidising solution, rinsed with dH_2O, incubated in silver stain; rinsed with dH_2O, then with 3% (w/v) Na_2CO_3 in dH_2O and developed in developing solution. When the protein bands had developed sufficiently, the reaction was stopped by the addition of citric acid (1 g per 50 ml developing solution used). For a permanent record, the stained gels were equilibrated for 5 minutes in gel drying buffer and dried as described in section 2.1.9.

2.1.11. Western Blotting

Western blot analysis was used to identify specific proteins from complex mixtures and to characterise mAbs.

Buffer	Composition
Transfer buffer	25 mM Tris, 191 mM glycine, 20% v/v methanol in dH_2O
Blocking buffer	5% w/v non-fat dried milk/0.1% Tween-20/PBS
Wash buffer	0.1% v/v Tween-20/PBS

Following SDS-PAGE, the gel was immediately equilibrated in transfer buffer for 10 minutes. The gel was placed on a sheet of nitrocellulose and further sandwiched between two sheets of filter paper, all of which had been pre-soaked in transfer buffer. The blotting apparatus was assembled according to the manufacturer's instructions with the gel to the anode side and the nitrocellulose to the cathode. The proteins were then transferred onto the nitrocellulose at 100 V for 1 hour at room temperature, in a tank filled with cooled transfer buffer. After this, the nitrocellulose blots were blocked for 1 hour in blocking buffer at room temperature with constant

mixing. The blots were rinsed with wash buffer and incubated with antibody raised against the antigen of interest (primary antibody), typically diluted to 1 µg/ml in wash buffer on a roller and incubated for 1 hour at room temperature or overnight at 4°C with constant mixing. The blots were washed in wash buffer five times for five minutes each at room temperature with constant mixing. Secondary antibody or HRPO-conjugated Extravidin (if the primary antibody was biotinylated), diluted 1/1000 –1/10,000 (depending on the agent) in wash buffer was incubated with the blots for 1 hour at room temperature with constant mixing. The blots were washed five times as described. The blots were developed and exposed in the same way as described in section 2.1.7.

2.1.12. ELISAs

Various ELISAs, developed in house, were used in the course of this work. All incubations were for 1 hour at 37°C, all wash steps comprised three washes (200 µl per well) with wash buffer. All dilutions were in blocking buffer (50 µl per well), except where stated. The buffer recipes are detailed below.

Buffer	Composition
ELISA coating buffer	0.1 M $NaHCO_3/Na_2CO_3$, pH9.6
Wash buffer	0.1% (v/v) Tween-20/PBS
Blocking buffer	1% (w/v) BSA/0.1% (v/v) Tween-20/PBS
ELISA developing solution	4 orthophenylenediamine (OPD) tablets (Dako) dissolved in 12 ml dH_20 plus 5 µl of 30% H_2O_2.
Quenching solution	10 % (v/v) H_2SO_4 in dH_2O.

2.1.12.1. Screening for anti-C6 mAbs by ELISA

Serum from immunised mice or supernatant from individual fusion wells were screened by an ELISA adapted for the purpose [484]. Ninety-six-well microtitre plates were coated with 1 µg/ml human C6 (Quidel Corporation, San Diego, USA – or purified in house) (50 µl per well) in ELISA coating buffer. After washing, the plates were blocked with blocking buffer (200 µl per well). The blocking agent was removed, the plates washed and 50 µl of test sample was added to each well. A control antibody against human C6 was included to demonstrate the assay was working correctly (WU 6.4, a gift from Professor Reinhardt Würzner, University of Innsbruck, Austria). After washing, peroxidase conjugated anti-mouse IgG (H & L chains) immunoglobulin or peroxidase conjugated anti-mouse IgG Fc_γ immunoglobulin was placed in each well, or for the rat anti-rat C6 hybridomas, HRPO-conjugated anti-rat immunoglobulin antibody was used. The plate was washed as described and the assay developed with ELISA developing solution (50 µl per

well). Colour development was stopped with quenching solution (50 µl per well) when the positive control had developed sufficiently so that it was highly positive and the negative control had not developed. Typically, this was within 5 minutes, but could be incubated for up to 1 hour. The absorbance of each well was measured at 490 nm. Cells from wells with the greatest colour development were taken forward.

2.1.12.2. Rat mAb Isotype ELISA

Ninety-six well microtitre plates were coated with 100 µl of hybridoma supernatant to be tested. After washing, the plates were blocked with 150 µl blocking buffer per well. The blocking agent was removed, the plate washed three times with washing buffer and 100 µl of biotinylated anti-rat isotype specific secondary antibodies (Table 2.1) were added in duplicate to individual wells at a concentration of 1 µg/ml. The plates were washed, 100 µl HRPO-Extravidin was added to each well and incubated at 37°C for 1 hour. After washing, the plate was developed with the addition of 100 µl per wll of developing solution for up to 1 hour. Colour development was stopped by adding 50 µl of quenching solution to each well and the absorbance of each well was measured at 490 nm.

2.1.13. Isotyping of Mouse mAbs

Mouse mAbs were isotyped using the IsoStrip mouse monoclonal antibody isotyping kit, according to manufacturer's protocols (Catalogue number 1 493 027; Boehringer-Mannheim, Roche Applied Science, Indianapolis, USA). This kit comprises a development tube containing lyophilised latex beads conjugated to anti-mouse light chain antibodies, and an isotyping strip (IsoStrip). The IsoStrip bears immobilised bands of goat anti-mouse antibodies corresponding to the mouse antibody isotypes IgG_1, IgG_{2a}, IgG_{2b}, IgG_3, IgM and IgA heavy chains and to the kappa and lambda light chains. Both sides of the strip also bear a positive control band, which indicates that the antibody-coated beads have travelled up the strip. When the latex beads are resuspended in the tissue culture medium being tested and an Isostrip is placed in the mixture, the latex beads move up the strip by capillary flow. The complex continues to flow up the strip until it binds the band of immobilised goat anti-mouse antibody specific for the monoclonal's isotype and also the band of immobilised antibody specfic for the monoclonal's light chain. This is visualised by the appearance of a blue band corresponding to the monoclonal's heavy and light isotype.

To do the test, conditioned medium was collected from the antibody-secreting clones and diluted 1 in 10 with PBS. One hundred and fifty microlitres of this freshly diluted sample was added to

each development tube and incubated for 30 seconds at room temperature. Each development tube was vortexed for 5 seconds to ensure the latex beads were completely resuspended. An IsoStrip was then added to each tube and allowed to soak up the liquid for between 5 and 10 minutes. Development of the strip was complete when the positive control band on each side of the strip turned blue, which is between 5 and 10 minutes. After this time, the IsoStrips were examined and the antibody isotype interpreted. For a permanent record, the IsoStrips were dried.

2.1.14. Purification of Immunoglobulins

2.1.14.1. Partial purification of rabbit immunoglobulins

Solid polyethylene glycol (PEG)-6000 (15% (w/v)) was added to rabbit serum and stirred for 30 minutes at 4°C. The Ig were precipitated by centrifugation at 12, 000 g for 30 minutes at 4°C and resuspended in PBS, quantified by BCA assay and stored at -20°C.

2.1.14.2. Purification of Mouse IgM

Salt precipitation and ion exchange chromatography was used to purify mouse IgM isotype mAbs. To antibody-containing tissue culture supernatant, ammonium sulphate was added to 45% saturation, stirred continuously for 30 minutes at 4˚C and centrifuged at 24000 *g* for 20 minutes. The supernatant was discarded and the pellet resuspended in 0.02 M K_2HPO_4/0.02 M KH_2PO_4, pH 6.5 (start buffer) and dialysed against start buffer overnight at 4˚C. The IgM enriched sample was applied to a Source 15Q column (Pharmacia), which had been equilibrated in start buffer. The column was washed through with two column volumes of start buffer to remove unbound proteins. A linear gradient of elution buffer (0.02 M K_2HPO_4/0.02 M KH_2PO_4, 0.5 M NaCl, pH6.5) was applied to the column to elute the IgM antibody and collected in 5 ml fractions. IgM containing fractions were identified by dot blot (section 2.1.8) using a HRPO-conjugated anti-murine IgM antibody and pooled. Purity of the pooled fractions was determined using SDS-PAGE and Western blot; concentration of the purified antibody was assessed using the Micro BCA assay (section 2.1.5).

2.1.14.3. Purification of IgG Isotype mAbs using a Prosep A column

Prosep®-A 'High Capacity' (Bioprocessing, Consett, UK) comprises Staphylococcal Protein A coupled to a porous glass bead matrix. Protein-A binds to subclasses of immunoglobulin (Ig) G from various animal species and with a particularly high capacity to those of murine, bovine, guinea pig, human and rabbit origin. A pre-column of Sepharose-4B (GE Healthcare) was used

to remove any protein that bound non-specifically to the sepharose. The pre-column and Prosep-A column were prepared by being washed out of their storage solutions separately with 200 ml PBS each. All solutions were passed over these columns under gravity. The washing and elution conditions for IgG_1 isotype antibodies were altered to reduce contamination with bovine Ig. It was not possible to do this for other IgG isotype antibodies.

For all IgG isotype antibodies, the antibody-containing supernatant was passed sequentially over the pre-column and Prosep A column and the flow through collected. The column was washed with up to 500 ml PBS, until no more protein was detected using Coomassie protein assay reagent. Bound antibody was then eluted with 0.1 M glycine - HCl, pH 2.5 in 5 ml fractions into tubes containing 500 µl 1M Tris pH 7.0 to neutralise the sample. The protein content of the fractions was monitored either using the Coomassie protein assay reagent or by measuring the A_{280nm}. Protein-containing fractions were pooled, dialysed against PBS overnight at 4°C and concentrated by ultrafiltration. The prosep A column was washed with PBS. To maximise yield, the flow through was again passed over the column and any bound antibody eluted, pooled, dialysed and concentrated as described above. The protein concentration of purified antibody was determined either by measuring the A_{280} (section 2.1.6) or using the Micro BCA assay (section 2.1.5). The extinction coefficient of IgG antibodies is 1.4. The purity of the antibody was assessed by SDS-PAGE. The column was cleaned with 10% w/v HCl, pH 1.5 and stored in 0.1% v/v NaN_3/PBS.

IgG_1 isotype antibody-containing supernatant was premixed in equal ratios with wash buffer (3 M NaCl, 1.5 M glycine, pH 8.9), passed over both columns in sequence and the run-through collected. The Prosep A column was washed with up to 500 ml of wash buffer until no more protein was detected in the eluate, using the Coomassie protein assay (section 2.1.4). Bound antibody was eluted with elution buffer (0.1 M citrate buffer (0.1 M sodium citrate; 0.1 M citric acid), pH 5.2) in 5 ml fractions over 24 fractions. The A_{280} of the fractions were measured to determine their protein content, as citrate interferes with the Coomassie protein assay reagent so this could not be used. The protein-containing fractions were pooled, dialysed, concentrated, quantified and sample purity assessed as described earlier in this section. The column was washed with wash buffer and to maximise the yield of mAb, the run through was re-applied to the column. Any bound antibody was eluted, pooled, dialysed, concentrated, quantified and purity assessed as described above. The column was cleaned with 10% w/v HCl, pH1.5 and stored in 0.1% NaN_3/PBS.

2.2. Animals

All animals used were adults and obtained from breeding colonies in the Biomedical Services Unit, at the University of Wales College of Medicine (UWCM), Cardiff. To generate monoclonal antibodies, PVG C6 deficient rats [485] and C6 deficient Peru-Coppock mice, bred onto a C3H background were used. To generate polyclonal antibodies, C6 deficient rabbits [486] were used. These deficiencies had arisen spontaneously. Balb/c mice were used as a source of macrophages.

2.2.1. Serum Preparation

Collected blood was allowed to coagulate in a glass collection tube at room temperature for 30 minutes, or at 4°C for blood collected from rabbits. The clotted blood was then centrifuged at 2000 rpm for 10 minutes. The serum fraction was removed, aliquoted and stored at -70°C.

2.2.2. Preparation of mouse peritoneal macrophages

Balb/c mice were sacrificed using a Schedule 1 method and washed with 70% ethanol. Ten ml ice-cold RPMI medium was injected into the peritoneal cavity using a 21 gauge needle. The mouse abdomen was gently massaged and the medium containing resident macrophages then slowly withdrawn. The macrophages were pelleted by centrifugation at 2000 rpm, for 10 minutes. Finally, the cells were resuspended in the appropriate culture medium for addition to hybridoma cultures. Typically, the peritoneal washout of one mouse would yield enough macrophages for 50 ml medium.

2.2.3. Polyclonal antibody production

A C6 deficient rabbit [486] was immunised subcutaneously (s.c) with normal rabbit serum diluted in PBS, emulsified with Complete Freund's adjuvant (CFA)(1.5 ml mannide monooleate, 8.5 ml paraffin oil, 5 mg *Mycobacterium butyricum* per 10 ml ampule, Difco). Two and four weeks after the first immunisation, boosts of C6 sufficient rabbit serum diluted in PBS and emulsified with Incomplete Freund's adjuvant (IFA)(1.5 ml mannide monooleate, 8.5 ml paraffin oil per 10 ml ampule, Difco) were administered, s.c. A test bleed was taken, serum prepared and tested for anti-C6 antibody titre by ELISA. When a high titre was achieved, the rabbit was exsanguinated under terminal anaesthesia. The collected blood was allowed to clot and the serum was separated from the clot by centrifugation at 2500 rpm at 4°C. The antiserum was aliquoted and stored at –70°C.

2.3. Tissue Culture

All tissue culture reagents, except where stated, were from Gibco, Invitrogen Corporation (Paisley, UK). Tissue culture was performed under sterile conditions using sterile tissue culture plates and flasks (Nunc). Cells were maintained in a 5% CO_2 in a humidified chamber at 37°C. Medium was pre-warmed to 37°C prior to administering to cells, except where stated.

2.3.1. Tissue culture cells and media

Mouse myeloma cell lines:	Ag14-SP2/0 NSO
Basic medium	RPMI 1640 Medium, supplemented with 50 U/ml penicillin/ 50 μg/ml streptomycin, 1 μg/ml amphotericin B, 2 mM L-glutamine and 1 mM sodium pyruvate.
F-5 medium	Basic medium supplemented with 5% v/v foetal calf serum (FCS).
F-10 medium	Basic medium supplemented with 10% v/v FCS.
F-15 Medium	Basic medium supplemented with 15% v/v FCS.
HAT medium	F-15 medium supplemented with 0.1 mM hypoxanthine, 0.4 μM aminopterin and 16 μM thymidine.
HT medium	F-15 medium supplemented with 0.1 mM hypoxanthine and 16 μM thymidine.
PEG-1500	50% w/v Polyethylene glycol 1500 in 75 mM HEPES, pH 8.0, Roche.
Freezing medium	10% v/v DMSO (Sigma) in FCS.

2.3.2. Freezing cells

Stocks of antibody secreting cells and myeloma cell lines were stored frozen in liquid nitrogen. Hybridoma and myeloma cells are weakly adherent to tissue culture flasks and therefore did not require trypsinisation before subcloning. Cells were detached from the surface on which they were growing by agitation. The suspended cells were pelleted by centrifugation at 1200 rpm for 5 minutes. The pellet from one 80 cm^2 flask was resuspended in 1 ml freezing medium and placed in cryovials (Greiner) [in aliquots of 1 x 10^6 cells in 1 ml in cryovials]. The cells were then slowly frozen in a Cryo 1° Freezing Container (Nalgene), which is designed to decrease in temperature by 1°C per minute when placed in a -70°C freezer. After approximately 24 hours, the frozen cells were transferred to liquid nitrogen for long-term storage.

2.3.3. Thawing cells

Frozen cells were stored in aliquots in liquid nitrogen and thawed rapidly by transferring to a 37°C water bath. The cells were immediately resuspended in F-15 medium and centrifuged at 1200 rpm for 5 minutes. The pelleted cells were resuspended in 20 ml F-15 medium and plated out in

T25 flasks. Freshly harvested mouse peritoneal macrophages were added to the culture medium to act as feeder cells.

2.3.4. Maintenance of myeloma cell lines

The mouse myeloma cell line Ag14-SP2/0 was used for fusion with mouse spleen cells and the mouse myeloma cell line NSO was used for fusion with rat spleen cells. These cell lines were obtained from The European Collection of Cell Cultures (ECACC). Both myeloma cell lines were maintained in F-10 medium in a volume of 20 ml in 80 cm^2 flasks. To expand cultures, the cells were split 1:1. The flasks were agitated to dislodge cells, 20 ml fresh medium added to the flask and 20 ml of this suspension removed and placed in a new flask.

2.3.5. Monoclonal Antibody Production

Monoclonal antibodies (mAbs) were generated according to modifications of the method of Kohler and Milstein [484,487].

2.3.6. Immunisations

The table below summarises the details of the animals used for mAb production, the immunising antigen and the fusion partner:

Animal species	Immunised with	Myeloma fusion partner
C6 deficient mouse	Purified human C6	Ag14-SP2/0
C6 deficient mouse	Normal mouse serum	Ag14-SP2/0
PVG/C6 deficient rat	Normal rat serum	NSO

The immunisation protocol was as follows: the first immunisation was administered s.c.; comprising 30 – 50 µg of the protein of interest in PBS, emulsified with CFA. Two and four weeks after the first immunisation, the animals were boosted (s.c.) with an equal volume of 30 – 50 µg antigen in PBS and emulsified with an equal volume of IFA. Several days following the last boost, the animals were tail-bled, serum prepared (section 2.2.1) and tested for anti-human C6 antibodies by ELISA (section 2.3.8). The animal with the highest anti-C6 titre was boosted by intraperitoneal injection (i.p.) with approximately 20 µg antigen, diluted in PBS, 48 hours prior to sacrifice.

2.3.7. Generation of hybridomas

Once the animal with highest antibody titre against human C6 had been identified, the next step was to immortalise and select those B cells secreting anti-C6 antibodies. All wash steps were achieved by centrifugation at 1000 rpm for 5 minutes. The animal was exsanguinated under terminal anaesthesia and serum prepared (section 2.2.1). Its spleen was removed and

repeatedly perfused with cold (4˚C) RPMI 1640 medium using a 5 ml syringe and a 19 gauge needle to release spleen cells. The released cells were washed in cold RPMI 1640 medium three times.

Myeloma cells (SP2/0 or NSO) growing in log phase were harvested and washed once in F-10 medium. Spleen cells were mixed with the myeloma cells at a ratio of 2:1, washed once in RPMI 1640 medium and pelleted. The supernatant was completely removed, leaving a dry pellet, which was loosened by gentle agitation. Fusion was induced by the gradual addition of 1 ml PEG-1500 dropwise to the cells over 1 minute with gentle agitation. The fused cells were left to rest for 30 seconds and then 50 ml RPMI 1640 pre-warmed to 37˚C was slowly added. The cells were washed by centrifugation and resuspended in 100 ml (150 ml for rat fusion) HAT medium, to select for hybrid cells. The aminopterin in the HAT medium inhibits the *de novo* purine and pyrimidine synthesis pathway, so that cells have to synthesize nucleotides via the salvage pathway, which requires the addition of hypoxanthine and thymidine [488]. Myeloma cells are immortal but are unable to utilise the salvage pathway due to a mutation in the enzyme hypoxanthine-guanine phosphoribosyl transferase (HPRT). Therefore, unfused myeloma cells will die in HAT medium. The unfused spleen cells will also die after a few days in culture, even though they are able to use the salvage pathway, because they are not immortal [489]. Hybridomas are immortal, due to the myeloma cell, and can utilise the salvage pathway, because of the splenocyte, and therefore will grow in HAT medium. Approximately 0.5 ml of cell suspension was added to each well of eight (twelve for rat fusion) 24-well plates that had previously been seeded with 0.5 ml (per well) of HAT medium containing mouse peritoneal macrophages to act as feeder cells. Approximately 10-14 days post-fusion visible clones were present in the majority of wells and were ready for screening for the presence of anti-C6 antibodies by ELISA (section 2.3.8). Positive wells were cloned by limiting dilution into HT medium in order to obtain a monoclonal antibody secreting cell line. Hypoxanthine and thymidine were provided in culture medium to ensure survival of the hybridomas during the transition from using the salvage pathway to the *de novo* purine and pyrimidine synthesis pathway. For cloning at limiting dilution, anti-C6 secreting cells were counted and adjusted so that sequential rows of wells in 96 well plates were seeded with 100, 30, 10, 3, 1, and 0.3 cells per well. One hundred microlitres of HT medium containing mouse peritoneal macrophages were also added to each well, as feeder cells. When visible clones were present in wells seeded with 1 and 0.3 cells per well, these were screened by ELISA and cloned out again as described above, but in F-15 medium only. Typically, a total of three rounds of screening and subcloning at this dilution were required to ensure monoclonality, although sometimes further rounds were required.

Once the cell lines were monoclonal, they were expanded, some were frozen down as stocks and the rest were expanded further into 175 cm^2 tissue culture flasks and maintained in 30 ml F-5 medium. Once a week, the medium was collected and replaced with fresh medium. The collected medium was centrifuged at 1000 rpm` to remove cell debris. Sodium azide (0.01% (v/v)) was added as a preservative and the supernatant stored at 4°C until the antibody was purified.

2.4. Haemolysis Assays

Classical pathway mediated haemolytic assays were used to identify functional C6-containing fractions whilst purifying $C6^{490}$, to determine the functional activity of purified C6 across species and to characterise the functional blocking activity of antibodies and phage-peptides generated against purified C6.

2.4.1. General materials

Complement Fixation Diluent (CFD): 1 tablet was dissolved in 100 ml of deionised water to a final concentration of 0.9 mM sodium barbital, 2.8 mM barbituric acid, 145 mM NaCl, 0.8 mM $MgCl_2$, 0.3 mM $CaCl_2$, pH 7.2 ± 0.2 (Oxoid, Basingstoke, UK).
Alsever's solution: 144 mM $Na_3C_6H_5O_7.2H_2O$, 27 mM glucose, 72 mM NaCl, pH 6.1.
Sheep blood in Alsever's solution, TCS Biosciences Ltd., Claydon, Buckinghamshire, UK.
Rabbit blood in Alsever's solution, BMS, UWCM.

2.4.2. Antibody-sensitisation of sheep and rabbit erythrocytes

To prepare a 2% stock solution of antibody-sensitised sheep erythrocytes (sheep EA) or rabbit erythrocytes (rabbit EA), 1 ml of sheep blood or 1 ml of rabbit blood was diluted in 20 ml CFD and centrifuged at 2000 rpm for 5 minutes. Four hundred µl of the packed erythrocytes (E) were removed and washed three times in CFD as described above, before being resuspended in 10 ml CFD and warmed at 37°C for 5 minutes. To sensitise the sheep E, 10 ml of pre-warmed CFD containing Amboceptor (rabbit anti-sheep E)(Dade-Behring, Marburg, Germany) diluted 1/250 was added to the warm sheep E and mixed gently at room temperature for 30 minutes. The rabbit E were sensitised in the same way, except that they were incubated with mouse anti-rabbit E (BMS, UWCM) at a dilution of 1/200. The antibody-sensitised erythrocytes were washed three times in CFD and resuspended in a final volume of 20 ml CFD. Sheep EA and rabbit EA were stored at 4°C for up to 1 week.

2.4.3 Titration of test serum

Doubling dilutions of the test serum were made into 50 µl CFD (final volume) in a round-bottomed microwell plate, to which a further 50 µl each of CFD and EA were then added. The maximum lysis control wells contained 100 µl dH_2O and 50 µl EA and the background lysis control wells contained 100 µl CFD and 50 µl EA. The plate was incubated at 37°C for 30 minutes before being centrifuged at 2500 rpm for 5 minutes to pellet the cells. Supernatant from each well (100 µl) was transferred to a flat-bottom microwell plate and the release of haemoglobin into the supernatant was measured at A_{415nm}.

To calculate the percentage of lysis, the following equation was used:

$$\% \text{ lysis} = 100 \times \frac{A_{415nm} \text{ (sample)} - A_{415nm} \text{ (background lysis control)}}{A_{415nm} \text{ (maximum lysis control)} - A_{415nm} \text{ (background lysis control)}}$$

A measurement of the serum complement haemolytic activity (CH_{50}) was obtained by plotting the calculated % lysis against serum dilution and the dilution of serum at which 50-70% haemolysis occurred was determined.

2.4.4. Reconstitution of C6 deficient serum with functional C6

Reconstitution experiments with C6 were performed - either to identify functionally active C6 containing fractions during C6 purification or to determine the minimal concentration of C6 required for C-mediated haemolysis to occur.

To identify functionally active C6 containing fractions, rat C6 deficient (C6D) serum was titrated in a similar way to that described in section 2.4.3. Two sets of doubling dilutions of rat C6D were made in 50 µl CFD (final volume) in a round bottom microwell plate. To one set 10 µl functionally active C6 in CFD was added; to the other set 10 µl CFD was added and to both sets 50 µl sheep EA were added. For the maximum lysis control 60 µl dH_2O was added to 50 µl sheep EA and for the background lysis control 60 µl CFD was added to 50 µl sheep EA. The plate was incubated at 37°C for 30 minutes before being centrifuged at 2500 rpm for 5 minutes to pellet the cells. Supernatant from each well (90 µl) was transferred to a flat-bottom microwell plate and the release of haemoglobin into the supernatant was measured at A_{415nm}. The percentage of lysis was calculated as detailed in section 2.4.3 and a CH_{50} value was obtained by plotting the calculated % lysis against serum dilution. A dilution of rat C6D serum at which 50-70%

haemolysis occurred when C6 was present, but at which dilution no lysis occurred when C6 was absent was chosen for the subsequent reconstitution assays.

To identify C6 containing fractions, 10 µl test sample (either neat or diluted 1:10 in CFD) was mixed with 50 µl C6D rat serum diluted in CFD at a pre-determined dilution and 50 µl of sheep EA in a round bottom microtitre plate. Maximum and background lysis controls, as well as a positive control containing 10 µl functionally active C6 were also included. The plate was incubated at 37°C for 30 minutes and centrifuged at 2500 rpm for 5 minutes. Supernatant from each well (90 µl) was transferred to a flat-bottom microwell plate and the release of haemoglobin into the supernatant was measured at A_{415nm}. The percentage of lysis was calculated as detailed in section 2.4.3.

To determine the minimal concentration of C6 required for C-mediated haemolysis to occur doubling dilutions of C6D serum were made in 50 µl CFD (final volume) in a round bottom microtitre plate. Ten microlitres human C6 (0-200 µg/ml) in CFD was added to each dilution of C6D serum along with 50 µl EA and incubated for 30 minutes at 37°C. Maximum and background lysis controls were also included. The plates were centrifuged at 2500 rpm, the supernatants collected (90 µl) to a flat bottom microtitre plate and A_{415nm} measured. The percentage of lysis was calculated and the CH_{50} obtained as described in section 2.4.3.

2.4.5. Haemolytic assay to test the activity of potential inhibitory agents

A titration was carried out to determine the dilution of serum that induced 80% haemolysis, as detailed in section 2.4.3. Serial dilutions of the test sample were made into CFD (50 µl total volume) in a 96-well round bottom plate. To this, serum (50 µl) at a predetermined dilution in CFD was added and the plate pre-incubated at 37°C for 30 minutes. Fifty microlitres EA were then added to each well and the plate incubated for a further 30 minutes at 37°C. Maximum and background lysis controls, as well as relevant controls for the test sample were included. For antibodies being tested this was an antibody that did not recognise C6 and was not a known blocker of C-mediated haemolysis. Wild-type phage was the control when phage-peptides were tested. The plate was centrifuged at 2500 rpm for 5 minutes, the supernatant from each well (100 µl) transferred to a flat-bottom microwell plate and the release of haemoglobin into the supernatant measured at A_{415nm}. The percentage of lysis was calculated as detailed in section 2.4.3. For a rapid screen enabling a higher throughput of phage-peptides on one plate, subsequent phage-peptides were screened at one dilution only to determine whether they had inhibitory activity.

2.5. Surface Plasmon Resonance (SPR) using the BIAcore 3000

The BIAcore [491] instrument provides the means to study protein-to-protein interactions in real time with small amounts of unlabelled material by measuring surface plasmon resonance (SPR). It comprises three major components: the sensor chip, a microfluidics system [492] and SPR detector. SPR is an electron charge density wave effect that arises at the surface of a metallic film (sensor chip) when light is reflected at the film under specific conditions. The resonance is a result of energy and momentum being transformed from incident photons into surface plasmons and is sensitive to the refractive index of the medium on the opposite face of the film from the reflected light. If a molecule binds to the chip surface, then there is a change in the refractive index of the medium and this is recorded on the sensorgram. All sensor chips comprise a glass slide coated with gold to which a matrix is attached. The ligand of interest is immobilised onto this matrix and the microfluidics system delivers the molecule of interest (analyte) to it in a controlled manner. Quantitative information about the specificity, kinetics, affinity and concentration of the analyte for the ligand can then be gathered.

The BIAcore 3000 was used in all experiments and all buffers used were filtered (0.2 μm) and degassed before use on the BIAcore 3000. As the coupling chemistry was the same for both types of sensor chip used, the immobilisation of ligand onto the sensor chip surface is detailed below. Methods specific to the experiments are described in the relevant chapter.

2.5.1. Immobilisation of Ligand onto the Sensor Chip Surface

A number of sensor chips with matrices of different compositions attached to the surface are available. These different matrices enable the favourable immobilisation of a wide range of ligands of interest onto the surface. In this study, the CM-5 sensor chip (BIAcore AB, Uppsala, Sweden) and the Pioneer Chip F1 (BIAcore AB, Uppsala, Sweden) were used. Carboxymethylated dextran is covalently attached to the surface of both chips, but the dextran molecules on the Pioneer Chip F1 are shorter than those on the CM-5 chip. However, the ligand is covalently coupled (immobilised) onto both types of sensor chip via amine groups and so the immobilisation methods are identical. For immobilisation, the ligand interacts with the chip surface via electrostatic interactions – this usually occurs maximally below the pI of the ligand and therefore, the optimal pH for achieving maximal attachment of ligand to the surface of the chip was determined. Ligand diluted in 10 mM sodium acetate buffer, pH range 3.5 – 5.0, was injected over the sensor chip surface. Having selected the pH at which to carry out the immobilisation, the ligand was immobilised onto the flow cell surface (figure 2.1). To 'activate' the sensor chip surface, a mixture of NHS (0.05 M N-hydroxysuccinimide in H_2O)(BIAcore AB,

Figure 2.1 Chemistry of amine coupling of ligand to the CM-5 or Pioneer F1 sensor chip surface

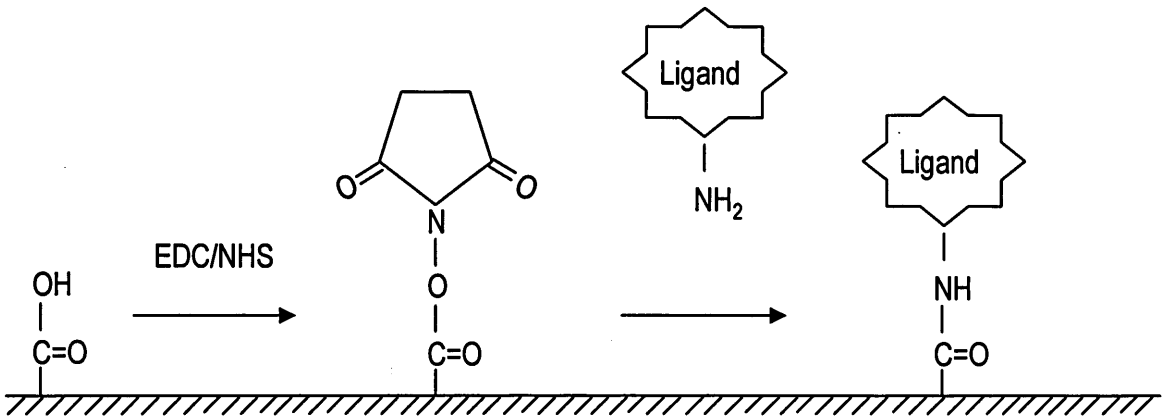

To immobilise a ligand onto the surface of a CM-5 or Pioneer F1 chip by amine coupling, the surface of the sensor chip is first activated by passing a mixture of freshly mixed 0.2M 1-ethyl-3-(3-dimethylaminopropyl)-carbodiimide (EDC) (final concentration) and 0.05 M N-hydroxsuccinimide (NHS) (final concentration) over it. This alters the surface chemistry, so that when the ligand with free amine groups is flowed over the sensor chip surface, the ligand forms a covalent bond with the surface via the amine group. When the target RU has been reached, 1 M ethanolamine-HCl pH 8.5 is passed over the surface, blocking any free reactive groups, so that no other proteins can bind to the surface.

Uppsala, Sweden) and EDC (0.2 M N-ethyl-N'-(dimethylaminopropyl)-carbodiimide in H_2O)(BIAcore AB, Uppsala, Sweden) was injected over it. The ligand was injected over the sensor chip and allowed to covalently bind to the surface. To block any free reactive groups remaining, ethanolamine (1M ethanolamine hydrochloride, adjusted to pH 8.5 with NaOH)(BIAcore AB, Uppsala, Sweden) was passed over the sensor chip surface. Noncovalently bound material was removed by flowing 10 mM sodium hydroxide over the flow cell. On the CM-5 chips, an additional flow cell was treated in a similar way, but omitting the immobilisation of ligand, so that it could be used as a reference blank flow cell. For the Pioneer F1 chip, an irrelevant peptide was immobilised onto the sensor chip and used as a reference.

Chapter 3: Purification and functional characterisation of human C6 and reconstitution of C activity in C6 deficient human and rodent sera with human C6

3.1. Introduction

The C protein C6 is a central target of this study. Therefore, before work could start on generating agents that block C6 activity, pure C6 was required. Although pure human C6 is available commercially (Quidel,San Diego, California, USA), it is expensive and sold in small amounts (250 µg costs approximately £150.00). As C6 is present in human plasma at up to 100 mg/L and out-of-date plasma was freely available from the Welsh Blood Transfusion Service, it was cost-effective to develop our own in-house methods of C6 purification. Traditionally, multi-step classical methods including ion exchange chromatography have been used for purifying C6 and other C proteins from human plasma [490]. Ion exchange chromatography is ideal for purifying from complex mixtures of proteins as it separates proteins according to charge. Various classical methods have been published for purifying C proteins [490,493-495] and these have now been further modified and optimised for use in-house. Such methods, however, are time consuming, inefficient and importantly often the functional activity of the protein is either significantly reduced or lost – this is particularly the case with C6 [496]. Therefore, better purification methods were required. Affinity chromatography separates proteins on the basis of a specific and reversible interaction between a protein (or group of proteins) and a particular ligand, coupled to a chromatographic matrix. It is the only purification technique that enables the purification of a biomolecule on the basis of its biological function or individual chemical structure [497]. For this to be successful, the coupled ligand must retain its specific binding affinity for the target molecules and after washing away unbound material, the binding between the ligand and target molecule must be reversible to allow the target molecules to be removed in an active form. The target protein can be eluted from the affinity medium either specifically using a competitive ligand, or non-specifically, by changing the pH, ionic strength or polarity, depending on the nature of the target-ligand interaction. Various biological interactions can be exploited in this way, including those between glutathione and glutathione-S-transferase (GST), lectins and glycoproteins as well as antibodies and antigens. Due to the specificity of these interactions, the target protein can be collected in a purified, concentrated and biologically active form from a complex mixture of proteins in one step. Purification that would otherwise be time-consuming, difficult or even impossible using other techniques can often be easily achieved with affinity chromatography.

This has been done successfully for other C proteins, using specific anti-C antibodies coupled to a matrix. Small quantities of human C6 have previously been purified by affinity chromatography [498] using the anti-human C6 mAb WÜ 6.4 [458]. However, attempts to purify greater amounts of C6 have been hampered by the fact that large quantities of antibody are required for column preparation. As the hybridoma cell line secreting WÜ 6.4 is not available to provide sufficient quantities of mAb, an in house anti-C6 secreting hybridoma would be of significant benefit, enabling affinity purification of C6 to be performed in house.

The requirements of a reliable C6 purification protocol were twofold: first, to be capable of purifying large quantities of C6 speedily and efficiently; secondly, the purified C6 should be biologically active. This would enable functional studies to be performed using classical haemolytic assays with C6 deficient human sera and reconstituting activity using purified C6. In addition, mouse, rat and rabbit C6 deficient sera were available in house, allowing the investigation of the functional homology of C6 across species, both in vitro and in vivo. For example, human C6 has been shown to reconstitute C6 activity in C6-deficient rats in previous studies [274,498]. Also, pure, biologically active C6 was an essential tool for later investigations in this study, including generating anti-C6 antibodies, identifying phage-peptides that recognise C6, and further characterising these reagents in functional blocking assays.

The aims of the investigations described in this chapter were threefold: first, to develop and optimise an efficient method for the purification of human C6, free of contaminating serum proteins and free of other C proteins. Second, to determine the functional activity of the purified C6 by reconstituting human C6 deficient serum in C-mediated lytic assays. Finally, to test the capacity of purified C6 to restore C-haemolytic activity in rodent C6 deficient sera both in vitro and in vivo.

3.2. Specific Methods

3.2.1. The Purification of Human C6

As pure human C6 was required for this project, one of the first tasks was to purify it. Various purification methods were developed and used. These techniques are detailed in the following section, but are summarised schematically in figure 3.1.

3.2.1.1. Enrichment of C6 using PEG Precipitation

Human C6 was purified from fresh frozen plasma obtained from the Welsh Blood Transfusion Service (WBTS). Whether classical or affinity methods were used to purify C6, a precipitation

Figure 3.1 A summary of the methods used to purify C6 from human serum

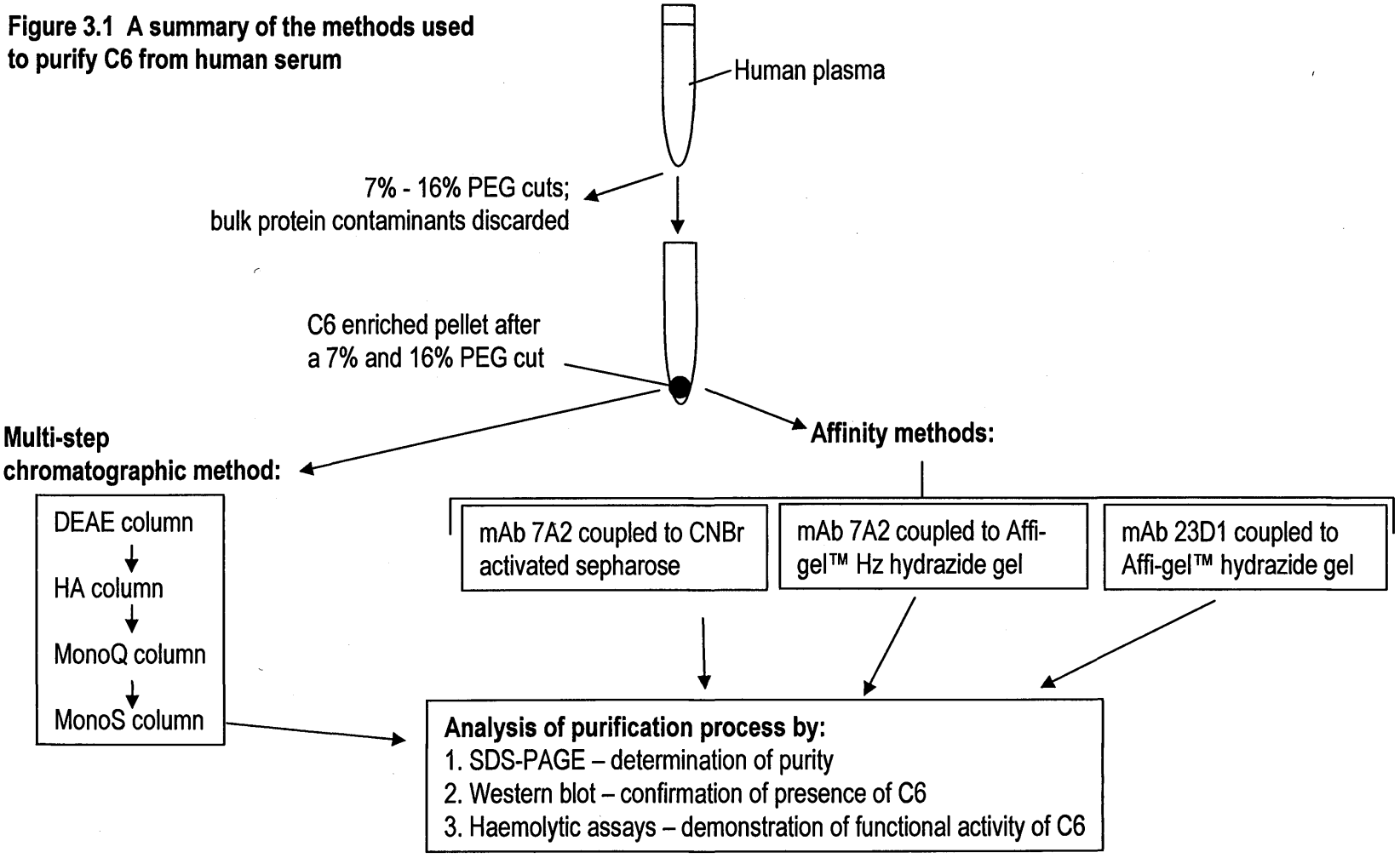

step was performed to enrich the preparation with C6 and reduce the volume to be applied to columns. All steps were performed at 4°C in order to minimise the loss of functional activity of C6, as human C6 rapidly and spontaneously becomes non-functional at room temperature. The protease inhibitors PMSF and benzamidine were added at 1 mM final concentration to human plasma, mixed and centrifuged at 15, 000 *g* for 10 minutes. To the supernatant, polyethylene glycol (PEG)-4000 was added from a 21% (w/v) stock solution in water to a final concentration of 7% (w/v), stirred for 30 minutes, and centrifuged at 24,000 *g* for 20 minutes, 4°C. The resulting pellet containing high molecular weight contaminants was discarded. The 7% PEG-supernatant was adjusted to 16% (w/v) PEG-4000 by the addition of solid PEG-4000 (9g of PEG-4000 per 100 ml supernatant), mixed and centrifuged as described above. The resulting pellet which contained the enriched C6 was then suspended in the relevant buffer for the purification method, whilst the supernatant was discarded.

3.2.1.2. Ion Exchange Chromatography

Ion exchange chromatography separates proteins with differences in charge. The separation is based on the reversible interaction between a charged protein and an oppositely charged chromatographic medium. Proteins bind to the chromatographic medium as they are loaded onto a column, then, by altering the conditions – usually increasing the salt concentration or changing the pH, the bound substances are eluted differentially. In this way, target proteins are concentrated during binding and collected in a purified, concentrated form.

C6 was purified from human plasma by published classical methods [493-495]. As contaminating proteins were present after the first three chromatographic steps, an additional purification step was added - the Mono S column. All steps were performed at 4°C. The C6-enriched pellet from section 3.2.1.1. was dissolved in 25 mM NaBarbitone buffer, containing 5mM EDTA, 0.5 mM PMSF, 0.02% sodium azide, pH 7.2. The sample was then subjected to various ion exchange chromatographic steps, using several matrices (Table 3.1). All columns were equilibrated and all samples dialysed in the relevant start buffer prior to the application of sample to the column. Bound sample was eluted with a continuous linear gradient varying salt (NaCl) or phosphate concentration as appropriate. Fractions containing functional C6 were identified by haemolytic assay (section 2.4.4), pooled and dialysed in the relevant start buffer. If necessary, sample was concentrated using ultrafiltration (section 2.1.2) and filtered through a 0.2 μm filter prior to being applied to a column.

After each chromatographic step, the C6-containing fractions were identified by haemolytic assay (section 2.4.4.) and pooled for the next chromatographic step. After the final step, fractions were

subject to SDS-PAGE electrophoresis and western analysis to assess the purity of C6. The concentration of C6 was determined either using the BCA assay (section 2.1.4) or measuring the absorbance of each fraction at 280 nm (extinction coefficient = 1.1) and stored in aliquots at -70°C until use. This helped retain the functional activity of C6 as it was lost when stored at -20°C.

Table 3.1. The sequential chromatographic steps C6 purification.

Chromatographic matrix	Functional group	Start buffer	End buffer
DEAE-Sephacel (anion exchange)	Diethylaminoethyl	25mM NaBarbitone, 5 mM EDTA, 0.5mM PMSF, 0.02% NaN_3, pH 7.2	Start buffer + 1M NaCl, pH 7.2
Hydroxyapatite	Calcium phosphate	5 mM KPhosphate, pH 7.0	300 mM Kphosphate, pH 7.0
Mono Q (anion exchange)	Quaternary amine	20 mM KPhosphate, pH 7.0	Start buffer + 1 M NaCl, pH 7.0
♦Mono S (cation exchange)	Sulfonate	20 mM KPhosphate, pH 5.0	Start buffer + 0.5 M NaCl, pH 5.0

All matrices, apart from hydroxyapatite, were purchased from Amersham Pharmacia Biotech (Chalfont, Buckinghamshire, UK). Hydroxyapaptite is not an ion exchange matrix and was purchased from Bio-Rad (Hercules, California, USA).
♦Additional step added to classical methods to improve the purity of C6.

3.2.1.3. Affinity Chromatography

3.2.1.3.1. Preparation of an affinity column using Cyanogen Bromide (CNBr) activated sepharose

Cyanogen bromide (CNBr)-activated Sepharose 4B (Amersham Biosciences, USA) is a preactivated gel for immobilisation of ligands containing primary amines.

Buffers	Composition
Coupling buffer	0.1 M $NaHCO_3$ pH 8.3, 0.5M NaCl.
Swelling buffer	1 mM HCl.
Blocking buffer	0.1 M Tris-HCl, pH 8.0.
Low pH wash buffer	0.1 M sodium acetate buffer pH 4.0, 0.5 M NaCl.
High pH wash buffer	0.1 M Tris-HCl buffer, pH 8.0, 0.5 M NaCl.

Ten milligrams of purified antibody was coupled to CNBr-activated Sepharose 4B using the buffers listed above as detailed in the manufacturer's instructions (Catalogue number: 17-0430-01) (www1.amershambiosciences.com). Freeze-dried gel (1g per 3 mg of antibody) was washed and swelled on a sintered glass filter using approximately 200 ml swelling buffer per gram of freeze-dried powder. The gel was mixed with the antibody (1 mg/ml, which had been dialysed into coupling buffer) and mixed end over end for 1 hour at room temperature. After this, the gel

was washed with a minimum of 5 gel volumes of coupling buffer and the coupling efficiency analysed by quantifying unbound antibody using the Coomassie protein assay. The remaining active groups on the sepharose gel were deactivated or blocked after coupling by incubating the gel for 2 hours in blocking buffer. As Tris-HCl was used, this added an excess of small primary amine. The gel was then washed, alternating between low and high pH wash buffers, at least three times in order to remove excess of uncoupled ligand. This ensured that no free ligand remained ionically bound to the immobilised ligand. Columns were stored in 0.1% sodium azide (NaN_3)/PBS.

3.2.1.3.2. Preparation of an affinity column using Affi-Gel® Hz Hydrazide Gel

Although activated sepharose coupled antibodies efficiently, the coupled anti-C6 antibody was prone to leaching from the column, so that very quickly the coupled antibody was eluted from the column, making it useless. Affi-Gel® Hz Hydrazide Gel (Bio-Rad Laboratories, Hercules, California, USA) is an agarose support which reacts with the aldehydes of oxidized carbohydrates, forming stable, covalent hydrazone bonds. The F_c region of IgG isotype antibodies comprises approximately 3% carbohydrate and by oxidation, it can be coupled to the Affi-Gel Hz gel. As the F_c region of the antibody is coupled to the matrix, it is more likely that the antibody will be presented on the matrix in an orientation that will be optimal for affinity purification. Antibody was coupled to the Affi-Gel® Hz Hydrazide Gel, according to the manufacturers instruction manual (www.bio-rad.com, catalogue number 153-6060). All steps were performed at 4°C, except where specified.

Buffer	Composition
Affi-gel coupling buffer	Made up from Affi-gel 10X Coupling buffer (Cat No 153-6054, BioRad), adjusted to pH 5.5.
Sodium periodate stock solution	25mg sodium periodate dissolved in 1.2 ml dH_2O.

The purified mAb to be coupled was prepared for oxidation by dialysing it against two changes of Affi-gel coupling buffer overnight to achieve a 1,000-fold excess of buffer to antibody. To oxidise the mAb, one tenth the volume of sodium periodate stock solution was added to the mAb (e.g. 2 ml stock solution to 20 ml antibody at 1 mg/ml) and the solution mixed gently in the dark for 1 hour at room temperature. Glycerol was immediately added to the oxidised antibody at a final concentration of 20 mM and allowed to mix for 10 minutes. The antibody was dialysed against two changes of Affi-gel coupling buffer overnight to achieve a 1,000-fold (v/v) excess of buffer to antibody.

The Affi-gel Hz gel was prepared as follows: to remove the isopropanol in which it was stored, the gel/isopropanol slurry was transferred to a container and the gel allowed to settle. The isopropanol supernatant was removed and Affi-gel coupling buffer added at twice the gel volume. This was mixed well and the gel allowed to settle. The supernatant was removed and the gel wash repeated. Finally, an equal volume of coupling buffer was added to the gel and mixed. The slurry was then added to a leak-proof reaction container and allowed to settle. The buffer above the settled gel was removed.

For optimal coupling to Affi-gel Hz gel it is recommended the IgG concentration should be 1-10 mg/ml. The oxidised, desalted IgG was added to the washed affi-gel Hz hydrazide gel. The mAb was coupled to the gel by mixing overnight at room temperature. The gel/IgG slurry was poured into a column, the eluant collected and the volume measured. The gel was washed with one column volume of 20 mM K_2HPO_4/20 mM KH_2PO_4, 0.5 M NaCl, pH 7.0. The column eluant was collected and saved for coupling efficiency determination. The column was washed with 20 mM K_2HPO_4/20 mM KH_2PO_4, 0.5 M NaCl, 0.02% v/v sodium azide and stored at 4°C until used.

To calculate the coupling efficiency of the mAb to the column, the absorbance at 280 nm in the eluates was measured against an appropriate buffer blank. The following equations were then used:

Abs_{280nm} / 1.4 = (mg IgG/ml) x dilution x volume = **total IgG**

[total coupled protein] =

[total protein before coupling]-[total uncoupled protein (eluant + 0.5 M NaCl wash)]

% protein coupled = 100 X ([total coupled protein] / [total protein before coupling])

The column was pre-conditioned by applying 2-4 bed volumes of 0.1% v/v diethylamine (DEA) in PBS, pH 11.5. The column was regenerated with at least 5 bed volumes of PBS before use.

3.2.1.3.3. Affinity purification of human C6

The C6 enriched PEG pellet (section 3.2.1.1.) was dissolved in PBS and centrifuged at 15000 *g* for 20 minutes to remove undissolved material before passing it over the affinity column. The C6 affinity column was pre-equilibrated with 10 column volumes PBS and the C6 containing solution passed over it at approximately 0.5 ml per minute. The breakthrough was retained and the column washed with at least 20 column volumes PBS until no more protein was detected in the run through by Coomassie protein reagent. Bound C6 was eluted from the column with elution buffer (0.5% v/v DEA in PBS, pH 11.5) in 1 ml fractions until no more protein was detected using

Coomassie reagent. Fractions were neutralised by the addition of 200 µl 1M Tris-HCl, pH 7.0. The column was rinsed with PBS to remove elution buffer from the column and the breakthrough re-applied to the column to maximise yield. Bound C6 was eluted as described above; the column was washed with PBS and stored in 0.01% NaN_3 v/v in PBS at 4°C.
Protein containing fractions (1 ml) were assayed for C6 activity by haemolytic assay (section 2.4.4), pooled, dialysed against PBS overnight and concentrated by ultrafiltration. The protein concentration of the concentrate was determined by measuring A_{280} or using the BCA assay, functional activity was determined using a haemolytic assay and purity was determined by SDS-PAGE and western blot. Finally, the purified C6 was aliquoted and stored at -70°C.

3.2.2. Reconstitution of C6 deficient serum with purified human C6

3.2.2.1. Reconstitution of different species sera in vitro with purified human C6

The following experiments were performed using sera from humans, mice, rats and rabbits that had previously been confirmed as genetically deficient in C6 and dysfunctional in haemolytic assays. The aim of the investigations described was to determine whether human C6 was capable of restoring C lytic function to the aforementioned deficient sera. Sheep EA were used for all sera tested, apart from mouse serum, for which rabbit EA were used. The concentration of C6 in normal human blood ranges between 20 - 80 µg/ml [499], therefore the concentration range of C6 used to reconstitute C6 deficient (C6D) serum was 1 – 200 µg/ml.
For the reconstitution assay, 10 µl C6 (1 - 200 µg/ml final concentration) was added to 50 µl C6D human serum (diluted 1 in 5 – 1 in 640 in CFD, except for experiments involving mouse sera, in which case dilutions were in CFD supplemented with 0.1% (w/v) gelatine and 2.5% (w/v) dextrose) and incubated together with 50 µl 2% sheep EA for 30 minutes at 37°C (described in section 2.4.). After centrifugation at 1500 *g*, the supernatants were collected and absorbance at 415nm measured. The percentage of lysis was calculated and the CH_{50} value calculated according to the instructions in section 3.2.2.3.

3.2.2.2. Reconstitution of C6 deficient mice in vivo with human C6

To investigate whether the haemolytic activity of C6 deficient mice could be restored over 12 hours with human C6, purified human C6 (300 µg per mouse) was administered (i.p. injection) to C6 deficient mice. Thirty minutes and 2 hours post-injection, the mice were tail-bled and serum prepared (section 2.2.1). Twelve hours post-injection, the mice were exsanguinated under terminal anaesthesia and serum prepared. To determine whether the administration of human

C6 had reconstituted haemolytic activity, haemolytic assays were performed (section 2.4.) using rabbit EA and the CH_{50} at each timepoint calculated as below.

3.2.2.3. Calculation of Complement Haemolytic activity required to achieve 50% haemolysis of activated sheep erythrocytes (CH_{50}) via the C classical pathway

CH_{50} describes the amount of complement haemolytic activity in serum required to produce 50% haemolysis of antibody sensitised erythrocytes under specific conditions. The CH_{50} is inversely proportional to the amount of serum required to produce 50% haemolysis of activated erythrocytes, referred to as the X_{50}. The X_{50} and CH_{50} values for the C6 reconstitution assays performed in this chapter were calculated by a method adapted from the standard operating procedure (SOP) for serum complement haemolytic activity (CH_{50}) used in the Cellular Immunology Laboratory, Section of Immunology, Department of Medical Biochemistry and Immunology at the University Hospital of Wales.

After the haemolytic assays had been performed, the X value, the volume (µl serum/well) per well was calculated and the $\log_{10}$ for each point determined. The Y value, the percentage of cells lysed was calculated and then the value of $\log_{10}(Y/1-Y)$ determined. To determine X_{50}, the volume of serum required to produce haemolysis of 50% of activated erythrocytes, $\log_{10}X$ was plotted against $\log_{10}(Y/1-Y)$.

At 50% haemolysis, Y = 0.5, hence (Y/1-Y) = 1,

therefore $\log_{10}(Y/1-Y) = \log_{10}1 = 0$.

A trendline was fitted to the data and the equation of the line determined. This equation was then used to calculate the value of:

$\log_{10}X$ at $\log_{10}(Y/1-Y) = 0$,

which is the $\log_{10}$ of the X_{50}. The antilog (10^{X50}) was calculated, giving the X_{50} for that serum sample.

CH_{50} Units/ml = $1/X_{50} \times 2000$.

The normal range for classical pathway CH_{50} values in human serum are 1000 – 2000 when performed with 1% EA; in these experiments, 2% EA were used. This may result in an altered normal range for the CH_{50} values.

3.3. Results

3.3.1. Purification of human C6 using ion exchange chromatography

Human plasma, obtained from the WBTS (1L starting volume) was subject to PEG precipitation, followed by a series of column purification steps (described in section 3.2.1.). At each point in this process, material was reserved and analysed by SDS-PAGE and in parallel by western blot under non-reducing conditions in order to assess the degree of purification achieved (Figure 3.2). Owing to the complex nature of the sample, the C6 PEG enriched pellet is seen as a broad smear of proteins with no discernable band corresponding to C6 either on the coomassie blue stained gel or the western blot. Following elution from the DEAE column, the pooled fractions are better resolved on both gels, demonstrating the removal of major contaminating proteins and enrichment of C6 as a band of 100 kDa. The mono Q column removed the majority of the remaining contaminants, leaving two major bands, one consistent with C6, the other with a molecular weight of approximately 70 kDa. The identification of the protein peak containing functionally active C6 (as determined by haemolytic assay) corresponds to 2 peaks of absorbance at 280 nm on the chromatogram (Figure 3.3). In order to remove the remaining contaminants the pooled fractions were passed over the mono S column. Fractions of the protein peak containing functionally active C6 (as determined by haemolytic assay) correspond to a single peak on the chromatogram (Figure 3.4) and the coomassie stained gel and western blot (Figure 3.2) shows that most of the contaminating proteins were removed and the major band corresponds to C6. However, an additional band of 70 kDa remained in all but one of the fractions and was also detected by western blot, confirming it is a fragment of C6. The mAb WU 6.4, the detecting antibody used for figure 3.2b recognises a truncated form of C6 as well as full length C6. Truncated C6 is made by individuals with a subtotal deficiency in C6 and has a molecular weight of 79 - 80 kDa [499,500]. It is unlikely that plasma collected from normal individuals contained a truncated form of C6, but more likely that the C6 degraded either during storage in the expired plasma or as it was being purified. Gel filtration was not used to separate these different molecular weight proteins, as they were such similar molecular weights they would have co-eluted from a column together. Although C6 was successfully purified, the yield was 0.56 mg per 1 L volume of starting material. Assuming there is 80 mg/L C6 in plasma, the yield of purified C6 using this method is less than 1%. The functional quality of the purified C6 was also poor and the process time consuming. Therefore, better methods of C6 purification needed to be developed.

Figure 3.2 Purification of human C6 using ion exchange chromatography

A. Coomassie Staining

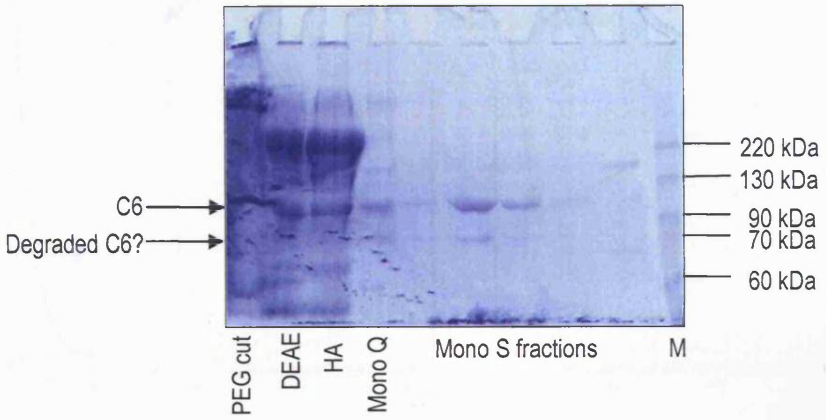

B. Western Blot analysis

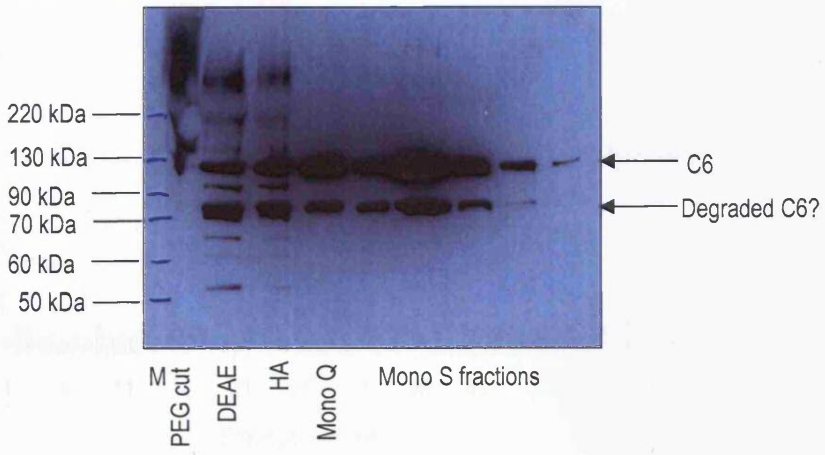

Collected fractions containing functional C6 activity at each purification step were pooled and passed over the next chromatographic column. Pooled material was retained at each step and equal volumes of sample analysed under non-reducing conditions by (A) SDS PAGE, stained with Coomassie blue reagent to assess the degree of purification reached at each step. The same material was also subject to (B) Western blotting. After SDS PAGE and transfer to nitrocellulose, protein was probed with the anti-human C6 antibody WU6.4 (1 μg/ml) and anti-mouse Ig-HRPO (1/1000) as a secondary antibody. Bands were detected with ECL and visualised by autoradiography. Protein molecular weight markers (M) were also run.

Figure 3.3 Typical chromatogram of partially purified C6 being passed over a MonoQ column

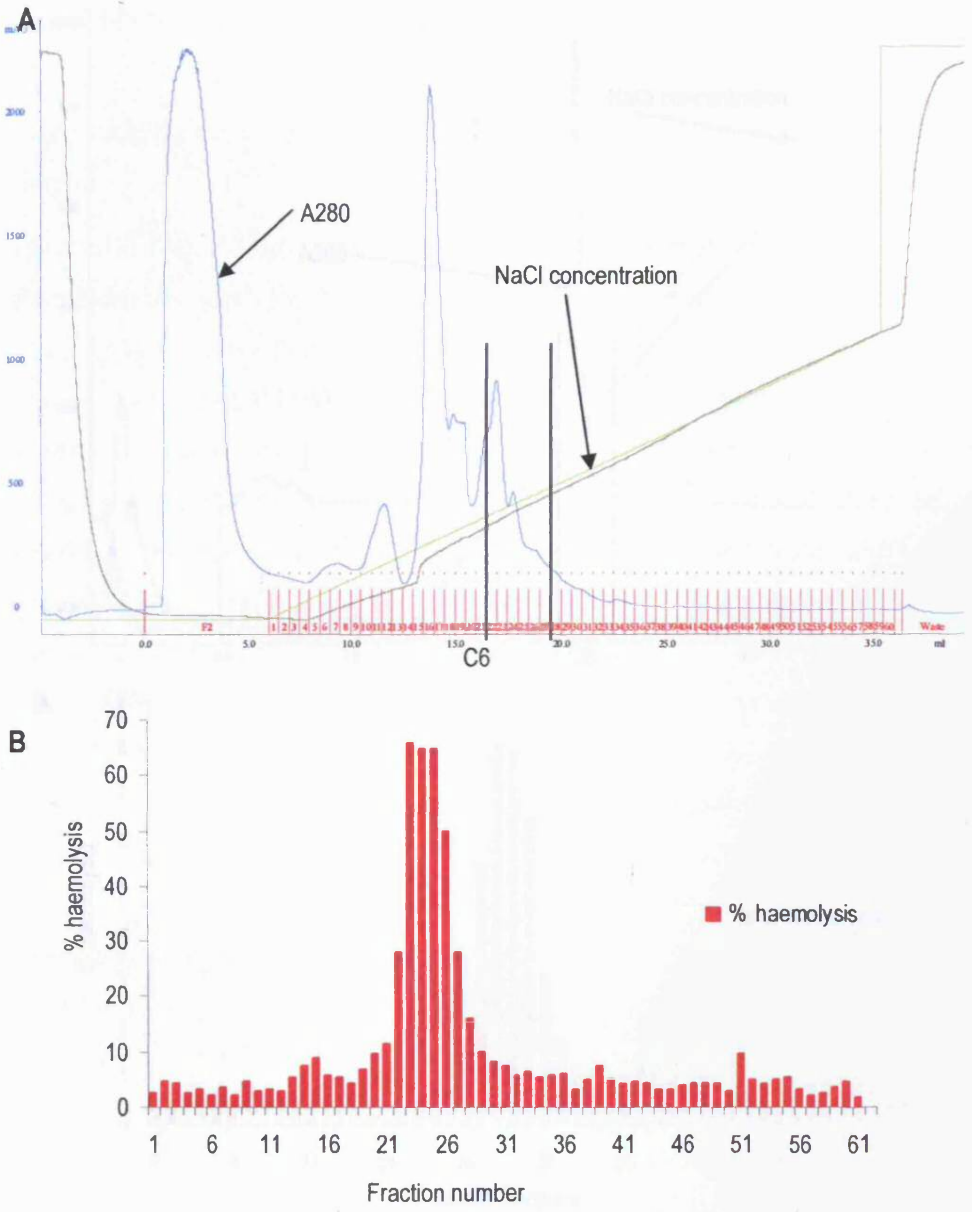

C6-containing fractions eluted from an HA column were pooled, dialysed against MonoQ start buffer and applied to a MonoQ column pre-equilibrated with MonoQ start buffer. To elute proteins from the column, a linear salt gradient was applied and a chromatogram recorded (A). To identify the C6-containing fractions, 10 µl of each fraction was incubated with rat C6 deficient serum and 2% sheep EA for 30 minutes and centrifuged. The supernatants were collected and the A415 nm measured. As can be seen from Figure 3.3B, C6 was eluted between fractions 19-31. Fractions 22-27 were pooled and dialysed against Mono S start buffer.

Figure 3.4 Typical chromatogram of partially purified C6 being passed over a MonoS column

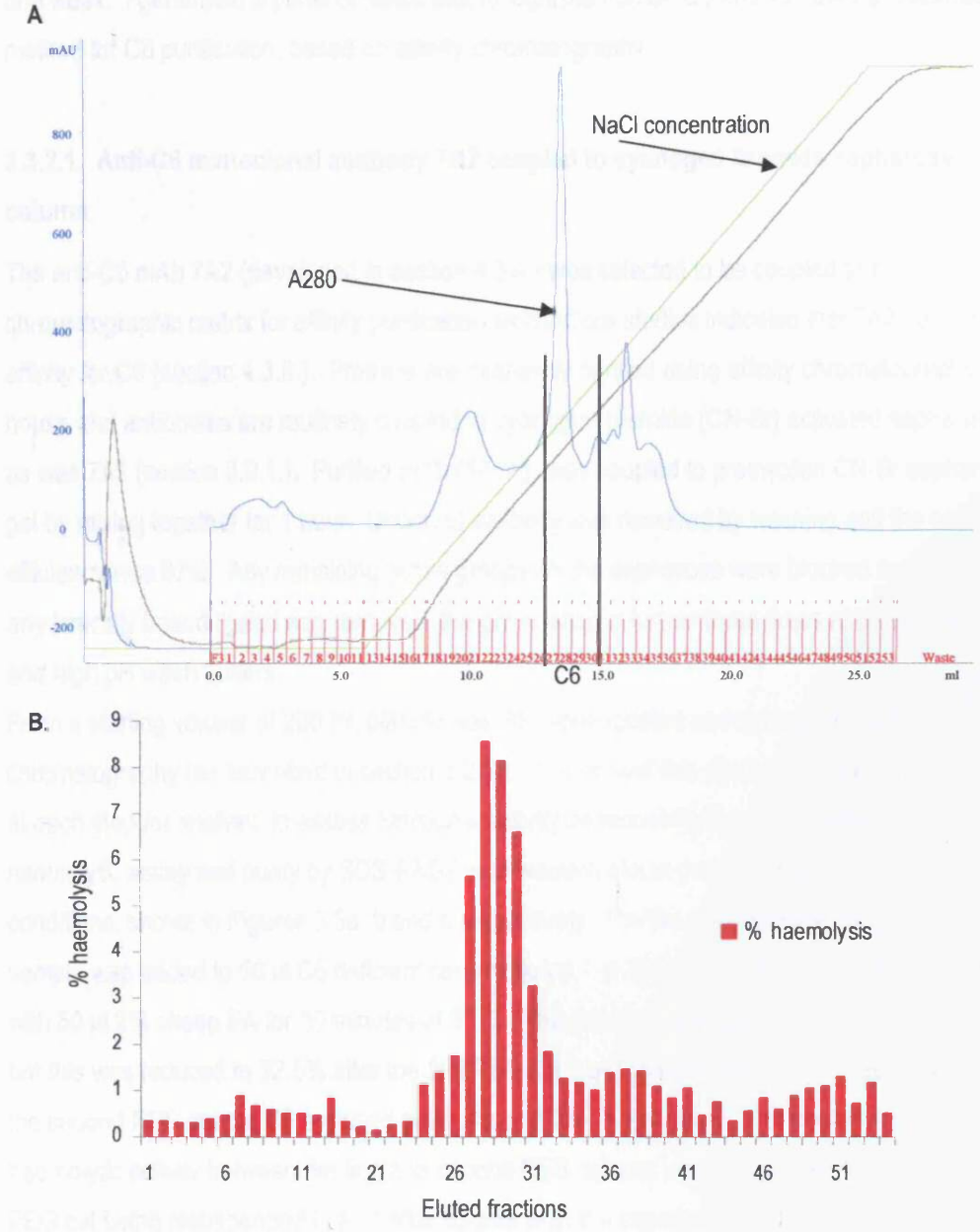

C6-containing fractions eluted from the MonoQ column were pooled, dialysed against MonoS start buffer and applied to a MonoS column pre-equilibrated with MonoS start buffer. To elute proteins from the column, a linear salt gradient was applied and a chromatogram recorded (A). To identify the C6-containing fractions, 10 µl of each fraction was incubated with rat C6 deficient serum and 2% sheep EA for 30 minutes and centrifuged. The supernatants were collected and the A415 nm measured. As can be seen from Figure 3.4B, C6 was eluted between fractions 27-30. These fractions correspond to the largest fraction peak in Figure 3.4A.

3.3.2. Purification of human C6 using affinity chromatography

Although C6 had been successfully purified using classical chromatographic methods, the process was inefficient, with a yield of less than 1% and time consuming, taking approximately one week. I generated a panel of mAbs that recognised human C6 and so I tried an alternate method for C6 purification, based on affinity chromatography.

3.3.2.1. Anti-C6 monoclonal antibody 7A2 coupled to cyanogen bromide sepharose column

The anti-C6 mAb 7A2 (developed in section 4.3.4.) was selected to be coupled to a chromatographic matrix for affinity purification as BIACore studies indicated that 7A2 had a high affinity for C6 (section 4.3.6.). Proteins are frequently purified using affinity chromatography in house and antibodies are routinely coupled to cyanogen bromide (CN-Br) activated sepharose, as was 7A2 (section 3.2.1.). Purified mAb (10 mg) was coupled to preswollen CN-Br sepharose gel by mixing together for 1 hour. Unbound antibody was removed by washing and the coupling efficiency was 97%. Any remaining active groups on the sepharose were blocked and to ensure any ionically bound ligand was removed, the gel washed a further three times alternately with low and high pH wash buffers.

From a starting volume of 200 ml, plasma was PEG-precipitated and subjected to affinity chromatography (as described in section 3.2.1.). Throughout this process, material was retained at each step for analysis to assess functional activity by reconstitution of C6 deficient serum in a haemolytic assay and purity by SDS-PAGE and western blot in parallel under non-reducing conditions, shown in Figures 3.5a, b and c respectively. For the reconstitution assay, 1 µl of test sample was added to 50 µl C6 deficient serum diluted 1 in 200 in CFD and incubated together with 50 µl 2% sheep EA for 30 minutes at 37°C. The starting material caused 96% haemolysis, but this was reduced to 32.5% after the first PEG cut, suggesting some C6 had been lost; after the second PEG cut the C6 enriched pellet caused 45% haemolysis. The apparent increase in haemolytic activity between the first and second PEG cut was due to the pellet from the second PEG cut being resuspended in a smaller volume than the supernatant of the first PEG cut. Of the eluted fractions, only fractions 2 - 4 had haemolytic activity, causing 6.3%, 5.4% and 3.8% haemolysis respectively and demonstrating the presence of C6. Owing to the complex nature of the sample, the plasma, C6 PEG enriched supernatant and C6 PEG enriched pellet are seen as broad smears of proteins with no discernable band corresponding to C6 either on the coomassie stained gel or the western blot. The major band in eluted fractions 1 – 6 had a molecular weight

Figure 3.5 Purification of human C6 using affinity chromatography: 7A2 coupled to cyanogen bromide (CNBr) activated sepharose

A. C6 reconstituting activity of fractions collected from column

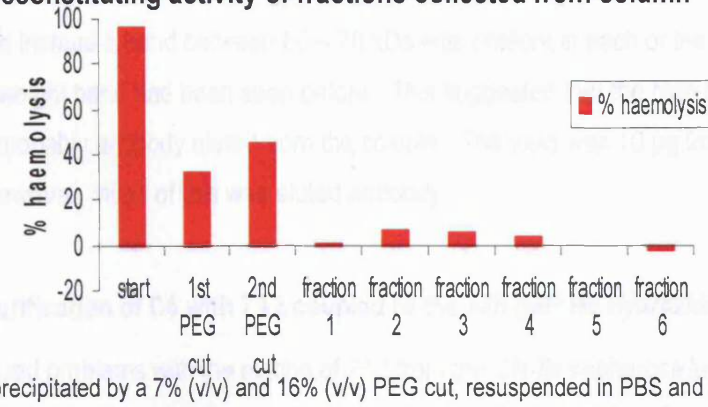

C6 was precipitated by a 7% (v/v) and 16% (v/v) PEG cut, resuspended in PBS and applied to the 7A2 coupled CNBr-activated sepharose column. The breakthrough was reserved and the column washed with PBS. C6 was eluted from the column with 0.5% DEA in PBS and protein containing fractions collected. These were subject to a haemolytic assay using C6D rat serum.

B. Coomassie staining

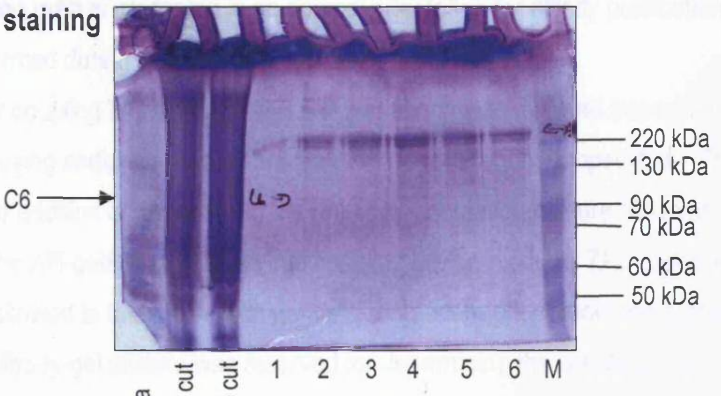

C. Western Blot

Equal volumes of samples collected at each purification step of affinity purification using the anti-C6 antibody, 7A2, coupled to cyanogen bromide sepharose were run under non-reducing conditions on a 7.5% SDS PAGE gel and either **B.** stained with coomassie blue reagent or **C.** blotted onto nitrocellulose. Protein was probed with the rabbit anti-rabbit C6 polyclonal antibody R1075 (1:1000) and goat anti-rabbit Ig-HRPO (1:1000) as a secondary antibody. Bands were detected with ECL and visualised by autoradiography. M - protein molecular weight markers.

of approximately 220 kDa. A faint band of 100 kDa corresponding to C6 was visible in fraction 2 and the haemolytic assay data confirmed that this was functionally active. In a subsequent experiment, the fractions were subject to SDS-PAGE electrophoresis under reducing conditions and stained with coomassie blue (Figure 3.6). The 220 kDa high molecular weight band was not present and instead a band between 60 – 70 kDa was present in each of the wells where the high molecular weight band had been seen before. This suggested that the high molecular weight band was probably antibody eluted from the column. The yield was 10 µg from 200 ml starting material, however, much of this was eluted antibody.

3.3.2.2. Purification of C6 with 7A2 coupled to the Affi-gel® Hz hydrazide matrix

The continued problems with the elution of 7A2 from the CN-Br sepharose led to the search for alternative matrices to couple 7A2. Affi-gel® Hz hydrazide gel forms covalent hydrazone bonds with oxidized carbohydrates, which are present in the F_c region of IgG isotype mAbs. This is advantageous as the mAb is presented in an optimal orientation for affinity purification and the hydrazone bond formed during coupling is very stable.

To prepare 7A2 for coupling to the Affi-gel®, 3.5 mg antibody was dialysed into coupling buffer and then oxidised using sodium periodate solution for 1 hour at room temperature. The reaction was stopped by the addition of glycerol and the antibody-containing mixture dialysed against coupling buffer. The Affi-gel® was washed into coupling buffer, oxidised 7A2 added and the coupling reaction allowed to take place with gentle mixing overnight at room temperature. The eluant from the antibody-gel mixture was reserved for determining the coupling efficiency, which was 67.7%. The column was washed with 20 mM Kphosphate buffer, 0.5M NaCl, 0.02% (v/v) NaN_3, which removed some of the antibody, reducing the coupling efficiency to 45.2%. The column was stored in this buffer at 4˚C until required.

From a starting volume of 250 ml, plasma was PEG-precipitated and subjected to affinity chromatography (described in section 3.2.1.). Throughout this process, material was retained at each step for analysis to assess functional activity by reconstitution of C6 deficient serum in a haemolytic assay and purity by SDS-PAGE and western blot in parallel under non-reducing conditions, shown in Figures 3.7a, b and c respectively. For the reconstitution assay, 1 µl of test sample was added to 50 µl C6 deficient serum diluted 1 in 200 in CFD and incubated together with 50 µl 2% sheep EA for 30 minutes at 37˚C. Fractions 2 - 15 had abundant haemolytic activity, peaking at 41.4% haemolysis in fraction 6. Owing to the complex nature of the sample, the C6 PEG enriched supernatant, C6 PEG enriched pellet and breakthrough from the column

Figure 3.6 Analysis of reduced samples from Figure 3.5 by SDS-PAGE

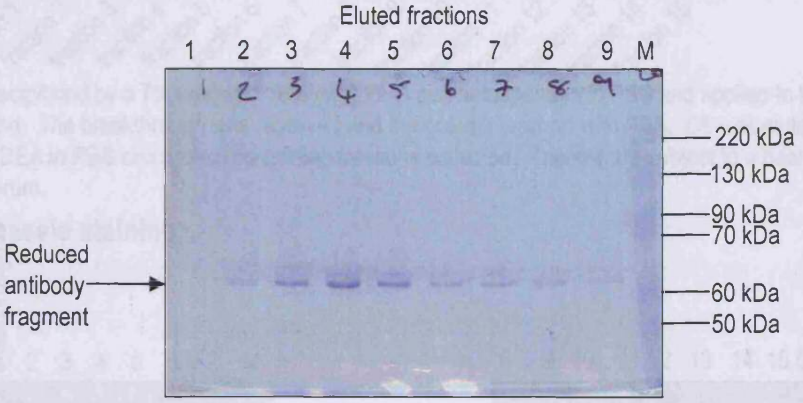

Twenty microlitres of each fraction eluted from the affinity column comprising the anti-C6 antibody 7A2, coupled to cyanogen bromide sepharose were run under reducing conditions on a 7.5% SDS PAGE gel and stained with coomassie blue reagent. M - protein molecular weight markers.

Figure 3.7 Purification of human C6 using affinity chromatography: 7A2 coupled to Affi-gel® Hz hydrazide gel

A. C6 reconstituting activity of fractions collected from column

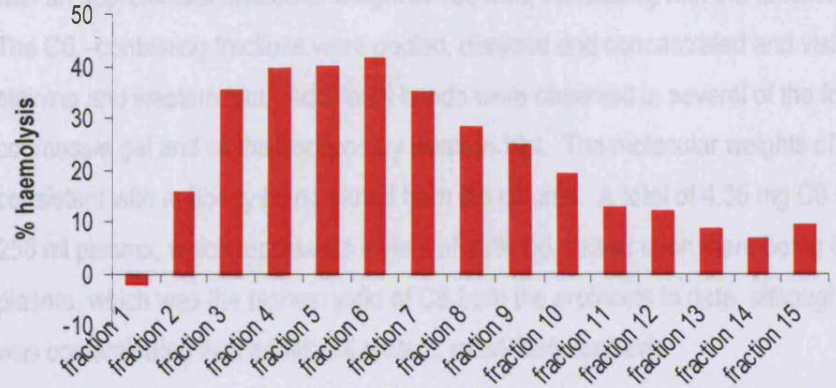

C6 was precipitated by a 7% (v/v) and 16% (v/v) PEG cut, resuspended in PBS and applied to the 7A2 coupled affi-gel® column. The breakthrough was reserved and the column washed with PBS. C6 was eluted from the column with 0.5% DEA in PBS and protein containing fractions collected. These were subject to a haemolytic assay using C6D rat serum.

B. Coomassie staining

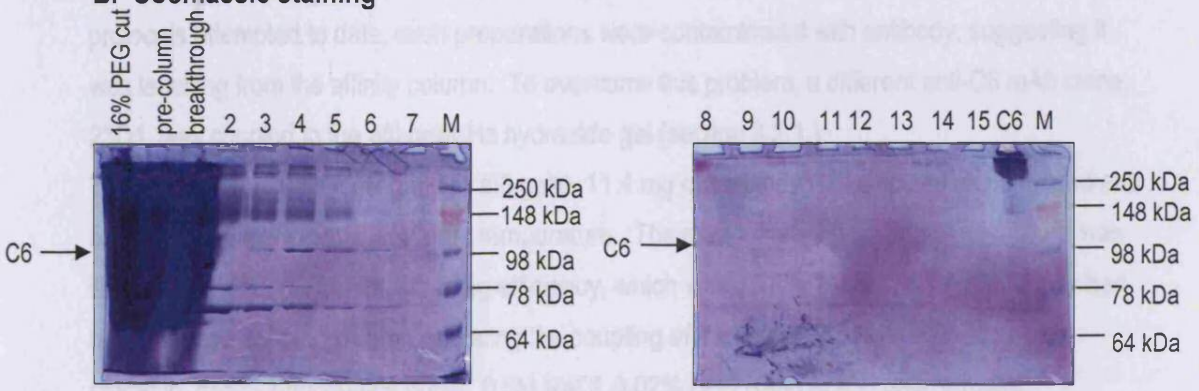

C. Western blot

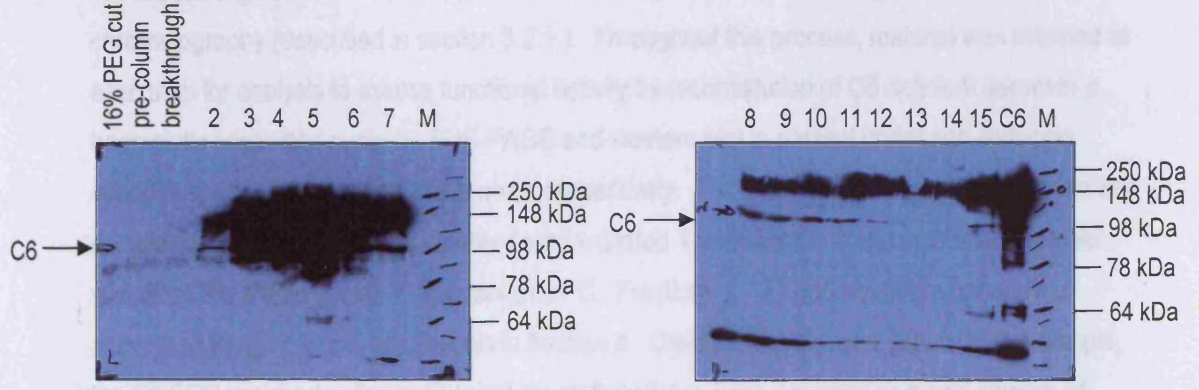

Samples collected at each purification step: resuspended C6 enriched pellet following 16% PEG cut, C6 enriched supernatant after removal of particular debris by centrifugation, breakthrough from column, fractions 2 – 7 collected from column, (M) protein molecular weight markers, fractions 8 – 15 collected from column, purified pooled C6, (M) protein molecular weight markers and run under non-reducing conditions on 7.5% SDS PAGE gel and either **B.** stained with coomassie blue reagent or **C.** blotted onto nitrocellulose. Protein was probed with mouse anti-human C6 mAb 23D1 (1 μg/ml) (developed in section 4.3.4.) and goat anti-mouse Ig-HRPO (1:2000) as a secondary antibody. Bands were detected with ECL and visualised by autoradiography.

are seen as broad smears of proteins with no discernable band corresponding to C6 either on the coomassie stained gel or the western blot. Although C6 was not the major band, it was clearly visible in fractions 3-8 on the coomassie gel and detectable by western blot in fractions 2 – 12, with an approximate molecular weight of 100 kDa, correlating with the functional data obtained. The C6 –containing fractions were pooled, dialysed and concentrated and visible by coomassie staining and western blot. Additional bands were observed in several of the fractions on the coomassie gel and all the fractions by western blot. The molecular weights of these bands were consistent with antibody being eluted from the column. A total of 4.35 mg C6 was purified from 250 ml plasma, which represents a yield of 22% C6, based upon there being 80 mg/L C6 in plasma, which was the highest yield of C6 from the protocols to date, although the preparation was contaminated with additional protein, most likely antibody.

3.3.2.3. Purification of C6 with 23D1 coupled to the Affi-gel® Hz hydrazide matrix

Although the coupling of 7A2 to affi-gel® had yielded the greatest amount of purified C6 from the protocols attempted to date, such preparations were contaminated with antibody, suggesting it was leaching from the affinity column. To overcome this problem, a different anti-C6 mAb clone, 23D1, was coupled to the affi-gel® Hz hydrazide gel (section 3.2.1.).

To prepare 23D1 for coupling to the affi-gel®, 11.4 mg of antibody was oxidised as described and allowed to couple overnight at room temperature. The eluant from the antibody-gel mixture was reserved for determining the coupling efficiency, which was 60.3%. After washing, antibody had been washed from the column, reducing the coupling efficiency to 34.3%. The column was stored in 20 mM Kphosphate buffer, 0.5M NaCl, 0.02% (v/v) NaN_3 at 4°C until required.

From a starting volume of 200 ml, plasma was PEG-precipitated and subjected to affinity chromatography (described in section 3.2.1.). Throughout this process, material was retained at each step for analysis to assess functional activity by reconstitution of C6 deficient serum in a haemolytic assay and purity by SDS-PAGE and western blot in parallel under non-reducing conditions, shown in Figures 3.8a,b and c respectively. For the reconstitution assay, 10 µl of test sample was added to 50 µl C6 deficient serum diluted 1 in 200 in CFD and incubated together with 50 µl 2% sheep EA for 30 minutes at 37°C. Fractions 2 - 21 had abundant haemolytic activity, peaking at 29.8% haemolysis in fraction 4. Owing to the complex nature of the sample, the C6 PEG enriched pellet and breakthrough from the column are seen as broad smears of proteins with no discernable band corresponding to C6 on the coomassie stained gel. C6 was the major band in fractions 2 – 18 on the coomassie stained gel and fractions 2 – 20 by western

Figure 3.8 Purification of human C6 using affinity chromatography: 23D1 coupled to Affi-gel® Hz hydrazide gel

A. C6 reconstituting activity of fractions collected from column

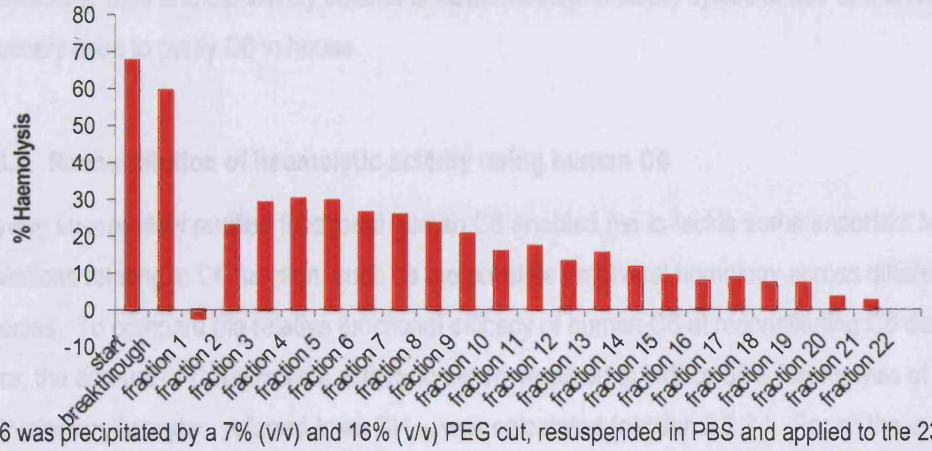

C6 was precipitated by a 7% (v/v) and 16% (v/v) PEG cut, resuspended in PBS and applied to the 23D1 coupled affi-gel® column. The breakthrough was reserved and the column washed with PBS. C6 was eluted from the column with 0.5% DEA in PBS and protein containing fractions collected. These were subject to a haemolytic assay using C6D rat serum.

B. Coomassie staining

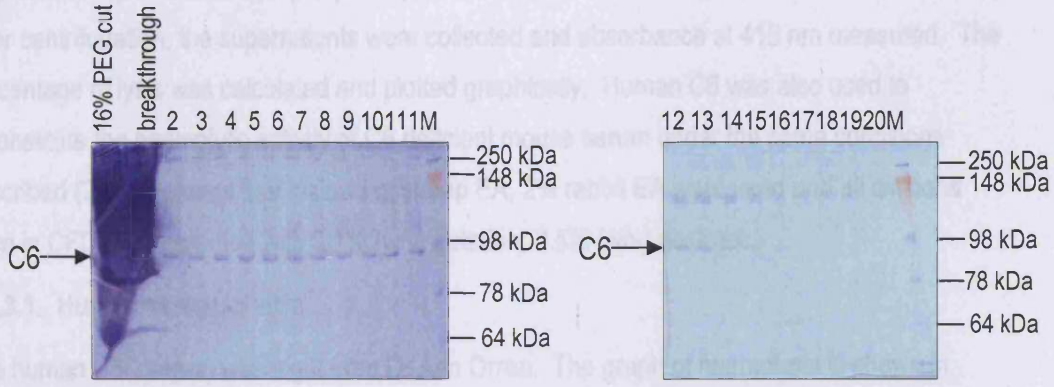

C. Western Blotting

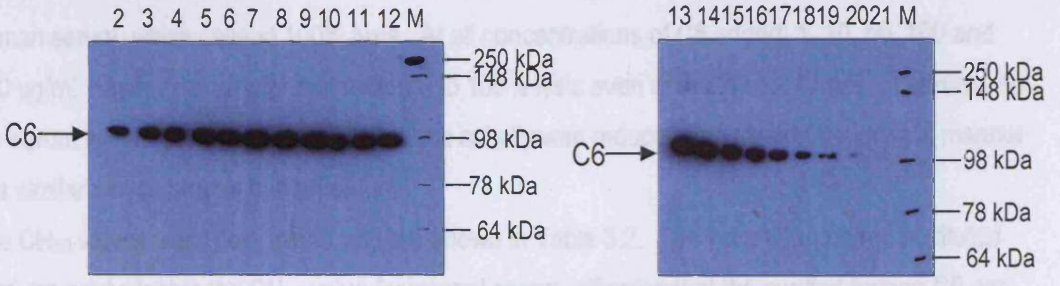

Samples collected at each purification step **B.** resuspended C6 enriched pellet following 16% PEG cut, breakthough collected from column, fractions 2 – 11 collected from column, (M) protein molecular weight markers, fractions 12 – 20 collected from column, (M) protein molecular weight markers and run under non-reducing conditions on 7.5% SDS PAGE gel and stained with coomassie blue reagent. **C.** Samples were blotted onto nitrocellulose after being subject to SDS-PAGE, fractions 2 – 12 collected from column, (M) protein molecular weight markers, fractions 13 – 21 collected from the column, (M) protein molecular weight markers. Protein was probed with mouse anti-human C6 mAb 27B1 (1 μg/ml) and goat anti-mouse Ig-HRPO (1:2000) as a secondary antibody. Bands were detected with ECL and visualised by autoradiography.

blot, with a molecular weight of 100 kDa, correlating with the functional data obtained. A total of 3.95 mg C6 was purified from 200 ml plasma, representing a yield of 25% C6 based upon there being 80 mg/L of C6 in plasma. This was the largest amount of C6 yielded from the purification protocols to date and the affinity column is stable through multiple cycles of use and is now routinely used to purify C6 in house.

3.3.3. Reconstitution of haemolytic activity using human C6

Having successfully purified functional human C6 enabled me to tackle some important biological questions relating to C6 function, such as the possible functional homology across different species. To compare the relative functional efficacy of human C6 at reconstituting C6 deficient sera, the amount of C haemolytic activity in serum required to induce 50% haemolysis of activated erythrocytes, referred to as CH_{50}, was calculated (section 3.2.3.). For all the in vitro reconstitution assays, 10 µl C6 (1 – 200 µg/ml final concentration) was added to 50 µl C6 deficient serum (human, rabbit or rat) diluted 1 in 5 – 1 in 640 in CFD and incubated together with 50 µl 2% sheep activated sheep erythrocytes for 30 minutes at 37°C (described in section 2.4.4.). After centrifugation, the supernatants were collected and absorbance at 415 nm measured. The percentage of lysis was calculated and plotted graphically. Human C6 was also used to reconstitute the haemolytic activity of C6 deficient mouse serum under the same conditions described (2.4.4.), except that instead of sheep EA, 2% rabbit EA were used and all dilutions were in CFD supplemented with 0.1% (w/v) gelatine, 2.5% (w/v) dextrose.

3.3.3.1. Human serum in vitro

The human C6D serum was a gift from Dr Ann Orren. The graph of haemolysis is shown in Figure 3.9. C6-deficient serum had no detectable haemolytic activity, in comparison to normal human serum, which caused 100% lysis. At all concentrations of C6 added; 1, 10, 50, 100 and 200 µg/ml, haemolytic activity was restored to 100% lysis even at the lowest dilution of serum. As the serum was further diluted, the haemolytic activity was reduced in a dilution dependent manner in a similar way to normal human serum.

The CH_{50} values were determined and are shown in Table 3.2. The values for the reconstituted sera are equivalent to the CH_{50} value for normal serum, affirming that the purified human C6 can restore full C haemolytic activity to C6D human serum and that C6 is not a limiting component for C lysis. This is in agreement with other studies [501,502].

Figure 3.9 The reconstitution of human C6 deficient serum with purified human C6

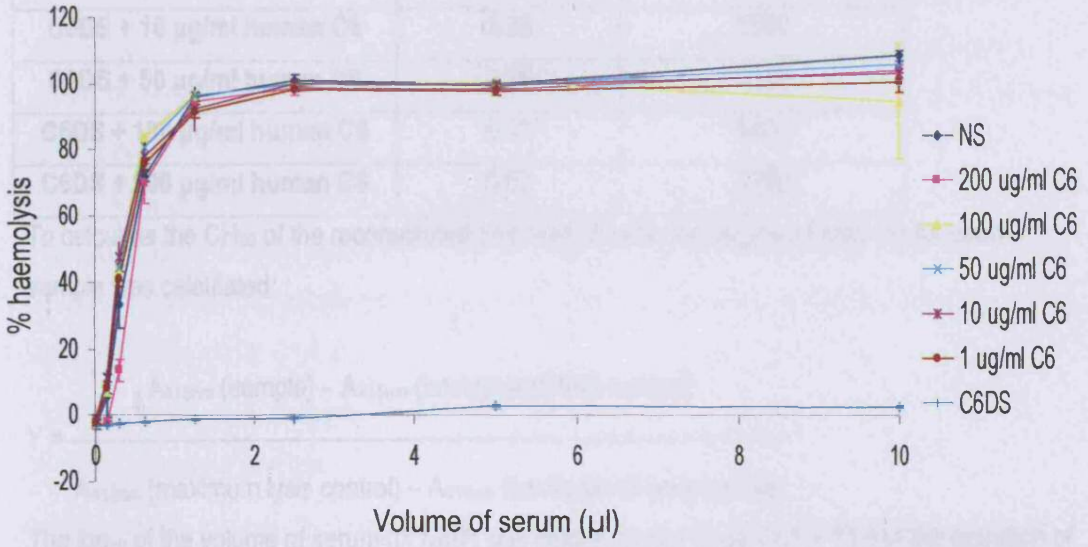

The ability of purified human C6 to reconstitute C-mediated lytic activity to genetically C6 deficient human serum was investigated in a haemolytic assay. In a round-bottomed 96-well plate, C6 deficient serum (50 µl), diluted over the range 1 in 5 – 1 in 640 was reconstituted with 10 µl purified human C6 to give final concentrations of: 1µg/ml, 10 µg/ml, 50 µg/ml, 100 µg/ml or 200 µg/ml C6. 2% sheep EA (50 µl) was added to each well and the plate incubated at 37°C for 30 minutes. After centrifugation, the supernatants were collected and transferred to a flat-bottomed plate and the absorbance measured at 415 nm. For comparison, unreconstituted C6 deficient serum and normal human serum were also included in the assay. For each dose of C6 used to reconstitute the C6 deficient serum, the percentage of haemolysis was calculated and plotted on the graph above. Each data point represents the mean of value +/- standard deviation of the mean of a single experiment performed in triplicate.

Table 3.2 Calculation of X_{50} and CH_{50} values of C6 deficient human serum reconstituted with purified human C6.

Sample	X_{50} (µl serum)	CH_{50}
Normal human serum	0.44	4540
C6 deficient serum (C6DS)	-	-
C6DS + 1 µg/ml human C6	0.41	4880
C6DS + 10 µg/ml human C6	0.36	5560
C6DS + 50 µg/ml human C6	0.36	5560
C6DS + 100 µg/ml human C6	0.37	5400
C6DS + 200 µg/ml human C6	0.53	3780

To calculate the CH_{50} of the reconstituted and normal sera, the degree of lysis (Y) for each sample was calculated:

$$Y = \frac{A_{415nm}\text{ (sample)} - A_{415nm}\text{ (background lysis control)}}{A_{415nm}\text{ (maximum lysis control)} - A_{415nm}\text{ (background lysis control)}}$$

The $\log_{10}$ of the volume of serum (µl /well) was plotted against $\log_{10}$ (Y/1 – Y) and the equation of the line determined. At 50% haemolysis, the Y-axis, $\log_{10}$ (Y/1-Y) = 0. The equation of the line was then used to calculate the value of $\log_{10}X$ at $\log_{10}$(Y/1-Y) = 0, which is the $\log_{10}$ of the X_{50}. The antilog (10^{X50}) was calculated, giving the X_{50} for that serum sample. The CH_{50} was calculated according to the equation:

$$CH_{50} = \frac{1}{X_{50}} \times 2000$$

3.3.3.2. Rabbit serum in vitro

To determine whether purified human C6 could reconstitute haemolytic activity to C6 deficient rabbit serum, human C6 was incubated with C6 deficient rabbit serum. The percentage of lysis was calculated and plotted graphically, shown in Figure 3.10.

Unreconstituted C6-deficient serum had no detectable haemolytic activity, in comparison to normal rabbit serum, which caused 50% lysis. At concentrations between 50 – 200 µg/ml C6 added haemolytic activity was restored to an either equal or greater level than that for normal serum. When the serum was reconstituted with 1 or 10 µg/ml C6, haemolysis occurred at a lower level than that for normal serum.

The CH_{50} values were calculated and these values are shown in Table 3.3. The CH_{50} values for the reconstituted sera are equivalent to the CH_{50} value for normal rabbit serum, affirming that the purified human C6 can restore full C haemolytic activity to C6D rabbit serum and that C6 is not a limiting component for C lysis.

3.3.3.3. Rat serum in vitro

Purified human C6 was incubated with C6 deficient rat serum to determine whether it could reconstitute C-mediated haemolytic activity of C6 deficient rat serum. A graph of the percentage of haemolysis is shown in Figure 3.11. C6-deficient rat serum had no detectable haemolytic activity, in comparison to normal rat serum, which caused 100% lysis. At all concentrations of C6 added, 1 – 200 µg/ml, the haemolytic activity of the serum was restored to a level equivalent to normal serum.

The CH_{50} values were calculated and these values are shown in Table 3.4. The CH_{50} value for the unreconstituted C6D rat serum is close to zero, whilst the CH_{50} values for the reconstituted serum are either equivalent to or greater than the CH_{50} values for normal rat serum, confirming that the purified human C6 can restore full C haemolytic activity to C6D rat serum and that C6 is not a limiting component for C lysis.

3.3.3.4. Mouse serum in vitro

The ability of purified human C6 to reconstitute C-mediated haemolytic activity of C6 deficient mouse serum was also addressed. The percentage of lysis was calculated and plotted on a graph (Figure 3.12).

Figure 3.10 The reconstitution of rabbit C6 deficient serum with purified human C6

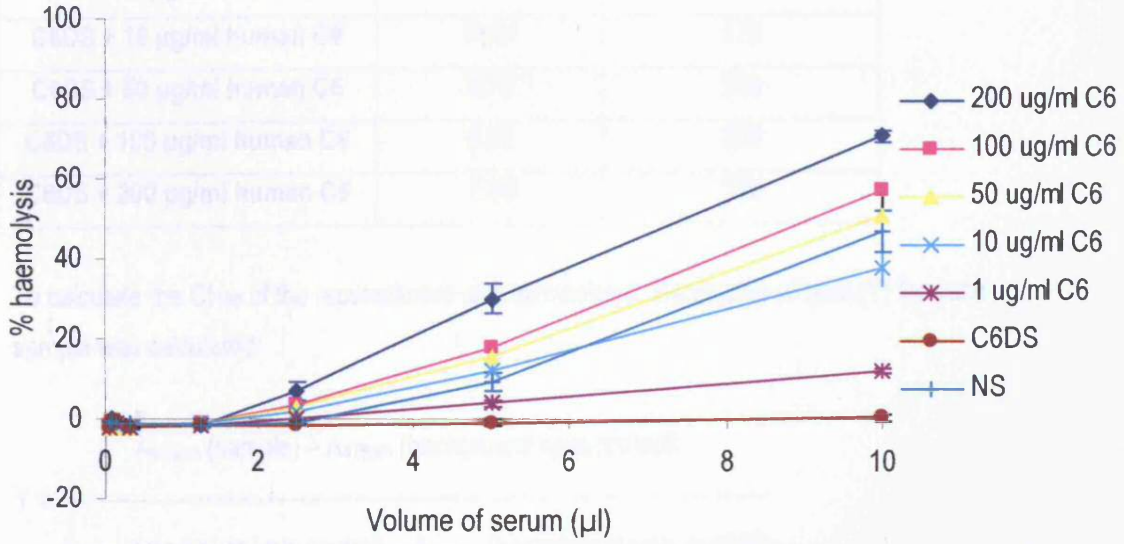

The ability of purified human C6 to reconstitute C-mediated lytic activity to genetically C6 deficient rabbit serum was investigated in a haemolytic assay. In a round-bottomed 96-well plate, C6 deficient serum (50 µl), diluted over the range 1 in 5 – 1 in 640 was reconstituted with 10 µl purified human C6 to give final concentrations of: 1µg/ml, 10 µg/ml, 50 µg/ml, 100 µg/ml or 200 µg/ml C6. 2% sheep EA (50 µl) was added to each well and the plate incubated at 37°C for 30 minutes. After centrifugation, the supernatants were collected and transferred to a flat-bottomed plate and the absorbance measured at 415 nm. For comparison, unreconstituted C6 deficient serum and normal rabbit serum were also included in the assay. For each dose of C6 used to reconstitute the C6 deficient serum, the percentage of haemolysis was calculated and plotted on the graph above. Each data point represents the mean of value +/- standard deviation of the mean of a single experiment performed in triplicate.

Table 3.3 Calculation of X_{50} and CH_{50} values of C6 deficient rabbit serum reconstituted with purified human C6.

Sample	X_{50} (µl serum)	CH_{50}
Normal rabbit serum	10.38	194
C6 deficient serum (C6DS)	-	-
C6DS + 1 µg/ml human C6	*	*
C6DS + 10 µg/ml human C6	11.41	176
C6DS + 50 µg/ml human C6	9.72	200
C6DS + 100 µg/ml human C6	8.82	220
C6DS + 200 µg/ml human C6	7.06	280

To calculate the CH_{50} of the reconstituted and normal sera, the degree of lysis (Y) for each sample was calculated:

$$Y = \frac{A_{415nm}\text{ (sample)} - A_{415nm}\text{ (background lysis control)}}{A_{415nm}\text{ (maximum lysis control)} - A_{415nm}\text{ (background lysis control)}}$$

The $\log_{10}$ of the volume of serum (µl /well) was plotted against $\log_{10}$ (Y/1 – Y) and the equation of the line determined. At 50% haemolysis, the Y-axis, $\log_{10}$ (Y/1-Y) = 0. The equation of the line was then used to calculate the value of $\log_{10}X$ at $\log_{10}$(Y/1-Y) = 0, which is the $\log_{10}$ of the X_{50}. The antilog (10^{X50}) was calculated, giving the X_{50} for that serum sample. The CH_{50} was calculated according to the equation:

$$CH_{50} = \frac{1}{X_{50}} \times 2000$$

* It was not possible to calculate the CH_{50} for reconstitution with 1 µg/ml human C6 as the raw data gave negative results when attempting to calculate log values.

Figure 3.11 The reconstitution of rat C6 deficient serum with purified human C6

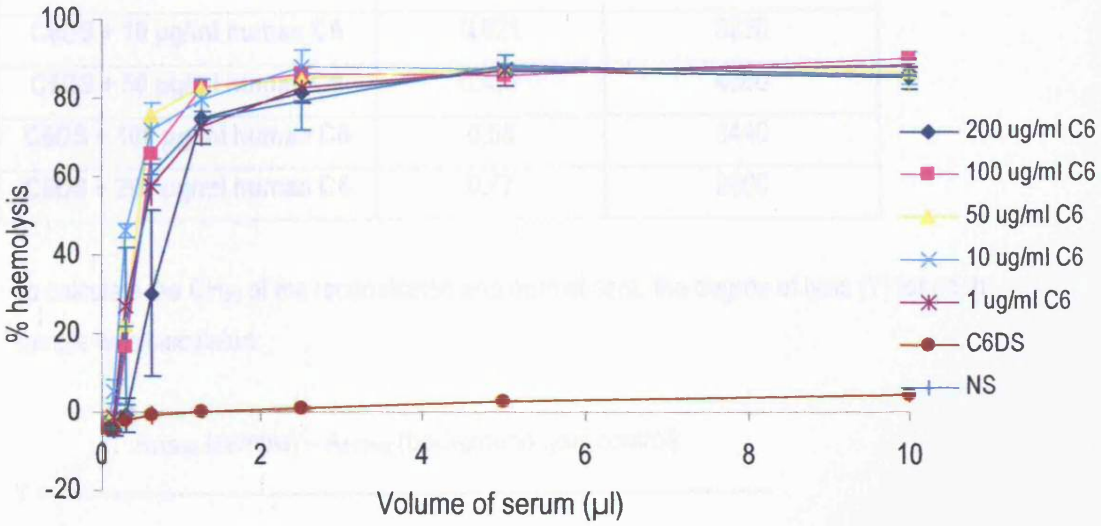

The ability of purified human C6 to reconstitute C-mediated lytic activity to genetically C6 deficient rat serum was investigated in a haemolytic assay. In a round-bottomed 96-well plate, C6 deficient serum (50 µl), diluted over the range 1 in 5 – 1 in 640 was reconstituted with 10 µl purified human C6 to give final concentrations of: 1µg/ml, 10 µg/ml, 50 µg/ml, 100 µg/ml or 200 µg/ml C6. 2% sheep EA (50 µl) was added to each well and the plate incubated at 37°C for 30 minutes. After centrifugation, the supernatants were collected and transferred to a flat-bottomed plate and the absorbance measured at 415 nm. For comparison, unreconstituted C6 deficient serum and normal rat serum were also included in the assay. For each dose of C6 used to reconstitute the C6 deficient serum, the percentage of haemolysis was calculated and plotted on the graph above. Each data point represents the mean of value +/- standard deviation of the mean of a single experiment performed in duplicate.

Table 3.4 Calculation of X_{50} and CH_{50} values of C6 deficient rat serum reconstituted with purified human C6.

Sample	X_{50} (µl serum)	CH_{50}
Normal rat serum	0.686	2920
C6 deficient serum (C6DS)	84.1	20
C6DS + 1 µg/ml human C6	0.567	3520
C6DS + 10 µg/ml human C6	0.621	3220
C6DS + 50 µg/ml human C6	0.457	4380
C6DS + 100 µg/ml human C6	0.58	3440
C6DS + 200 µg/ml human C6	0.77	2600

To calculate the CH_{50} of the reconstituted and normal sera, the degree of lysis (Y) for each sample was calculated:

$$Y = \frac{A_{415nm}\text{ (sample)} - A_{415nm}\text{ (background lysis control)}}{A_{415nm}\text{ (maximum lysis control)} - A_{415nm}\text{ (background lysis control)}}$$

The $\log_{10}$ of the volume of serum (µl /well) was plotted against $\log_{10}$ (Y/1 – Y) and the equation of the line determined. At 50% haemolysis, the Y-axis, $\log_{10}$ (Y/1-Y) = 0. The equation of the line was then used to calculate the value of $\log_{10}X$ at $\log_{10}(Y/1-Y) = 0$, which is the $\log_{10}$ of the X_{50}. The antilog (10^{X50}) was calculated, giving the X_{50} for that serum sample. The CH_{50} was calculated according to the equation:

$$CH_{50} = \frac{1}{X_{50}} \times 2000$$

Figure 3.12 The reconstitution of mouse C6 deficient serum with purified human C6

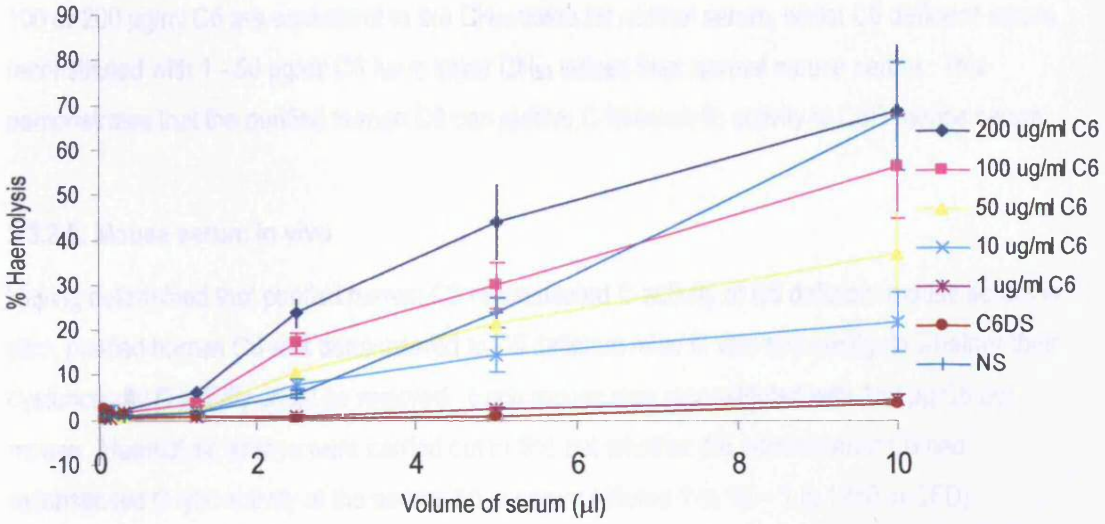

The ability of purified human C6 to reconstitute C-mediated lytic activity to genetically C6 deficient mouse serum was investigated in a haemolytic assay. In a round-bottomed 96-well plate, C6 deficient serum (50 µl), diluted over the range 1 in 5 – 1 in 640 was reconstituted with 10 µl purified human C6 to give final concentrations of: 1µg/ml, 10 µg/ml, 50 µg/ml, 100 µg/ml or 200 µg/ml C6. 2% sheep EA (50 µl) was added to each well and the plate incubated at 37°C for 30 minutes. After centrifugation, the supernatants were collected and transferred to a flat-bottomed plate and the absorbance measured at 415 nm. For comparison, unreconstituted C6 deficient serum and normal mouse serum were also included in the assay. For each dose of C6 used to reconstitute the C6 deficient serum, the percentage of haemolysis was calculated and plotted on the graph above. Each data point represents the mean of value +/- standard deviation of the mean of a single experiment performed in triplicate.

C6-deficient serum caused a maximum of 3.5% haemolysis and when reconstituted with 1 µg/ml C6 a similar level of lysis was caused - 4.4%. Normal mouse serum caused an average of 67% lysis and an equivalent amount of lysis occurred when the C6 deficient serum was reconstituted with 200 µg/ml purified human C6 - 68%. At concentrations between 10 – 100 µg/ml C6 added, haemolytic activity was restored to lower activity than normal mouse serum.
The calculated CH_{50} values are shown in Table 3.5. The CH_{50} values for sera reconstituted with 100 or 200 µg/ml C6 are equivalent to the CH_{50} value for normal serum, whilst C6 deficient serum reconstituted with 1 - 50 µg/ml C6 have lower CH_{50} values than normal mouse serum. This demonstrates that the purified human C6 can restore C haemolytic activity to C6D mouse serum.

3.3.3.5. Mouse serum in vivo

Having determined that purified human C6 reconstituted C activity of C6 deficient mouse serum in vitro, purified human C6 was administered to C6 deficient mice in vivo to investigate whether their dysfunctional C activity could be restored. Each mouse was reconstituted with 150 µg C6 per mouse. Haemolytic assays were carried out to find out whether the administered C6 had reconstituted C lytic activity of the serum, 50 µl serum (diluted 1 in 10 – 1 in 1280 in CFD) collected at each timepoint was incubated with 50 µl 2% rabbit EA for 30 minutes at 37˚C (section 2.4.). The percentage of lysis was plotted graphically (Figure 3.13).
As expected, C6-deficient mouse serum had no detectable haemolytic activity. Thirty minutes after the C6 had been administered to the mice the haemolytic activity of the serum had increased to 42.8% at the lowest dilution of serum. Two hours after the administration of C6, the haemolytic activity of the serum collected from the mice had increased to 62% at the lowest serum dilution. Twelve hours after the administration of C6, the haemolytic activity of the serum collected from the mice had increased further still to 100% at the lowest dilution of serum.
The CH_{50} values for the reconstituted sera at the collection timepoints were calculated and are shown in Table 3.6. The CH_{50} values for the reconstituted sera increase over the time course. This is in comparison to C6 deficient rats reconstituted with human C6, in which the reconstituted haemolytic activity was still detectable 24 hours after reconstitution, although it was decreasing [498]. It was anticipated that serum would have contained greatest haemolytic activity 30 minutes post administration of C6. One explanation for this may be that C6 was slowly absorbed from the peritoneum following the i.p. injection and that if the C6 had been injected intravenously, the expected results may have been obtained. Nevertheless, these data do demonstrate that the C lytic activity of C6 deficient mice can be reconstituted by the administration of human C6 and that

Figure 3.13 The reconstitution in vivo of C6 deficient mice with purified human C6

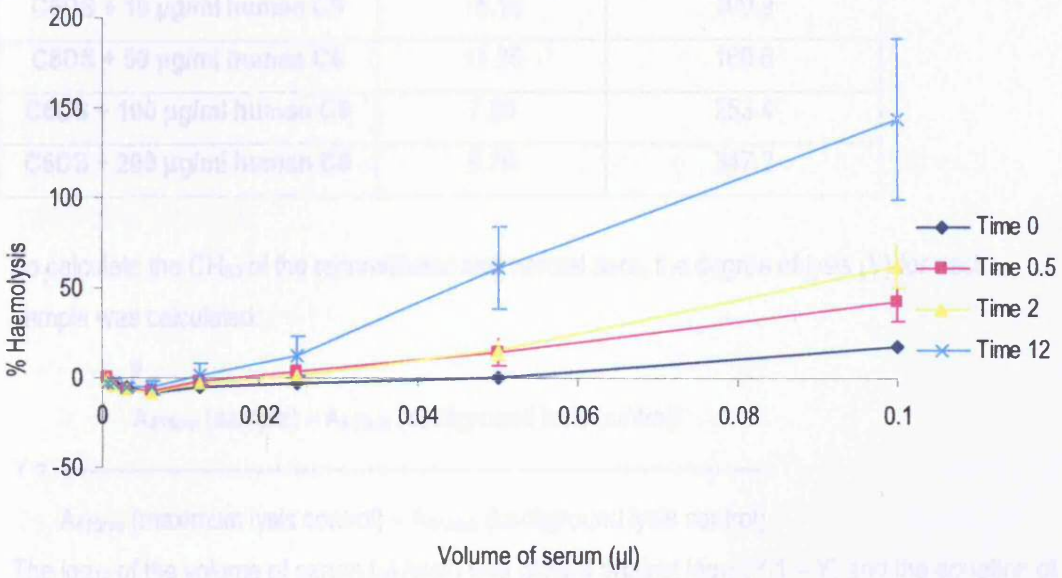

The ability of purified human C6 to reconstitute genetically C6 deficient mouse serum in vivo was investigated. Three hundred micrograms of purified human C6 was administered by i.p. injection to each mouse. Thirty minutes, two hours and twelve hours post C6 administration, blood was collected from each mouse and serum prepared. To determine whether the purified human C6 had reconstituted C activity in the C6 deficient mice, the collected serum was assessed in a haemolytic assay. In a round-bottomed 96-well plate, serum collected at each timepoint (50 µl), diluted over the range 1 in 10 – 1 in 1280 was incubated with 2% rabbit EA (50 µl) at 37°C for 30 minutes. After centrifugation, the supernatants were collected and transferred to a flat-bottomed plate and the absorbance measured at 415 nm. For comparison, serum collected from a C6 deficient mouse which had not received human C6 was also included in the assay. For each timepoint after the administration of purified human C6 to the C6 deficient mice, the percentage of haemolysis was calculated and plotted on the graph above. Each data point represents the mean of value +/- standard error of the mean of a single experiment performed in triplicate.

Table 3.5 Calculation of X_{50} and CH_{50} values of C6 deficient mouse serum reconstituted with purified human C6.

Sample	X_{50} (µl serum)	CH_{50}
Normal mouse serum	7.75	258.0
C6 deficient serum (C6DS)	-	-
C6DS + 1 µg/ml human C6	226.9	8.8
C6DS + 10 µg/ml human C6	18.19	109.9
C6DS + 50 µg/ml human C6	11.86	168.6
C6DS + 100 µg/ml human C6	7.89	253.4
C6DS + 200 µg/ml human C6	5.76	347.2

To calculate the CH_{50} of the reconstituted and normal sera, the degree of lysis (Y) for each sample was calculated:

$$Y = \frac{A_{415nm}\text{ (sample)} - A_{415nm}\text{ (background lysis control)}}{A_{415nm}\text{ (maximum lysis control)} - A_{415nm}\text{ (background lysis control)}}$$

The $\log_{10}$ of the volume of serum (µl /well) was plotted against $\log_{10}$ (Y/1 – Y) and the equation of the line determined. At 50% haemolysis, the Y-axis, $\log_{10}$ (Y/1-Y) = 0. The equation of the line was then used to calculate the value of $\log_{10}X$ at $\log_{10}(Y/1-Y) = 0$, which is the $\log_{10}$ of the X_{50}. The antilog (10^{X50}) was calculated, giving the X_{50} for that serum sample. The CH_{50} was calculated according to the equation:

$$CH_{50} = \frac{1}{X_{50}} \times 2000$$

Table 3.6 Calculation of X_{50} of serum collected from C6 deficient mice after reconstitution with purified human C6.

Sample	X_{50} (µl serum)	CH_{50}
0 hours	-	-
0.5 hours	5.78	340
2 hours	4.28	460
12 hours	2.2	900

To calculate the CH_{50} of the reconstituted and normal sera, the degree of lysis (Y) for each sample was calculated:

$$Y = \frac{A_{415nm}\text{ (sample)} - A_{415nm}\text{ (background lysis control)}}{A_{415nm}\text{ (maximum lysis control)} - A_{415nm}\text{ (background lysis control)}}$$

The $\log_{10}$ of the volume of serum (µl /well) was plotted against $\log_{10}$ (Y/1 – Y) and the equation of the line determined. At 50% haemolysis, the Y-axis, $\log_{10}$ (Y/1-Y) = 0. The equation of the line was then used to calculate the value of $\log_{10}X$ at $\log_{10}$(Y/1-Y) = 0, which is the $\log_{10}$ of the X_{50}. The antilog (10^{X50}) was calculated, giving the X_{50} for that serum sample. The CH_{50} was calculated according to the equation:

$$CH_{50} = \frac{1}{X_{50}} \times 2000$$

the C6 retains its functional activity in the circulation for at least twelve hours after the administration of the C6.

3.4. Discussion

This chapter describes and compares methods for C6 purification and culminates in the development of a fast, reliable purification protocol for human C6 that is now routinely used within the department. The purified human C6 was free of contaminating proteins, including other C proteins and was shown to be functionally active in restoring C-induced lysis in C6D human serum. In addition, the cross-species activity of the purified human C6 was also investigated. In vitro haemolytic assays demonstrated that human C6 was effective in restoring C activity in C6 deficient rat, rabbit and mouse sera. This effect was also tested in vivo when C activity in C6 deficient mice was fully restored for at least 12 hours post administration of human C6 (300 µg) by i.p. injection.

Classical methods for C6 purification involved several chromatographic steps typically taking 7-10 days for completion. The isolated C6 had a molecular weight of 100 kDa and an additional protein band at approximately 70 kDa, both detectable on Coomassie stained polyacrylamide gels and by western blot. Typically the yield of C6 was 0.56 mg from a starting serum of 1 L. The expected yield (based on a normal serum range of 80 µg/ml (equivalent to 80 mg/L of C6) from 1L of serum, if 100% C6 was purified would be 80 mg. This discrepancy highlights that the process was very inefficient, with more than 99% of C6 available in plasma being lost during purification. In addition to the poor yield, there was also some evidence of C6 degradation, as highlighted by western blot analysis (Figure 3.2) in which the mAb WU 6.4 stained two bands, one at 100 kDa and a smaller band at 70 kDa. This smaller C6 fragment was co-purified with full length C6, suggesting that these molecules shared the same ionic properties even though they had different molecular weights. It is unclear whether C6 was already degraded in the expired plasma or whether it degraded during the purification procedure, even though preventative measures, such as including protease inhibitors and carrying out the process at 4˚C were taken. However, the process took several days and pure, concentrated proteins are always more stable than proteins at low concentration in complex mixtures; the protein concentration of the preparation decreased during the procedure. In other studies, samples containing C6 in serum, which is a complex, concentrated protein mixture, have been left at room temperature apparently without deleterious effects [499,503].

Due to the poor yield and degradation of C6 using classical purification methods, affinity chromatographic methods were attempted. The mAb 7A2 was first coupled to CN-Br activated sepharose, leading to the isolation of C6 as detected by SDS-PAGE with Coomassie staining and western blot with a band of 100 kDa. However, the major protein eluted from the column had a molecular weight of 220 kDa and upon reduction several bands were observed with molecular weights consistent with antibody, suggesting that it was leaching from the column. The mAb 7A2 was then coupled to Affi-gel™ leading to the isolation of functional C6, with a molecular weight of 100 kDa, detectable by SDS-PAGE with Coomassie staining and western blot. From a starting volume of 250 ml, 4.35 mg of C6 was purified, representing a yield of 22% - a significant improvement on all previous attempts at purifying C6. However, contaminating protein was present, again consistent with antibody leaching from the column. This suggested that the antibody leaching was occurring not due to the properties of the column matrix but due to the properties of the antibody itself. Finally, the mAb 23D1 (developed in section 4.3.4.) was coupled to Affi-gel™ and a single band of 100 kDa, detectable by SDS-PAGE and western blot was purified, with no contamination. From a starting volume of 200 ml, 3.95 mg of C6 was purified, representing a yield of 25%. This was the highest yielding protocol for C6 purification and the mAb was stable on the column. This method has now become the routine method for C6 purification in house.

The concentration of C6 in the serum of healthy individuals varies widely, ranging between 20 – 80 µg/ml [499]. Patients with C6 levels between 0.3 – 3.0 µg/ml are classified as having a subtotal C6 deficiency (C6SD) [499] and those in which C6 is undetectable or the levels are below 0.3 µg/ml are considered to be totally C6 deficient (C6Q0) [499,503]. C6Q0 individuals are susceptible to Neisserial infections, but patients with C6SD are not [503], even though levels of C6 in their serum are very low. The concentrations of C6 used to reconstitute C6Q0 serum in this study ranged from 1 – 200 µg/ml, a range that covered the abnormally low levels of C6 detected in C6SD patients, normal C6 levels and abnormally high levels of C6. The added C6 reconstituted haemolytic activity of the C6Q0 serum to similar levels of normal human serum at all concentrations tested. Taken together with the literature that C6SD individuals are not susceptible to Neisserial infections and the C6 they produce is functionally active [499] these findings suggests that even very low levels of C6 are sufficient to afford protection against such diseases. These data suggest that in the human terminal pathway C6 concentration cannot be limiting, considering that the range of C6 concentrations used in these assays resulted in similar levels of haemolysis. However, these results are not directly comparable to published analyses of C6SD patients [503] as the haemolytic assays were carried out in a different way. It was also

found that all of the C6SD patients tested made a truncated form of C6 only, with a molecular weight of 85 kDa and it is possible that this form of C6 does not have the same activities as normal C6, although it has been shown that it is bactericidally active [500].

The reconstitution assays demonstrate that human C6 can be used to reconstitute not only human C6 deficient serum, but also C6 deficient serum from mice, rats and rabbits. It has previously been shown that the rat C6 sequence is 82% homologous to the human C6 sequence [485] whilst the mouse C6 amino acid sequence is 75% homologous to the human C6 sequence [504] and the data presented here showed there is functional equivalence of C6 between the species tested, even though the molecular weights of mouse and rat C6 differ from that of human C6 [485,505-507]. In addition to their sequence similarity, mouse and human C6 share a similar modular structure. All C6 sufficient mice produce C6A which has a molecular weight of 91 kDa and lacks the factor I modules (FIMs) of human C6 [504]. Some mouse strains produce additional forms of C6, designated C6B and C6C with molecular weights of 107 kDa and 91 – 107 kDa [504-507]. Rat C6 has a molecular weight of approximately 90 kDa [485]. Following the discovery of a strain of C6 deficient rats (PVG/C6$^-$) [508], the strain was characterised [485]. Full length human C6 cDNA was used as a probe to clone rat C6 from a C6 sufficient strain rat liver cDNA library for comparative purposes. Confirmation of the identity of the putative rat C6 cDNA sequence was based upon homology with the human C6 cDNA sequence, demonstrating the sequence similarity between C6 of the two species. Currently, nothing has been published regarding the sequence of rabbit C6. Genetically C6-deficient rabbits were identified over 40 years ago [486]; this deficiency arises as a result of a single gene defect that is not known to be associated with other genetic abnormalities [509]. C6 deficient rabbits have been used in various disease models, such as investigating the influence of C5b-9 on reperfusion injury [510]. C6 deficient rabbit serum has also been reconstituted with human C6 [501], demonstrating that there is functional homology between rabbit and human C6.

Purified human C6 has previously been used successfully in vivo in two studies to reconstitute PVG/C6$^-$ rats in models of disease [274,498]. In the study by Mead et al [498], a model of human demyelinating multiple sclerosis was induced in C6 sufficient and deficient rats. C6-deficient rats displayed no demyelination and had a reduced clinical score in comparison to the C6 sufficient rats. Reconstitution of the C6-deficient rats with human C6 at a dose of 8 mg/kg restored serum haemolytic activity to 70 – 100% of that in C6 sufficient rats for at least 24 hours and induction of disease resulted in pathology indistinguishable from that of the C6 sufficient rats. In the C6 reconstitution in vivo experiment in mice in the current study, haemolytic activity took time to be restored after C6 had been administered and was only fully restored at the last time point taken,

12 hours after C6 had been administered. On first inspection, the time taken for haemolytic activity to be restored seems to be a long time – however, the C6 had been administered by i.p. injection meaning that it would have to enter the bloodstream before it could be detected and this might take some time. In the study by Mead et al [498], the human C6 was administered i.v. and reconstituted haemolytic activity measured 24 hours later. There is no data available on how quickly the C6 activity was functionally reconstituted.

In addition to demonstrating that human C6 can be used to restore the haemolytic activity of mouse, rat and rabbit serum, this investigation confirmed previous reports that C6 is not a rate-limiting component of the terminal pathway in humans [502]. Furthermore, these data suggest that C6 is not a rate-limiting component of the terminal pathway in rats, rabbits or mice.

In summary, a fast and efficient affinity protocol for purifying human C6 has been developed, using an antibody generated during the course of this study. The C6 purified in this way is functionally active and is capable of reconstituting C6 deficient human, rat, rabbit and mouse serum in vitro. Moreover, the purified human C6 also reconstituted C6 deficient mice in vivo to generate functionally active serum complement from these mice as determined in haemolytic assays. The purified C6 will be useful in generating further antibodies and peptide fragments that recognise C6 and in the characterisation of these reagents.

Chapter 4: The Generation and Characterisation of anti-C6 antibodies.

4.1. Introduction

Inappropriate and chronic C activation is implicated in the initiation or progression of various autoimmune diseases, such as rheumatoid arthritis, multiple sclerosis, glomerulonephritis or as a consequence of ischemia-reperfusion injury [251]. The pro-inflammatory by-products of C activation C3a and C5a, recruit and activate neutrophils, whilst the MAC can initiate signalling cascades within cells possibly leading to apoptosis or kill them directly [110,112,113]. By using C component deficient animals in models of C-mediated disease, the contribution of those components to the development of the disease can be elucidated.

Multiple sclerosis and the corresponding animal models, experimental allergic encephalomyelitis (EAE) and Ab-mediated demyelinating EAE (ADEAE) have traditionally been considered to be T cell-mediated diseases [511]. However, the activities of the MAC, formed as a result of C activation, have recently been highlighted in the development of pathology in these diseases in studies using C6 deficient PVG ($PVG/C6^{-}$) rats. In the first seminal study, EAE was induced in normal PVG rats and $PVG/C6^{-}$ rats by immunisation with myelin basic protein (MBP). ADEAE was also induced, with an additional injection of anti – myelin oligodendrocyte glycoprotein (MOG) mAb [498]. Demyelination, mononuclear cell infiltration and axonal injury was observed in the normal rats, but neither demyelination nor axonal injury was observed in the $PVG/C6^{-}$ rats even though the levels of mononuclear cell infiltration were equivalent to those seen in the normal rats. Reconstitution of the C6 deficiency with human C6 lead to pathology and clinical disease indistinguishable from that in the normal rats, demonstrating the involvement of the MAC in the progression of this disease. In the second study, the induction of EAE led to the development of symptoms in 70% of the $PVG/C6^{-}$ rats and 95% of the normal rats immunized [512], although these were significantly milder in the C6-deficient rats. Similar levels of C3 deposition were seen in the spinal cords of the normal and C6-deficient rats, whilst C9 deposition was detected only in the spinal cords of normal rats, consistent with the inability of the C6-deficient rats to form MAC. The anti-MBP response was similar in both strains, but the numbers of white blood cells, neutrophils and basophils in the peripheral blood increased more in the normal rats. RT-PCR showed no differences in cytokine profiles of CD4+ T cells between C6 deficient and normal rats, although the infiltrate of CD4+ T cells was significantly lower in the C6-deficient rats. Taken together with results from other studies [513-516], these experiments strongly suggest that the MAC plays a critical role in the progression of this disease and that inhibiting C6 activity might be clinically beneficial.

Despite evidence demonstrating the clear involvement of MAC in contributing to the development of various pathologies, there are currently very few examples in the literature of inhibitory antibodies being raised against any of the terminal complement components with the intention of developing them for therapeutic use. An inhibitory anti-human C8 mAb, clone 133.3, was tested in ex vivo models of hyperacute rejection (HAR) [517] and CPB [518]. In both studies, the mAb inhibited sC5b-9 formation. In the HAR model, this inhibition protected rat hearts from organ damage when perfused with human serum. In the CPB model, platelet activation was observed in control experiments, but this was inhibited in samples to which the anti-C8 mAb had been added. Although these results are encouraging, this mAb has not been developed further.

The anti-C6 mAb, clone WU 6.4 was generated with a view to making an inhibitor of sC5b-9 formation [458]. Extensive characterisation in vitro demonstrated it inhibited C-mediated haemolysis and TCC generation, but not sufficiently well to be developed as an anti-C6 drug.

Polyclonal anti-C6 inhibitory Fab fragments were used to elucidate the role of the MAC in acute passive transfer experimental autoimmune myasthenia gravis (EAMG) [519]. These were co-administered with the EAMG inducing agent, an anti-acetylcholine receptor (AChR) mAb. Serum C6 was reduced to 8% in rats receiving the highest dose of anti-C6 Fab (0.12 mg/ml) and symptoms and signs associated with acute EAMG, such as muscle weakness, electrophysiologic abnormalities and loss of AChR were inhibited. Clinical symptoms were also inhibited in rats receiving a lower dose of anti-C6 Fab (0.08 mg/ml), although muscle AChR were still lost. Macrophage accumulation at muscle motor end-plates was inhibited by both doses of anti-C6 Fab. This study not only demonstrates the role played by MAC in this model, but highlights the therapeutic potential of developing anti-terminal complement component antibodies, in particular against C6.

Several anti-human C5 mAbs have been described, including clone N19-8 [458], which blocked C5a generation and inhibited MAC formation although its scFv antibody counterpart lacked the ability to inhibit C5a generation [458,459,468]. The anti-C5 mAb clone 5G1.1 has been made into two products [469]; an scFv antibody, marketed as Pexelizumab™ and the humanised mAb, now called Eculizumab™. All of these anti-C5 mAbs are discussed in greater detail in section 1.9.8.

Blocking mAbs raised against rat C5 and murine C5 have also been described [520]. An anti-murine C5 mAb provided protection against C5b-9 mediated damage in collagen-induced arthritis [521]. Anti-rat C5 mAb, clone 18A inhibited C5b-9 mediated haemolysis and significantly reduced cell apoptosis, necrosis and infiltration by polymorphonuclear leukocytes in a model of myocardial ischemia-reperfusion (I/R) injury [520]. Anti-C5 mAbs not only block C5b-9 formation, but also

inhibit C5a generation. To specifically inhibit MAC formation only, mAbs need to be raised against one of the terminal complement complex components: C6, C7, C8 or C9.
As so few anti-C6 antibodies have been described, the main aim of this chapter was to generate polyclonal and monoclonal antibodies against human, rabbit, rat and mouse C6. The ultimate aim of this study is to generate agents that inhibit C6 activity. Therefore, these antibodies were assayed for C6 blocking activity in classical pathway mediated haemolytic assays using human serum. Inhibitory antibodies with an IgG isotype were further characterised, to determine whether any of the mAbs recognised and functionally inhibited C6 from other species. Finally, the binding affinities of selected mAbs for human C6 were measured and epitope mapping studies carried out.

4.2. Specific methods and protocols

4.2.1. Determination of Binding Affinities and Epitope Mapping of anti-C6 mAbs using Surface Plasmon Resonance Technology

Surface plasmon resonance (SPR) technology using the BIAcore 3000 was used to measure the binding affinities of the anti-C6 mAb clones 7A2 and 23D1 for C6. The same technology was also used to determine the epitope each mAb recognised.

4.2.1.1. Determining the binding affinity of mAbs for C6

The affinity of the anti-C6 mAbs for human C6 was assessed on the BIAcore 3000. C6 was immobilised onto the flow cell of a CM5 sensor chip as described (section 2.5.1.). A reference flow cell on the same chip was prepared by activating the surface and blocking it. This ensured that control flow cell would have the same surface charge as the experimental flow cell.
For the binding affinity experiments, mAb (100 µl) was injected over the flow cell on which C6 was immobilised at a variety of concentrations (10.4 nM – 1 µM) over 5 minutes at a flow rate of 20 µl/minute. The dissociation of mAb from C6 as HBS-EP buffer (10 mM HEPES, pH 7.4, 150 mM NaCl, 3 mM EDTA, 0.005% (v/v) Surfactant-P20) was flowed over the sensor chip surface was monitored over 15 minutes and the data recorded on a sensorgram. The mAb was passed over the reference flow cell at the same time. Any mAb remaining bound to the flow cell surfaces at the end of this time was removed by flowing over 0.2% (v/v) diethylamine in PBS. To calculate the net RU change when a mAb bound and dissociated from C6, the reference flow cell sensorgram was subtracted from the C6 immobilised flow cell sensorgram. A program in the

BIAcore 3000 controlling software was used to fit various models to the data; this was then interpreted to determine the affinity of the mAb for C6.

For each set of affinity binding experiments, a control experiment to assess whether any mass transfer effects were occurring was carried out. The aim of these experiments is to determine whether the observed on-rates when analyte is flowed over the ligand are diffusion limited. If they are diffusion limited, then as the flow rate is altered, the on-rate will change and mass transfer effects are occurring. If the mass transfer effects are minimal, then when superimposed upon each other, the gradients of the observed on-rates gradients for each sensorgram as the mAb is passed over should be identical. Briefly, mAb (3.125 μg/ml) was passed over the C6 immobilised and reference flow cell surfaces at flow rates of 5, 15 and 75 μl per minute and the sensorgrams compared. All solutions used on the BIAcore 3000 were filtered and degassed before use.

4.2.1.2. Epitope mapping experiments

To investigate the antigenic sites on C6 recognised by the anti-C6 mAbs, the BIAcore 3000 was used. Rabbit anti-mouse immunoglobulins (RAM Ig) were immobilised onto the flow cell surface of a CM - 5 sensor chip (section 2.5.1.). To ensure the reference flow cell surface had the same charge as the experimental flow cell surface, the reference flow cell was subject to the same immobilisation procedure, omitting the immobilisation of anything onto the surface.

A two-site assay was used to map the epitopes on C6 recognised by the anti-C6 mAbs. The first anti-C6 mAb (100 μg/ml) was passed over the flow cell on which the RAM Ig had been immobilised and allowed to bind. C6 (100 μg/ml) was then injected over the flow cell and allowed to bind to the anti-C6 mAb already bound. To avoid binding of the second mAb to unoccupied RAM Ig sites, purified mouse Ig (100 μg/ml) was injected over the antibody-C6 complex to block these sites. The second anti-C6 mAb (100 μg/ml) was then injected over the flow cell. At the end of the experiment, the bound components were removed by injecting 10 mM glycine, pH 1.7 (20 μl) over the surface. All the data were recorded on a sensorgram. At the same time, the same components were passed over the reference blank flow cell and recorded on a sensorgram. For analysis, the reference sensorgram was subtracted from the experimental sensorgram. To ensure that the binding of the second antibody was specific for human C6, the experiment was repeated, but with the omission of passing over the C6.

The flow rate during each experiment was 20 μl per minute; each component was passed over the flow cell for 5 minutes. All experiments were carried out in HBS-EP buffer (0.01 M HEPES pH 7.4, 0.15 M NaCl, 3 mM EDTA, 0.005% (v/v) Surfactant-P20) and all components were in HBS-EP buffer.

4.3. Results

4.3.1. Rabbit anti-rabbit C6 polyclonal antibody

Western blotting (section 2.1.11.) was used to determine the specificity of the rabbit anti-rabbit C6 polyclonal antibody (section 2.2.3) for other species C6 (Figure 4.1). This antibody recognised two bands in the normal human serum sample, the upper at the expected molecular weight of C6. The lower may have been a degradation product of C6. The antibody did not recognise any components of C6 deficient human serum. This antibody did not appear to recognise mouse C6 as no staining was detected in the normal mouse serum or the C6 deficient serum. It did recognise a band just below 98 kDa in the normal rat serum sample, which is consistent with the molecular weight of rat C6. A band of a similar molecular weight was observed in the C6 deficient rat serum sample, suggesting that the band was not specific for C6. Single bands of a similar molecular weight as the human C6 were observed for guinea pig, goat and sheep serum. No staining was observed for the chicken serum sample. As this antiserum recognised C6 in the human serum sample but did not recognise mouse C6, it was not characterised further.

4.3.2. Rat anti-rat C6 monoclonal antibodies

Two C6 deficient rats were immunised with normal rat serum containing rat C6, as described in section 2.3.6. and tested for anti-C6 antibodies by ELISA using human C6 (Figure 4.2). Rat 2 had the highest titre and was exsanguinated under terminal anaesthesia, its spleen removed and used to generate hybridomas (section 2.3.7.). Two anti-C6 mAbs were isolated, clones 2D1 and 7D1. Both mAbs inhibited C-mediated haemolysis of erythrocytes when human serum was used as the source of C in a dose-dependent manner (Figure 4.3), suggesting that these antibodies were functionally blocking for human C6. Antibody 2D1 inhibited C-mediated haemolysis by up to 90.5%; 7D1 by up to 62.6%. Neither mAb recognised human C6 by western blot (data not shown). Clone 2D1 had an IgM isotype, whilst the 7D1 was weakly positive for all isotypes tested, suggesting that it was not actually monoclonal. Clone 2D1 was not further characterised due to its isotype and 7D1 was not investigated further because it was not monoclonal.

4.3.3. Mouse anti-mouse C6 antibodies

Three C6 deficient mice were immunised with C6 sufficient mouse serum (section 2.3.6.) and tested for anti- C6 antibodies by ELISA using human C6 (Figure 4.4). B cells were isolated from

Figure 4.1 Western blot to determine whether the polyclonal rabbit anti-rabbit C6 antibody recognises other species C6

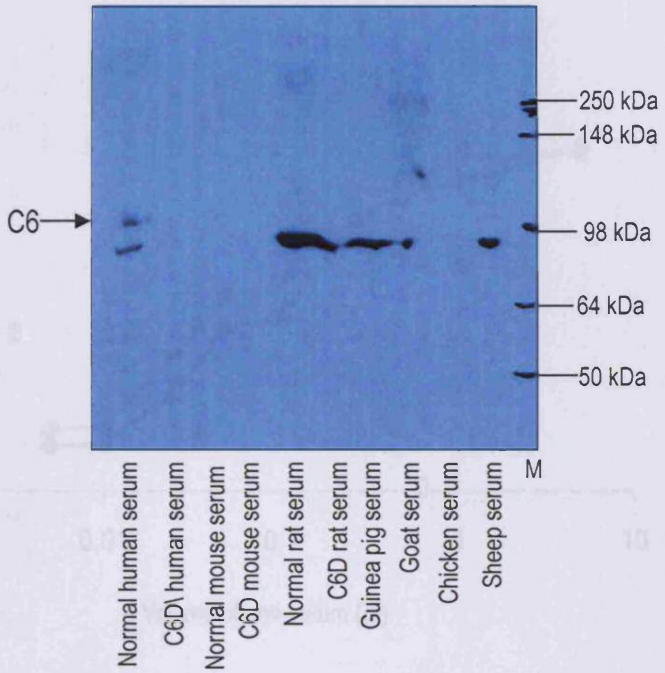

Serum (2 μl) was diluted in dH_2O (2 μl) and non-reducing buffer (2 μl), run on a 7.5% SDS-PAGE gel and transferred to nitrocellulose by electroblotting for 1 hour. Protein was probed with the rabbit anti-rabbit C6 antibody (1:5000) and goat anti-rabbit Ig-HRPO (1:25000) as a secondary antibody. Bands were detected with ECL and visualised by autoradiography. M – protein molecular weight markers.

Figure 4.2 Screening ELISA to determine the rat with the highest rat anti-rat C6 antibody titre

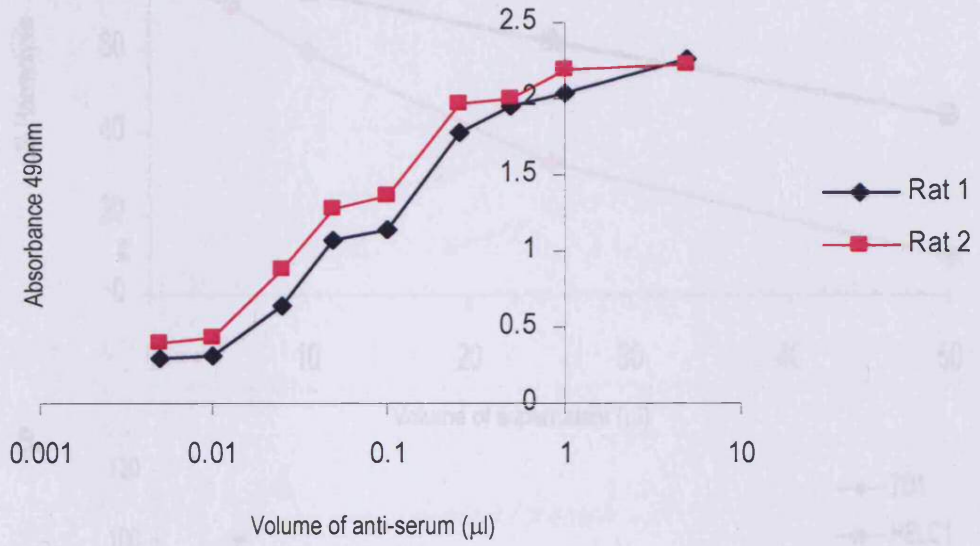

The two immunised rats were tail bled, the collected blood allowed to clot and serum prepared. To determine which rat had the highest titre of anti-rat C6 antibodies, a screening ELISA was used. All incubations were for 1 hour at 37°C and all wash steps comprised three washes. A 96-well ELISA plate was coated with 10 µg/ml human C6 (50 µl/well). After washing, the plate was blocked in blocking buffer. The plate was washed again and the rat anti-rat C6 anti-serum was added to the plate at several dilutions in blocking buffer. The anti-serum was removed, the plate washed and HRP-conjugated anti-rat immunoglobulins diluted 1/1000 in blocking buffer. After washing, the plate was developed with OPD substrate. Development was stopped with 10% (v/v) H_2SO_4 and the plate was read at 490 nm. Above, the volume of anti-serum has been plotted on a logarithmic scale against A_{490}. As rat 2 had a slightly higher titre against C6, it was chosen to be sacrificed and its spleen used in a fusion.

Figure 4.3 Haemolytic assays to investigate whether the rat anti-rat C6 antibodies, 2D1 and 7D1 are able to inhibit C-mediated lysis.

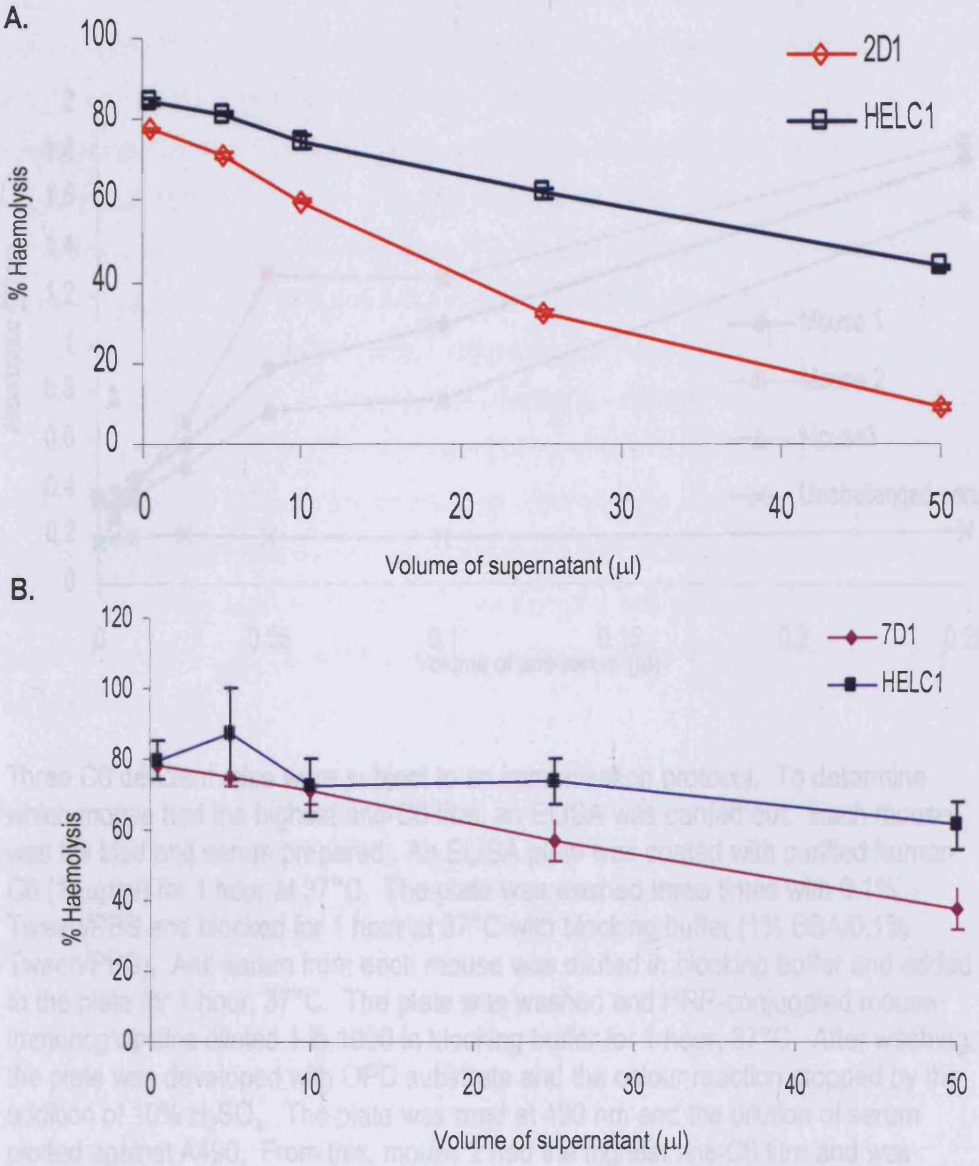

Supernatant was collected from hybridoma cell lines and dilutions made over a range in CFD. Fifty microlitres were added to 50 µl diluted human serum and 50 µl 2% sheep EA in a 96 round-bottomed well. This mixture was incubated at 37°C for 30 minutes. The plates were then centrifuged at 2500 rpm for 5 minutes and the supernatants transferred to a flat-bottomed microtitre plate and the absorbance measured at 415 nm. The percentage of haemolysis was calculated for each sample and plotted against the volume of supernatant. The graph show the mean for each sample point ± the standard error of the mean. For 2D1, n=2; 7D1, n=6. As a non-inhibitory antibody secreting cell line control, supernatant collected from the hybridoma cell line secreting the anti-human CD59 mAb, clone HEL-C1 was included in each assay.

Figure 4.4 Screening C6 deficient mice immunised with normal mouse serum to establish titre levels for anti human C6 antibodies

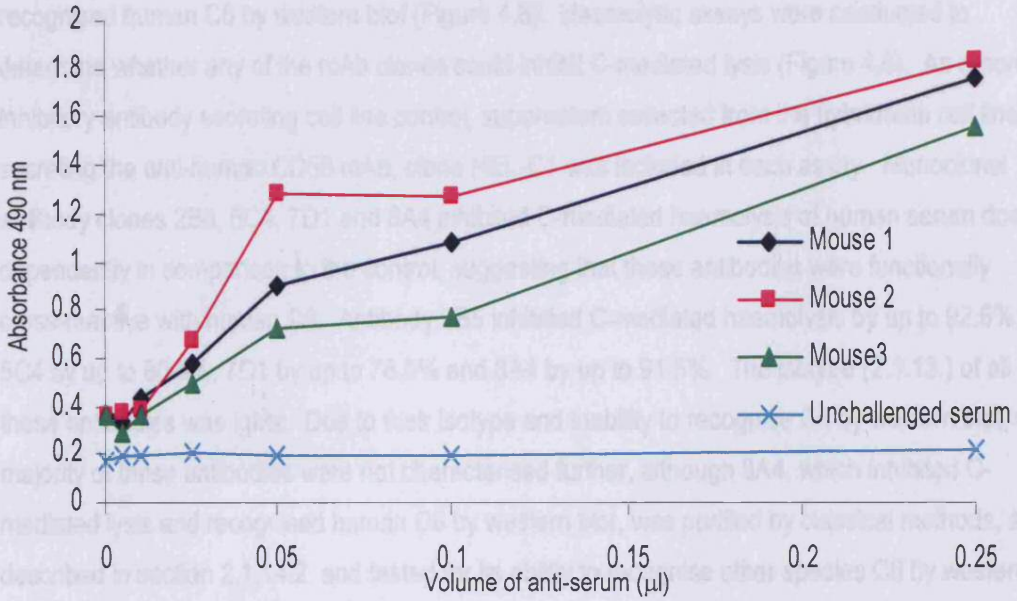

Three C6 deficient mice were subject to an immunisation protocol. To determine which mouse had the highest anti-C6 titre, an ELISA was carried out. Each mouse was tail bled and serum prepared. An ELISA plate was coated with purified human C6 (1 µg/ml) for 1 hour at 37°C. The plate was washed three times with 0.1% Tween/PBS and blocked for 1 hour at 37°C with blocking buffer (1% BSA/0.1% Tween/PBS). Anti-serum from each mouse was diluted in blocking buffer and added to the plate for 1 hour, 37°C. The plate was washed and HRP-conjugated mouse immunoglobulins diluted 1 in 1000 in blocking buffer for 1 hour, 37°C. After washing, the plate was developed with OPD substrate and the colour reaction stopped by the addition of 10% H_2SO_4. The plate was read at 490 nm and the dilution of serum plotted against A490. From this, mouse 2 had the highest anti-C6 titre and was selected to use for a fusion in the first instance. Ultimately, all three mice were used in fusions.

the spleen of the mouse with the highest titre of anti-C6 antibodies and fused with the mouse myeloma cell line SP2/0 (section 2.3.7.). Mouse anti-C6 secreting cells were selected for by screening against human C6, ensuring the antibodies would be cross-reactive with both mouse C6 and human C6. Ultimately, all three mice were used for the fusions. From these three fusions, eight mAbs were identified, designated 1B1, 1C1, 2B5, 4A5, 5A5, 5C4, 7D1 and 8A4. Supernatants collected from these cell lines were used to characterise the properties of each mAb clone and this data is summarised in Table 4.1. Two of the mAbs, clones 5C4 and 8A4 recognised human C6 by western blot (Figure 4.5). Haemolytic assays were conducted to determine whether any of the mAb clones could inhibit C-mediated lysis (Figure 4.6). As a non-inhibitory antibody secreting cell line control, supernatant collected from the hybridoma cell line secreting the anti-human CD59 mAb, clone HEL-C1 was included in each assay. Monoclonal antibody clones 2B5, 5C4, 7D1 and 8A4 inhibited C-mediated haemolysis of human serum dose-dependently in comparison to the control, suggesting that these antibodies were functionally cross-reactive with human C6. Antibody 2B5 inhibited C-mediated haemolysis by up to 92.6%; 5C4 by up to 80.5%, 7D1 by up to 78.5% and 8A4 by up to 91.5%. The isotype (2.1.13.) of all of these antibodies was IgMκ. Due to their isotype and inability to recognise C6 by western blot, the majority of these antibodies were not characterised further, although 8A4, which inhibited C-mediated lysis and recognised human C6 by western blot, was purified by classical methods, as described in section 2.1.14.2. and tested for its ability to recognise other species C6 by western blot (section 4.3.3.1.).

Table 4.1 Summary of the characterisation of the mouse anti-mouse C6 mAbs.

Clone	Recognition of human C6 by ELISA	Recognition of human C6 by Western blot	Capable of inhibiting C-mediated haemolysis when human serum used	Isotype
1B1	Yes	No	Weakly inhibitory	IgMκ
1C1	Yes	No	Weakly inhibitory	IgMκ
2B5	Yes	No	Yes	IgMκ
4A5	Yes	No	No	IgMκ
5A5	Yes	No	Weakly inhibitory	IgMκ
5C4	Yes	Yes	Yes	IgMκ
7D1	Yes	No	Yes	IgMκ
8A4	Yes	Yes	Yes	IgMκ

Figure 4.5 Detection of human C6 by mouse anti-mouse C6 antibodies, A. 5C4 and B. 8A4

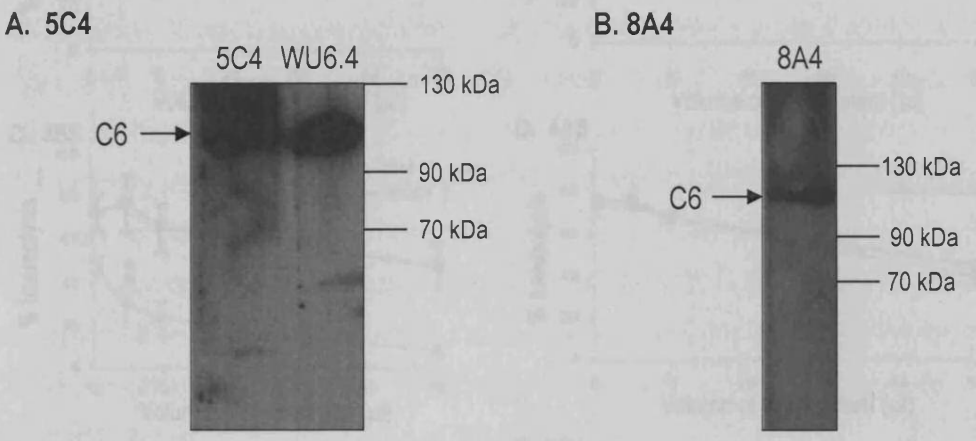

Serum (15 μl) was diluted in dH_2O (85 μl) and non-reducing loading buffer (50 μl) and applied to a 4% stacking gel with a single well and electrophoresed through on a 7.5% SDS-PAGE running gel and transferred to nitrocellulose by electroblotting for 1 hour. The nitrocellulose was then cut into strips running the length of the gel before supernatant containing the test antibody, 5C4 and 8A4 diluted 1:1 with 0.1% tween/PBS or control antibody WU 6.4 (1 μg/ml) diluted in 0.1% tween/PBS was incubated with each strip (2 ml). After washing, bound antibody was probed with goat anti-mouse Ig-HRPO (1:2000) (Bio-rad) as a secondary antibody. Bands were detected with ECL and visualised by autoradiography.

Figure 4.5 Detection of human C6 by mouse anti-mouse C6 antibodies, A. 5C4 and B. 8A4

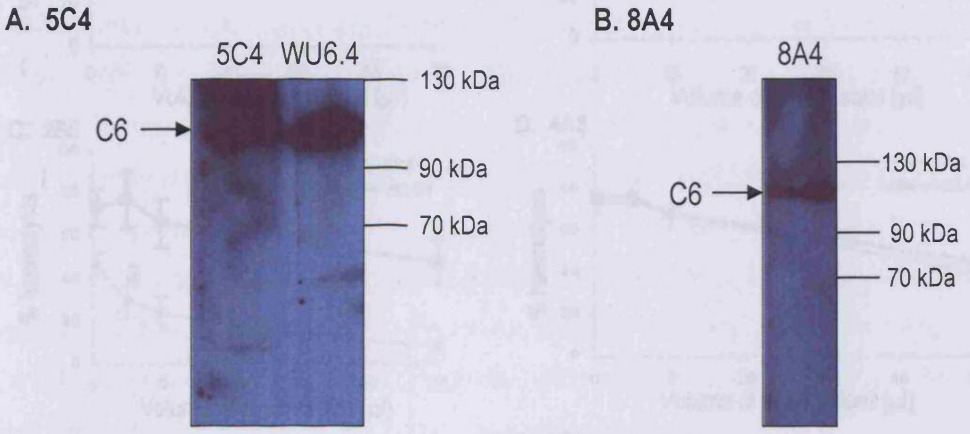

Serum (15 μl) was diluted in dH_2O (85 μl) and non-reducing loading buffer (50 μl) and applied to a 4% stacking gel with a single well and electrophoresed through on a 7.5% SDS-PAGE running gel and transferred to nitrocellulose by electroblotting for 1 hour. The nitrocellulose was then cut into strips running the length of the gel before supernatant containing the test antibody, 5C4 and 8A4 diluted 1:1 with 0.1% tween/PBS or control antibody WU 6.4 (1 μg/ml) diluted in 0.1% tween/PBS was incubated with each strip (2 ml). After washing, bound antibody was probed with goat anti-mouse Ig-HRPO (1:2000) (Bio-rad) as a secondary antibody. Bands were detected with ECL and visualised by autoradiography.

Figure 4.6 Haemolytic assays to investigate whether the monoclonal mouse anti-mouse C6 antibodies inhibit C-mediated lysis.

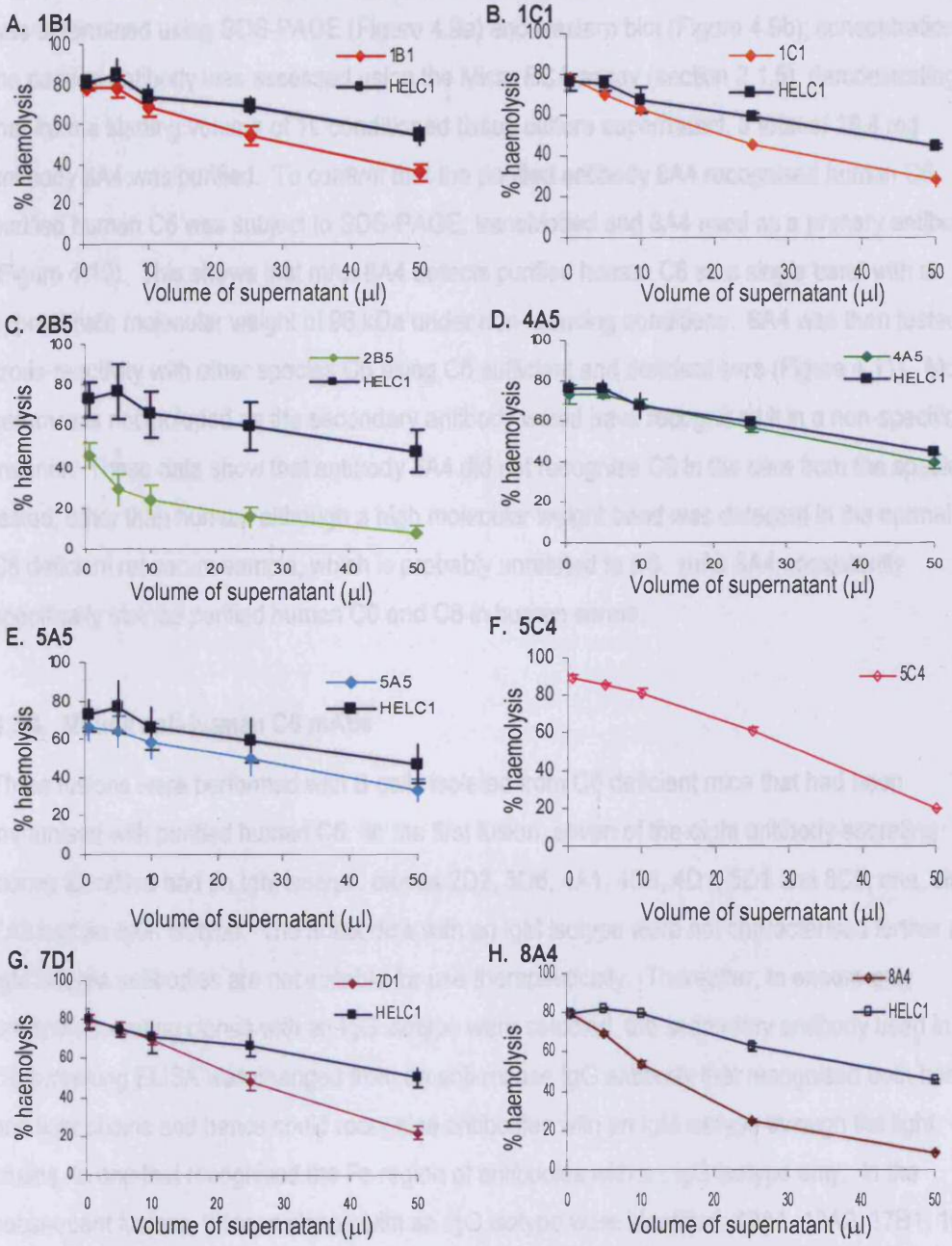

Supernatant was collected from hybridoma cell lines and dilutions made over a range in CFD. Fifty microlitres were added to 50 µl diluted human serum and 50 µl 2% sheep EA in a 96 round-bottomed well. This mixture was incubated at 37°C for 30 minutes. The plates were then centrifuged at 2500 rpm for 5 minutes and the supernatants transferred to a flat-bottomed microtitre plate and the absorbance measured at 415 nm. The percentage of haemolysis was calculated for each sample and plotted against the volume of supernatant. For 1B1, n=14; 1C1, n=12; 2B5, n=18; 4A5, n=10; 5A5, n=10; 5C4, n=3, 7D1, n=12; 8A4, n=6. Error bars are the standard error of the mean.

4.3.3.1. The purification of the mouse anti-mouse C6 mAb, clone 8A4

The chromatogram of the purification of mAb 8A4 is shown in Figure 4.7. IgM containing fractions were identified by dot blot (section 2.1.8) using an HRPO-conjugated anti-murine IgM antibody (Figure 4.8), pooled and concentrated using ultrafiltration. Purity of the pooled fractions was determined using SDS-PAGE (Figure 4.9a) and western blot (Figure 4.9b); concentration of the purified antibody was assessed using the Micro BCA assay (section 2.1.5), demonstrating that from a starting volume of 1L conditioned tissue culture supernatant, a total of 16.4 mg antibody 8A4 was purified. To confirm that the purified antibody 8A4 recognised human C6, purified human C6 was subject to SDS-PAGE, transblotted and 8A4 used as a primary antibody (Figure 4.10). This shows that mAb 8A4 detects purified human C6 as a single band with an approximate molecular weight of 98 kDa under non-reducing conditions. 8A4 was then tested for cross-reactivity with other species C6 using C6 sufficient and deficient sera (Figure 4.11). Mouse serum was not included as the secondary antibody would have recognised it in a non-specific manner. These data show that antibody 8A4 did not recognise C6 in the sera from the species tested, other than human, although a high molecular weight band was detected in the normal and C6 deficient rat serum sample, which is probably unrelated to C6. mAb 8A4 consistently specifically stained purified human C6 and C6 in human serum.

4.3.4. Mouse anti-human C6 mAbs

Three fusions were performed with B cells isolated from C6 deficient mice that had been immunised with purified human C6. In the first fusion, seven of the eight antibody-secreting clones identified had an IgM isotype; clones 2D2, 3D6, 4A1, 4C6, 4D1, 5D1 and 8C5; one, clone 7A2 had an IgG_1 isotype. The antibodies with an IgM isotype were not characterised further as IgM isotype antibodies are not suitable for use therapeutically. Thereafter, to ensure only antibody-secreting clones with an IgG isotype were selected, the secondary antibody used in the C6 screening ELISA was changed from an anti-mouse IgG antibody that recognised both heavy and light chains and hence could recognise antibodies with an IgM isotype through the light chains, to one that recognised the Fc region of antibodies with an IgG isotype only. In the subsequent fusions, thirteen clones with an IgG isotype were identified: 12A1, 13A2, 17B1, 18A1, 22B1, 23D1, 24C2, 25C5, 26C2, 26B4 and 27B1.

Supernatants collected from these cell lines were investigated for their ability to inhibit C-mediated lysis in a haemolytic assay (Figure 4.12). Initially, supernatant collected from the hybridoma cell line secreting HELC1, an antibody raised against human CD59 was used as an

Figure 4.7 Chromatogram of partially purified antibody, 8A4 being passed over a SourceQ column

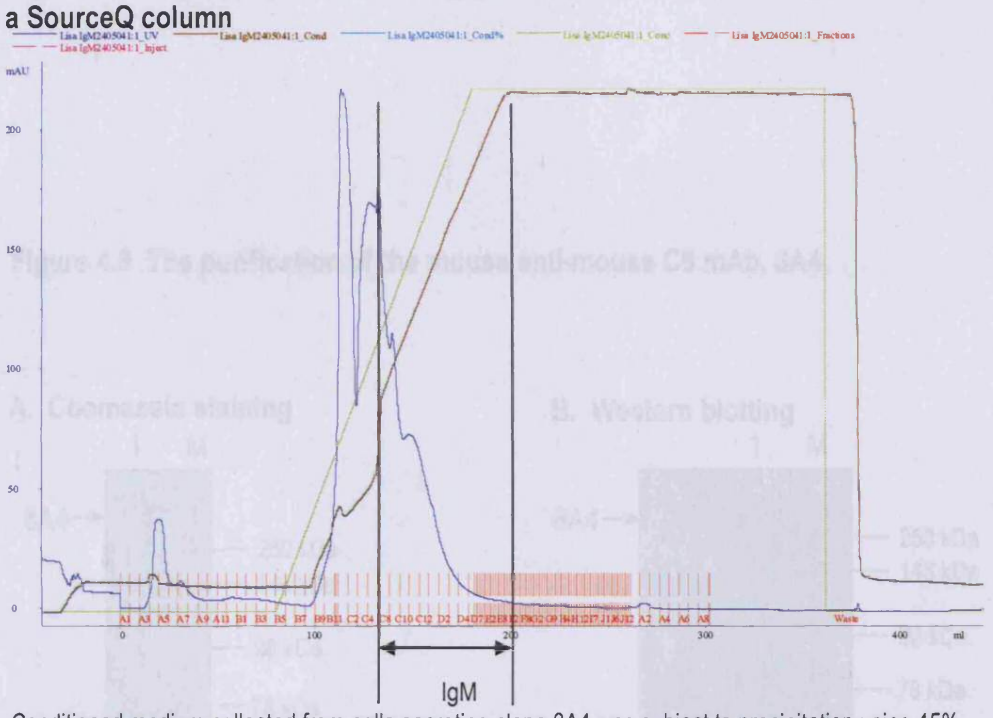

Conditioned medium collected from cells secreting clone 8A4 was subject to precipitation using 45% $AmSO_4$ saturation. After centrifugation, the supernatant was discarded and the pellet resuspended in a minimal volume of 20 mM K2HPO4/20 mM KH2PO4, pH 6.5 (start buffer) and dialysed against this overnight. The IgM enriched sample was applied to a Source 15Q column pre-equilibrated in start buffer and an increasing linear gradient of end buffer (start buffer containing 0.5M NaCl) applied. The FPLC was programmed to collect the eluate in 5ml fractions.

Figure 4.8 Dot blot of fractions from eluted column to find the IgM containing peak

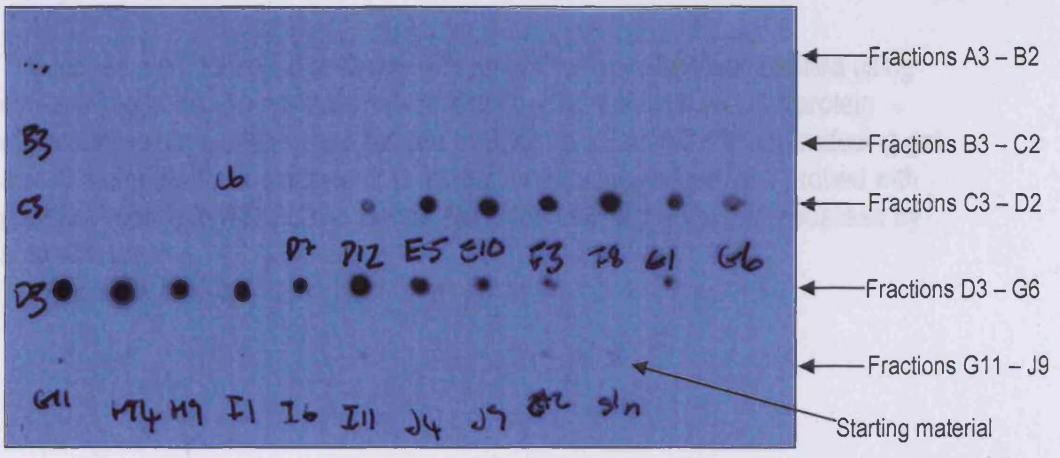

Two microlitres of each fraction (A3 – D12; thereafter every fifth fraction) was dotted onto nitrocellulose membrane and allowed to dry at room temperature, before being blocked with 5% (w/v) milk/0.1% (v/v) Tween/PBS for 30 minutes at room temperature. After washing, the blot was incubated with HRPO-anti-mouse IgM (μ-chain specific) antibody diluted 1:5000 in 0.1% (v/v) Tween/PBS and incubated at room temperature for 1 hour. After five washes with 0.1% (v/v) Tween/PBS, the blot was developed with the addition of ECL.

Figure 4.9 The purification of the mouse anti-mouse C6 mAb, 8A4

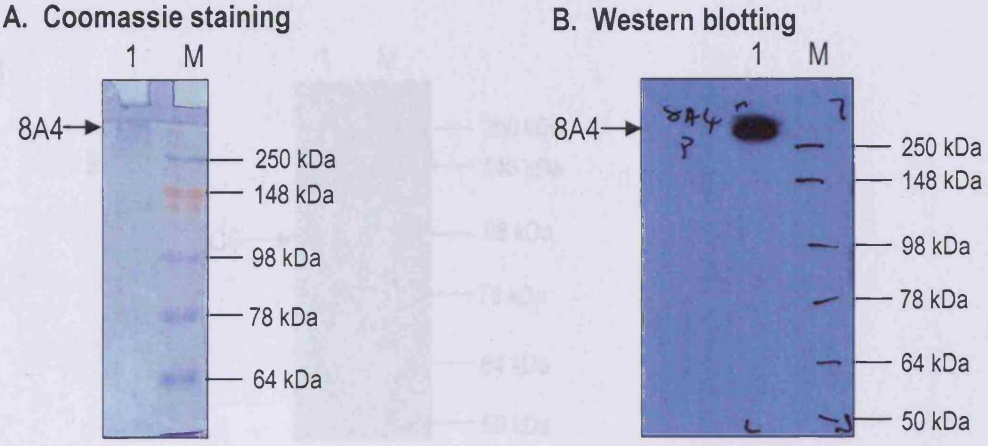

The mouse anti-mouse C6 antibody with an IgM isotype, 8A4 was purified using classical methods. To assess purity, the purified sample (1) and (M) protein molecular weight markers were subject to SDS-PAGE on a 7.5% non-reducing gel and **A.** stained with Coomassie or **B.** blotted onto nitrocellulose, and probed with goat anti-mouse IgM (1:2000). Bands were detected with ECL and visualised by autoradiography.

Figure 4.10 The detection of human C6 with the mouse anti-mouse C6 mAb, 8A4

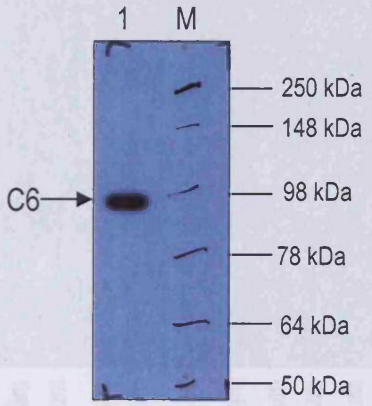

Purified human C6 (1) and (M) protein molecular weight markers were subject to 7.5% SDS-PAGE, electroblotted onto nitrocellulose and probed with the mouse anti-mouse C6 mAb, 8A4 (2µg/ml) and goat anti-mouse IgM (1:1000) as a secondary antibody. Bands were detected with ECL and visualised by autoradiography.

Figure 4.11 Western blot to determine the cross-reactivity of the mouse anti-mouse C6 mAb 8A4 for C6 from other species serum

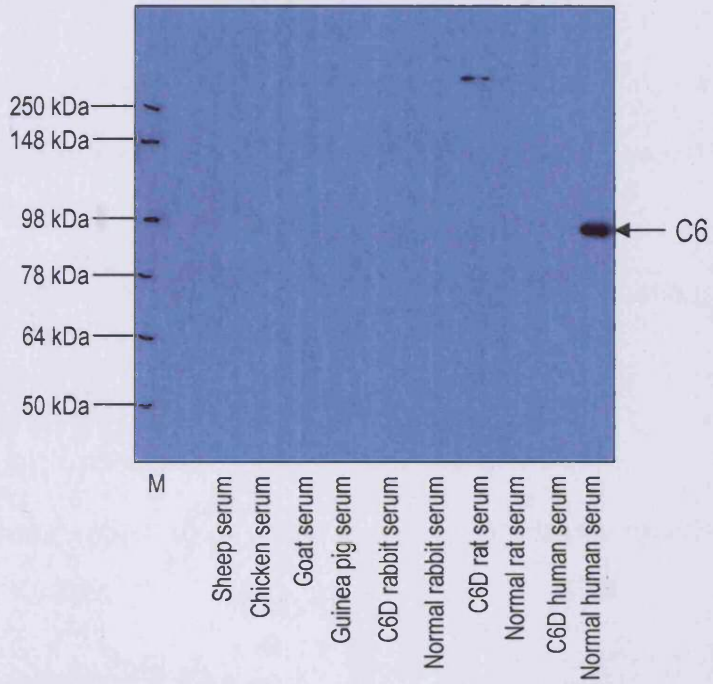

Different species of animal sera, as well as human sera were run under non-reducing conditions on 7.5% SDS PAGE gel and transferred onto nitrocellulose by electoblotting. After blocking the blot with 5% (w/v) milk/0.1% Tween/PBS, protein was probed with mouse anti-mosue C6 mAb 8A4 (4 μg/ml) and goat anti-mouse IgM-HRPO (1:1000) as a secondary antibody. Bands were detected with ECL and visualised by autoradiography.

Figure 4.12 Haemolysis assay to determine whether the monoclonal mouse anti-human C6 antibodies inhibit C-mediated lysis

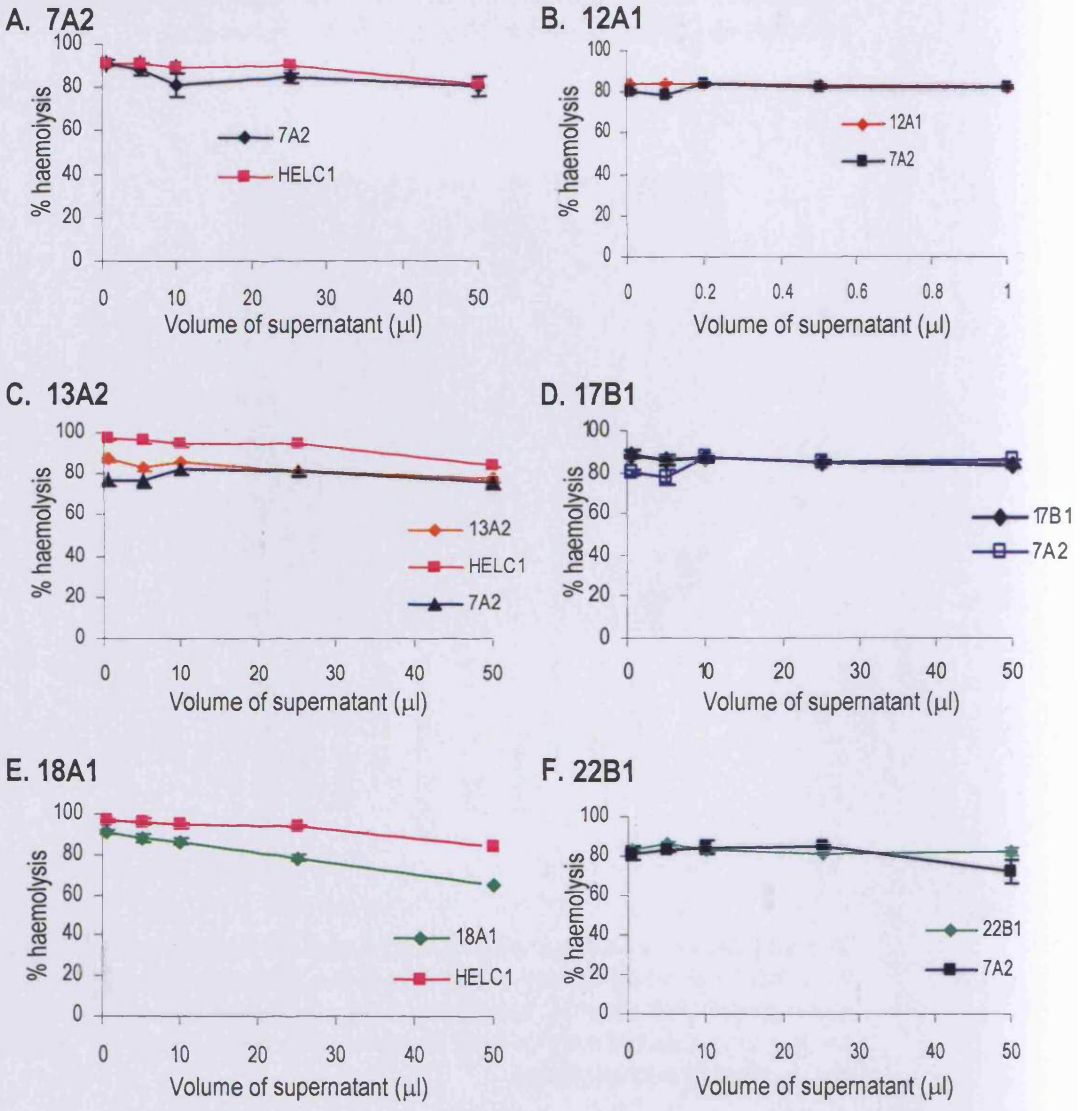

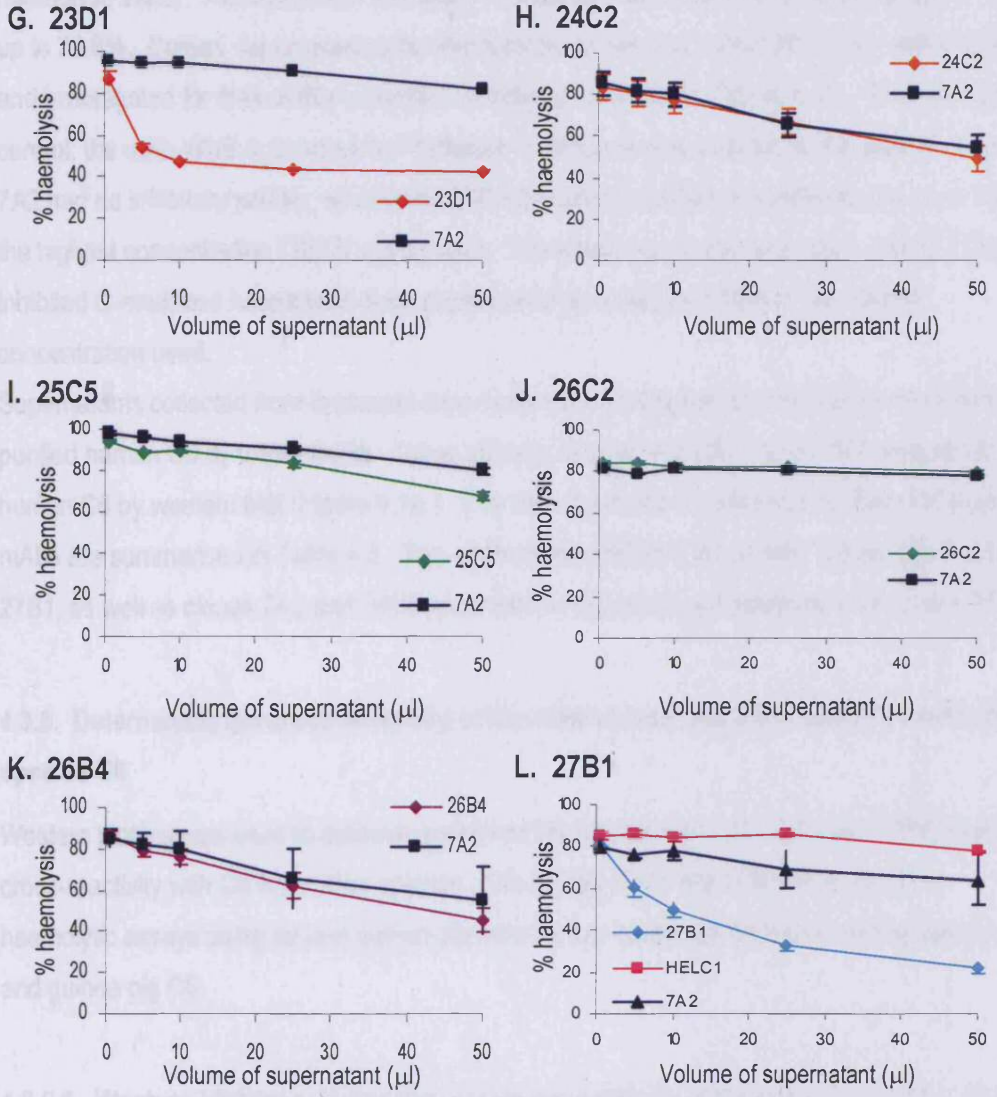

Supernatant was collected from hybridoma cell lines and dilutions made over a range in CFD. Fifty microlitres were added to 50 µl diluted human serum and 50 µl 2% sheep EA in a 96 round-bottomed well. This mixture was incubated at 37°C for 30 minutes. The plates were then centrifuged at 2500 rpm for 5 minutes and the supernatants transferred to a flat-bottomed microtitre plate and the absorbance measured at 415 nm. The percentage of haemolysis was calculated for each sample, averaged and plotted against the volume of supernatant. For 7A2, n=4; 12A1, n=6; 13A2, n=12; 17B1, n=6; 18A1, n=4; 22B1, n=4; 23D1, n=16; 24C2, n=12; 25C2, n=2; 26C2, n=6; 26B4, n=10; 27B1, n=20. Error bars are the standard error of the mean.

antibody secreting cell line control. However, the mouse anti-human C6 antibody, clone 7A2 had such a similar non-inhibitory activity that it was subsequently used as the control antibody supernatant. Out of all the antibodies tested, 23D1 and 27B1 inhibited C-mediated haemolysis of human serum dose-dependently in comparison to the control. Antibody clones 24C2, 25C5 and 26B4 showed some inhibitory activity in comparison to the control when used neat in the haemolytic assay. Antibody 23D1 inhibited C-mediated haemolysis by up to 58.0% and 27B1 by up to 78.6%. Culture supernatant collected from the clones 7A2, 23D1 and 27B1 were purified and investigated for their ability to inhibit C-mediated haemolysis (Figure 4.13). As an inhibitory control, the mAb WU6.4, donated by Professor R. Würzner was included in the assays. Clone 7A2 had no inhibitory activity, whilst mAb 23D1 inhibited C-mediated haemolysis by up to 99% at the highest concentration (187.5 µg/ml) used. This effect was dose-dependent. Clone 27B1 also inhibited C-mediated haemolysis dose-dependently up to almost 100% at the highest concentration used.

Supernatants collected from these cell lines were also investigated for their ability to recognise purified human C6 by western blot. Three of them, clones 7A2, 23D1 and 27B1 recognised human C6 by western blot (Figure 4.14.). The data regarding the characterisation of all these mAbs are summarised in Table 4.2. Two of the three inhibitory antibodies, clones 23D1 and 27B1, as well as clones 7A2 and 24C2, were further characterised (sections 4.3.5. and 4.3.6.).

4.3.5. Determining the cross-reactivity of the mAb clones 7A2, 23D1 and 27B1 with other species C6

Western blotting was used to determine whether the mAb clones 7A2, 23D1 and 27B1 had any cross-reactivity with C6 from other species. The clones 23D1 and 27B1 were tested in haemolytic assays using rat and guinea pig sera for any functional inhibitory activity against rat and guinea pig C6.

4.3.5.1. Western blotting to determine the cross-reactivity of the mAb clones 7A2, 23D1 and 27B1 with other species C6

The anti-C6 mAb clones 7A2, 23D1 and 27B1 were assessed for their ability to recognise rat, mouse, rabbit, guinea pig, goat, chicken, sheep and bovine C6 by western blot. To confirm the specificity of the test antibody for C6, C6 deficient sera was included on the western blot alongside normal serum, if available, to provide a means of comparison. Samples of purified

Figure 4.13 Haemolytic assay demonstrating that the inhibitory properties of the monoclonal antibodies 23D1 and 27B1 are retained when purified.

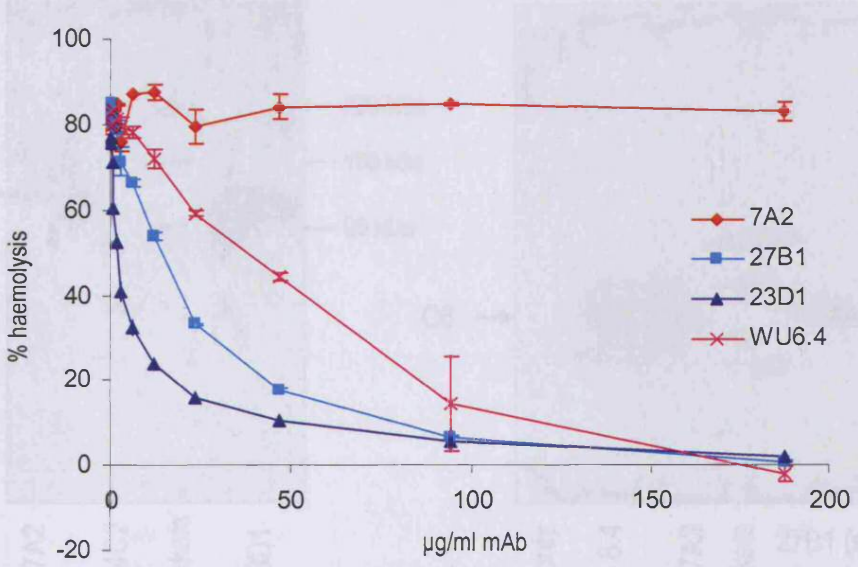

Purified mAb was diluted over the range 0 – 187.5 µg/ml in CFD. Fifty microlitres were added to 50 µl diluted human serum and 50 µl 2% sheep EA in a 96 round-bottomed well. This mixture was incubated at 37°C for 30 minutes. The plates were centrifuged at 2500 rpm for 5 minutes and then the supernatants were transferred to a flat-bottomed microtitre plate. The absorbance was measured at 415 nm. The percentage of haemolysis was calculated for each sample and plotted against the concentration of mAb. Error bars are the standard error of the mean; n=2 for each condition.

Figure 4.14 Western blot to determine whether the mouse anti-human C6 mAbs 7A2, 23D1, 24C2 and 27B1 recognise purified human C6 by Western blot

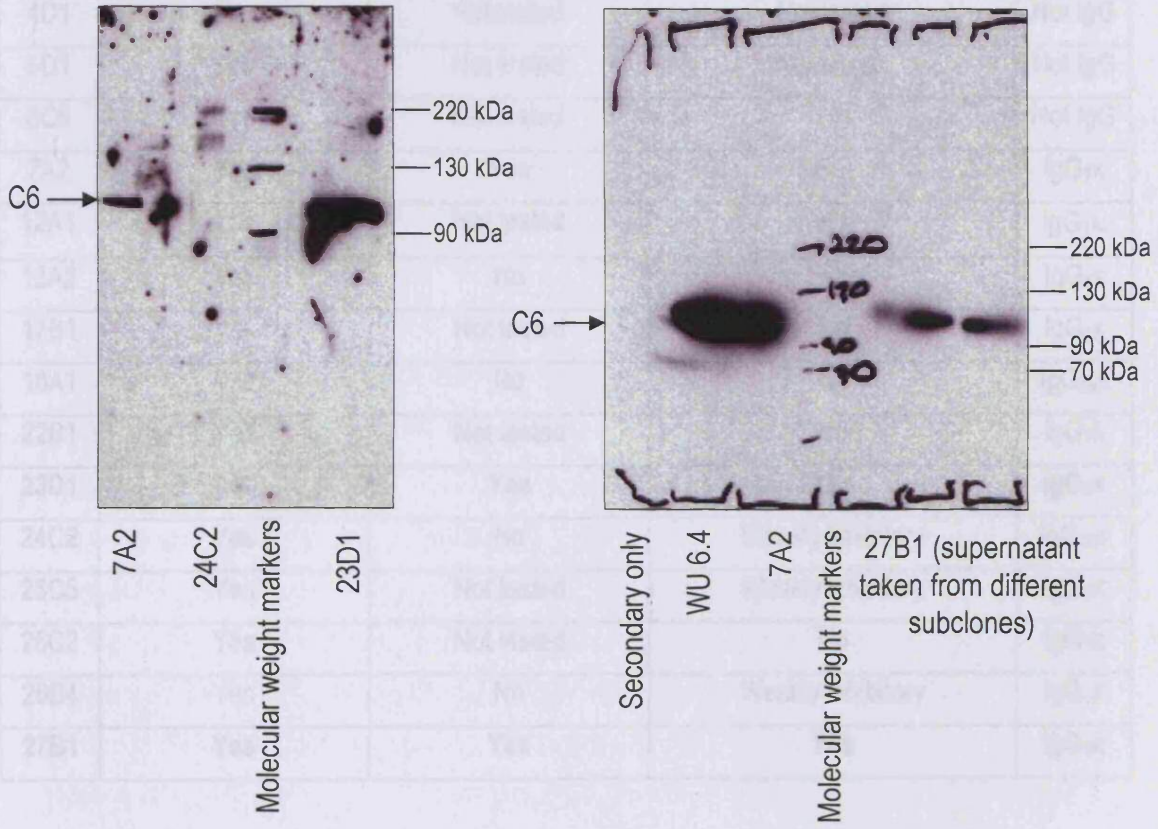

Serum (15 μl) was diluted in dH_2O (85 μl) and non-reducing loading buffer (50 μl) and applied to a 4% stacking gel with a single well and electrophoresed through on a 7.5% SDS-PAGE running gel and transferred to nitrocellulose by electroblotting for 1 hour. The nitrocellulose was then cut into strips running the length of the gel before supernatant containing the test antibodies, 23D1, 24C2 and 27B1 diluted 1:1 with 0.1% tween/PBS, or in the case of 7A2 diluted to 1 μg/ml in 0.1% tween/PBS. A control antibody WU 6.4 (1 μg/ml) diluted in 0.1% tween/PBS was also incubated with each strip (2 ml). To determine whether there was any non-specific binding of the secondary antibody to the serum, one strip was incubated in secondary antibody only. After washing, bound antibody was probed with goat anti-mouse Ig-HRPO (1:2000) (Bio-rad) as a secondary antibody. Bands were detected with ECL and visualised by autoradiography.

human C6, normal human serum and C6 deficient human serum were included on the western blots as a reference.

Clones 7A2 (figure 4.15), 27B1 (figure 4.16) and 23D1 (figure 4.18) all recognised purified human C6 and C6 in normal human serum, but did not recognise any component of C6 deficient human serum. Clone 7A2 (figure 4.15) stained a single band with a molecular weight of approximately 64 kDa weakly in both the normal and C6 deficient rat and rabbit serum and also the guinea pigserum. This is not specific for C6, as C6 deficient rats do not make a truncated form of C6 [485,508]; neither do C6 deficient rabbits [486,509]; also the molecular weight of rat C6 is approximately 90 kDa [485]. Single bands with a molecular weight in excess of 250 kDa were seen for human, C6 deficient human, goat, chicken, sheep and bovine sera in the westerns probed with 7A2 (figure 4.15) and 27B1 (figure 4.16). An identical blot was probed only with secondary antibody (figure 4.17) and similar staining of high molecular weight bands was observed in these samples as well, suggesting that the observed staining of the high molecular weight bands was due to the secondary antibody recognising protein in a non-specific manner.

4.3.5.2. Haemolytic assays to determine whether mAbs 27B1 and 23D1 were functionally cross-reactive with other species sera

Purified anti-human C6 mAbs 23D1 and 27B1 were tested in haemolytic assays using rat and guinea pig sera for functional inhibitory activity against rat and guinea pig C6 (Figures 4.19A and B respectively). The non-inhibitory mAb, 7A2 was used as a reference non-inhibitory control, as was the mAb WU 6.4, which had previously been shown not to recognise rat or guinea pig C6 in serum by ELISA [522]. Both the rat and guinea pig sera were diluted 1 in 100 as this dilution resulted in 80% haemolysis of sheep EA. In humans, the concentration of C6 in serum ranges between 20 – 80 μg/ml [499]. Based upon there being a similar concentration of rat or guinea pig C6 in the relevant sera, there would be approximately 10 – 40 ng of C6 per well in these experiments, whilst the concentration of antibody ranged between 1.85 ng (37 ng/ml) and 3.75 μg (75 μg/ml) per well.

At the highest concentration added 75 μg/ml, there was 51% haemolysis in the presence of the non-inhibitory mAb, 7A2. This inhibition was not present when mAb 7A2 was diluted out further in comparison to no antibody being present (72% haemolysis). The mAbs 23D1, WU6.4 and 27B1 all inhibited C-mediated haemolysis to some degree when present at high concentrations, 36.5%, 26.5% and 45% respectively, and these effects were dose-dependent, but as with 7A2, these effects were rapidly diluted out. Given the excess the mAbs present were in relative to rat C6 in

Figure 4.15 Western blot to determine the cross-reactivity of the mouse anti-human C6 mAb 7A2 with C6 from other species

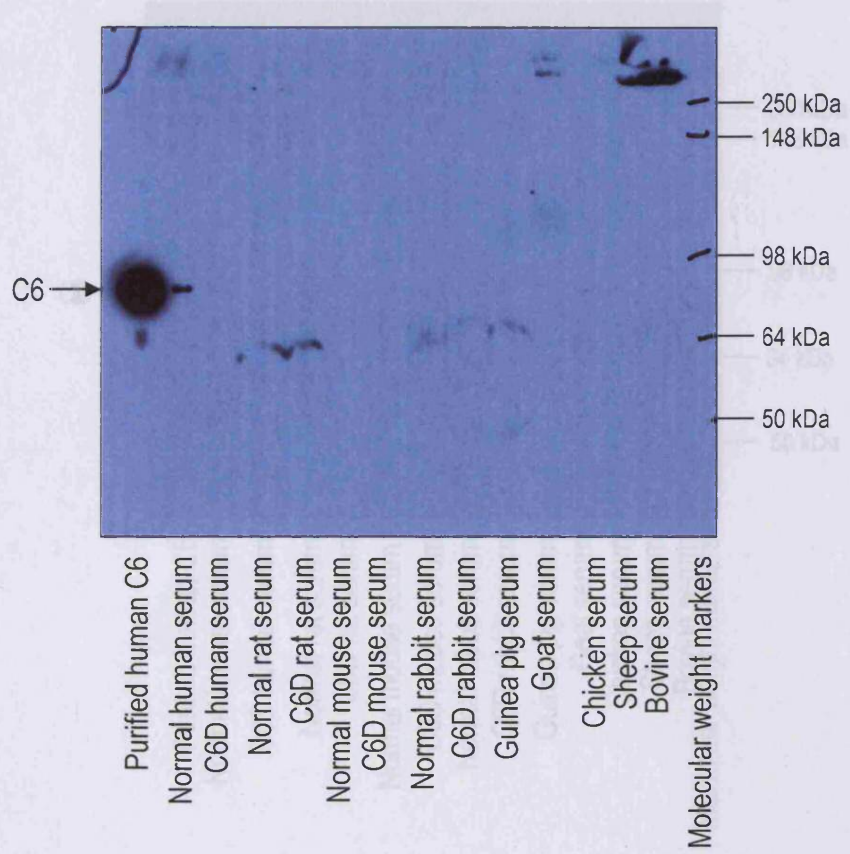

To determine if the mouse anti-human C6 mAb, 7A2 recognised other species C6, serum collected from the species listed above and purified human C6 were subject to SDS-PAGE, transblotted and 7A2 (1 µg/ml) was used as a primary antibody to detect C6. Secondary antibody was anti-mouse Ig-HRPO (1:10, 000 dilution) and bands were detected with ECL and visualised by autoradiography. Protein markers are depicted to the right of the figure.

Figure 4.16 Western blot to determine the cross-reactivity of the mouse anti-human C6 mAb 27B1 with C6 from other species

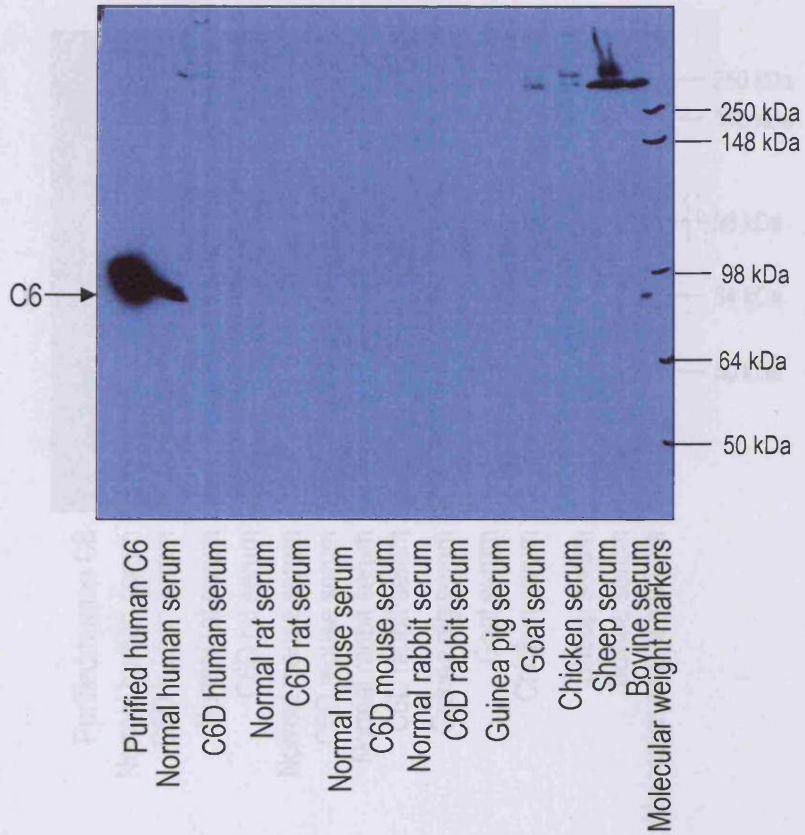

To characterise the ability of the mouse anti-human C6 mAb, 27B1 to recognise other species C6, serum collected from the species listed above as well as purified human C6, were subject to SDS-PAGE, transblotted and 27B1 (1 µg/ml) was used as a primary antibody to detect C6. Secondary antibody was anti-mouse Ig-HRPO (1:10,000 dilution) and bands were detected with ECL and visualised by autoradiography. Protein markers are shown on the right of the figure.

Figure 4.17 Western blot probed with secondary antibody only to determine the specificity of the primary antibodies 7A2 and 27B1

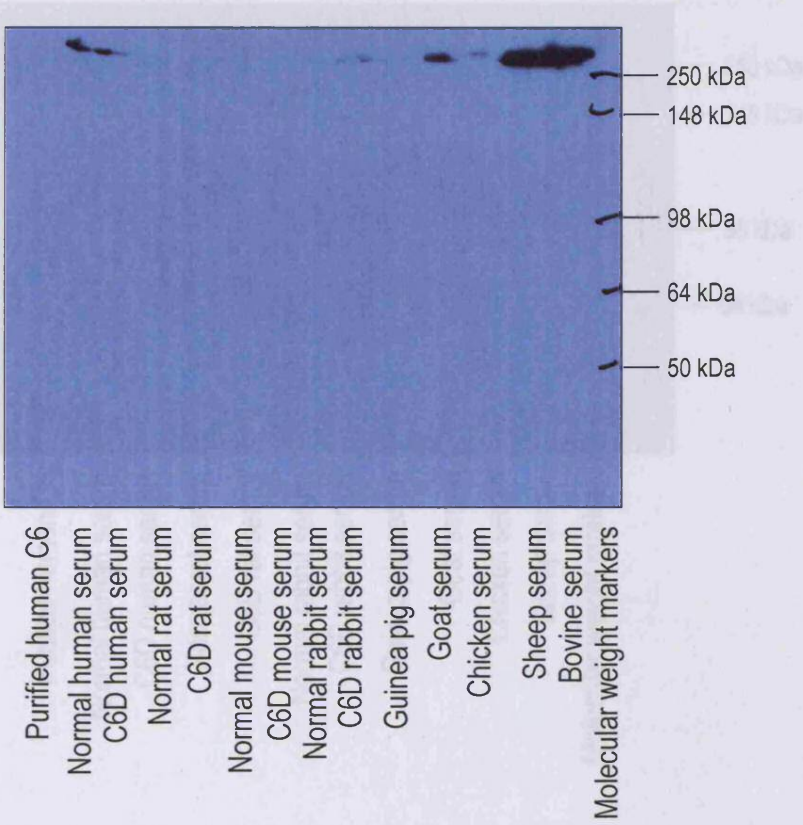

To confirm the specificity of the mouse anti-human C6 mAbs 7A2 and 27B1 for various species C6, serum collected from the species listed above as well as purified human C6, were subject to SDS-PAGE, transblotted and probed only with the secondary antibody anti-mouse Ig-HRPO (1:10,000 dilution). Any bands were detected with ECL and visualised by autoradiography. Protein markers are shown on the right of the figure.

Figure 4.18 Western blot to determine the cross-reactivity of the mouse anti-human C6 mAb 23D1 with C6 from other species

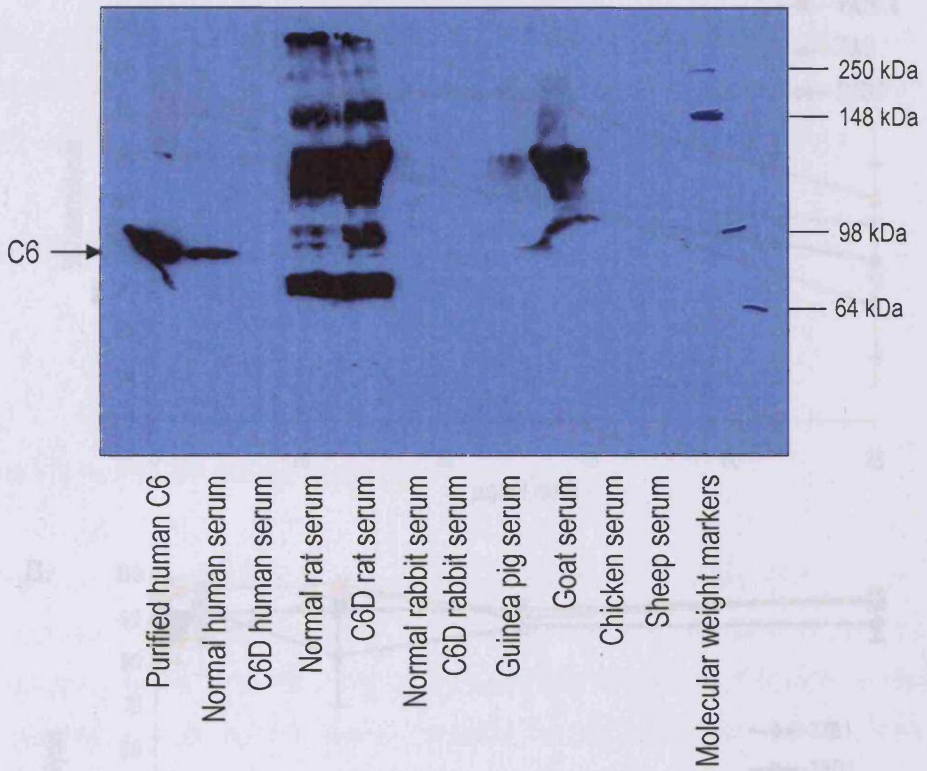

To determine if the mouse anti-human C6 mAb, 23D1 recognised other species C6, serum collected from the species listed above and purified human C6 were subject to SDS-PAGE, transblotted and 23D1 (1 µg/ml) was used as a primary antibody to detect C6. Secondary antibody was anti-mouse Ig-HRPO (1:10, 000 dilution) and bands were detected with ECL and visualised by autoradiography.

Figure 4.19 Haemolytic assay using rat serum to determine whether the antibodies 23D1 or 27B1 have inhibitory activity against either A. rat C6 or B. guinea pig C6.

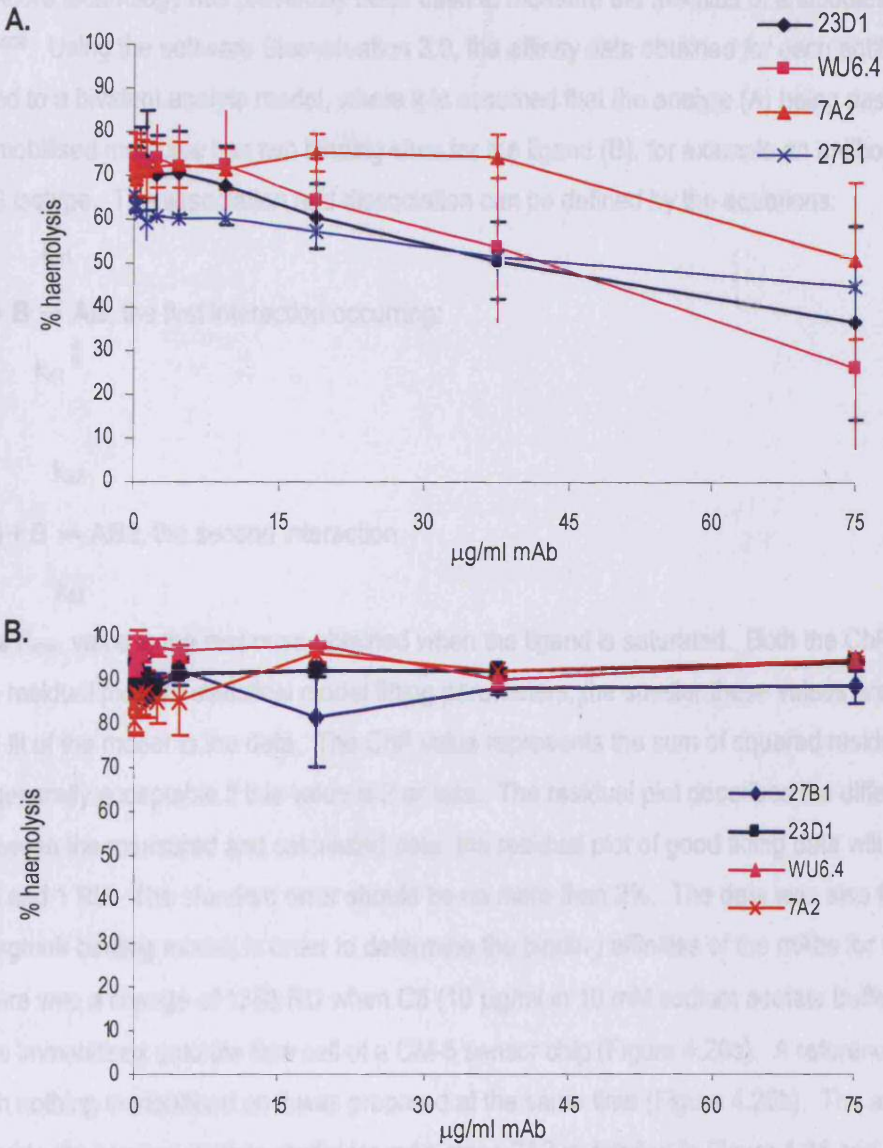

A dilution range of purified mAb was made (0 – 75 µg/ml) in CFD. Fifty microlitres were added to either 50 µl diluted rat or guinea pig serum and 50 µl 2% sheep EA in a 96 round-bottomed well. This mixture was incubated at 37°C for 30 minutes. The plates were then centrifuged at 2500 rpm for 5 minutes and the supernatants transferred to a flat-bottomed microtitre plate and the absorbance measured at 415 nm. The percentage of haemolysis was calculated for each sample and plotted against the concentration of mAb. Error bars are the standard error of the mean; n=2 for each condition.

order to be able to measure inhibition, these mAbs are at best weakly inhibitory of rat C6 activity. When guinea pig serum was used, no inhibition of guinea pig C6 activity was observed.

4.3.6. Measuring the affinity of the anti-human C6 mAbs 7A2 and 23D1 for human C6 using the BIAcore

BIAcore technology has previously been used to measure the affinities of antibodies for antigens [523-526]. Using the software Biaevaluation 3.0, the affinity data obtained for each antibody was fitted to a bivalent analyte model, where it is assumed that the analyte (A) being passed over the immobilised molecule has two binding sites for the ligand (B), for example an antibody with an IgG isotype. The association and dissociation can be defined by the equations:

k_{a1}

A + B $\rightleftharpoons$ **AB**, the first interaction occurring:

k_{d1}

k_{a2}

AB + B $\rightleftharpoons$ **AB2**, the second interaction

k_{d2}

The R_{max} value is the response obtained when the ligand is saturated. Both the Chi^2 value and the residual plot are statistical model fitting parameters; the smaller these values are, the better the fit of the model to the data. The Chi^2 value represents the sum of squared residuals – the fit is generally acceptable if this value is 2 or less. The residual plot describes the difference between the measured and calculated data; the residual plot of good fitting data will be between 0.5 and 1 RU. The standard error should be no more than 2%. The data was also fitted to a 1:1 Langmuir binding model, in order to determine the binding affinities of the mAbs for C6.
There was a change of 1383 RU when C6 (10 μg/ml in 10 mM sodium acetate buffer, pH 4.0) was immobilised onto the flow cell of a CM-5 sensor chip (Figure 4.20a). A reference flow cell with nothing immobilised on it was prepared at the same time (Figure 4.20b). The affinity data fitted to the bivalent analyte model for mAb clone 7A2 is detailed in Figure 4.21 and fitted to the 1:1 Langmuir model in Figure 4.22. The sensorgram for the corresponding control experiment to determine if mass transfer effects had occurred during experiments is shown in Figure 4.23. The sensorgrams overlay each other perfectly, demonstrating that mass transfer effects were kept to a minimum in this experiment. The bivalent analyte model fits well to the data obtained for the

Figure 4.20 A. Immobilisation of purified human C6 on a CM-5 sensor chip and B. preparation of a control surface

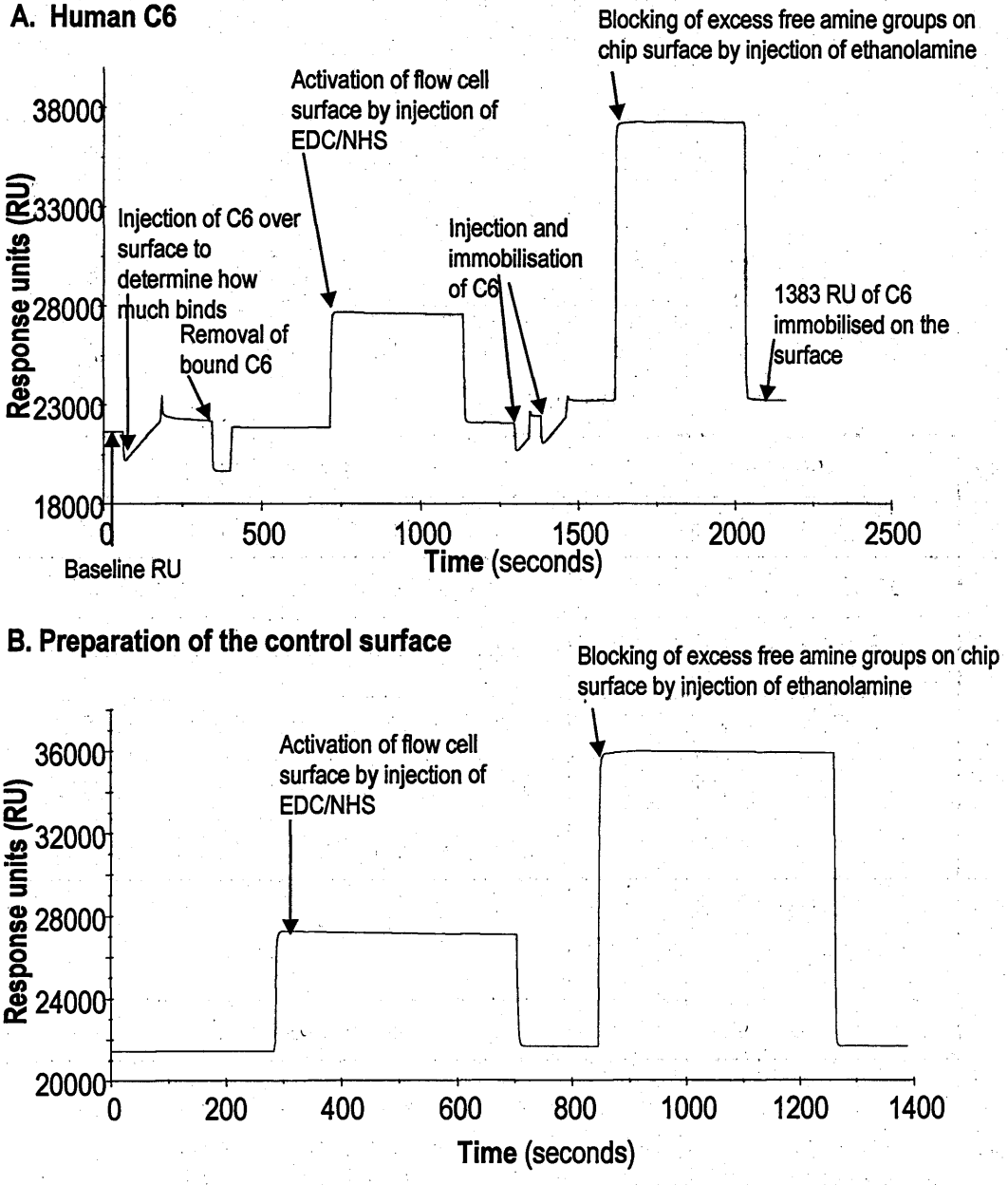

A. After determining the rate at which purified human C6 (10 µg/ml in 10 mM sodium acetate buffer, pH 4.0) bound to the chip, the surface was activated by passing EDC/NHS over and then the C6 was injected over the chip and allowed to covalently couple to it. When the target RU had been reached, ethanolamine was passed over the flow cell surface to block any free amine groups remaining. **B.** The control surface (nothing bound) was prepared by activating the surface and then blocking it as described.

Figure 4.21 Analysis of the binding affinity of the anti-C6 mAb clone 7A2 for human C6 fitted to a bivalent analyte model

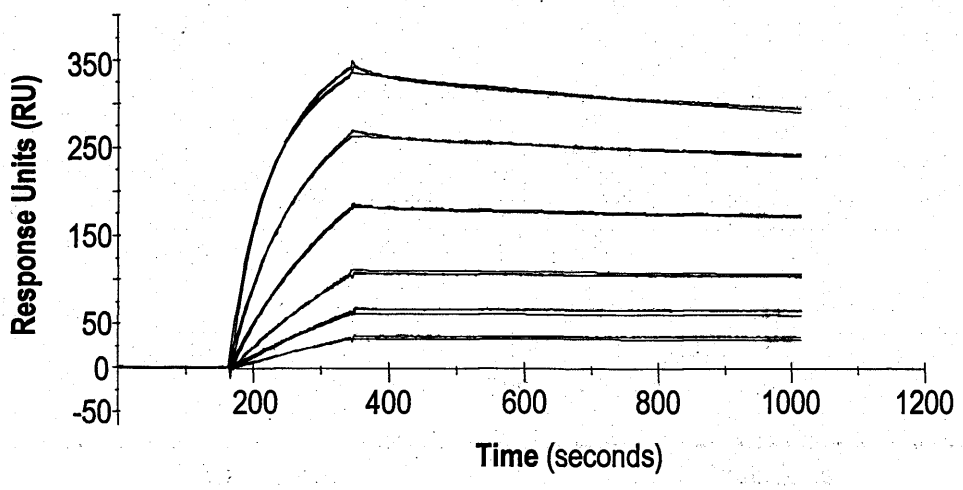

Parameters	Calculations
First association rate constant, k_a1	$3.11 \times 10^4 \pm 89.2$ $M^{-1}s^{-1}$
First dissociation rate constant, k_d1	$6.02 \times 10^{-4} \pm 6.61 \times 10^{-6}$ s^{-1}
Second association rate constant, k_a2	$1.99 \times 10^{-3} \pm 1.23 \times 10^{-4}$ $RU^{-1}s^{-1}$
Second dissociation rate constant, k_d2	$0.0407 \pm 2.47 \times 10^{-3}$ s^{-1}
First association equilibrium constant, K_A	5.17×10^7 M^{-1}
First dissociation equilibrium constant, K_D	1.9×10^{-8} M
R_{max}	586 ± 1.19 RU
Chi^2	9.2
Residual plot	-20 - +10

The anti-C6 mAb 7A2 was injected over human C6 which had been immobilised onto a CM5 chip at a range of concentrations (10.4 nM – 1.0 μM). At the end of each injection, the mAb was allowed to dissociate for 15 minutes. The data was recorded and fitted to a model of bivalent analyte binding to ligand. This is represented graphically above, where the coloured lines of each trace represent the experimental data obtained and the black lines represent the corresponding curve-fit. The interpreted data is summarised in the table above. The numbers following the ± represent the Standard Error.

Figure 4.22 Analysis of the binding affinity of the anti-C6 mAb clone 7A2 for human C6 fitted to a Langmuir binding model

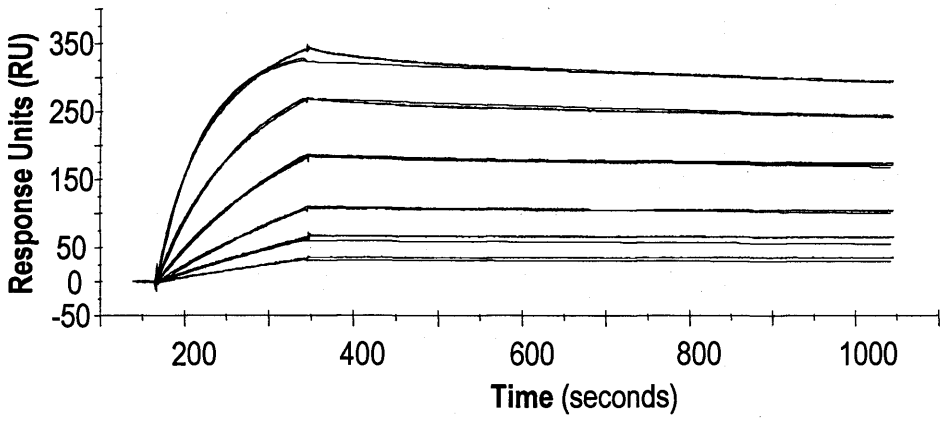

Parameters	Calculations
Association rate constant, k_a	$1.1 \times 10^5 \pm 120\ M^{-1}s^{-1}$
Dissociation rate constant, k_d	$1.41 \times 10^{-4} \pm 1.29 \times 10^{-6}\ s^{-1}$
Association equilibrium constant, K_A	$7.83 \times 10^8\ M^{-1}$
Dissociation equilibrium constant, K_D	1.28×10^{-9} M
R_{max}	339 ± 0.222
Chi^2	18.6
Residual plot	-10 - + 20

Human C6 was immobilised onto a CM5 chip. To determine the affinity of the anti-C6 mAb 7A2 for C6, it was passed over the immobilised C6 at a range of concentrations (10.4 nM – 1.0 μM). At the end of each injection, the mAb was allowed to dissociate for 15 minutes. The data was recorded and fitted to a model of analyte binding to ligand in a 1:1 ratio (Langmuir). This is represented graphically above, where the coloured lines of each trace represent the experimental data obtained and the black lines represent the corresponding curve-fit. The interpreted data is summarised in the table above. The numbers following the ± represent the Standard Error.

Figure 4.23 Experiment to determine whether mass transfer effects occurred during the binding affinity measurements of mAb 7A2 for human C6

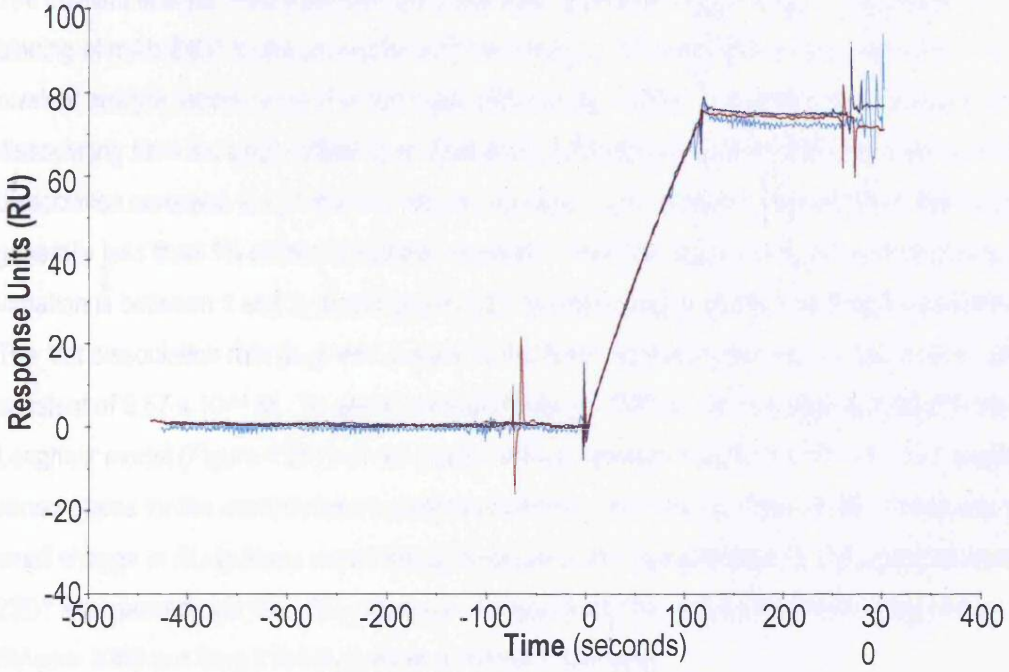

The mAb 7A2 (3.125 μg/ml in HBS-EP buffer) was passed over a flow cell on which human C6 had been immobilised at flow rates of 5 (turquoise line), 15 (navy line) and 75 (red line) μl per minute. Sensorgrams of each experiment were recorded and have been superimposed on each other to determine whether any mass transfer effects are occurring. As the gradient of each trace are identical, this suggests that there were no mass transfer effects in this experiment.

anti-C6 mAb 7A2 binding to human C6 (Figure 4.21). The data in the accompanying table shows that in general the standard errors for the calculated constants are less than 2%. The k_d1 value is very small, suggesting that mAb 7A2 has a slow dissociation rate from human C6, which is seen on the graph. The Chi^2 value and the residual plot value are both higher than desirable. By dividing the first dissociation rate (k_{d1}) by the first association rate (k_{a1}), an affinity constant of mAb 7A2 for C6 could be calculated, which was 1.9×10^{-8} M. The calculated affinity constant of mAb 7A2 for C6 from the 1:1 curve-fit was 1.28×10^{-9} M.

The bivalent analyte fitted data for mAb clone 23D1 is shown in Figure 4.24. This shows the binding of mAb 23D1 to the immobilised C6 at a range of concentrations (coloured lines) and the bivalent analyte model curve fit to that data with the black lines. The mAb does not seem to be dissociating from the chip surface over time and is reflected in the very small value for the first dissociation constant, k_d1, in the accompanying table. Apart from this, the standard errors are generally less than 1% of the calculated constants. The Chi^2 value is below 2 and the residual variation is between 1 and 3, illustrating that the bivalent analyte model has fitted to the data well. The first dissociation rate (k_{d1}) was divided by the first association rate (k_{a1}) to calculate an affinity constant of 9.57×10^{-11} M. To get an overall affinity of 23D1 for C6, the data was fitted to the Langmuir model (Figure 4.25) and the overall affinity constant was 6.18×10^{-13} M. The overlayed sensorgrams for the control mass transfer experiment are shown in Figure 4.26. There was a small change in RU in these experiments, because of the concentration (3.125 µg/ml) at which 23D1 was passed over C6. The change in RU approach the minimal sensitivity level of the BIAcore 3000 and thus it is not possible to interpret this data.

4.3.7. Epitope mapping of the antibodies using SPR technology

The BIAcore was also used to determine the epitope specificities of the anti-human C6 mAbs 7A2, 23D1, 24C2 and 27B1. Each mAb binds an epitope on the antigen; a pair of mAbs which bind to closely situated epitopes will interfere sterically with each other's binding, whilst mAbs recognising distant epitopes will bind independently of each other. SPR technology has previously been used in epitope mapping studies [527-529].

Epitope mapping was carried out according to the manufacturers recommended protocols as detailed in section 4.2.3.2. 7245.7 RU of RAM Igs (BIAcore, cat no BR-1005-14) (30 µg/ml in 10 mM sodium acetate buffer, pH 5.0) were immobilised onto the surface of a CM-5 sensor chip (Figure 4.27a). A reference flow cell surface was prepared by subjecting it to the immobilisation procedure, without immobilising anything onto it (Figure 4.27b).

Figure 4.24 Analysis of the binding affinity of the anti-C6 mAb clone 23D1 for human C6 fitted to a bivalent analyte model.

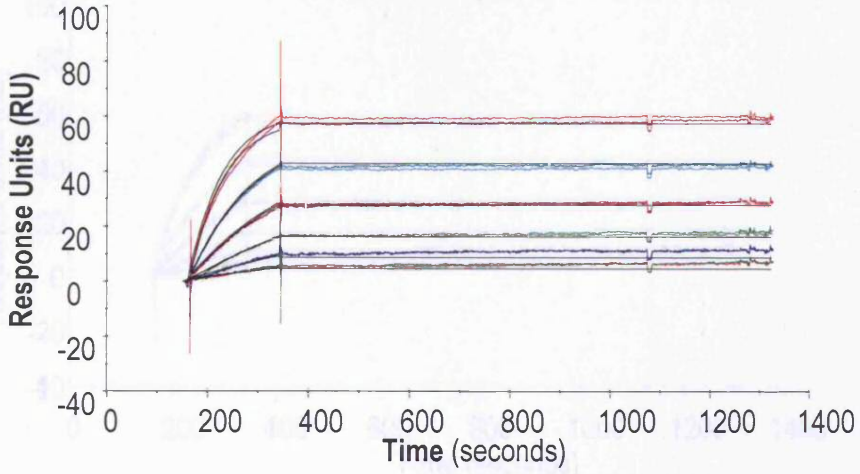

Parameters	Calculations
First association rate constant, k_{a1}	$2.8 \times 10^{4} \pm 177\ M^{-1}s^{-1}$
First dissociation rate constant, k_{d1}	$2.68 \times 10^{-6} \pm 8.9 \times 10^{-7}\ s^{-1}$
Second association rate constant, k_{a2}	$2.31 \times 10^{-4} \pm 6.41 \times 10^{-6}\ RU^{-1}s^{-1}$
Second dissociation rate constant, k_{d2}	$5.92 \times 10^{-4} \pm 4.48 \times 10^{-6}\ s^{-1}$
First association equilibrium constant, K_A	$1.04 \times 10^{10}\ M^{-1}$
First dissociation equilibrium constant, K_D	$9.57 \times 10^{-11}\ M$
R_{max}	88.4 ± 0.554 RU
Chi^2	1.68
Residual plot	1 - 3

The mAb, 23D1 was passed over human C6 over a concentration range (5.21×10^{-9} M – 1.67×10^{-7} M). At the end of each injection, the mAb was allowed to dissociate for 15 minutes. The data was recorded and the software, BIAevaluation 3.0 used to align each trace and fit the data to a bivalent analyte model of binding. The coloured lines of each trace represent the experimental data obtained and the black lines represent the corresponding curve-fit.

Figure 4.25 Analysis of the binding affinity of the anti-C6 mAb clone 23D1 for human C6 fitted to a 1:1 (Langmuir) binding model.

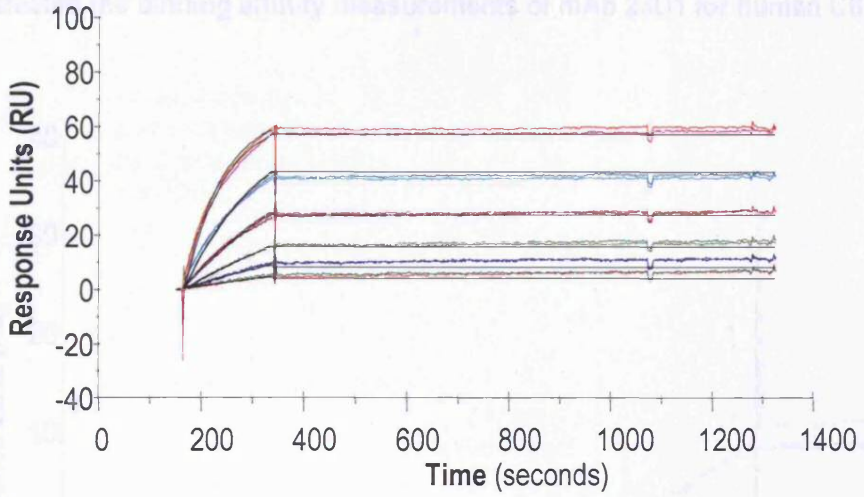

Parameters	Calculations
Association rate constant, k_a	7.9 x 104 ± 197 $M^{-1}s^{-1}$
Dissociation rate constant, k_d	4.88 x 10^{-8} ± 4.28 x 10^{-7} s^{-1}
Association equilibrium constant, K_A	1.62 x10^{12} M^{-1}
Dissociation equilibrium constant, K_D	6.18 x 10^{-13} M
R_{max}	63.7 ± 0.077 RU
Chi^2	2.33
Residual plot	-4 - +5

Several concentrations (5.21 x 10^{-9} M – 1.67 x 10^{-7} M) of the anti-C6 mAb 23D1 were passed over a sensor chip surface on which human C6 had been immobilised and allowed to dissociate for 15 minutes. The data was recorded and the software BIAevaluation 3.0 used to align each trace and fit the data to a 1:1 Langmuir binding model. The coloured lines of each trace represent the experimental data obtained and the black lines represent the corresponding curve-fit.

Figure 4.26 Experiment to determine if mass transfer effects might have affected the binding affinity measurements of mAb 23D1 for human C6

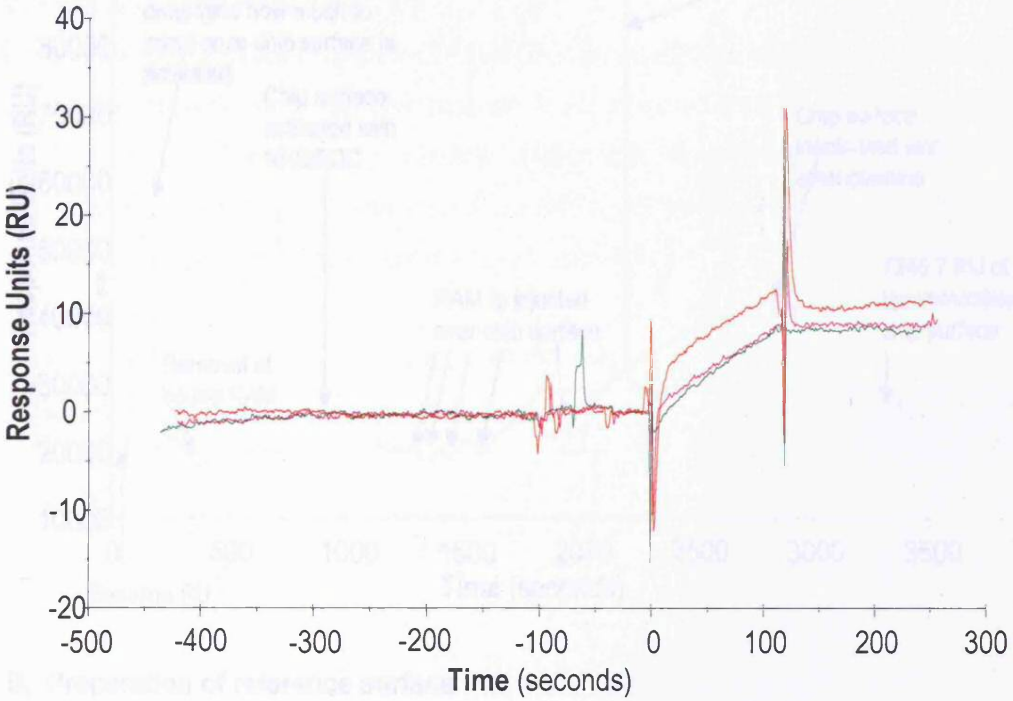

The monoclonal antibody 23D1 (3.125 μg/ml) was injected over a sensor chip on which human C6 had previously been immobilised at flow rates of 5 (red line), 15 (pink line) and 75 (green line) μl per minute. Sensorgrams were recorded of each experiment and above have been superimposed upon each other.

Figure 4.27 Immobilisation of A. rat anti-mouse immunoglobulins (RAM Igs) onto a CM-5 sensor chip and B. preparation of a reference surface.

A. RAM Igs

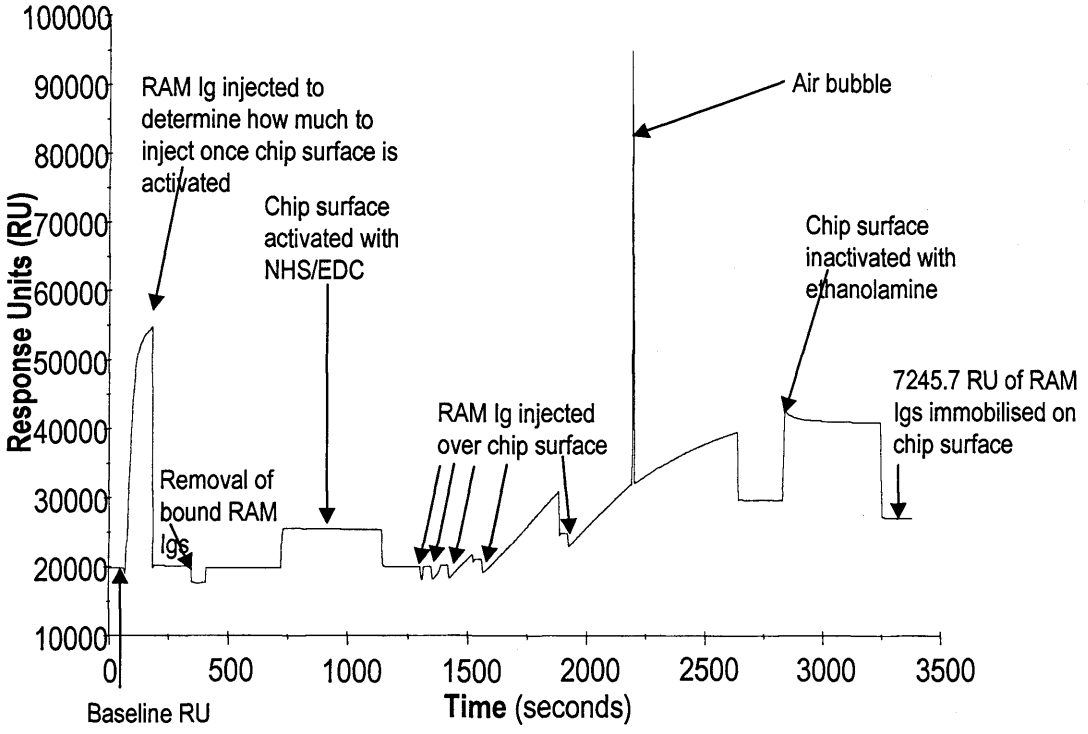

B. Preparation of reference surface

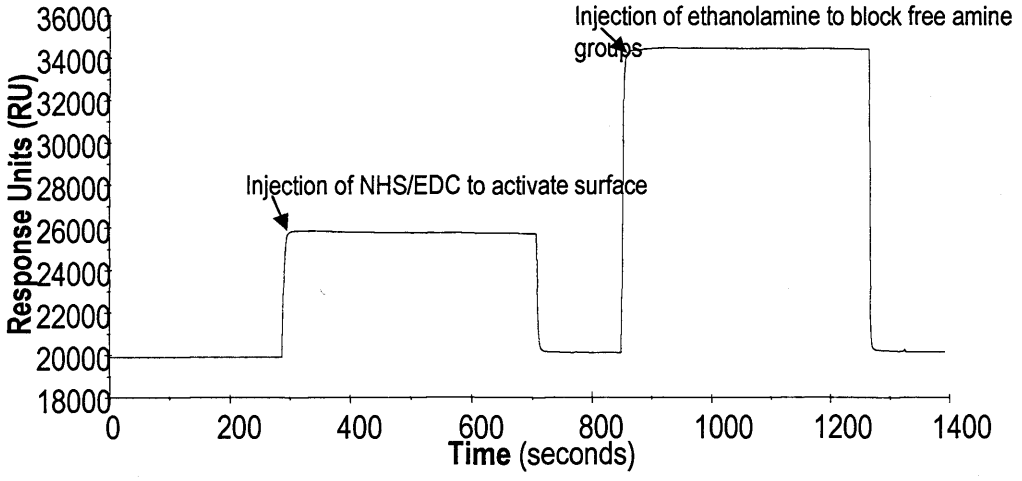

A. The rate at which RAM Igs (30 μg/ml in 10 mM sodium acetate buffer, pH 5.0) was determined. The chip surface was activated by passing NHS/EDC over and then RAM Igs were injected and allowed to couple to it. The activated surface was blocked by passing ethanolamine over. **B.** The control surface was prepared by activating it and then blocking free amine groups as described.

The first set of epitope mapping experiments was carried out with the mAb clone 23D1 being flowed over the RAM Ig immobilised flow cell and also the reference surface, to act as a capture antibody for C6 and then either mAb clone 7A2, 27B1, 24C2 or WU 6.4 being passed over the captured C6. The anti-human C6 mAb clone WU 6.4 recognises the third thrombospondin repeat of C6 (modular structure shown in figure 1.2) [522] and was included in this experiment to gain more information about the epitopes recognised by the antibodies being characterised. A typical sensorgram of the epitope mapping experiment is shown in figure 4.28. The data from these experiments is summarised in table 4.3.

Although the specificity of the mAbs for C6 had been determined either by ELISA or Western blot, control experiments to confirm that the increases in RU observed when the mAbs were passed over the captured C6 were due to a specific interaction with C6 were carried out. Briefly, the same experiment was carried out for each of the antibodies, but with the omission of C6 being injected over the chip. This data is summarised in table 4.4.

Table 4.3. 23D1 versus 7A2, 27B1, 24C2 and WU 6.4

Capture mAb 23D1 (RU)	Human C6 (RU)	Blocking agent Mouse Ig (RU)	Second mAb			
			7A2 (RU)	27B1 (RU)	24C2 (RU)	WU 6.4 (RU)
850.5	369.8	944.4	305.7	-	-	-
751.0	436.0	977.9	-	166.4	-	-
667.9	364.8	1123.9	-	-	129.0	-
528.8	337.9	1223.1	-	-	-	281.2

Table 4.4 23D1 versus 7A2, 27B1, 24C2 and WU 6.4 in the absence of human C6.

Capture mAb 23D1 (RU)	Blocking agent Mouse Ig (RU)	Second mAb			
		7A2 (RU)	27B1 (RU)	24C2 (RU)	WU 6.4 (RU)
289.6	756.6	194.8	-	-	-
305.8	764.9	-	403.7	-	-
311.4	758.6	-	-	117.6	-
309.2	749.4	-	-	-	73.2

Each of the mAb tested bound to C6 captured by immobilised 23D1 (Table 4.3). However, all of the mAbs also bound to the sensor chip in the absence of C6 (Table 4.4). As the mAbs had been shown to specifically recognise C6, the data suggest that the chip surface had not been completely blocked using mouse Ig. This makes it impossible to accurately interpret the data shown in Table 4.3 or similar studies with the other mAbs captured on the chip. Due to time constraints, the epitope mapping experiments were not further optimised.

Figure 4.28 Typical sensorgram of an epitope mapping experiment

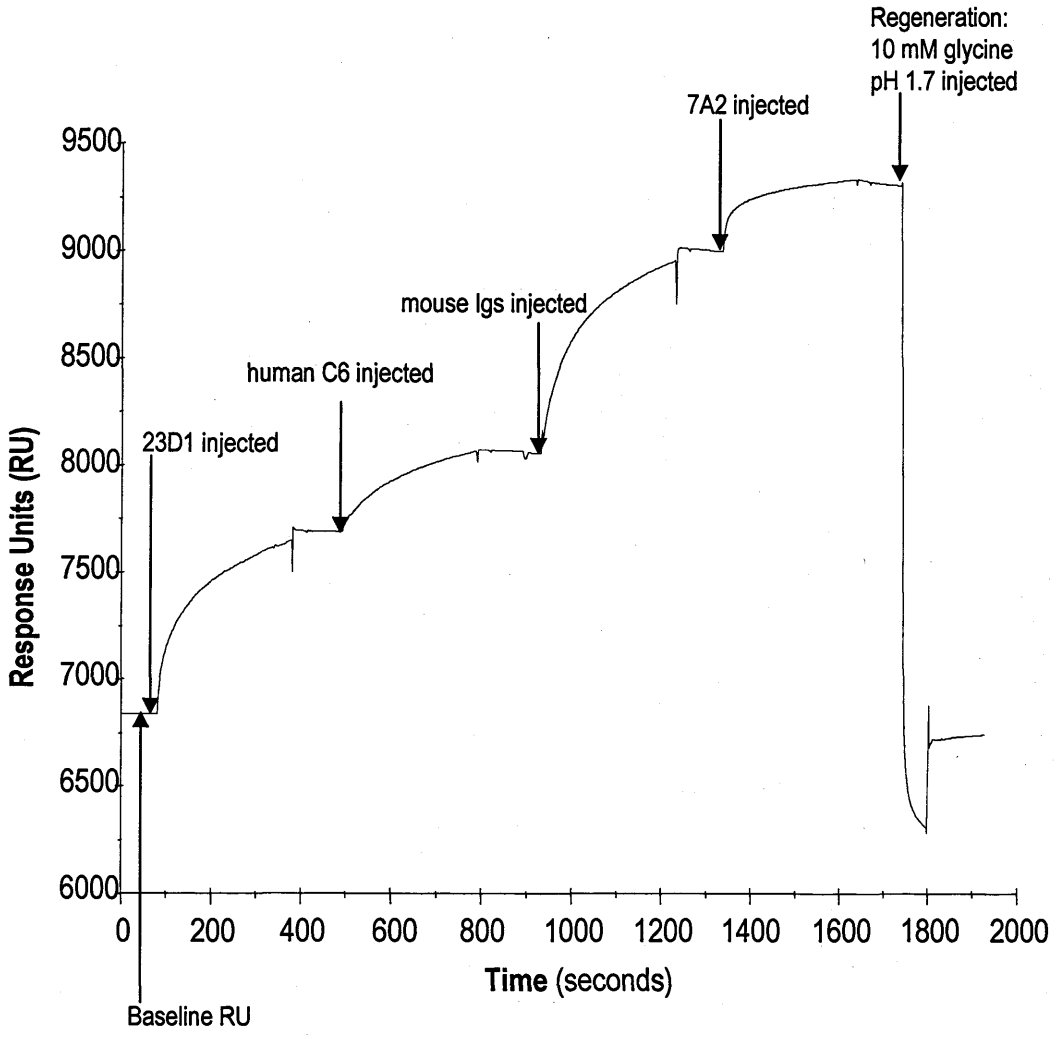

Each reagent was injected over the flow cell to which the RAM Igs had been immobilised and the control cell at a concentration of 100 μg/ml, a flow rate of 20 μl/min for 5 minutes each. At the end of each experiment, the surfaces were regenerated with 10 mM glycine, pH 1.7. In this experiment mAb 23D1 was the capture antibody for C6 and mAb 7A2 was the secondary antibody.

Less mAb 23D1 was captured on the chip surface for the control experiments (Table 4.4) than in the epitope mapping experiments (Table 4.3). This might indicate that the immobilised ligand was gradually denaturing, probably due to 10 mM glycine, pH 1.7 being passed over the surface at the end of each experiment to remove any remaining analyte. This is normal and defines the lifespan of the sensor chip and the decrease in RU observed when 23D1 was passed over the chip is likely a reflection of this phenomenon.

4.3.8. Analysis to determine whether any contamination was present in the samples passed over the BIAcore.

Data obtained from experiments involving the BIAcore, in particular the epitope mapping experiments indicated that the samples of mAb used might be of insufficient purity. The most probable source of contaminant would have been the medium in which the anti-C6 secreting hybridomas were cultured as this contained bovine Ig. To investigate this, aliquots (10 μg) of mAbs and mouse immunoglobulins used in the epitope mapping experiments were subject to SDS-PAGE and in parallel, stained with coomassie blue (figure 4.29a) or subject to western blot and probed with either an anti-mouse immunoglobulin antibody (figure 4.29b), or an anti-bovine immunoglobulin antibody (figure 4.29c), each of which were non-cross species reactive. Coomassie staining showed that all of the samples – purified mAbs 7A2, 23D1, 27B1, 24C2, WU 6.4 and mouse IgG contained protein with a molecular weight consistent with that of IgG. Western blotting of the mAbs and mouse IgG showed that they all contained mouse Ig, as expected. However, by probing with the anti-bovine Ig antibody, it could be seen that all of the purified mAbs, apart from WU6.4 were contaminated with bovine Ig. As would be expected, the sample of mouse IgG did not contain any bovine Ig, having been prepared from mouse serum. It is possible that the bovine Ig retained in these preparations were competing with the anti-mouse Ig immobilised on the sensor chip, limiting the amount of mouse Ig able to bind to the anti-mouse Ig.

4.4 Discussion

This chapter describes the generation of a panel of polyclonal and monoclonal antibodies (mAbs) raised against rabbit, rat, mouse or human C6, that all recognise human C6. Many of the mAbs inhibited C-mediated haemolysis, presumably by interacting with C6. As the point of this work was to identify an inhibitory C6 mAb with a minimal C-activating isotype, two mAbs were selected

Figure 4.29 Coomassie staining and Western blotting to determine the purity of reagents used in BIAcore experiments

A. Coomassie stained acrylamide gel

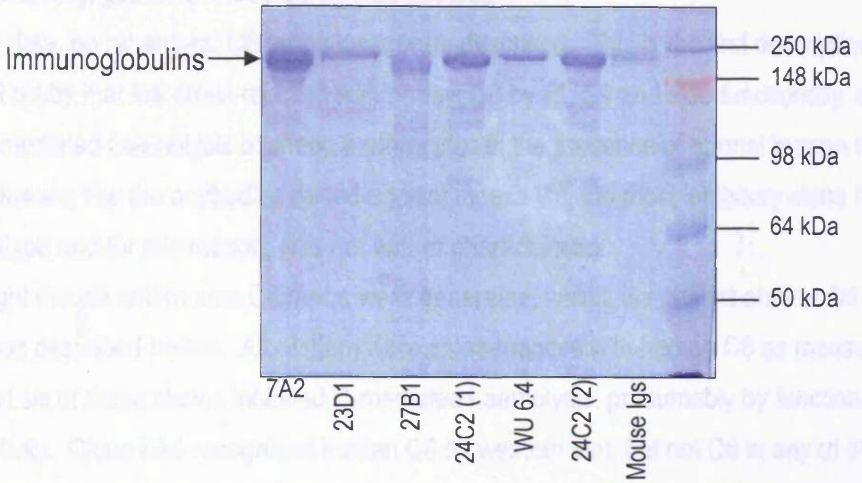

B. Western blot for mouse immunoglobulins

C. Western blot for bovine immunoglobulins

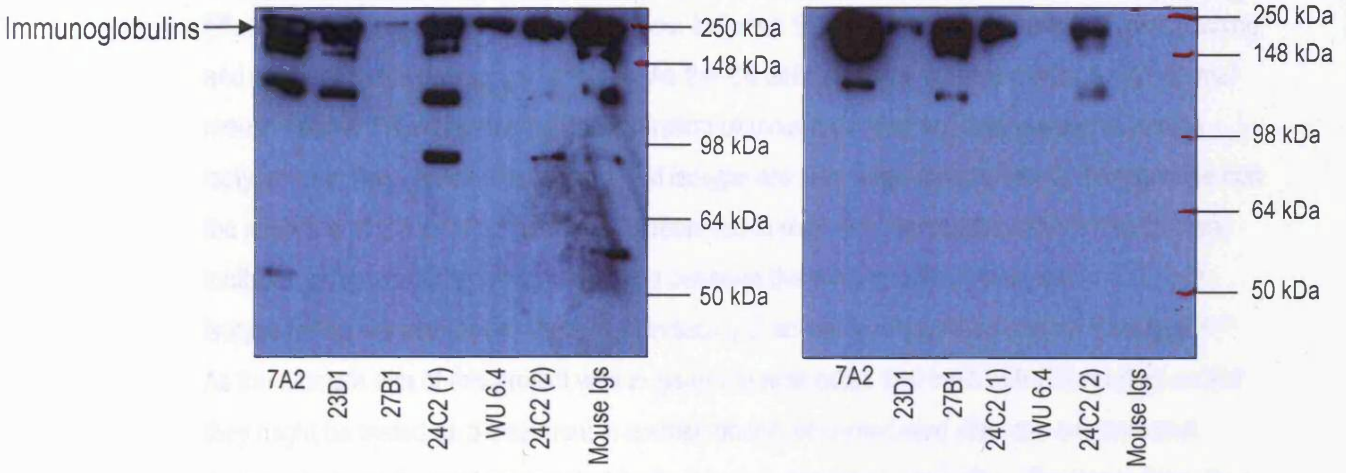

To determine whether the mAbs purified from tissue culture supernatant also contained bovine Ig, samples (10 μg) of the mAbs were subject to SDS-PAGE and either **A.** stained with Coomassie, or transblotted to nitrocellulose, blocked and **B.** incubated with non-species cross reactive anti-mouse Igs or **C.** incubate with non-species cross-reactive anti-bovine Igs. The blots were developed with ECL and visualised by autoradiography. 24C2 (1) and 24C2 (2) refer to different aliquots of stocks of this mAb.

for more detailed characterisation, based upon their C6-inhibitory properties and isotype. For comparison, a non-inhibitory anti-C6 mAb with an identical isotype to the two inhibitory mAbs, clone 7A2, was also further characterised.

Of the antibodies raised against C6, the anti-rabbit C6 polyclonal antibody recognised two bands in human serum by western blot. The higher one had a molecular weight consistent with C6, the lower one was likely a degradation product of C6. In addition, this polyclonal antibody recognised guinea pig, goat and sheep C6 by western blot.

To date, no rat anti-rat C6 mAbs have been described. This is the first description of rat anti-rat C6 mAbs that are cross-reactive with human C6 by ELISA and also functionally, as they inhibited C-mediated haemolysis of sheep erythrocytes in the presence of normal human serum. However, like the antibodies raised against mouse C6, the most inhibitory clone had an IgM isotype and for this reason, was not further characterised.

Eight mouse anti-mouse C6 mAbs were generated, which, like the rat anti-rat C6 mAbs have not been described before. All of them were cross-reactive with human C6 as measured by ELISA and six of these clones inhibited C-mediated haemolysis, presumably by functionally inhibiting C6 activity. Clone 8A4 recognised human C6 by western blot, but not C6 in any of the other species sera tested. All of these mAbs had an IgM isotype: the first phase of the humoral immune response is characterised by an early rise of antigen-specific IgM due to clonal B-cell expansion [530]. In the second phase, interactions occur between B- and T-cells, leading to isotype switching and memory B-cell development [531,532]. As the C6 deficient mice were immunised with normal mouse serum, it is likely that the concentration of mouse C6 was not high enough to induce isotype switching. Antibodies with an IgM isotype are very large molecules and it is possible that the inhibition of C-mediated haemolysis observed in experiments may have been due to steric inhibition rather than a specific interaction between the mAb and the 'active site' of C6. IgM isotype mAbs are also more effective at inducing C activation than those of an IgG isotype [30,31]. As the ultimate aim of this project was to generate antibodies that inhibit MAC formation so that they might be tested as a treatment in animal models of C-mediated disease, any potential therapeutic benefit would be negated by their own C-activating properties. For this reason, these antibodies were not characterised further, although clone 8A4 was very good at recognising human C6 by western blot and will be a useful antibody for detecting C6.

Nineteen mouse anti-human C6 mAbs were identified, presenting a new and valuable resource to be used in research involving human C6. Seven of these had an IgM isotype and for reasons already discussed, were not further characterised. Of the twelve remaining, the three most interesting mAbs were selected for further characterisation: all of them - clones 7A2, 23D1 and

27B1, recognised C6 by western blot. Clone 7A2 did not inhibit C-mediated haemolysis, whilst clones 23D1 and 27B1 did.

Western blotting was performed to determine whether clones 7A2, 23D1 and 27B1 recognised other animal species C6. Clones 27B1 and 23D1 detected human C6, but did not detect C6 in other sera tested. At high concentrations, mAbs 23D1 and 27B1 were weakly inhibitory against rat serum and had no activity against guinea pig serum in haemolytic assays. The functional data strongly suggest that mAb 7A2 recognises a different epitope from mAbs 23D1 and 27B1. The FIMs domains of C6 enhance its activity, by forming the first reversible interactions with the C345C domain of C5 [83,85], whilst the C control protein (CCP) modules are critical for its activity (discussed in section 1.1.2.) [84], suggesting that C6 binds irreversibly to C5b through its CCP domains. C7 binds to the C345C domain of C5b through its FIMs domains with a higher affinity than C6 [85], leading to the suggestion that during the initial stages of MAC formation, C6 interacts with C5b through its FIMs domains, which leads to interactions between other regions of C6, such as the CCP domains and regions of C5. The C7 FIMs domains then displace the C6 FIMs domains, forming C5b-7. Therefore, it is probable that mAbs 23D1 and 27B1 recognise either the FIMs domains or the CCP domains of C6. With hindsight, it would have been informative to perform reactive lysis assays to determine whether mAbs 23D1 and 27B1 inhibited C5b6 formation or C7 binding to form a complex with C5b6.

SPR was used to measure the binding affinities of the anti-human C6 mAbs 7A2 and 23D1 for human C6. Data obtained from both experiments appeared to fit well to the bivalent analyte binding model. However, statistical analysis of the curve-fitting data showed that whilst this was true for mAb 23D1, the fit was not quite so accurate for mAb 7A2. The binding affinity of a mAb for antigen is usually in the order of 10^{-9} M [533]. The anti-C6 mAb 7A2 had an affinity of 1.9×10^{-8} M when the data was fitted to the bivalent analyte model and 1.28×10^{-9} M when fitted to the 1:1 model of interaction. These binding affinities are in the lower range of the expected binding affinity of a mAb for antigen. The difference between the two affinities is most likely due to the way they were calculated. For example, the affinity from the bivalent analyte fitted data refers to the first interaction only, whereas in the 1:1 model, there is only one interaction characterised. Antibody 23D1 had a particularly high affinity for human C6, which was 9.57×10^{-11} M when fitted to the bivalent analyte model and 6.18×10^{-13} M when fitted to the 1:1 Langmuir model. These high affinities were mainly due to the slow dissociation rate of 23D1 from C6. On the sensorgram, it looked like the interaction between the mAb and the immobilised C6 was essentially irreversible. This is probably an indication that the observed slow rate was due to avidity rather than affinity. There are other instances in the literature where the affinities of mAbs

from antigens have been determined using BIAcore technology and similar slow dissociation rates between antibody and antigen have been observed. For example, a mAb has been identified that binds to thrombin [534] and has a very slow dissociation rate that is almost irreversible [535].

Results from epitope mapping experiments initially looked very promising, but control experiments highlighted a lack of specificity of many of the mAb preparations and made it impossible to draw any meaningful conclusions as to the epitopes recognised by the mAbs. Western blotting showed that some of the samples were heavily contaminated with bovine Ig. This was probably co-purified with the mouse Ig during the purification of the mouse Ig, as bovine Ig also has a high affinity for protein A. It is also possible that the rabbit anti-mouse (RAM) Ig immobilised on the chip surface may have been cross-species reactive with bovine Ig, so that the bovine Ig were captured by the immobilised RAM Ig. One way around this contamination problem would have been to culture the hybridomas in serum-free chemically defined culture medium, such as CD hybridoma medium (Invitrogen). In house, a number of measures have recently been instigated to deal with this problem. To minimise the presence of the bovine Ig in the culture medium, the hybridoma cell lines are now cultured in culture medium supplemented with low Ig-containing bovine serum instead of normal bovine serum. In addition, the hybridomas are cultured in high expression systems including Integra™ flasks (IBS Integra Biosciences, Switzerland) and the Technomouse™ system (IBS Integra Biosciences, Switzerland). Both of these systems are improvements upon standard tissue culture cultivation techniques in that nutrients and oxygen are delivered to the cells cultured within a compartment and simultaneously waste products and carbon dioxide are diffused out of the cell culture compartment, encouraging maximal cell growth and protein secretion, leading to the accumulation of milligrams of protein. As well as altering the culture conditions, changes to the purification protocol of the mAbs from culture supernatant have been made. Both bovine Ig and mouse IgG_1 have a high affinity for prosep-G [536], meaning that bovine Ig can also be co-purified from the prosep-G. Mouse $IgG_{1\kappa}$ binds to prosep-A at a capacity of approximately 13 mg/ml whilst bovine Ig binds to prosep-A at a capacity of 27 mg/ml [537], but bovine Ig elutes from prosep-A at a different pH from mouse IgG_1. These properties can be made use of by incorporating washes to specifically elute the bovine Ig before eluting the mAb of interest, allowing a greater degree of purity to be achieved.

In conclusion, a panel of nearly 30 different antibodies have been raised against rabbit, rat, mouse or human C6 and all recognise human C6. Anti-rat C6 and anti-mouse C6 mAbs have not been previously described and although the ones generated in this work were not further

characterised, they will be useful tools in any research requiring anti-rat or anti-mouse C6 mAbs. Many of the antibodies had inhibitory activity in haemolytic assays and two with an IgG isotype were further characterised. These were found to be specific for human C6, meaning that their therapeutic potential cannot be investigated in animal models of disease in which C plays a role, although it will be possible to carry out further ex vivo studies using human serum (chapter 6).

Chapter 5: The Identification of Peptides that bind C6 using Phage Display.

5.1 Introduction

The pharmaceutical industry is increasingly interested in developing peptides as drug candidates because they can be synthesised cheaply, and are stable, so that they can be stored for long periods at room temperature [538]. The development of phage display technology has enabled peptides specifically recognising a protein to be rapidly identified. Phage display is a selection technique in which DNA encoding a peptide sequence or protein is fused to a gene encoding a coat protein of a bacteriophage (phage). This results in the expression or display of the peptide on the surface of the virion (Figure 5.1). Phage display provides a physical link between a vast library of random peptide sequences and the DNA encoding each sequence, allowing rapid identification of peptide ligands for a variety of target molecules, including antibodies, enzymes and cell-surface receptors, by an *in vitro* selection process called *panning* [539,540]. In its simplest form, panning is performed by incubating a library of phage-displayed peptides with immobilised target protein (on plates or beads), washing away the unbound phage, and eluting the specifically-bound phage. The eluted phage are then amplified and taken through additional panning and amplification cycles to significantly enrich the pool in favour of sequences that specifically bind the target protein. After 3 - 4 rounds of panning, individual clones are characterised by DNA sequencing. This process is depicted schematically in Figure 5.2.
Often, the panning procedure is more complex than that described above. For example, phage-peptides have been panned against immobilised, purified receptors [541] as well as against intact cells [542-544] leading to the identification of functionally active peptides. Affinity tags can be attached upstream from the randomised region of the phage. This has enabled the substrates of enzymes to be determined, as it becomes possible to separate cleaved from uncleaved phage with the appropriate affinity matrix [545]. It is also possible to fuse longer DNA sequences to the phage genome, resulting in larger proteins being displayed by the phage, such as antibodies [546], hormones [547], protease inhibitors [355], enzymes [548] and DNA binding proteins [549]. The endless variations in the nature of the substrate the phage-peptides can be panned against, together with the fact that the DNA sequences of binding proteins can be rapidly obtained and thus used as source material to generate phage peptide libraries, makes phage display an extremely powerful tool that can be applied to many different fields in medical research [348-350,550-555] and the pharmaceutical industry [328,556-563].
Phage display has been used to identify C- inhibitory agents with therapeutic potential. For example, Compstatin, a peptide that blocks C3 convertase formation, was discovered by panning

Figure 5.1 A schematic diagram of the surface of a phage displaying peptides.

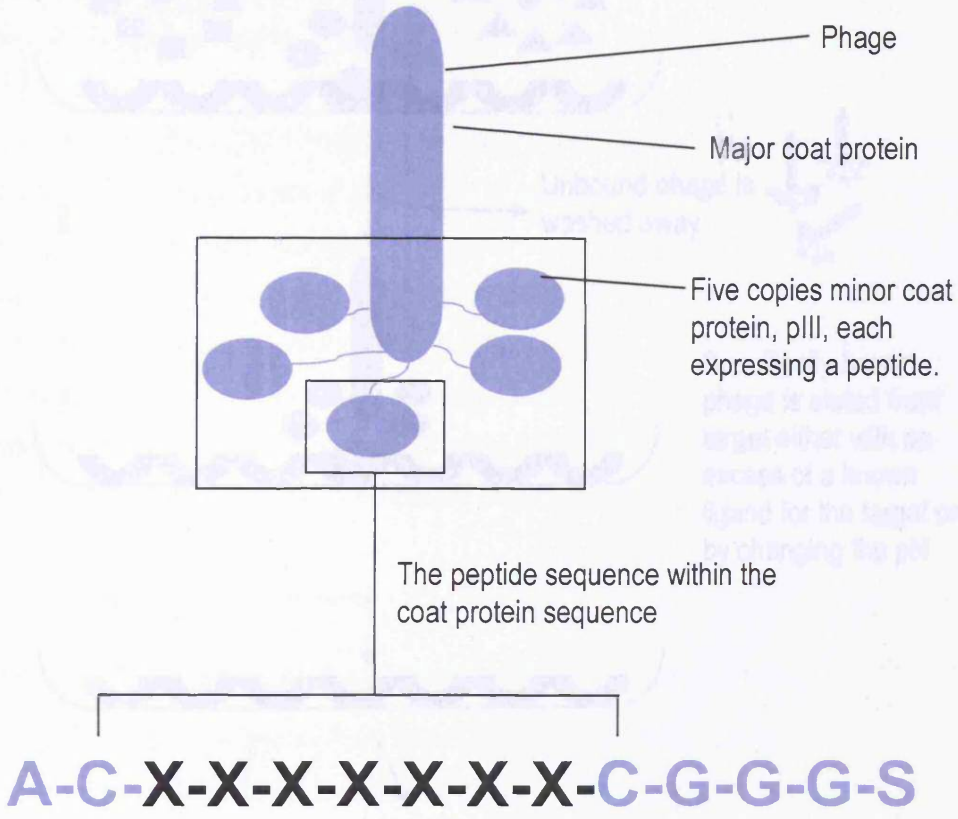

The surface of the bacteriophage (phage) comprises at least two types of protein, the major coat protein and the minor coat protein. Five copies of the minor coat protein, pIII, are expressed per phage. In this example of phage display, DNA encoding random heptamer peptide sequences has been fused to the minor coat protein gene, gIII. These are expressed along with the coat protein when it is made, resulting in the display of the peptide on the surface of the virion, as above.

Figure 5.2 A schematic diagram of the process of biopanning

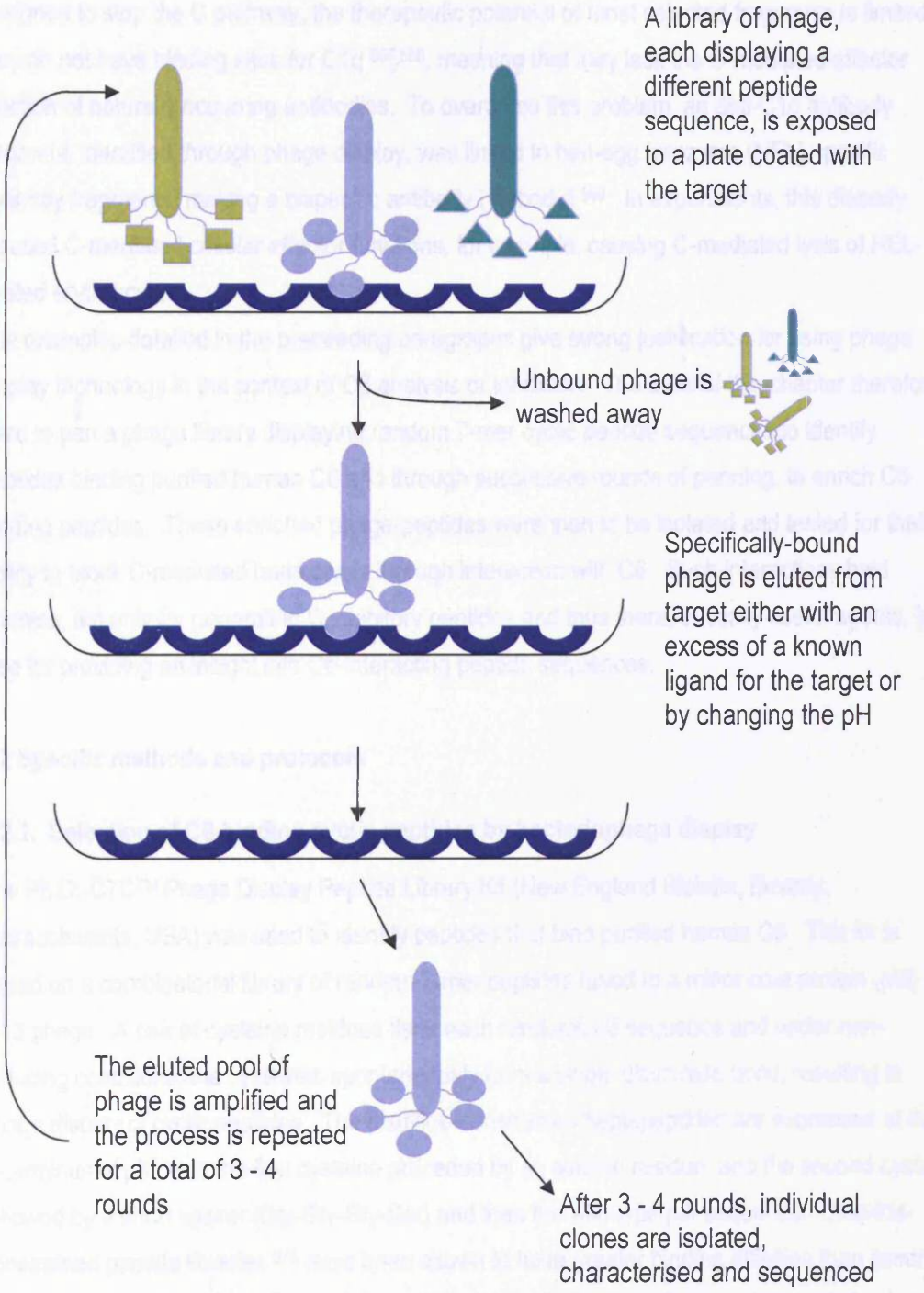

Adapted from the Ph.D.-C7C™ Phage Display Peptide Library Kit instruction manual (New England Biolabs)

a library against C3b [361]. Peptide 2J, which inhibits C1q activity was discovered by screening against C1q [359,360]; both are described in further detail in section 1.9.5. Several anti-C5 scFV inhibitory antibodies have been developed in this way, including the licensed drug Pexelizimab™ [471,564,565] (section 1.9.8.) and also TS-A12/22 [566]. Although these particular scFv antibodies are designed to stop the C pathway, the therapeutic potential of most selected fragments is limited as they do not have binding sites for C1q [567,568], meaning that they lack the C-mediated effector function of naturally occurring antibodies. To overcome this problem, an anti-C1q antibody fragment, identified through phage display, was linked to hen-egg lysozyme (HEL)-specific antibody fragments, making a bispecific antibody (diabody) [569]. In experiments, this diabody induced C-mediated cellular effector functions, for example, causing C-mediated lysis of HEL-coated erythrocytes.

The examples detailed in the preceeding paragraphs give strong justification for using phage display technology in the context of C6 analysis or inhibition. The aims of this chapter therefore, were to pan a phage library displaying random 7-mer cyclic peptide sequences to identify peptides binding purified human C6 and through successive rounds of panning, to enrich C6-binding peptides. These enriched phage-peptides were then to be isolated and tested for their ability to block C-mediated haemolysis through interaction with C6. Such interactions held promise, not only for generating C inhibitory peptides and thus therapeutically useful agents, but also for providing an insight into C6-interacting peptide sequences.

5.2 Specific methods and protocols

5.2.1. Selection of C6-binding cyclic peptides by bacteriophage display

The Ph.D.-C7C™ Phage Display Peptide Library Kit (New England Biolabs, Beverly, Massachusetts, USA) was used to identify peptides that bind purified human C6. This kit is based on a combinatorial library of random 7-mer peptides fused to a minor coat protein (pIII) of M13 phage. A pair of cysteine residues flank each randomised sequence and under non-reducing conditions, the cysteines spontaneously form a single disulphide bond, resulting in phage display of cyclic peptides. The disulfide-constrained heptapeptides are expressed at the N-terminus of pIII, with the first cysteine preceded by an alanine residue, and the second cysteine followed by a short spacer (Gly-Gly-Gly-Ser) and then the wild-type pIII sequence. Disulfide-constrained peptide libraries [570] have been shown to have greater binding affinities than linear peptide libraries [347,351,352,571] and have also been useful in the identification of structural epitopes [572,573]. The library consists of 1.2 x 10^9 electroporated sequences, amplified once to yield

approximately 200 copies of each sequence in 10 µl of the supplied phage. Extensive sequencing of the naïve library has revealed a wide diversity of sequences with no obvious positional biases [574].

Table 5.1 Kit components used:

Disulfide constrained heptapeptide phage display library	100 µl, 2 x 10^{13} pfu/ml. Supplied in TBS with 50% glycerol. Complexity = 1.2 x 10^{9} transformants
-96 gIII sequencing primer	– 5' – ^{HO}CCC TCA TAG TTA GCG TAA CG – 3', 100 pmol, 1pmol/µl
E.coli ER2738 host strain	F'lacI^{q} Δ(lacZ)M15 proA^{+}B^{+} zzf::Tn10(Tet^{R})/fhuA2 supE thi Δ(lac-proAB)Δ(hsdMS-mcrB)5(r_k-m_k-McrBC-). Host strain supplied as 50% glycerol culture; not competent.

5.2.1.1. Additional Buffers and Broths Required

All techniques described below were carried out with autoclaved tips, vials, flasks and solutions to prevent bacterial and DNAase contamination.

Table 5.2 The composition of buffers and broths used:

Lauria-Bertani (LB) broth:	1% tryptone w/v (Oxoid), 1% w/v NaCl, 0.5% w/v yeast extract (Oxoid) in dH_2O.
LB agar:	As for LB, but with 1.5% w/v agar (Oxoid)
LB Tet plates:	Tetracycline (20 µg/ml) was added to LB agar when the broth had cooled to 50°C.
Agarose Top:	1 % w/v bacto-tryptone, 0.5% w/v yeast extract, 0.5 g w/v NaCl, 0.1% w/v $MgCl_2.6H_2O$, 0.7 % w/v agar in dH_2O.
Glycerol stock solution	50% glycerol v/v in LB broth. Filter sterilised.
Coating buffer:	0.1 M $NaHCO_3$, 0.1 M Na_2CO_3, pH 9.6 in dH_2O.
Blocking buffer:	0.5% w/v BSA and 0.02% v/v NaN_3 in coating buffer.
Washing buffer:	0.1 % v/v Tween-20 in PBS.
Stringent washing buffer:	0.5% v/v Tween-20 in PBS.
Elution buffer:	20 mM diethylamine, pH 11 in autoclaved dH_2O.
Neutralisation buffer:	1 M Tris-HCl buffer, pH 7.0 in dH_2O.
DH_2O:	Deionised H_2O.
Precipitation solution:	20% w/v/ PEG-8000, 2.5 M NaCl in dH_2O.
Iodide buffer:	10 mM Tris-HCl, pH8.0, 1mM EDTA, 4 M NaI in dH_2O
Sodium acetate buffer:	Sodium acetate buffer: 3 M sodium acetate, adjusted pH 4.6 with acetic acid

5.2.1.2. Maintenance of the M13 Strain

M13 is a male-specific coliphage and therefore all cultures for M13 propagation were in colonies grown on media selective for presence of the F-factor. The F-factor of the host strain supplied,

Escherichia coli (*E.coli*) ER2738 contains a mini-transposon that confers tetracycline (Tet) resistance. These were selected by growing on tetracycline – containing media.
For general maintenance, ER2738 was streaked out from the glycerol stock onto an LB-Tet plate. The plate was inverted and incubated at 37˚C overnight and stored wrapped with parafilm at 4˚C in the dark for a maximum of 1 month.

5.2.1.3. Culture of ER2738 for infection by phage

Ten millilitres of LB broth was inoculated with a single colony of ER2738 from the maintenance plate (section 2.6.2) and incubated with shaking at 37˚C until mid-log phase (OD_{600} = 0.5, approximately 8 hours) growth was reached.

5.2.1.4. Phage Titering

Phage stocks were titered by diluting prior to infection, so that the multiplicity of infection (MOI) was much less than 1 (i.e. cells are in excess), ensuring that each plaque contained only one phage peptide sequence.
Three millilitres melted agarose top was dispensed into sterile culture tubes, one per expected phage dilution, and incubated at 45˚C until use. LB agar plates were poured; one per expected dilution. Ten-fold serial dilutions of phage in LB broth were made. For amplified phage culture supernatants, dilution ranges were 10^8-10^9; for unamplified panning eluates; 10^1-10^4. A fresh pipette tip was used for each dilution. Two hundred microlitres of culture of ER2738 in mid-log phase (section 5.2.3) was dispensed into microfuge tubes, one for each phage dilution. Ten microlitres of each phage dilution was added to each tube, vortexed and incubated at room temperature for 1-5 minutes to allow the phage to infect the bacteria. Each dilution of infected cells were transferred to a culture tube containing the agarose top, vortexed, poured immediately onto the LB plate and spread evenly. The plates were allowed to cool, inverted and incubated overnight at 37˚C. The plaques on each plate were counted on plates having approximately 100 plaques. To calculate the phage titre in plaque forming units (pfu) per 10 µl, each number was multiplied by the dilution factor for that plate.

5.2.1.5. Panning Procedure

The selection for phage-peptides that bind human C6 was carried out according to the manufacturers' methods. Briefly, ten wells of a 96-well microtitre plate were coated overnight at 4°C with 100 µl per well of purified human C6 diluted to 100 µg/ml in coating buffer. The coating solution was removed and the wells blocked for 1 hour at 4°C with 200 µl blocking buffer per well. After removal of the blocking solution, the wells were washed five times with washing buffer (200

µl per well). Phage (2×10^{11}) were added to each well and incubated at room temperature for 1 hour to permit binding. Following binding, the wells were washed with stringent washing buffer (200 µl per well) ten times to remove non-specifically binding phage. Specifically bound phage were eluted by incubation with elution buffer (100 µl per well) for 10 minutes and then transferred to fresh wells. Fifteen microlitres of neutralisation buffer was added to each well to neutralise the elution buffer. The eluate was titered as described in section 5.2.4. in order to determine how many phage-peptides had been eluted from this round of panning - referred to as output pfu. One hundred microlitres of the pooled eluate was reserved and stored at 4°C; the rest was amplified in the host strain by adding it to 10 ml *E.coli* ER2738 in early-log phase growth and incubated at 37°C with vigorous shaking for 4-6 hours. The culture was transferred to a centrifuge tube and centrifuged at 12000 *g* for 10 minutes at 4°C. The supernatant was transferred to a fresh tube and centrifuged again. The upper 80% of the supernatant was carefully removed and transferred to a fresh tube, to which 1/6 volume of precipitation solution was added. The phage were allowed to precipitate overnight at 4°C. The precipitated phage were centrifuged for 15 minutes, 12000 *g*, 4°C. The supernatant was decanted and the tubes re-spun briefly. Any residual supernatant was removed with a pipette. The pellet was resuspended in 1 ml PBS and transferred to a microcentrifuge tube and centrifuged at 1000 *g* for 5 minutes at 4°C to pellet residual cells. The supernatant was transferred to a fresh microcentrifuge tube and subject to a second precipitation with 1/6 volume of precipitation solution, on ice for 60 minutes. The tubes were centrifuged at 1000 *g* for 10 minutes at 4°C. The supernatant was discarded and the tubes briefly re-spun and any residual supernatant carefully removed. The pellet was resuspended in 200 µl PBS and microcentrifuged at 1000 *g* for 1 minute to pellet any remaining insoluble matter. The amplified eluate (supernatant) was transferred to a fresh tube and titered again (section 5.2.4.) to determine how many phage-peptides would be used in the next round of panning – referred to as input pfu. This represented the end of the first round of panning. The second and third rounds of panning were conducted as described for the first round of panning, except that the amplified phage eluate from the first round was incubated with the C6 coated plate in the second round and the amplified phage eluate from the second round was incubated with the C6 coated plate in the third round of panning (Figure 5.2).

The percentage recovery of phage-peptides from each round of panning was calculated using the following equation:

Percent recovery of pfu = (output pfu / input pfu) x 100

The degree of enrichment at each biopanning step was calculated by dividing the percentage recovery of phage peptides from a panning round by the percentage recovery of phage peptides from the first round of panning.

5.2.1.6. Isolation of phage-peptide DNA

Five hundred microlitres of phage-containing supernatant from the first centrifuge step in section 5.2.4 were transferred to a fresh eppendorf tube and precipitation buffer (200 µl) was added. The tube was inverted to mix the solutions, left to stand for 10 minutes at room temperature, then centrifuged at 1000 *g*, at room temperature, for 10 minutes. The supernatant was discarded; the tube was re-spun briefly and any remaining supernatant carefully removed with a pipette. The pellet was resuspended thoroughly in 100 µl iodide buffer to lyse the phage. The mixture was incubated for 10 minutes at room temperature and centrifuged at 1000 *g*, 10 minutes. The supernatant was discarded and the pellet resuspended in 100 µl sodium acetate buffer and 250 µl ethanol to precipitate the single stranded DNA and incubated for 10 minutes. The mixture was centrifuged at 1000 *g* for 10 minutes, the supernatant discarded and the pellet washed once by centrifugation at 1000 *g*, 10 minutes in 75% (v/v) ethanol. After removing the ethanol, the pellet was allowed to air dry and it was then suspended in 30 µl sterile H_2O.

5.2.1.7. DNA sequencing of phage-peptides

PCR was used to amplify isolated phage-peptide DNA for automated dideoxy DNA sequencing. DNA extension was performed in one direction only and dye-labelled dideoxynucleotides were included in the reaction mixture. When a dideoxynucleotide was incorporated into the extending DNA, extension terminated. This resulted in cDNA of different lengths with a terminal dye-labelled dideoxynucleotide. Different dyes were used for each of the four dideoxynucleotides and when the PCR was applied to the automated sequencer the machine detected which dideoxynucleotide was present at the length of each length of cDNA. In this way, the sequence of the DNA was determined. The ABI Big Dye™ Terminator Cycle Sequencing Kit (Perkin Elmer) was used and the manufacturer's recommended protocol was followed. PCR was performed on 2.5 µl isolated phage-peptide DNA, in 15 µl final volume of 3.2 pmole primer, 1 µl of Big Dye premix, containing Ampli Taq® DNA polymerase, 5 µl Better Buffer. Thermal cycling was carried out in an OmniGene thermal cycler (Hybaid) with heated lid. As the PCR was being performed for sequencing, one primer only was required, to ensure the DNA extended in one direction only. This was supplied with the phage display peptide library kit and was specific for gIII, the gene the DNA for the peptide sequence had been fused to.

Amplification was accomplished using the following conditions:

Table 5.3 Cycling conditions for sequencing PCR:

Cycle number	Cycle conditions
1 Cycle	96°C, 3 minutes
25 cycles	Denature - 96°C, 15 secs
	Anneal - 50°C, 10 secs
	Extend - 60°C, 4 minutes

The amplified DNA was precipitated by the addition of 2 µl sodium acetate buffer (section 5.2.5) and 95% (v/v) ethanol (50 µl) to the reaction tube. The mixture was mixed, incubated on ice for 10 minutes, centrifuged at 1000 *g* for 30 minutes and the supernatant carefully removed. The pellet was washed in 250 µl 75% (v/v) ethanol and centrifuged at 1000 *g* for 10 minutes. Sequencing was carried out in house using an ABI model 373A automated DNA sequencer (Perkin Elmer).

5.2.1.8. Calculation of representation of a given peptide motif in library

According to the manufacturer's instructions, the likelihood that the Ph.D.-C7C library contains a given peptide motif could be calculated using the data in Table 5.4 as follows. First, the observed frequencies of each residue in the motif (expressed as decimal values) in Table 5.4 were multiplied by each other in order to obtain the absolute probability *p* of obtaining that sequence. The expected number λ, of independent clones within the library displaying a given motif was calculated by multiplying *p* by the complexity of the library, *n* (1.2×10^9).

The probability P(*k*) that the library contained exactly *k* clones displaying a particular motif was calculated using the Poisson distribution, $P(k) = e^{-\lambda}\lambda^k/k!$.

If K=0 (i.e. the library does not contain the desired motif), then the equation is reduced to:

$P(0) = e^{-\lambda} = e^{-np}$.

Therefore, the probability P(*k*>0) that the library contains at least one independent clone displaying a given motif was calculated from the equation: $P(k>0) = 1-P(0) = 1-e^{-np}$.

5.2.2. Reconstitution of synthetic peptides

The sequences of the synthetic peptides made were: SACNNQPYKMCGGG and SACKTHTMHWCGGG (Severn Biotech Ltd., Kidderminster, UK) and were cyclised and purified to greater than 80% purity. The peptides were supplied as a lyophilised powder and due to their hydrophobic nature, reconstituted in DMSO (5% v/v in H_2O) to dissolve the peptide. PBS was added, to make a final concentration of 100 µM of peptide. The dissolved peptides were aliquoted and stored at -70°C until use.

pIII leader sequence ↓ Start of mature peptide-pIII fusion ↓

5' - ... TTA TTC GCA ATT CCT TTA GTG GTA CCT TTC TAT TCT CAC TCT GCT TGT

3' - ... AAT AAG CGT TAA GGA AAT CAC CAT GGA AAG ATA AGA GTG AGA CGA ACA

... Leu Phe Ala Ile Pro Leu Val Val Pro Phe Tyr Ser His Ser Ala Cys

NNK NNK NNK NNK NNK NNK NNK TGC GGT GGA GGT TCG GCC GAA ACT GTT GAA

NNM NNM NNM NNM NNM NNM NNM ACG CCA CCT CCA AGC CGG CTT TGA CAA CTT

Xxx Xxx Xxx Xxx Xxx Xxx Xxx Cys Gly Gly Gly Ser Ala Glu Thr Val Glu

└— Random peptide sequence —┘

AGT TGT TTA GCA AAA TCC CAT ACA GAA AAT TCA TTT ACT AAC GTC TGG AAA GAC

TCA ACA AAT CGT TTT AGG GTA TGT CTT TTA AGT AAA TGA TTG CAG ACC TTT CTG

Ser Cys Leu Ala Lys Ser His Thr Glu Asn Ser Phe Thr Asn Val Trp Lys Asp

GAC AAA ACT TTA GAT CGT TAC GCT AAC TAT GAG GGC ... - 3'

CTG TTT TGA AAT CTA GCA ATG CGA TTG ATA CTC CCG ... - 5'

Asp Lys Thr Leu Asp Arg Tyr Ala Asn Tyr Glu Gly ...

↑

-96 sequencing primer

Figure 5.3. The N-terminal sequence of random disulfide-constrained heptapeptide-pIII fusion, taken from the Ph.D.- C7C™ phage display peptide library kit instruction manual. The pIII fusion leader sequence is removed upon secretion at the position indicated by the arrow. The alanine preceeding the first cysteine residue of the crosslink is the first amino acid residue at the N-terminus of the mature fusion protein. The hybridisation position of the –96 primer which is used for the sequencing PCR is indicated.

Table 5.4 Amino acid distribution of the Ph.D.-C7C™ library

Amino Acid		Codons	Expected frequency*	Observed frequency
3 letter code	1 letter code			
Arg	R	CGK, AGG	9.4%	4.3% (25/581)†
Leu	L	CTK, TTG	9.4%	9.6% (56/581)
Ser	S	TCK, AGT	9.4%	8.6% (50/581)
Ala	A	GCK	6.2%	6.5% (38/581)
Gly	G	GGK	6.2%	2.2% (13/581)
Pro	P	CCK	6.2%	10.7% (62/581)
Thr	T	ACK	6.2%	13.1% (76/581)
Gln	Q	CAG, TAG	6.2%	7.1% (41/581)
Val	V	GTK	6.2%	1.9% (11/581)
Asn	N	AAT	3.1%	6.4% (37/581)
Asp	D	GAT	3.1%	4.1% (24/581)
Cys	C	TGT	3.1%	0% (0/581)†
Glu	E	GAG	3.1%	3.1% (18/581)
His	H	CAT	3.1%	6.9% (40/581)
Ile	I	ATT	3.1%	2.1% (12/581)
Lys	K	AAG	3.1%	3.8% (22/581)
Met	M	ATG	3.1%	3.3% (19/581)
Phe	F	TTT	3.1%	2.1% (12/581)
Trp	W	TGG	3.1%	1.9% (11/581)
Tyr	Y	TAT	3.1%	2.4% (14/581)

*Expected frequency = # codons for that amino acid ÷ 32 codons x 100%. Note use of reduced genetic code NNK (32 codons) in library construction.

†Arginines and single cysteines in the displayed peptide sequence interfere with secretion of pIII and phage infectivity, respectively; consequently, clones with peptides containing Arg or Cys are selected against [575].

‡The stop codon TAG is suppressed by Gln in the strain used to propagate the library.

The library was supplied as having a complexity of 1.2 x10^9 transformants. The diversity of the library was not confirmed before use.

Reproduced from the Ph.D.-C7C™ phage display peptide library kit instruction manual.

5.2.3. ELISA to determine whether synthetic peptides bind to C6

The peptides of two of the inhibitory phage peptides were synthesised and their ability to bind C6 was tested by ELISA. Wells of a 96-well ELISA plate were coated with varying concentrations of peptide CNNQPYKMC (0 - 7.75 µM) or peptide CKTHTMHWC (0 – 12.5 µM) in carbonate coating buffer (50 µl per well) for 2 hours at 37°C. The plates were gently washed three times with 0.1% Tween/PBS (washing buffer) (200 µl per well) and then blocked for 1 hour, 37°C with 1% BSA/0.1% Tween/PBS (blocking buffer) (100 µl per well). After washing once with washing buffer, human C6 (1 µg/ml) (50 µl per well) diluted in blocking buffer was added to each well and incubated for 1 hour at 37°C. After the plates were washed three times with washing buffer, the anti-human C6 antibody, WU 6.4 (1 µg/ml in blocking buffer) (50 µl per well) was added to each well and the plate incubated for 1 hour at 37°C. The plates were washed as described and incubated with anti-mouse Ig diluted 1 in 10,000 in blocking buffer (50 µl per well) for 1 hour at 37°C. The plates were washed three times with washing buffer and developed with the addition of OPD substrate (50 µl per well) and quenched with 10% H_2SO_4 (50 µl per well). The absorbance was measured at 490 nm.

5.2.4. Analysis of specificity of the synthetic peptides for C6 using Surface Plasmon Resonance

Surface plasmon resonance (SPR) using the BIAcore 3000 was used to determine whether human C6 bound to the peptides of interest. The synthetic peptides were immobilised onto a Pioneer F1 sensor chip (BIAcore AB, Uppsala, Sweden), which has a short dextran matrix attached to its surface. Any changes in response units (RU) when the large C6 molecule was passed over the immobilised peptides would be more easily detected due to the short matrix than if the peptides had been immobilised onto the more often used CM-5 sensor chip surface that has a longer dextran matrix attached to it. The peptides were immobilised onto the sensor chip surface as described (section 2.5.1.) at pH 3.5 in 10 mM sodium acetate buffer.

5.2.4.1. Studies to determine whether C6 and C9 interact with peptides immobilised on a BIAcore F1 Pioneer Chip

A baseline value of RU was recorded, with HBS-EP (0.01M HEPES pH 7.4, 0.15M NaCl, 3 mM EDTA, 0.005% (v/v) Surfactant-P20) buffer flowing over the flow cells of the F1 pioneer chip. Purified human C6 or C9 in PBS were injected over the flow cells and at the end of the injection

time, the change in RU was recorded. To remove analyte bound to the immobilised peptide, 0.2% (v/v) diethylamine in PBS was injected over the chip.

5.2.5. C6 'add-back' haemolytic assays to investigate the functional activity of synthetic peptide

To investigate whether the synthetic peptides CNNQPYKMC and CKTHTMHWC had any C6 functional inhibitory activity, a 'C6-add back' haemolytic assay was used. Briefly, genetically C6 deficient rat serum was reconstituted with purified human C6. To test whether the peptides had any C6 inhibitory activity, varying concentrations of the peptides were pre-incubated with the C6, then the C6 deficient serum was added, followed by activated sheep erythrocytes (sheep EA). When peptide was not present, the sheep EA lysed. If the peptides had inhibitory properties, then lysis of the sheep EA would occur to a lesser extent or not at all.

To determine the dilution of C6 deficient rat serum and concentration of purified human C6 to use, a haemolytic assay was performed. C6 deficient rat serum was diluted in CFD over the range 1in 50 to 1 in 400 and 50 µl pre-incubated with varying concentrations of human C6 (0.039 – 5 µg/ml) (50 µl) at 37°C for 30 minutes. To this mixture, 50 µl 2% sheep EA was added and the mixture incubated for 30 minutes at 37°C. After centrifugation, the supernatants were collected and absorbance measured at 415 nm. The percentage haemolysis was calculated (section 2.4). The dilution of C6 deficient rat serum and concentration of human C6 at which approximately 80% of sheep EA were lysed was selected.

To determine whether the peptides could inhibit C6 activity, 50 µl peptide CNNQPYKMC (0 – 7.75 µM) or peptide CKTHTMHWC (0 – 12.5 µM) was pre-incubated with 50 µl human C6 (1.25 nM) for 1 hour at 37°C. Fifty microlitres C6 deficient rat serum, diluted 1 in 50 was added to the mixture and incubated for a further hour at 37°C. 2% Sheep EA (50 µl) were then added and the mixture incubated for 30 minutes at 37°C. After centrifugation, the supernatants were transferred to a flat-bottomed microtitre plate and the absorbance measured at 415 nm. The percentage of lysis was calculated and a graph of peptide concentration versus percentage of lysis plotted.

5.3 Results

5.3.1. Identification and characterisation of phage-peptides that interact with human C6

5.3.1.1. Enrichment of the phage library during biopanning

C6 binding phage-peptides were selected for by panning 2 x 10^{11} plaque forming units (pfu) of phage-peptides on a C6 coated microtitre plate. Non-specifically binding phage were removed by

washing and specifically bound phage eluted by incubation with elution buffer. The eluate was titered in order to determine how many phage had been eluted, so that the percentage of recovery and enrichment factor of C6 binding phage-peptides could be calculated. Briefly, the phage were diluted and allowed to infect the bacterial strain of *E.coli*, ER2738. The infected bacteria were mixed with an agarose containing growth medium, spread evenly over an LB plate and grown overnight at 37°C. The plaques on each plate were counted and multiplied by the dilution factor of the phage to give the number of pfu or output at the end of the panning round. The phage in the eluate were then amplified and titered, to determine the number of pfu to be input into the next round of panning. This process was carried out for each round of panning. The percentage recovery of the phage peptides was calculated by dividing the number of pfu eluted by the number of pfu panned against C6 in a panning round and multiplying this figure by 100. The degree of enrichment at each biopanning step was calculated by dividing the percentage recovery of phage peptides from a panning round by the percentage recovery of phage peptides from the first round of panning. These data are summarised in Table 5.5.

Table 5.5 The recovery of phage-peptides and the degree of enrichment reached during the rounds of biopanning

Biopanning	Input (number of plaque forming units (pfu per 10 µl)	Output (pfu per 10 µl)	% Recovery of pfu (output pfu/ input pfu) x100	Enrichment factor (present round % recovery/ round 1 percent recovery)
Round 1	2×10^{11}	7.95×10^{3}	0.00000397%	1
Round 2	1.4×10^{6}	1.65×10^{2}	0.0118 %	2969
Round 3	2.3×10^{4}	1.03×10^{4}	44.78%	11,279,597

After the first round of biopanning, the input number of pfu into the two subsequent rounds decreased. This was unexpected and the manufacturers protocols recommended that 2×10^{11} pfu were used in each round of biopanning to ensure that optimal enrichment of the target specific phage-peptides was occurring. It is possible that the infectivity of the phage were reduced, due to the sequences of the peptides they presented. No guidance was supplied by the manufacturer's for the output pfu that could be expected. As can be seen from Table 5.5, only 7950 virions were eluted from the first round of panning and this is reflected in the percentage of virions recovered, 3.975×10^{-6}%. In the second round of biopanning, 165 virions were eluted and

the percentage recovery rose from 3.975 x 10^{-6}% in the first round to 0.0118% in the second round. In the final round of panning, 10,300 virions were recovered, representing a recovery of 44.78%. The degree of enrichment was 1.128 x 10^7 from the first round to the final round. As the phage-peptide library originally contained 1.2 x 10^9 different sequences, this suggests that approximately 100 sequences may have been enriched from the original library, although many of these may be identical to each other.

5.3.1.2. The identification of inhibitory C6 binding phage-peptides

After three rounds of panning, ER2738 were infected with the enriched phage-peptide library and cultured on a plate. Individual clones were selected, amplified, isolated and either titered to investigate their potential inhibitory activity in haemolytic assays or DNA prepared for sequencing analysis (described in section 5.2).

Initially, to investigate whether the phage-peptides inhibited C-mediated lysis, equivalent numbers of phage were serially diluted and incubated with human serum in haemolytic assays (described in section 2.3.12.4). This data is shown in Figure 5.3, along with the corresponding sequence data. This shows that all of the phage-peptides tested inhibited C-mediated haemolysis in a dose-dependent manner and the negative control, wild-type phage had no inhibitory activity. Two consensus sequence peptides were identified; CKTHTMHWC and CNNQPYKMC. In further experiments, the haemolytic assay was used as a screen to test the inhibitory activity of phage-peptides at a single dose of equivalent numbers of phage in duplicate. This is summarised in Table 5.6; the percentage inhibition in the presence of 1 x 10^{11} phage particles is shown, together with corresponding sequence data. For completeness, the data in Figure 5.3 is also included. Information on the inhibitory activity of two of the clones sequenced was not obtained. Of the seventeen clones sequenced, nine different sequences were isolated. The sequence NNQPYKM was present in six independent clones, five of which had inhibitory activity between 75.3 - 100%, whilst the clone KNQPPST which shared the consensus NQP, inhibited haemolysis by nearly 80%. The two clones with the sequence KTHTMHW completely inhibited C-mediated lysis at the dose tested. Clones with the sequence FPIPLGS and the similar sequence clone FPIPLPS also fully inhibited C-mediated haemolysis. The clones TAKLENW and EPARSLQ almost completely inhibited haemolysis in the assay, whereas the phage displaying the sequence KTTSTSH inhibited haemolysis by 50%, the lowest degree of inhibition recorded. Inhibitory data for the phage-peptide with the sequence TAAGALS was not obtained. Peptides with consensus

Figure 5.3 Inhibition of C-mediated haemolysis by phage-peptides that bind C6

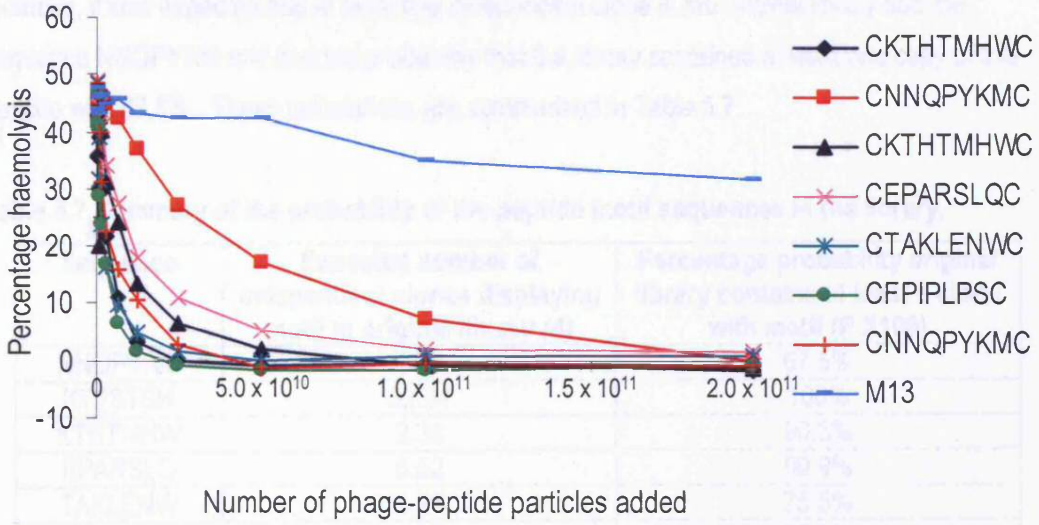

To investigate whether the phage-peptides inhibited C-mediated lysis, equivalent numbers of phage were serially diluted and pre-incubated with human serum diluted 1 in 80 for 30 minutes at 37°C. 2% sheep EA was then added to the mixture and incubated for a further 30 minutes at 37°C. The samples were centrifuged and the absorbance of the supernatants read at 415 nm. The percentage of haemolysis was calculated and the values plotted as above. Phage-peptides displaying the same sequence are labelled with the same sequence and plotted in the same colour. M13, wild type phage negative control.

sequences are underlined in Table 5.6. These are NQP, contained in the sequences NNQPYKM and KNQPPST, and FPIPLXS, which represents the sequences FPIPLPS and FPIPLGS.

5.3.1.4 Calculation of representation of a given peptide motif in library

Once the peptide sequences had been determined, using data supplied by the manufacturers about the amino acid distribution in this particular library, it was possible to calculate the expected number (λ) of independent clones within the library displaying a particular sequence and also the probability of at least one copy of that peptide occurring in the library (section 5.2.8.). For example, it was expected that at least one independent clone in the original library had the sequence NNQPYKM and that the probability that the library contained at least one copy of this peptide was 67.5%. These calculations are summarised in Table 5.7.

Table 5.7 Summary of the probability of the peptide motif sequences in the library.

Sequence	Expected number of independent clones displaying motif in original library *(λ)*	Percentage probability original library contains at least 1 clone with motif (P X100)
NNQPYKM	1.12	67.5%
KTTSTSH	52.31	100%
KTHTMHW	2.34	90.3%
EPARSLQ	6.52	99.9%
TAKLENW	1.41	75.5%
FPIPLPS	5.35	99.5%
TAAGALS	7.84	100%
KNQPPST	26.73	100%
FPIPLGS	1.1	66.7%

These data demonstrate that after three successive rounds of biopanning, the library was enriched for C6 binding phage-peptides. Furthermore, in the original library one clone only of three of the C6 binding phage-peptides was predicted to be present. This demonstrates that the process of panning is not only highly specific but is also highly sensitive, because a single peptide clone in the original library can be successfully selected and enriched for.

5.3.1.5. Searching NCBI Blast for sequence similarities with proteins

The NCBI BLAST website (address: htttp://www.ncbi.nlm.nih.gov/BLAST/) [576] was searched for short, nearly exact similar matches with proteins for each of the peptide sequences. On average, there were approximately 100 blast hits for each query sequence with varying degrees of match. Many were labelled unknown and hypothetical proteins, whose functions may in the future be

Table 5.6 A summary of phage-peptide inhibitory activity and matching sequence data

Peptide	Percentage Inhibition (1×10^{11} phage peptides)	Sequence
1	100	CKTHTMHWC
2	92.6	CNNQPYKMC
3	100	CKTHTMHWC
4	98.2	CEPARSLQC
5	99.5	CTAKLENWC
6	100	CFPIPLPSC
7	100	CNNQPYKMC
8	80.2	CNNQPYKMC
9	75.3	CNNQPYKMC
10	49.8	CKTTSTSHC
11	Not tested	CNNQPYKMC
12	Not tested	CTAAGALSC
13	91.9	CNNQPYMC
14	96.2	CKTHTMHWC
15	79.8	CKNQPPSTC
16	100	CFPIPLGSC
17	98.1	CFPIPLGSC

Peptides 1 – 17 were tested for their ability to inhibit C-mediated lysis in a haemolysis assay. 1×10^{11} phage peptide particles were pre-incubated with human serum diluted 1 in 80 for 30 minutes at 37°C before 2% sheep EA were added and the mixture incubated for a further 30 minutes at 37°C. The samples were centrifuged, the supernatants collected and their absorbance measured at 415 nm. The percentage of inhibition was then calculated. The DNA of the phage-peptides was also collected and subject to sequencing by PCR with dideoxynucleotides. Underlined sequences show consensus sequences between different peptide sequences. Note: the first seven peptides are those shown in Figure 5.3

defined and found to interact with C6. Some were not physiologically relevant, for example, six of the seven residues in the sequence FPIPLGS, FPIPL-S matched an unknown protein from a plant, Oryza sativa (japonica cultivar) and five residues in the sequence NNQPYKM, QPYKM, matched maturase K, an enzyme present in various species of Lily. However, two of the matched proteins were connected with the C system. Six of the seven residues in the sequence FPIPLPS, FPIPLP, shared sequence similarity with human, pig, sheep and rabbit pulmonary surfactant-associated protein B (SP-B). Six of the seven residues in the sequence TAAGALS, TAAGAL, had sequence similarity with human mannan-binding lectin serine protease 2 (MASP-2) and the 19 kDa isoform of MASP-2, sMAp. The sequence mapped to the EGF-like domain of MASP-2 and its smaller isoform, sMAp19.

The RGD motif in matrix proteins recognised by integrin $\alpha_5\beta_1$ was identified by phage display [577,578]. This suggests that short peptide sequences of three amino acids can be sufficient to allow important interactions between proteins to take place. It was investigated whether any three amino acid sequences within the 7-mer peptide sequences (identified as binding C6) had homology to the protein sequences of human C5, C6 or C7. Three amino acid sequences were compared with protein sequences of C5 (accession number P01031) [579-587], C6 (accession number P13671) [81,588-593] and C7 (accession number P10643) [593-599] that had been downloaded from the NCBI Entrez Protein database (http://www.ncbi.nlm.nih.gov/entrez/viewer). The data is shown in Table 5.8 and the arrangement of the protein modules are described in section 1.1.2. In all of the 7-mer sequences, apart from EPARSLQ, there was at least one three amino acid sequence that was homologous to C5, C6 or C7. All the motifs with homology to C5 were within regions of C5 that become C5b following cleavage of C5. NNQPYKM contained three motifs: two homologous to C5b and one homologous to C6. The sequence KTTSTSH also contained three motifs that matched sequences in C5b, C6 and C7. One of the motifs within TAKLENW was homologous with sequences in C5b, C6 and C7. The sequences FPIPLPS and FPIPLGS are very similar and they contained two identical motifs that were homologous with sequences in C5b and C6.

5.3.2. Characterisation of selected peptides

Two of the sequences showing good inhibition of haemolysis as phage peptides, CNNQPYKMC and CKTHTMHWC, were made as cyclic peptides (Severn Biotech, Kidderminster, UK and Eurogentec, Belgium). These were then tested in an ELISA for the ability to recognise C6, their inhibitory properties of C-mediated lysis and their ability to bind C6 on the BIACore.

Table 5.8 Summary of areas of homology between 3 amino acid motifs in 7-mer peptides and Complement components C5, C6 and C7.

7-mer peptide sequence	3 amino acid sequence	Residues homologous to in C5, C6 or C7	Protein modules residues are in
NNQPYKM	PYK	351-353 in C5	β chain
	YKM	1326-1328 in C5	C5α' chain
	NNQ	825-827 in C6	1st FIMs domain
KTHTMHW	KTH	1200-1202 in C5	C5α' chain
KTTSTSH	TST	1368-1370 in C5	C5α' chain
		211-213 in C7	Perforin-like domain
	STS	876-878 and 903-905 in C6	2nd FIMs domain
	TSH	236-238 in C7	Perforin-like domain
TAKLENW	LEN	1176-1178 in C5	C5α' chain
		236-238 in C6	Perforin-like domain
		356-358 in C7	Perforin-like domain
	KLE	155-157 in C6	LDL-receptor class A domain
FPIPLPS	IPL	963-965 in C5	C5α' chain
	PIP	186-188 in C6	Perforin-like domain
	LPS	424-426 in C5	β chain
		283-285 in C7	Perforin-like domain
FPIPLGS	IPL	963-965 in C5	C5α' chain
	PIP	186-188 in C6	Perforin-like domain
TAAGALS	GAL	1321-1323 in C5	C5α' chain
		821-823 in C7	2nd FIMs domain
KNQPPST	PPS	527-529 in C7	2nd TSP type-1 domain
EPARSLQ	-	-	-

5.3.2.1. Assessing the binding of C6 to the peptides

5.3.2.1.1. ELISA to determine whether the selected peptides bind human C6

An ELISA plate was coated with varying concentrations of peptide CNNQPYKMC (0 - 7.75 µM) or peptide CKTHTMHWC (0 – 12.5 µM) for 2 hours, washed and blocked. After further washing, 1µg/ml human C6 added to each well for 1 hour and the plate washed before the anti-human C6 antibody, WÜ 6.4 (1 µg/ml) was added to each well for 1 hour. After washing, anti-mouse Ig diluted 1 in 10,000 was added to each well and incubated for a further hour. The plates were washed and developed with the addition of OPD substrate. The reaction was stopped with the addition of 10% H_2SO_4 to each well and the absorbance measured at 490 nm. There was no evidence of binding above background with peptide NNQPYKM (Figure 5.4), suggesting that this peptide might not bind C6, or that when bound to plastic its binding activity was lost. However, the ELISA in which peptide KTHTMHW was coated on the plate developed in a dose-dependent manner (Figure 5.4). This suggested that KTHTMHW when coated on plastic did bind C6.

5.3.2.1.2. The use of SPR to determine whether the selected peptides bind human C6

To better determine whether the two peptides bound to C6 surface plasmon resonance (SPR) was used. To ascertain whether this was a specific interaction, the terminal C pathway component C9 was also passed over the immobilised peptides.

5.3.2.1.2.1. The immobilisation of peptides onto the surface of the F1 pioneer chip

Peptides CNNQPYKMC and CKTHTMHWC and a reference peptide, P_0 were immobilised on a Pioneer F1 sensor chip as described in section 2.5.1.at pH 3.5 in 10 mM sodium acetate buffer. The target RU change for immobilising each peptide onto the sensor chip was 1000 based upon the manufacturers' recommendations. The net change in RU after immobilisation of each peptide is shown in Table 5.9.

Table 5.9 Change in Response Units of each flow cell after immobilisation of peptide

Flow cell	Peptide	Net change in Response Units (RUs) after immobilisation
1	CNNQPYKMC	1825.8
2	CKTHTMHWC	1028.0
3	P_0, irrelevant peptide	723.2

Figure 5.4 ELISA to determine whether human C6 binds to peptides CNNQPYKMC and CKTHTMHWC

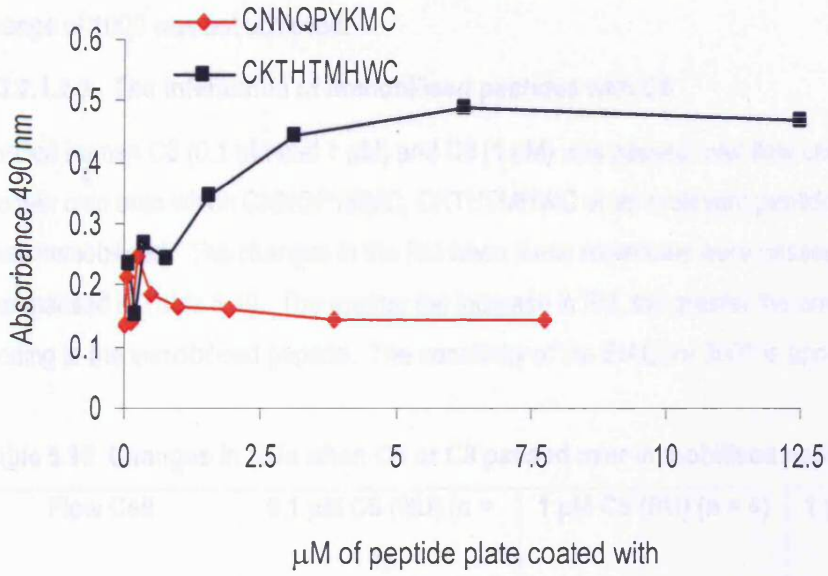

A 96-well ELISA plate was coated with varying concentrations of peptide CNNQPYKMC (0 – 7.75 μM) or peptide CKTHTMHWC (0 – 12.5 μM). All incubations were for 1 hour at 37°C and plates were washed a total of 3 times at each wash step. The plate was washed, blocked, washed and human C6 (1μg/ml) added to each well. After washing, the anti-human C6 antibody, WU 6.4 (1 μg/ml) was added to each well. The plate was washed and an anti-mouse immunoglobulin antibody was added to each well (diluted 1 in 10, 000). After washing, the ELISA was developed by the addition of OPD substrate and the reaction stopped by the addition of 10% H_2SO_4. The absorbance of each well was measured at 490 nm.

There was a change of 1825.8 RU when peptide CNNQPYKMC was immobilised onto flow cell 1 of the F1 pioneer chip. When peptide CKTHTMHWC was immobilised onto flow cell 2 of the same chip there was a change of 1028 RU. Figure 5.5 shows the sensorgram of the immobilisation of peptide CKTHTMHWC. This is a typical representation of the immobilisation of the peptides onto the flow cells of the sensor chip. Towards the end of the immobilisation, as more peptide was injected over the flow cell, it failed to bind to the surface, demonstrating that it had become saturated with peptide. When peptide P_0, an irrelevant peptide was bound onto the surface of flow cell 3, there was a change of 723.2 RU. Like the immobilisation of peptide CKTHTMHWC, the immobilisation of peptide P_0 had reached saturation and the target RU change of 1000 was not achieved.

5.3.2.1.2.2. The interaction of immobilised peptides with C6

Purified human C6 (0.1 µM and 1 µM) and C9 (1 µM) was passed over flow cells of the F1 pioneer chip onto which CNNQPYKMC, CKTHTMHWC or an irrelevant peptide control, P_0 had been immobilised. The changes in the RU when these molecules were passed over are summarised in Table 5.10. The greater the increase in RU, the greater the amount of analyte binding to the immobilised peptide. The sensitivity of the BIACore 3000 is approximately 4 RU.

Table 5.10 Changes in RUs when C6 or C9 passed over immobilised peptides

Flow Cell	0.1 µM C6 (RU) (n = 1)	1 µM C6 (RU) (n = 4)	1 µM C9 (RU) (n = 3)
CNNQPYKMC	12.7	27.1	5.5
CKTHTMHWC	6.6	19.8	5.0
Irrelevant peptide	4.3	6.9	3.8

The change in RU when 0.1 µM C6 was passed over a flow cell on which CNNQPYKMC had been immobilised was 12.7 and increased to 27.1 when 1 µM C6 was passed over. When 1 µM C9 was passed over the same flow cell, the average change in RU was 5.5. This showed that peptide CNNQPYKMC specifically recognised C6 but not C9 and that the observed changes in RU were dependent on the concentration of C6. The change in RU when 0.1µM C6 was passed over the flow cell on which CKTHTMHWC had been immobilised was 6.6 and increased to 19.8 when 1 µM C6 was passed over. In contrast, the average change in RU when 1 µM C9 was passed over the same flow cell was 5.0. This demonstrated that peptide CKTHTMHWC also recognised C6 but not C9 and that the observed changes in RU were dependent on the

Figure 5.5 The immobilisation of peptide CKTHTMHWC onto the flow cell surface of an F1 pioneer chip

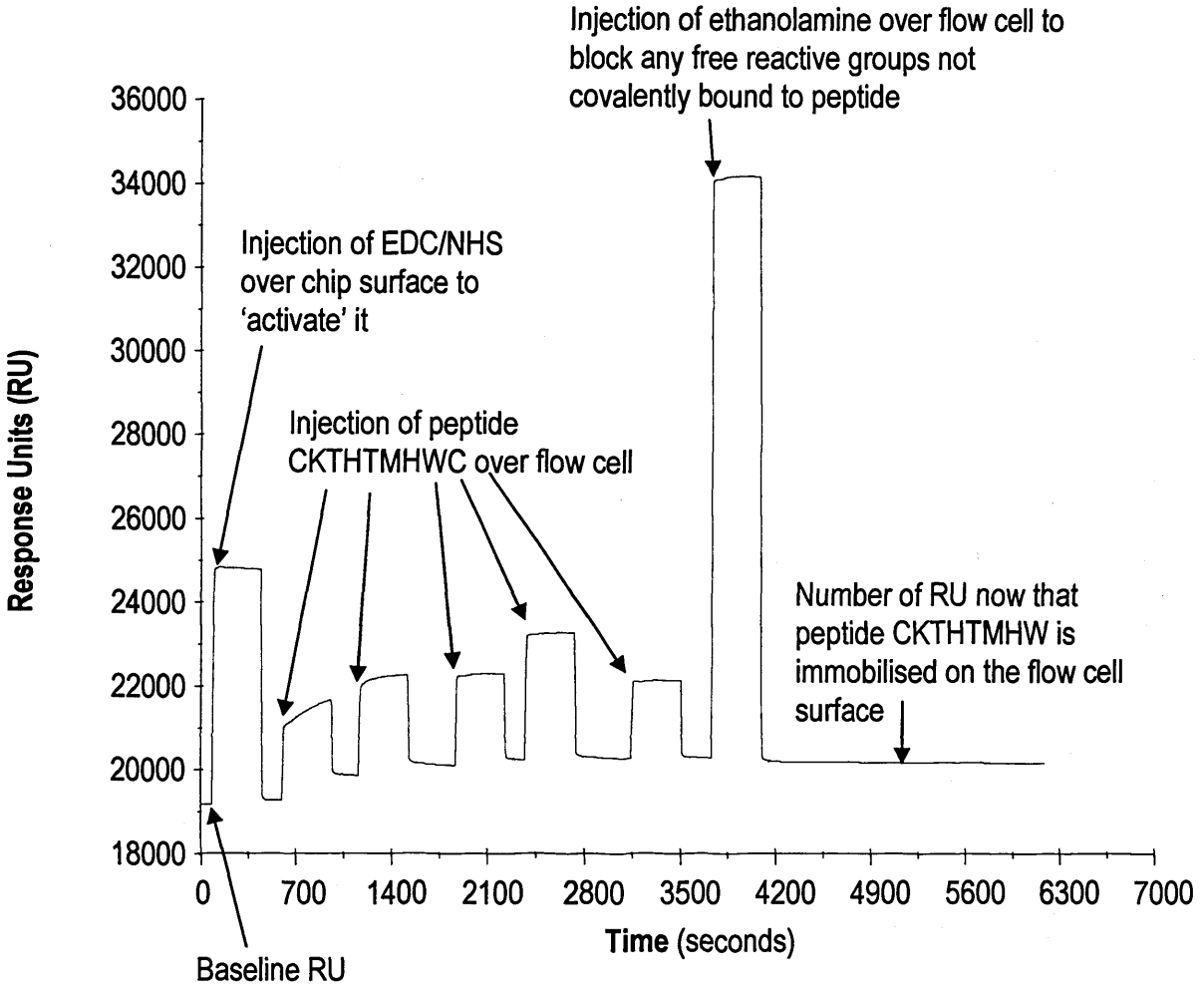

An F1 pioneer chip was docked in the BIACore 3000 and HEPES buffered saline flowed over and a baseline response unit (RU) value recorded. To 'activate' the flow cell surface, a mixture of EDC/NHS was injected over the flow cell. Peptide CKTHTMHWC was then passed over the flow cell and a measurement of RU was recorded before and after to determine whether it was binding to the surface. This was repeated a further four times, until no more peptide bound to the surface. Another sign the peptide was binding to the surface is that once it was starting to be injected over the flow cell, the RUs increased, as can be seen from the slope the first time the peptide is passed over. As the surface became saturated with peptide the gradient of the slope decreased with subsequent injections, until a flat plateau was reached. To block any remaining free reactive groups on the surface of the flow cell, ethanolamine was passed over. A reading was then taken to determine how many RUs of peptide had covalently bound to the flow cell surface.

concentration of C6. When 0.1 µM C6 was passed over the flow cell on which P_0 peptide had been immobilised, the change in RU was 4.3 and increased to 6.9 when 1 µM C6 was passed over. When 1 µM C9 was passed over the same flow cell, the average change in the RU was 3.8, which is below the sensitivity of the BIACore 3000. This shows that the P_0 peptide did not bind C6 or C9.

In summary, these data recorded on the BIACore suggest that both peptides specifically bind C6, but not C9. However, the changes in RU were low when C6 was passed over at both concentrations, which were in the micromolar range, suggesting that C6 has a low affinity for both peptides. Another reason for the small change in RU when C6 was passed over the flow cells might be due to the orientations and conformations of the peptides immobilised onto the chip surface. It would have been interesting to immobilise C6 onto a chip and pass the peptides over, but this was not done, mainly because the peptides are so small that if they had bound to immobilised C6, the change in RU might have been undetectable.

5.3.2.2. Assay to determine whether the selected peptides inhibit C-mediated haemolysis

The potential of the synthetic peptides CNNQPYKMC and CKTHTMHWC to functionally inhibit C6 activity was investigated in a 'C6-add back' haemolytic assay. First, to determine the dilution of C6 deficient rat serum and concentration of purified human C6 to use, a haemolytic assay was performed, diluting the concentrations of these two components (Figure 5.6). The dilution of C6 deficient rat serum and concentration of human C6 at which approximately 80% of sheep EA were lysed was selected. Diluted peptide was pre-incubated with human C6 (1.25 nM – up to 10,000 fold less than the highest concentration of peptide used) for 1 hour at 37°C before genetically C6 deficient rat serum, diluted 1 in 50 was added and incubated for a further hour at 37°C. Sheep EA were then added and the mixture incubated for 30 minutes at 37°C. After centrifugation, the supernatants were transferred to a flat-bottomed microtitre plate and the absorbance measured at 415 nm.

The concentration range of peptide CNNQPYKMC was 0 – 7.75 µM and for peptide CKTHTMHWC, 0 – 12.5 µM. The graph in Figure 5.7 shows that over these concentration ranges, neither peptide CNNQPYKMC nor peptide CKTHTMHWC was able to functionally inhibit C-mediated lysis.

Figure 5.6 Haemolytic assay to determine the dilution of C6 deficient rat serum and the concentration of human C6 required to lyse 80% of activated sheep erythrocytes

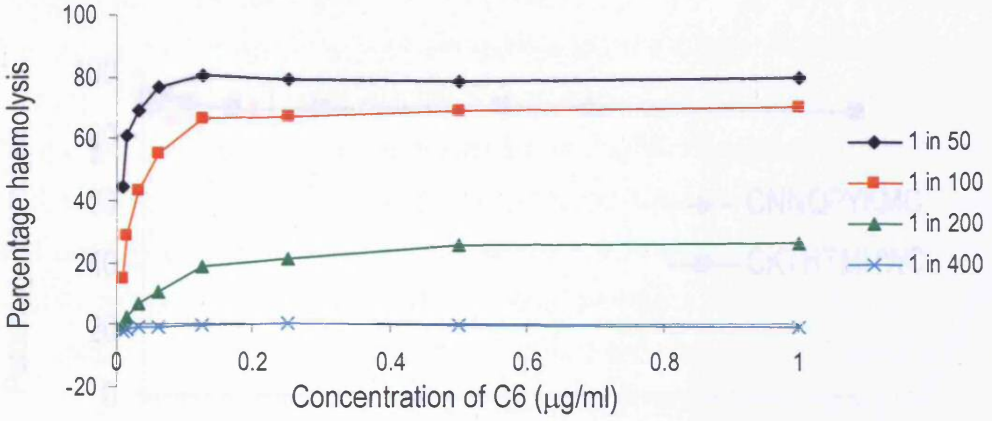

To determine the dilution of C6 deficient rat serum and concentration of purified human C6 to use in the 'C6 add back' haemolytic assay, a haemolytic assay was performed, diluting the concentrations of these two components. The dilution of C6 deficient rat serum and concentration of human C6 at which approximately 80% of sheep EA were lysed was selected.

Figure 5.7 Assay to determine whether the synthetic peptides CNNQPYMC and CKTHTMHWC can inhibit Complement-mediated haemolysis

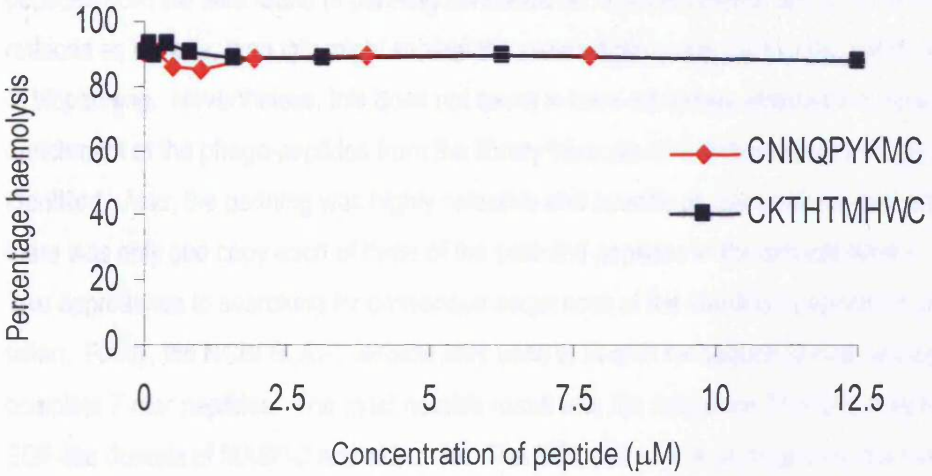

Diluted peptide was pre-incubated with human C6 (1.25 nM) for 1 hour at 37˚C before genetically C6 deficient rat serum, diluted 1 in 50 was added and incubated for a further hour at 37˚C. Sheep EA were then added and the mixture incubated for 30 minutes at 37˚C. After centrifugation, the supernatants were transferred to a flat-bottomed microtitre plate and the absorbance measured at 415 nm.

5.4 Discussion

This chapter described the selection of phage-peptides that bound human C6 through multiple rounds of biopanning and enrichment, the identification of selected phage-peptides that inhibited C-mediated haemolysis and the sequences of the respective peptides. The ability of two of these identified peptides to bind C6 and inhibit C-mediated haemolysis was also investigated.

In the second and third rounds of panning, the number of input pfu was below the optimum recommended, suggesting that phage infectivity may have been reduced in some way. The manufacturers instruction manual states that arginine and single cysteine residues displayed in the peptide sequence interfere with the secretion of pIII and also phage infectivity, therefore, clones with peptides containing Arg or Cys are selected against [575]. One of the selected phage-peptides from the final round of panning contained an arginine residue and if its infectivity was reduced as is likely, then this might explain the reduced pfu being put into the subsequent rounds of biopanning. Nevertheless, this does not seem to have adversely affected the selection or enrichment of the phage-peptides from the library because nine independent sequences were identified. Also, the panning was highly selective and specific as calculations showed it was likely there was only one copy each of three of the selected peptides in the original library.

Two approaches to searching for consensus sequences of the identified peptides in proteins were taken. Firstly, the NCBI BLAST website was used to search for sequence matches against the complete 7-mer peptides. The most notable result was the sequence TAAGAL matching the EGF-like domain of MASP-2 and sMAp 19. The MBL pathway is analogous to the start of the classical pathway of the C system but there has been no documented evidence of components of the MBL pathway interacting with the terminal pathway to date. Two of the peptides contained the consensus sequence FPIPLXS. However, BLAST searches failed to select the same protein matches when conducting searches for these sequences, making the other notable result, the sequence FPIPLP matching the leader sequence of the precursor pulmonary surfactant protein-B less significant. The second approach was to search the published sequences of C5, C6 and C7 for shorter matching sequences within the isolated peptide sequences. When motifs three amino acids long were searched for, there were several hits. All motifs that had homology with C5 mapped to the portion of the molecule that becomes C5b after C5 is cleaved by C5 convertase and had homology with residues in the α2-macroglobulin C-terminal region, apart from two motifs that had homology with the α2-macroglobulin N-terminal region of C5b. None of these matched the C345C domain that binds reversibly to the FIMs domains of C6 and C7 (described in section 1.1.2. and figure 1.3) [83,600]. The FIMs domains in C7 are important for the ability of C7 to bind to

C5b6 [85]. However, for C6, whilst the FIMs domains of C6 reversibly bind to C5b, it is the CCP domains in C6 that are essential for its activity [84]. One motif had homology for a sequence within the second FIMs domain in C7; given that the FIMS domains of C7 displace the FIMs domains of C6 from the C345C domain of C5, this could potentially represent a way of inhibiting C6 activity. In addition to the CCP domains of C6, it is thought that hydrophobic regions in both C6 and C5b are also involved in C5b6 formation, but the precise interactions remain to be elucidated [83]. It may be significant that two of the motifs that had homology with C5 were close to each other in the amino acid sequence: GAL at residues 1321-1323 and YKM at residues 1326-1328.
Although the FIMs domains within C7 are important for its activity, it is interesting that the other sequences with homology to C7 were of a hydrophobic nature; one of the motifs had similarity with the thrombospondin domain in C7 and four had homology with sequences in the perforin-like domain of C7. These results may be useful in investigating which areas of C5b, C6 and C7 interact with each other during MAC formation.
Of those tested, all of the phage-peptides almost completely inhibited lysis in C-mediated haemolytic assays apart from one, CKTTSTSHC, which inhibited haemolysis by less than 50%. This sequence did not contain any hydrophobic residues, whilst the other sequences with greater inhibitory activity contained amino acid residues that were predominantly uncharged or hydrophobic.
The peptide CKTHTMHWC bound C6 in an ELISA and both sequences specifically bound to C6 on the BIACore. Although the phage-peptide versions of the synthetic peptides inhibited C-mediated cell lysis dose-dependently in haemolytic assays, the peptides had no inhibitory activity. The phage-peptides may have inhibited C6 due to their size through steric effects and therefore this lack of inhibition for free peptide may be due the smaller size. It is recognised that some phage-peptides lose their binding ability or functional activity after being synthesised as peptides, as the phage coat can interfere with assays [601,602]. Some of the peptides contained more than one three amino acid motif that had homology with C5, C6 or C7 and five copies of peptide were displayed on the surface of each phage. These were in relative proximity to each other and it may be this pentameric conformation was critical to the observed properties of the inhibitory peptides because each peptide might have bound to a different region of C6 or interfered with C5b binding to C6 and C7 binding to C5b6. It would be interesting either to couple single and multiple units of peptides to a larger protein or make a fusion protein containing the peptide and investigate whether the inhibitory activity of these peptides could be restored. This was not possible in this study, due to the constraints of time and limited amounts of the peptides available.

Compstatin is a well-characterised peptide that binds C3 and was identified through screening a random phage display library expressing 27-mer peptide sequences against C3 [361]. It was assumed that long peptides might adopt a secondary structure more conducive to binding than short peptides. However, in contrast to the library we used, these long peptides were not constrained by a pair of cysteine residues, although it was expected a certain proportion of peptides would contain pairs of cysteines capable of forming intramolecular disulfide bonds [603], thereby constraining the peptides in a potentially favourable conformation [604]. The Ph.D.-C7C™ phage display library that we used was designed specifically to display peptides constrained in one conformation only, making the analysis of the characterisation of selected phage-peptides more reliable. However, in retrospect, in terms of having a greater chance of identifying a peptide with sequence similarity to a terminal C component or being able to select a peptide with functional blocking activity for C6, it may have been better to choose a phage-peptide library that displayed longer sequences of peptides.

In summary, the work conducted in this chapter has led to the identification of several phage-peptide clones that inhibit C-mediated haemoiytic activity. These clones were sequenced and 35% of them had the identical sequence NNQPYKM; 18% of them had the sequence KTHTMHW. Based upon their frequency and inhibitory activity as phage-peptides, synthetic peptides with these sequences were made. Haemolytic assays showed that these peptides no longer had inhibitory activity. However, studies on the BIAcore demonstrated that the peptides specifically bound to human C6, as opposed to another terminal complex component, C9. Although the 7-mer sequences did not share similarity with significant proteins when compared with databases, motifs three amino acids long did have homology with areas in C5b and C7 and represent an interesting area to explore in determining in particular the domains of C5b involved in binding to C6 during C5b6 and MAC formation.

Chapter 6: Establishing an ex vivo model of cardiopulmonary bypass for the assessment of the capacity of anti-human C6 antibodies to inhibit formation of soluble C5b-9.

6.1. Introduction

Having generated antibodies that recognise and inhibit C6 in Chapter 4, the obvious next step was to test the most promising inhibitory antibodies of C6 activity in a model of pathology in which damage is mediated by the terminal complement complex. The anti-human C6 mAbs 23D1 and 27B1 were the best inhibitors but they did not recognise any other species C6 and so they could not be tested in animal models of disease. Therefore, an ex vivo model of extracorporeal circulation or cardiopulmonary bypass (CPB) was set up in order to test the therapeutic potential of these mAbs. CPB is a necessary component of many types of cardiac surgery, but postoperative complications can occur, including respiratory failure, renal dysfunction, bleeding disorders, neurologic dysfunction and altered liver function. In turn, these can result in multiple organ failure (MOF) and eventually the death of the patient [262-266]. These complications arise due to a complex systemic inflammatory response (Figure 6.1), initiated by several factors, including contact of blood components with the surface of the bypass circuit, thereby activating the C system and other proteolytic cascades, and endotoxemia [605]. Raised levels of C3a and C5b-9 have been detected in patients both during and following CPB [267,269-273], but not in those who have undergone cardiac or other major surgery not requiring CPB [267,272]. This is because C3 convertase inhibitors are expressed on the surfaces of endothelial cells (EC) to ensure that C activation is properly regulated, but they are not present on the surface of the extracorporeal circuit. This allows both the coagulation and C (via the alternative pathway) systems to become activated in an unregulated manner when blood comes into contact with this non-physiological surface. C3a and C5a are released, attracting and activating neutrophils via the C3a and C5a receptors respectively [145,146]. C3a and C3adesArg also induce the synthesis of the pro-inflammatory cytokines TNF-α, IL-1β and IL-6 [606,607], which in turn exert their own effects, mainly by stimulating transcription factor NF-κB [608].

Neutrophils are initially recruited to injured tissue through low affinity interactions with EC and platelets through L-, E- and P-selectins respectively. Once activated, the expression of CR3 (integrin CD11b/CD18) on the neutrophil cell surface is upregulated [609] and binds to various adhesion molecules including intercellular adhesion molecule (ICAM), vascular cell adhesion molecule (VCAM) and platelet-endothelial cell adhesion molecule (PECAM) on the EC surface. As a result of these interactions, the neutrophils migrate into the interstitial fluid phase whereupon the contents of their lysosomes, such as

Figure 6.1 Schematic representation of the inflammatory response to cardiopulmonary bypass

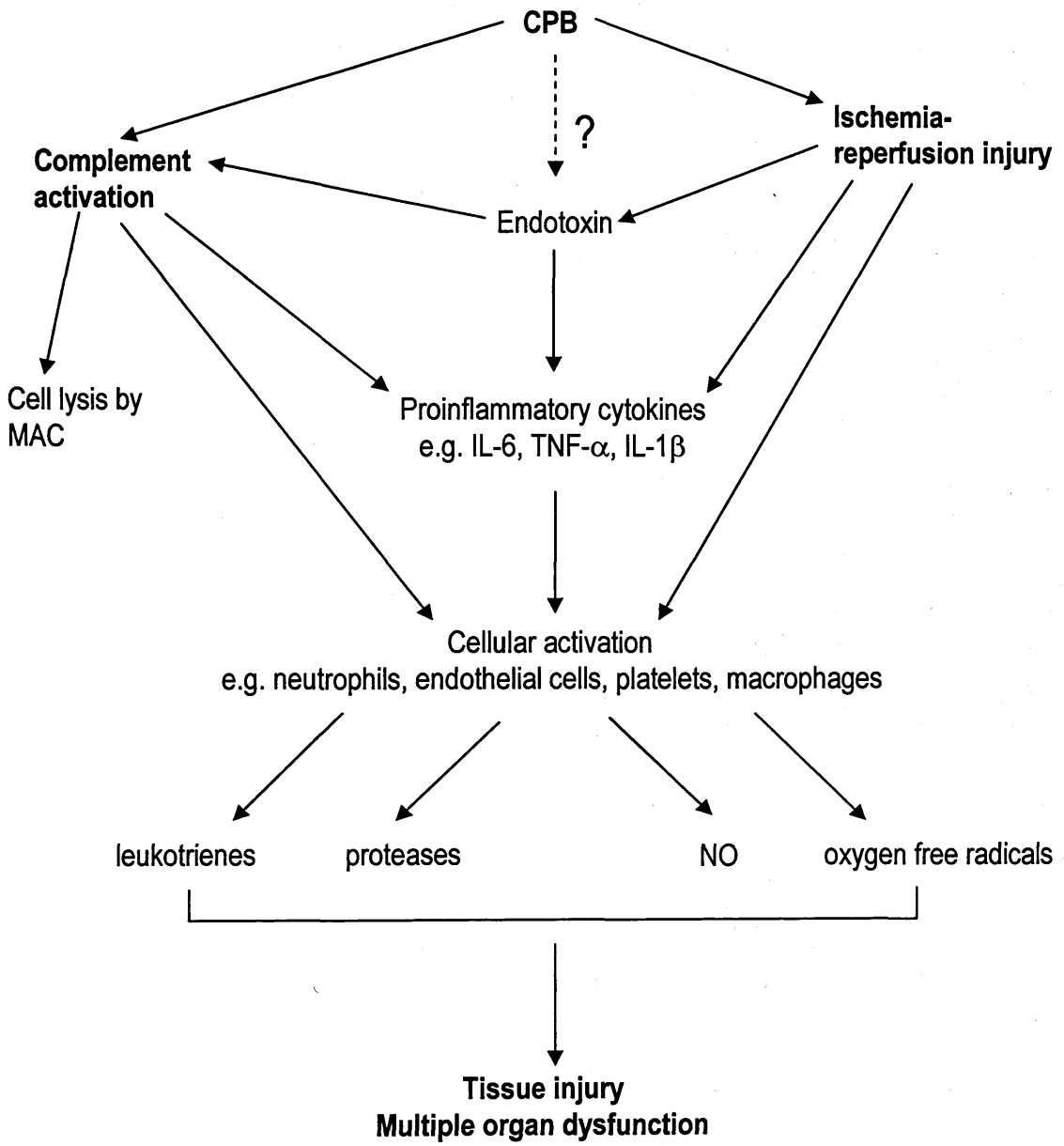

proteolytic enzymes, leukotrienes and oxygen free radicals, are released. These components can cause lipid peroxidation of EC and myocyte membranes, ultimately resulting in cellular dysfunction, oedema and cell death [610].

Circulating levels of endotoxin rise during and after CPB [270,611-614]. The gut is likely to be the main source of this, as changes in intestinal permeability occur during CPB [615-619] due to ischemia-reperfusion (I/R) injury and might lead to the release of endotoxin into the circulation. Once in the circulation, endotoxin can bind to EC, inducing IL-6 secretion [620] and to LPS-binding protein in the circulation, forming a complex. This complex binds to CD14 expressed on the surface of macrophages, stimulating their production of TNF-α [270,621]. Endotoxin will also activate the C system via the alternative pathway [32].

Nitric oxide (NO) production can increase significantly during and after CPB [622], leading to vasodilation and increased vascular permeability. This is mediated by inducible nitric oxide synthase (iNOS) which is activated by pro-inflammatory cytokines and endotoxin released during and after CPB [623-625]. However, NO produced by constitutive (c)NOS is believed to play a protective role and its release is impaired after CPB [626,627]. Clearly, the inflammatory response in patients undergoing CPB is very complex.

Therapeutic strategies to reduce systemic inflammation during and following CPB can be split into two broad scopes: a pharmacological-based approach and technical strategies. Steroids have a proven track record in reducing inflammation [628]. The pre-operative administration of methylprednisolone significantly reduces the levels of pro-inflammatory cytokines and increases the anti-inflammatory cytokine IL-10 [629,630]. Other studies have shown that steroid pre-treatment decreases endotoxin release [631] and expression of neutrophil integrins [632]. Steroids exert these effects by suppressing the induction of pro-inflammatory protein expression through the inhibition of several transcriptional pathways in different cell types [633-635].

Aprotinin (section 1.9.3.) was routinely used in the early 1980s, although it emerged that at high doses it increased the risk of patients suffering myocardial infarction and other complications during cardiac surgery [320]. However, it has continued to remain in use and a recent extensive meta-analysis demonstrated that aprotinin decreases mortality by up to 50%; the risk of peri-operative myocardial infarction is not increased, whilst the proportion of patients receiving blood components is reduced as is the frequency of surgical re-exploration [636]. Aprotinin can also reduce the expression of various inflammatory mediators by the same mechanisms as steroids in in vitro experiments [637-639]. However, there was no decrease in pro-inflammatory cytokine release or neutrophil activation in clinical trials [640].

Pexelizumab™ the anti-C5 antibody (section 1.9.8.) is currently being tested in phase III clinical trials of patients requiring CPB during coronary artery bypass graft surgery. Pexelizumab™ inhibits C5a and soluble C5b-9 generation and leukocyte accumulation, but does not affect C3a generation [520]. Its effectiveness in this context indicates that some of the harmful effects of CPB may be due to either C5a or SC5b-9 generation or both.

The routinely used technical strategy to lessen inflammation during and following CPB is the use of heparin-coated circuits. This reduces the direct contact of blood cells with foreign material, thereby decreasing C activation [641,642], cytokine release [643], kallikrein [644] and leukocyte activation [645]. However, there are conflicting reports as to the success of this strategy, with some publications demonstrating little benefit [646] whilst others show that high risk patients undergoing CPB with heparin-coated circuits have better clinical outcomes [647]. Some of the variability may be due to different coating techniques, for example, Duraflo II (Baxter Healthcare Corporation, California, USA) and Carmeda BioActive Surface (CBAS; Anaheim, California, USA) heparin coatings are used clinically. When compared against each other and an uncoated surface in trials, both coatings reduced C activation and neutrophil activation, although the CBAS system was more effective than the Duraflo II system [648].

Other technical strategies include ultrafiltration, maintaining a pulsatile flow during CPB and reducing temperature at which the surgery is carried out. Ultrafiltration is used during open-heart surgery to reduce excess body water accumulated during CPB and improve hemodynamic parameters [649]. Pro-inflammatory cytokine release is reduced in both paediatric and adult patients, but is not associated with improved clinical outcome in adults [650]. In paediatric patients there is decreased C activation and hemodynamic, pulmonary and hemostatic improvements have been demonstrated [651].

Blood flow occurs in a pulsatile manner under physiological conditions [626]. NO production is increased as a result of CPB, but it also modulates vasomotor tone in response to physiologic stimuli such as pulsatile flow and shear stress [652]. By ensuring that a pulsatile flow is maintained during CPB, this might minimise any systemic responses. Although some studies have reported a reduction of endotoxin and other pro-inflammatory mediators [653,654], others have not [655].

Various studies have been conducted comparing the clinical outcome of patients who have experienced normothermic (33 - 37°C) and hypothermic (26 - 28°C) CPB. The results are difficult to interpret due to the range of temperatures that CPB can be carried out at. Hypothermic CPB may provide better neuroprotection [656,657], but otherwise overall, the temperature at which CPB is carried out seems to make little difference [658-661], as hypothermic CPB delays but does not completely prevent neutrophil activation [662-664].

A study to discern which C components are responsible for mediating damage following I/R injury in the kidney, a side effect of CPB, was carried out in mice deficient in C3, C4, C5 or C6. All of the mice, apart from the C4-deficient mice, were protected, suggesting that C activation occurred via the alternative pathway and that the damage was mediated mainly by MAC formation. Inhibition of C5a activity in the C6-deficient mice did not provide them with further protection against I/R injury, confirming that the harmful aspects of C in this model were mainly due to C5b-9 production [513]. These data give strong justification for the development of an agent that specifically inhibits C5b-9 formation that could be used therapeutically in CPB.

The aims of this chapter were first to develop and characterise an ex vivo model of CPB based upon published methods [665,666] and second, to test the therapeutic potential of two of the inhibitory anti-C6 antibodies, 23D1 and 27B1 in this ex vivo model of CPB.

6.2. Specific methods and protocols

6.2.1. *Ex vivo* model of Cardiopulmonary Bypass (CPB)

An ex vivo model of CPB was set up based on published methods [665,666] to investigate the potential of anti-C6 blocking antibodies to inhibit C activation in a therapeutic setting. In the published methods, low density polyethylene tubing (I.D. 1.6 mm, O.D. 3.2 mm, Nalgene) was used. In this study, for comparative purposes and to add further clinical relevance, Tygon® S-50-HL hospital and surgical tubing (I.D. 3.2 mm, O.D. 4.8 mm) was also used. This medical grade tubing is used in CPB.

6.2.1.1. Collection of human blood and serum preparation

Blood was collected from volunteers by an appropriately qualified person and allowed to coagulate in a glass collection tube at room temperature for 30 minutes. The clotted blood was centrifuged at 2000 rpm for 10 minutes. The serum fraction was removed and used immediately. Serum was used rather than plasma as C activation occurs more readily in serum.

6.2.1.2. Tubing loop model

Human serum (3 ml) was placed in tubing (length 74 cm – to fit around the rotor). The two ends of the tubing length were joined together to make a continuous and enclosed loop using an additional piece of tubing. An air space was left in the tubing loop giving a gas volume of 2.23 ml air. The tubing loop was then attached to the rotor with tape and placed in an incubator pre-warmed to 37°C. The rotor was switched on and left to rotate the tubing at 60 rpm for 120 minutes. A schematic diagram is shown in Figure 6.2. After incubation, the tubing loops were

Figure 6.2 The *ex vivo* model of cardiopulmonary bypass (CPB)

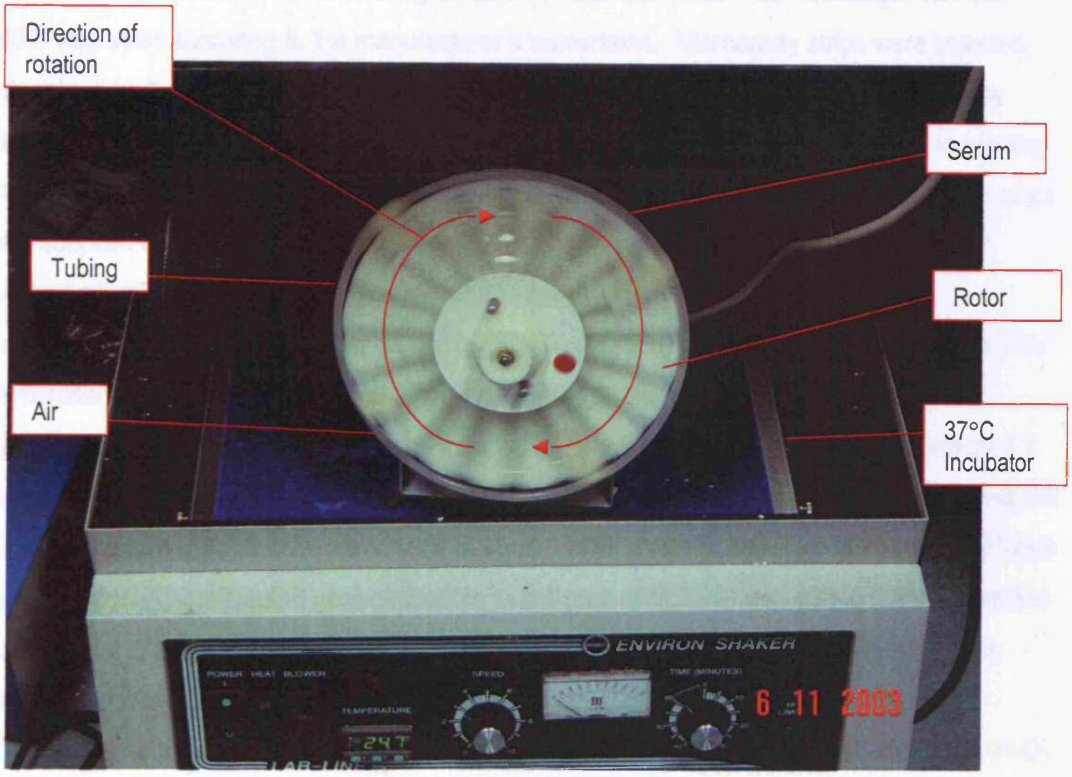

A diagram of the ex vivo cardiopulmonary bypass model. Tubing (polyethylene or Tygon™) was filled with 3 ml of serum, closed into a circuit and attached to a rotor. The tubing loop was rotated for 2 hours in a 37°C incubator at 60 rpm.

removed, opened and the serum samples poured into 5 ml tubes containing 0.2 M EDTA, giving a final concentration of 10 mM EDTA. A 0 minute sample was passed through the tube briefly and added to EDTA. The samples were stored at -70°C until analysis for the formation of soluble C5b-9 by ELISA. To test the inhibitory activity of the antibodies, these were added to the serum at a range of concentrations prior to being placed in the tubing and then treated in the same way as normal serum.

6.2.2. Soluble C5b-9 ELISA

The commercial ELISA kit for measuring sC5b-9 (Quidel, California, USA; Catalogue number A009) was used according to the manufacturer's instructions. Microassay strips were selected, determined by the number of blanks, standards and samples to be tested, and rehydrated by adding 300 µl wash buffer (0.05% Tween-20™, PBS, 0.01% Thimerosal) to each well, incubating for 2 minutes at room temperature and removing the liquid from each well. The microassay strips were supplied coated with a mouse monoclonal antibody specific for human sC5b-9. One hundred microlitres of blank, standard, control or sample diluted to the manufacturer's recommended dilution in specimen diluent (0.05% Tween-20 ™, Protein Stabilizers, PBS, 0.01% Thimerosal) were added to assigned microassay wells and incubated for 1 hour at room temperature. The wells were washed by adding 300 µl wash buffer to each well, incubated for 1 minute at room temperature and the liquid from each well removed. These steps were carried out a further four times, so that the wells were washed a total of five times. Fifty microlitres of sC5b-9 conjugate (HRPO-conjugated goat antibodies to antigens of sC5b-9) was added to each well and incubated for 1 hour at room temperature. The microassay strips were washed five times as described above and 100 µl prepared substrate solution (0.7% 2-2'-Azino-di-(3-ethylbenzthiazoline sulfonic acid) diammonium salt, diluted in 0.1M citrate buffer and 0.05% H_2O_2 added immediately prior to use) was added to each well and incubated at room temperature for 30 minutes. Fifty microlitres of stop solution was then added to each well and the absorbance read at 415 nm. The standard curve was plotted and the concentration of sC5b-9 in the samples calculated.

6.3. Results

6.3.1. The ex vivo model of CPB

Soluble C5b-9 formation occurred in serum after incubation for 2 hours in either the Tygon™ or polyethylene tubing in the CPB ex vivo model in comparison to 0 hours incubation in tubing (Figure 6.3). After 2 hours in the medical grade Tygon™ tubing in the CPB model, C activation in the serum had occurred, causing an increase from 254 ng/ml SC5b-9 before incubation, to 2012 ng/ml, which is a 7.92 fold increase. After being passed through the polyethylene tubing, the concentration of SC5b-9 in the serum was 345.2 ng/ml. After 2 hours in the CPB model, this had risen to 9443.5 ng/ml, which is a 27.36 fold increase in SC5b-9. In all of these conditions, results are means of duplicate measurements in the assay from single loops for each point. The physiological concentration of SC5b-9 in normal human serum is typically 100 – 250 ng/ml [667].

6.3.2. Characterisation of the ex vivo CPB model with the C inhibitor, soluble CR1 (sCR1)

Soluble CR1 (sCR1) (described in section 1.9.6.1.) inhibits the formation of the C3 and C5 convertases, ultimately preventing SC5b-9 formation [372,373]. In order to gain information about the degree of inhibition of SC5b-9 formation that could be expected to occur in this model, escalating doses of sCR1 (1, 2 and 5 µg/ml) were added to the serum being placed in the tubing at the start of the experiment.

The samples collected from the polyethylene or Tygon™ tubing were assayed for SC5b-9 (Figure 6.4). In the polyethylene tubing, there was a baseline reading of 8748.6 ng/ml SC5b-9 when no sCR1 was added. The baseline reading of SC5b-9 in the Tygon™ tubing in the absence of sCR1 was 4697.0 ng/ml. The addition of sCR1 at a dose of 1 µg/ml had no effect on the concentration of SC5b-9 in the polyethylene or Tygon™ tubing loops (SC5b-9 concentration was 9574.3 ng/ml and 4540.0 ng/ml, respectively). When sCR1 was added at a dose of 2 µg/ml, SC5b-9 formation was inhibited in the polyethylene and Tygon™ tubing by approximately 50% (4341.8 ng/ml and 2362.9 ng/ml sC5b-9 respectively) in comparison to control. In the presence of 5 µg/ml sCR1, SC5b-9 formation was inhibited in both types of loop by approximately 50% (4480 ng/ml and 1768.6 ng/ml SC5b-9 respectively) in comparison to control. For all of these conditions, results are the means of duplicate measurements in the assay from single loops for each data point.

Figure 6.3 Characterising an ex vivo model of CPB

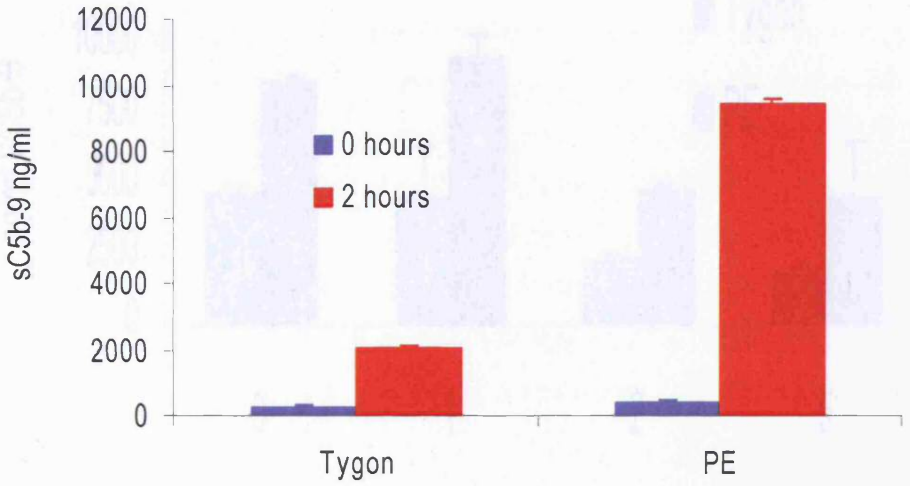

To determine whether medical grade Tygon™ tubing or polyethylene (PE) tubing could cause C activation 3 ml freshly prepared serum was placed in either tubing being tested; this was closed up and attached to a rotating device that rotated at 60 rpm and incubated at 37°C for 2 hours. At the end of this time, the tubing was removed, opened up and the serum drained out. To stop any further C activation, EDTA was added, making a final concentration of 10 mM and stored at -70°C until testing. For the 0 hours timepoint, fresh serum was passed through tubing and quenched and frozen as described. Soluble C5b-9 formation was measured by commercial ELISA and the measurements are presented graphically here. For experimental conditions, results are means of duplicate measurements in the assay from single loops for each data point. Error bars are standard deviation of the mean.

Figure 6.4 Inhibition of sC5b-9 formation by sCR1

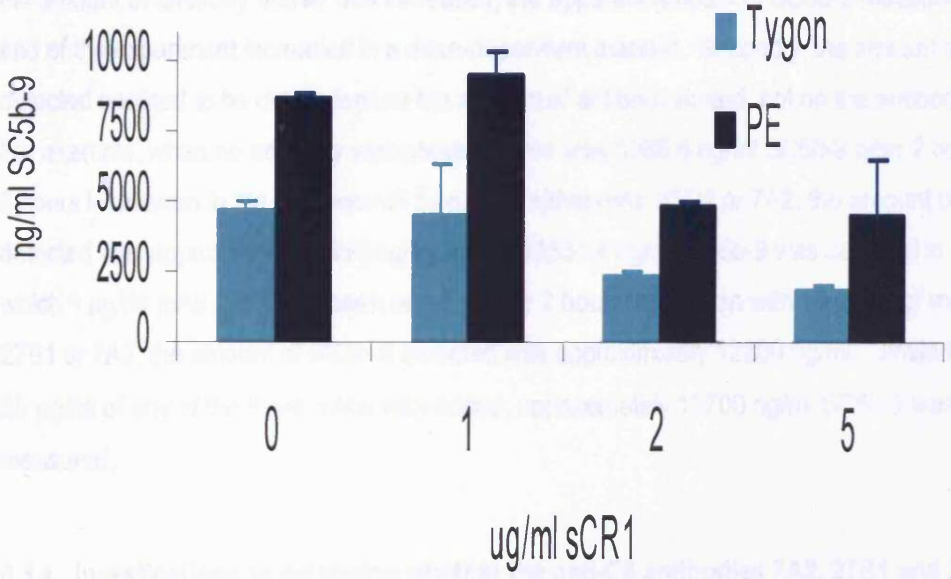

To determine whether the C inhibitor sCR1 inhibited C activation in this ex vivo model of CPB, escalating doses of sCR1 (1, 2 and 5 µg/ml) were added to freshly prepared serum and placed in either Tygon™ or polyethylene (PE) tubing. The tubing was closed up by joining them together and then attached to the rotating device for 2 hours at 37°C. The serum was removed and any potential C activation prevented by the addition of 10 mM EDTA (final concentration) and stored at -70°C until the concentration of sC5b-9 was assayed. As a control, serum without sCR1 added was also included in the experiment. Soluble C5b-9 formation was measured by ELISA and the measurements are shown on the graph above. For experimental conditions results are means of duplicate measurements in the assay from single loops for each data point. Error bars are standard deviation of the mean.

6.3.3. Testing the activities of the anti-C6 antibodies 7A2, 27B1 and 23D1 in the CPB model

The therapeutic potential of the two inhibitory anti-C6 antibodies 27B1 and 23D1 were tested in Tygon™ tubing at three doses over the concentration range (1 – 25 µg/ml). As a means of comparison, the same experiment was carried out in parallel using the non-inhibitory anti-C6 antibody 7A2. Each dose of antibody was added to the serum samples immediately prior to being placed into the tubing. The samples were assayed for SC5b-9 after the end of the experiment (Figure 6.5). There are two findings: firstly, that for each of the three antibodies, as the amount of antibody added was increased, the apparent amount of SC5b-9 measured at the end of the experiment increased in a dose-dependent manner. Secondly, the amount of SC5b-9 detected seemed to be dependent on the amount of antibody added, not on the antibody clone. For example, when no antibody was present, there was 5588.6 ng/ml SC5b-9 after 2 hours. After 2 hours incubation in the presence of 1 µg/ml of either mAb 23D1 or 7A2, the amount of SC5b-9 detected was approximately 5550 ng/ml, whilst 12331.4 ng/ml SC5b-9 was detected in serum to which 1 µg/ml mAb 27B1 had been added. After 2 hours incubation with 10 µg/ml of mAb 23D1, 27B1 or 7A2, the amount of SC5b-9 detected was approximately 12200 ng/ml. Similarly, when 25 µg/ml of any of the three mAbs was added, approximately 13700 ng/ml SC5b-9 was measured.

6.3.4. Investigations to determine whether the anti-C6 antibodies 7A2, 27B1 and 23D1 were interfering in the SC5b-9 ELISA

The preliminary data in section 6.3.3. were suggestive of the mAbs 7A2, 27B1 and 23D1 interfering in the SC5b-9 ELISA because the amount of SC5b-9 measured seemed to be dependent on the amount of mAb the serum was incubated with. These mAb preparations also contained bovine Ig (section 4.3.8.) as a result of the way in which they had been prepared. To test whether bovine Ig might be the agent interfering in the ELISA, as opposed to the mAbs themselves, mouse Ig prepared from mouse serum and two different preparations of a purified mAb clone TLD1C11, which was raised against an irrelevant rat antigen: one of which was pure; the other containing bovine Ig were added to freshly prepared serum. The mAb TLD1C11 has the same isotype as mAbs 7A2, 23D1 and 27B1 and is not raised against C6. The mAbs 7A2, 23D1 and 27B1 were also included in the experiment to determine whether they themselves were interfering in the SC5b-9 ELISA. Several concentrations of each antibody were added to the serum (1 – 25 µg/ml) in triplicate. Soluble C5b-9 in each sample was immediately measured.

Figure 6.5 Assessment of the inhibitory properties of antibody clones 27B1 and 23D1

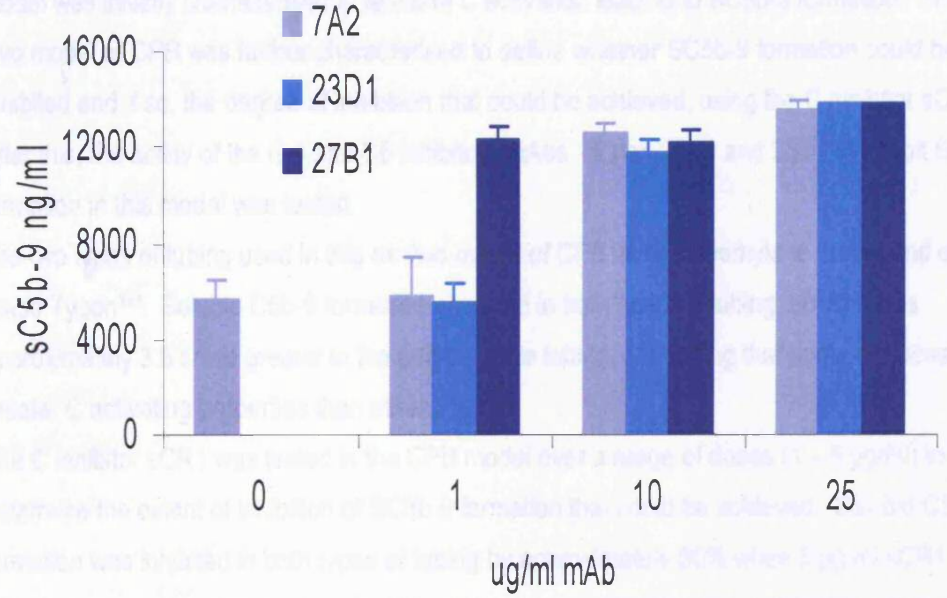

To investigate the C blocking properties of the inhibitory anti-C6 antibodies 23D1 and 27B1 in the ex vivo CPB model, fresh serum, together with either mAb 23D1 or 27B1 over the concentration range 1 – 25 μg/ml was placed in Tygon™ tubing. The ends of the tubing were closed and then each tubing loop was attached to the rotating device and rotated for 2 hours at 37°C. The serum was removed and further C activation prevented by the addition of 10 mM EDTA (final concentration) and stored at -70°C until the concentration of sC5b-9 was measured. The mAb clone 7A2 was included as an antigen specific isotype matched control which had had no inhibitory activity in previous tests. Serum without antibody present was also included in the experiment as a baseline measurement. Soluble C5b-9 formation was measured by ELISA and is shown on the graph above. Results are means of duplicate measurements in the assay from single loops for each point. The error bars are the standard deviation from the mean.

The samples contained no detectable SC5b-9 above serum background. These data show firstly, that under these conditions, bovine Ig does not interfere with the SC5b-9 ELISA. Secondly, these results indicate that the mAbs were not directly interfering with the ELISA under these experimental conditions.

6.4 Discussion

This chapter describes the development of an ex vivo model of CPB in two types of tubing. This model was initially characterised in terms of C activation leading to SC5b-9 formation. The ex vivo model of CPB was further characterised to define whether SC5b-9 formation could be inhibited and if so, the degree of inhibition that could be achieved, using the C inhibitor sCR1. After this, the ability of the two anti-C6 inhibitory mAbs, clones 27B1 and 23D1 to inhibit SC5b-9 formation in this model was tested.

The two types of tubing used in this ex vivo model of CPB were polyethylene tubing and clinical grade Tygon™. Soluble C5b-9 formation occurred in both types of tubing, but this was approximately 3.5 times greater in the polyethylene tubing, confirming that some surfaces have greater C activating properties than others.

The C inhibitor sCR1 was tested in the CPB model over a range of doses (1 – 5 µg/ml) to determine the extent of inhibition of SC5b-9 formation that could be achieved. Soluble C5b-9 formation was inhibited in both types of tubing by approximately 50% when 5 µg/ml sCR1 was added to serum. In retrospect, it would have been interesting to use a wider range of doses of sCR1 to fully inhibit SC5b-9 formation. Other groups have carried out in vivo in studies of CPB using sCR1. Soluble CR1 (TP10™, AVANT Immunotherapeutics, Needham, Massachusetts, USA) was administered to pigs (10 mg/kg i.v., which is equivalent to 100 – 200 µg/ml in plasma) undergoing CPB. At this dose, SC5b-9 formation was almost completely inhibited in comparison to the control group receiving no sCR1 [668]. Nevertheless, the ex vivo model of CPB set up in this chapter is sufficient to demonstrate the activity of a C inhibitor in a highly sensitive manner.

The C6 inhibitory antibodies 27B1 and 23D1 were tested in this CPB model and compared with the non-inhibitory anti-C6 isotype-matched mAb, 7A2. Surprisingly, the amount of SC5b-9 measured by ELISA did not decrease in response to any of the doses used. In fact, the higher the dose of antibody added the more sC5b-9 was detected. The amount of SC5b-9 detected in serum after being incubated with 10 µg/ml mAb for example, was very similar, irrespective of which clone had been used. This observation broadly applied to the three concentrations of mAb tested. However, mAbs 23D1 and 27B1 inhibited C-mediated haemolysis (Section 4.3.4.), a cell

based assay which measures MAC formation. Therefore, these data were suggestive that the mAbs might be interfering in the ELISA. All of the mAbs had been prepared in house and had been co-purified with bovine Ig (section 4.3.8.). To investigate if the bovine Ig and the mAbs themselves were interfering in the SC5b-9 ELISA, these mAbs, along with preparations of an irrelevant isotype matched mAb, clone TLD1C11, lacking or containing bovine Ig were added to freshly prepared serum and SC5b-9 measured in each sample immediately by ELISA. Soluble C5b-9 was barely detectable in any of the samples, demonstrating that neither the bovine Ig nor mAbs were directly interfering in the SC5b-9 ELISA. Therefore, the observed increases in the amount of SC5b-9 in the CPB model in the presence of the anti-C6 mAbs must either have been due to the presence of antibody or a phenomenon specific to these anti-C6 antibodies. One way of determining this would be to incubate serum in the CPB model with pure TLD1C11 and TLD1C11 containing bovine Ig and mouse Ig for 2 hours and measure SC5b-9. If the amount of SC5b-9 measured did not increase, then this would show that the observed increase in SC5b-9 in the presence of the mAbs 23D1, 27B1 and 7A2 were due specifically to these anti-C6 antibodies. This would indicate that these mAbs do not inhibit the fluid-phase generation of SC5b-9 and may even enhance its generation by cross-linking the complexes and causing C activation via the classical pathway, as opposed to the haemolytic assays used to establish the inhibitory activity of mAbs 23D1 and 27B1 which are a measure of MAC formation on the erythrocyte cell surface. This may suggest that mAbs 23D1 and 27B1 are inhibiting C6 by interfering with it embedding in the cell surface during MAC formation.

If the amount of SC5b-9 measured in serum did increase after incubation with irrelevant antibodies in the CPB model, this would suggest that the presence of antibodies is causing C activation via the classical pathway, resulting in increased levels of SC5b-9 formation. There are two ways around this problem: one is to make $F(ab')_2$ fragments of mAbs 23D1 and 27B1, so that they cannot activate the classical pathway; the other is to make scFv versions of these antibodies, which would also have less C activating properties than the parent molecules. Currently, there are two examples in the literature of inhibitory antibodies raised against C components being tested either in vivo or in an ex vivo model of CPB for their ability to block sC5b-9 formation. These are Pexelizumab™ (section 1.9.8.), the humanised scFV anti-C5 antibody [470], and $F(ab')_2$ fragments of an anti-properdin blocking mAb [669]. Both of these agents inhibited SC5b-9 formation in a dose-dependent manner. However, neither of them were tested as intact Ig molecules either in an ex vivo model of CPB or in vivo.

To summarise, an ex vivo model of CPB has been set up and C activation took place, because SC5b-9 formation occurred in the presence of serum in the Tygon™ and polyethylene tubing

used. The C inhibitor, sCR1 inhibited SC5b-9 formation in this model in a dose-dependent manner in both types of tubing, by up to approximately 50% at the maximal dose of sCR1 added (5 µg/ml). This was an important experiment that helped characterise this model in terms of the degree of inhibition of SC5b-9 formation that could be achieved with a previously defined C inhibitor [372,373]. The inhibitory anti-C6 mAbs 27B1 and 23D1 were tested for their ability to inhibit SC5b-9 in this model, along with the non-inhibitory anti-C6 mAb 7A2 as an isotype control. The incubation of the mAbs with serum resulted in an increase in SC5b-9 measured and this was dose dependent. Given the C6 inhibitory properties of the mAbs, these results were suggestive of some kind of assay interference. However, experiments designed to investigate this demonstrated that the mAb preparations were not interfering in the SC5b-9 ELISA. Nonetheless, this ex vivo CPB model will be useful as a preliminary tool in assessing the activities of C inhibitors of the human alternative and terminal C pathways before testing them in animal models of disease.

Chapter 7: General Discussion

7.1. Overview

The MAC is implicated in mediating the development of pathology in several autoimmune diseases such as rheumatoid arthritis and multiple sclerosis as well as due to clinical interventions, such as cardiopulmonary bypass (CPB). Currently, there are no drugs available that specifically inhibit MAC assembly. The advantage of blocking MAC formation as opposed to inhibiting the C cascade earlier on in the pathway is that there are many beneficial effects of C in the activation pathways, including the clearance of immune complexes and the chemattraction of neutrophils to areas of inflammation, ensuring that patients are not left vulnerable to infections. C6, a component of the MAC represents an ideal target for inhibition as it occurs early on in the terminal pathway and the complex it forms with C5b is not known to induce signalling cascades within cells or have any other effects outside the terminal pathway. Fortuitously, C6 deficient mice, rats and rabbits were available in house. The work described in this thesis sought to develop and characterise a panel of reagents that block C6 activity, with the ultimate aim of investigating their therapeutic potential in animal models of MAC mediated disease. To maximise the possibility of generating the greatest number of inhibitors, two approaches were used; one was to raise antibodies against C6 and the other was to pan a library of phage expressing peptides on their surface against C6.

Prior to the commencement of this project, attempts at making C inhibitory therapeutics had targeted the activating pathways and utilised recombinant technology to make soluble forms of membrane-associated C regulators. As a result of the successes achieved with these methodologies, similar approaches have been applied to making terminal pathway inhibitors. Soluble recombinant forms of the GPI-anchored membrane inhibitor, CD59 were made (sCD59) with a view to developing them as potential therapeutics [385,670,671], but were poor inhibitors of MAC formation when tested in vitro and in vivo [385,672]. To generate more active forms of sCD59, investigators have used a variety of techniques, including making chimeras, fusion proteins and attaching membrane-associating tags [400,404,673]. These measures improved the activity of the sCD59 in vitro in haemolytic assays. In vivo, attachment of a membrane-associating targeting moiety to soluble rat CD59 suppressed the development of disease in a rat model of rheumatoid arthritis. None of these agents have yet successfully been developed further for clinical use. Phage display is a young field and far fewer peptide inhibitors identified through this technique (excluding scFV) have been licensed for clinical use. With respect to C inhibitors, no peptides identified have been successfully developed for clinical use. Compstatin, which binds C3

inhibiting its cleavage, is the most famous example of using phage display to develop a C inhibitor, but is limited in its applications and has not been developed as a therapeutic [361-363]. One of the advantages of phage display is that phage-peptides that bind to the protein of interest can be rapidly identified and sequenced. In this project, after three rounds of panning, the phage-peptides were selected for sequencing on the basis of their ability to inhibit C-mediated haemolysis, but the corresponding synthetic peptides lost that ability, even though they still recognised C6. This is suggestive of the observed inhibitory properties of the phage-peptides being due to steric hindrance or possibly an avidity effect. This loss of function is not uncommon [601], but was a frustrating outcome and is a disadvantage of this type of approach to generating a peptide inhibitor. For this reason, this technique was probably not as good an approach to generating an inhibitor of C6 activity as making anti-C6 mAbs. There are many phage-peptide libraries commercially available and this is an important parameter that should be considered. The main variations between different phage-peptide libraries are the lengths of the presented peptides and also whether these are constrained by disulphide bonds. The amino acids in constrained sequences show more stringent sequence specificity than linear peptides selected for binding to the same targets [570]. Consequently, the library chosen for use in this study presented constrained peptides seven amino acids long. It may have been better to use a library displaying longer constrained peptides, or several libraries for comparison. In other studies in which inhibitory peptides of C components have been identified, the libraries used have displayed much longer peptide sequences than the 7-mer sequences used in this work [359,361]. The greater success might be due to the longer length of the peptide, as it is likely that for the peptide to bind, more of the residues interact with the target protein to allow binding to occur during panning. For this reason, such a peptide would likely have a greater affinity for the protein it was panned against than a shorter peptide.

A positive outcome from using this technique was that three amino acid motifs were identified within the C6 binding peptides that were found to share homology with regions of C5 and C7. Of particular interest were two motifs identified from different peptides that matched residues close together in the C5b sequence. Therefore phage display might provide an opportunity to study the interactions of the molecular domains of C5b and C6 with each other in detail, as C5b6 complex formation happens so fast that it isn't possible to study this in real time. If a particular sequence was found to bind to C6, this could in principal be made into an Fc fusion protein or attached to some other targeting molecule and tested for its ability to inhibit C6 activity. Mutation studies of the C6-binding peptide could be performed to determine sequences with a higher binding affinity.

Potentially, this could lead to the development of an efficient inhibitor of C6 suitable for clinical use.

An alternative to modifying C regulatory proteins was to generate monoclonal and scFv antibodies against the C protein of interest. Monoclonal and scFV antibodies are highly specific and tend to have a far higher affinity for the protein they recognise than peptides or other molecules. They are also retained in the circulation for some time, minimising the dose required for therapeutic benefit. Such reagents already have a proven track record in the treatment of various conditions, including cancer [408,444,445,447,449], and rheumatoid arthritis [674,675]. A precedent for inhibiting the C system has been set with the anti-C5 mAb Eculizumab™ approved to treat PNH [472,676], and its scFv analogue, Pexelizumab™ approved for use during CPB to inhibit systemic C activation and to treat myocardial infarction [471,564,565]. Both agents inhibit C-mediated haemolysis and C5a generation, but they are not terminal pathway specific and the loss of C5a with consequent inhibition of the beneficial chemattraction of neutrophils to the area of inflammation may have a deleterious effect on the patient's health.

Given the success of the mAbs developed for clinical use, raising mAbs against C6 was a logical approach to developing an agent that inhibited MAC formation. More than twenty different mAbs were raised against rat, mouse or human C6, and they all recognised human C6. Many also inhibited C-mediated haemolysis in the presence of human serum. All of the mAbs raised against rat or mouse C6 had IgM isotypes, an efficient C activating isotype and were therefore not further investigated [30,31]. Nevertheless, these mAbs are potentially useful as they were raised against and recognise mouse C6 and there are no commercially available anti-mouse C6 mAbs at present. Some, for example, might be suitable for use in immunocytochemistry for following the deposition of C6 in the MAC in histological specimens and would enable the assessment of MAC deposition in tissues in disease models in mice such as EAE. The fact that all of the mAbs raised against rat and mouse C6 had an IgM isotype was suggestive of the antigen challenge not being great enough to induce class switching in the B cells to secreting an IgG isotype antibody [531,532]. There are two ways of increasing the chances of this happening: one would have been to immunise the mice and rats with C6-enriched sera; the other to immunise with purified mouse and rat C6 respectively. It would have been relatively straightforward to enrich mouse and rat sera by performing PEG cuts and with hindsight, this simple approach would likely have been advantageous. To purify C6 from mouse and rat serum, classical methods would have needed to be used, as no anti-mouse C6 or anti-rat C6 antibodies were available at the start of this project for affinity purification. Classical purification methods were initially used to purify human C6 in

this study, but proved inefficient and time consuming. At least 100 ml serum as starting material would have been required to purify rat or mouse C6 and it would have been practical to collect this volume of rat serum. This would not have been so for mouse serum, as in excess of 200 mice would have had to be sacrificed to obtain this volume. Many anti-human C6 mAbs were made during the course of this study and as a consequence, some were used to affinity purify human C6. The yield and functional activity of the purified protein was much greater than using classical methods, because there were fewer steps making it much faster, so that C6 was less likely to be lost between steps and this also made the protein less prone to degradation. As a result of the work carried out during this project, anti-rat C6 and anti-mouse C6 mAbs are now available, making it possible to affinity purify rat and mouse C6 from small volumes of serum in the future.

The affinity purified human C6 was also used to determine its functional cross-species activity by being added to haemolytic assays using genetically C6-deficient rat, mouse and rabbit serum. These results clearly demonstrated that C6 is functionally conserved between these species, underlining the evolutionary importance of C proteins. Human C6 is a larger protein than rat or mouse C6, which share an 82% and 75% sequence homology with human C6 respectively [485,504]. Even so, it was surprising that the anti-human C6 mAbs, clones 23D1, 27B1 and 7A2 did not recognise other species C6, considering that they had been isolated from C6 deficient mice. It had originally been decided to immunise C6 deficient mice with normal mouse or purified human C6 to maximise the possibility of generating cross-species reactive mAbs. It is perhaps less unexpected that the inhibitory anti-human C6 mAbs, 23D1 and 27B1 do not recognise other species C6, as human C6 is a larger molecule than mouse and rat C6 because it contains two FIMS domains which enhance, but are not critical for its activity. An alternative approach to generating cross-species reactive anti-C6 mAbs with an IgG isotype would have been to be make recombinant proteins based upon regions of sequence similarity of C6 common to human, mouse and rat C6 and immunise mice and rats with these.

The species specificity of mAbs 23D1 and 27B1 for human C6 meant that it was not possible to test their inhibitory activity in vivo in animal models of C-mediated disease as had initially been anticipated. However, I wanted to test their therapeutic potential in a setting resembling a more clinical application than in vitro haemolytic assays. The activities of other C inhibitors have previously been investigated in ex vivo models of cardiopulmonary bypass (CBP) during which a complex inflammatory response is induced, including systemic C activation. The formation of C5b-9 is upregulated [267,270] mediating damage by causing cell lysis and can ultimately lead to multiple organ failure. For these reasons, an ex vivo model of CPB was established to test the

inhibitory anti-C6 mAbs. The model was initially characterised by determining that more soluble SC5b-9 was present in human serum after 2 hours circulation in comparison to serum not circulated in the model. The amount of sC5b-9 detected was also dependent on the type of tubing used. To demonstrate SC5b-9 formation could be inhibited, the inhibitor soluble (s)CR1 was added at various doses. The amount of SC5b-9 detected decreased dose-dependently to approximately 50% of that in the absence of sCR1 as the concentration of sCR1 added increased.

The abilities of mAbs 23D1 and 27B1 to inhibit MAC formation, together with a relevant isotype-matched control, were tested in the CPB model over a range of concentrations. Unexpectedly, for all of the mAbs, at each concentration of mAb incubated in the CPB model the concentration of SC5b-9 measured increased. In addition, the concentration of SC5b-9 measured in response to the same dose of different mAb was very similar, suggesting that the antibodies were interfering with the method used to measure SC5b-9; ELISA. This hypothesis was investigated and demonstrated that the mAbs were not directly interfering with the SC5b-9 ELISA. Therefore a logical interpretation of this data, in conjunction with the haemolytic assay data, is that mAbs 23D1 and 27B1 do not inhibit sC5b-9 formation in the fluid phase, but they do inhibit MAC formation at the cell surface, raising important implications for their mechanism of inhibition of C6 activity. These findings suggest that when either of these two mAbs bind to C6 they are not blocking its ability to bind to C5b to form the C5b6 complex; neither are they blocking the ability of C7 to bind to C5b6, but they are blocking the ability of this complex to insert into the cell membrane. The ex vivo CPB model happened to be very informative about the inhibitory action of mAbs 23D1 and 27B1, but as a model to test the therapeutic potential of agents, is probably more suited to testing the activity of fluid phase C inhibitors. These results also highlight the functional differences between cell-based assays and fluid-phase assays and the importance of carefully choosing a model to test an agent for the purpose it was intended. For example, the aim of this PhD was to generate inhibitors of C6 to block MAC formation in the cell membrane in order to prevent or stop the development of pathology in disease. It was of secondary consequence to inhibit sC5b-9 formation.

7.2. Future Directions

As a result of this work, many anti-C6 antibody secreting hybridoma cell lines have been created. Many had an IgM isotype, which meant that they were not further investigated, even though they functionally inhibited C6 activity. However, there are ways that these mAbs could be developed

further and investigated for their therapeutic potential; either by inducing 'class switching' so that they secrete mAbs with an IgG isotype, or by cloning the variable regions of the mAbs and ligating them to plasmids coding the F_c region of an IgG antibody to make a fusion protein. These would be interesting areas of research to pursue. Both of these approaches would also determine whether the observed inhibition of the intact antibody was due to a specific interaction with C6 at a region crucial for its activity, or whether this was due to steric hindrance. The advantage of developing these antibodies further is that they should recognise both mouse and human C6, so that their therapeutic potential can be tested in well-established animal models of MAC mediated disease.

Apart from generating mAbs and peptides that inhibit C6 activity an alternative approach would be to modifiy C inhibitory proteins made by infectious organisms. For example, bacteria and other parasitic organisms have evolved various strategies to evade the host immune system. These include making proteins that inhibit the activity of C components. The Schistosoma parasite makes at least two C inhibitory proteins during its lifecycle – one, complement C2 receptor inhibitor trispanning (CRIT) protein binds to C2 preventing it binding to C4b [677,678]. The other, schistosome C inhibitory protein type 1 (SCIP-1), is an analogue of CD59 and binds to C8 and C9 [679]. Apart from the specific targets that these proteins have evolved to inhibit, what is interesting about them is their sequence similarity with the host proteins they are mimicking. The region of CRIT that binds to C2 is homologous with a region within C4b [680], likewise, SCIP-1 is recognised by anti-human CD59 antibodies. These proteins yield important information about the regions of C2 and CD59 that interact with C4b and C8 and C9 respectively and represent an opportunity for the development of C-blocking therapeutics, specific against these regions. CRIT is currently being investigated for this purpose [681]. Similarly, there is also a bacterial protein that binds C6 and C7, made by some virulent strains of Streptococcus pyogenes called streptococcal inhibitor of complement (SIC) [682]. SIC inhibits C-mediated haemolysis, acting before the incorporation of fluid phase C5b-7 into cell membranes [683]. As the sequence of SIC has been determined [682], it would be possible to make recombinant truncated forms of it, determine the region of the protein that inhibits C-mediated haemolysis and use this as a basis for developing inhibitory peptides of sC5b-9 formation. It is likely that such studies would also yield important information about the regions of C6 that are important for its activity in forming MAC.

The two most promising C6 inhibitors, mAbs 23D1 and 27B1 were not tested in animal models of disease in which the MAC is implicated in playing a role, because they did not recognise other species C6. However, it may be possible to test these mAbs in an animal model of disease mediated by the MAC in C6 deficient animals reconstituted with human C6. A study investigating

the contribution of the MAC to disease progression in animal models of multiple sclerosis using normal and C6 deficient rats showed that the MAC formation mediates much of the pathology [498]. Upon reconstitution of the deficiency with human C6, the observed clinical disease and pathology in the C6 deficient rats became indistinguishable from that of the normal rats. This represents an opportunity to test the therapeutic potential of mAbs 23D1 and 27B1 to inhibit C6 activity. Following induction of disease in C6 deficient rats, when reconstituting the deficiency with human C6, the test mAb could be administered at the same time. If the rats did not develop disease or developed a milder pathology and disease than the relevant control groups, this would demonstrate the therapeutic potential of these mAbs as a proof of principle. Several disease models of multiple sclerosis and Guillan-Barre syndrome have been set up in house and C6 deficient rats and mice are available in house to carry this out.

The field of developing C inhibitors as potential therapies is continuing to expand and as knowledge grows, our understanding of the essential properties of a good inhibitor is also furthered. Despite the advances that have been made here and elsewhere, there are still no inhibitors available that inhibit MAC formation for the therapy of human diseases. The work described in this thesis contributes towards the development of such an inhibitor, demonstrating that it is possible to specifically inhibit MAC formation and helping to elucidate the best approaches to take when initially generating inhibitors. It is also clear from this work that determining the co-associating molecular domains of C5b and C6 that interact with each other and the sequence of events that occur during C5b6 formation will be essential for developing a rational and targeted strategy for inhibiting MAC assembly.

Bibliography

1. Buchner, H. Uber die nahere natur der bakterientoden substanz in blutserum. *Zentralbl Bakteriol* **6**, 561-5 (1889).
2. Ehrlich, P. & Morgenroth, J. Zur theorie der lysinwirkung. *Berlin Klinische Wochenschrift* **36**, 6-9 (1899).
3. Pepys, M. Role of complement in the induction of immunological responses. *Transplant Rev* **32**, 93-120 (1976).
4. Pepys, M., Mirjah, D., Dash, A. & Wansbrough-Jones, M. Immunosuppression by cobra factor: distribution, antigen-induced balst transformation and trapping of lymphocytes during in vivo complement depletion. *Cell Immunol* **21**, 327-36 (1976).
5. Klaus, G. & Humphrey, J. The generation of memory cells. I. The role of C3 in the generation of B memory cells. *Immunology* **33**, 31-40 (1977).
6. Walport, M. Complement First of Two Parts. *N Engl J Med* **344**, 1058-66 (2001).
7. Tranum-Jensen, J. & Bhakdi, S. Freeze-fracture analysis of the membrane lesion of human complement. *J Cell Biol* **97**, 618-26 (1983).
8. Bhakdi, S. & Tranum-Jensen, J. C5b-9 assembly: average binding of one C9 molecule to C5b-8 without poly-C9 formation generates a stable transmembrane pore. *J Immunol* **136**, 2999-3005 (1986).
9. Muller-Eberhard, H. Transmembrane channel-formation by five complement proteins. *Biochem Soc Symp* **50**, 235-46 (1985).
10. Podack, E., Biesecker, G. & Muller-Eberhard, H. Membrane attack complex of complement: generation of high-affinity phospholipid binding sites by fusion of five hydrophilic plasma proteins. *Proc Natl Acad Sci USA* **76**, 897-901 (1979).
11. Podack, E., Tschoop, J. & Muller-Eberhard, H. Molecular organization of C9 within the membrane attack complex of complement. Induction of circular C9 polymerization by the C5b-8 assembly. *J Exp Med* **156**, 268-82 (1982).
12. Tschopp, J., Podack, E. & Muller-Eberhard, H. Ultrastructure of the membrane attack complex of complement: detection of the tetramolecular C9-polymerizing complex C5b-8. *Proc Natl Acad Sci USA* **79**, 7474-8 (1982).
13. Tschopp, J. Ultrastructure of the membrane attack complex of complement. Heterogeneity of the complex caused by differing degrees of C9 polymerization. *J Biol Chem* **259**, 7857-63 (1984).
14. Podack, E. & Tschopp, J. Membrane attack by complement. *Mol Immunol* **21**, 589-603 (1984).
15. Esser, A., Kolb, W., Podack, E. & Muller-Eberhard, H. Molecular reorganisation of lipid bilayers by complement: a possible mechanism for membranolysis. *Proc Natl Acad Sci USA* **76**, 1410-4 (1979).
16. Shin, M., Rus, H. & Niculescu, F. Membrane attack by complement: assembly and biology of terminal complement complexes. in *Biomembranes* (ed. Lee, A.) 119-46 (JAI Press, Greenwich (CT), 1996).
17. Kinoshita, T. Biology of complement: the overture. *Immunol Today* **12**, 291-5 (1991).
18. Hugli, T. Structure and function of the anaphylatoxins. *Springer Semin Immunopathol* **7**, 193-219 (1984).
19. Müller-Eberhard, H. The membrane attack complex of complement. *Annu Rev Immnol* **4**, 503-28 (1986).
20. Hughes-Jones, N., Gorick, B., Miller, N. & Howard, J. IgG pair formation on one antigenic molecule is the main mechanism of synergy between antibodies in complement-mediated lysis. *Eur J Immunol* **14**, 974-8 (1984).

21. Loos, M. The complement system:activation and control. *Curr Topics Microbiol Immunol* **121**, 7-18 (1985).
22. Loos, M. 'Classical' pathway of activation. in *The complement system* (eds. Rother, K. & Till, G.) 136 (Springer, Berlin, 1988).
23. Ziccardi, R. & Cooper, N. The subunit composition and sedimentation properties of human C1. *J Immunol* **118**, 2047-52 (1977).
24. Ziccardi, R. The first component of human complement (C1): activation and control. *Springer Semin Immunopathol* **6**, 213-30 (1983).
25. Porter, R. & Reid, K. Activation of the complement system by antibody-antigen complexes: the classical pathway. *Adv Prot Chem* **33**, 1-71 (1979).
26. Reid, K. Proteins involved in the activation and control of the two pathways of human complement. *Biochem Soc Trans* **11**, 1-12 (1983).
27. Loos, M. & Colomb, M. C1, the first component of complement: structure-function-relationship of C1q and collectins (MBP, SP-A, SP-D, conglutinin), C1-esterases (C1r and C1s), and C1-inhibitor in health and disease. *Behring Institut Mitteilungen* **93**, 1-5 (1993).
28. Reid, K. Activation and control of the complement system. *Essays Biochem* **22**, 27-68 (1986).
29. Reid, K. & Day, A. Structure function relationships of the complement components. *Immunol Today* **10**, 177-80 (1989).
30. Perkins, S., Nealis, A., Sutton, B. & Feinstein, A. Solution structure of human and mouse immunoglobulin M by synchrotron X-ray scattering and molecular graphics modelling. A possible mechanism for complement activation. *J Mol Biol* **221**, 1345-66 (1991).
31. Schumaker, V., Calcott, M., Spiegelberg, H. & Muller-Eberhard, H. Ultracentrifuge studies of the binding of IgG of different subcalsses to the C1q subunit of the first component of complement. *Biochemistry* **15**, 5175-81 (1976).
32. Taylor, P. Non-immunoglobulin activators of the complement system. in *Activators and inhibitors of the complement system* (ed. Sim, R.) 37 (Kluwer, Amsterdam, 1993).
33. Levine, R. & Dodds, A. The thioester bond of C3. *Curr Top Microbiol Immunol* **153**, 73-82 (1990).
34. Arlaud, G., Colomb, M. & Gagnon, J. A functional model of the human C1 complex: Emergence of a functional model. *Immunol Today* **8**, 106-11 (1987).
35. Schumaker, V., Zavodszky, P. & Poon, P. Activation of the first component of complement. *Annu Rev Immnol* **5**, 21-42 (1987).
36. Nagasawa, S. & Stroud, R. Cleavage of C2 by C1s into the antigenically distinct fragments C2a and C2b: demonstration of binding of C2b to C4b. *Proc Natl Acad Sci USA* **74**, 2998-3001 (1977).
37. Morgan, B. & Harris, C. *Complement Regulatory Proteins*, (Academic Press, 1999).
38. Holers, V. Chapter 1: Complement as a regulatory and effector pathway in human diseases. in *Contemporary Immunology: Therapeutic Interventions in the Complement System* (eds. Lambris, J. & Holers, V.) 1-32 (Humana Press Inc, Totawa, NJ).
39. Stover, C. et al. The human gene for mannan-binding-lectin-associated serine protease-2 (MASP-2), the effector component of the lectin route of complement activation, is part of a tightly linked gene cluster on chromosome 1p36.2-3. *Genes Immun* **2**, 119-27 (2001).
40. Presanis, J., Kojima, M. & Sim, R. Biochemistry and genetics of mannan-binding lectin (MBL). *Biochem Soc Trans* **31**, 748-52 (2003).
41. Mullighan, C. et al. Mannose-binding lectin gene polymorphisms are associated with major infection following allogeneic hemopoietic stem cell transplantation. *Blood* **99**, 3524-9 (2002).

42. Law, S. & Levine, R. Interaction between the third complement protein and cell surface macromolecules. *Proc Natl Acad Sci USA* **74**, 2701-5 (1977).
43. Kinoshita, T. et al. C5 convertase of the alternative complement pathway: covalent linkage between two C3b molecules within the trimolecular complex enzyme. *J Immunol* **141**, 3895-901 (1988).
44. Kozono, H. et al. Localization of the covalent C3b-binding site on C4b within the complement classical pathway C5 convertase, C4b2a3b. *J Biol Chem* **265**, 14444-9 (1990).
45. Takata, Y. et al. Covalent association of C3b with C4b within C5 convertase of the classical complement pathway. *J Exp Med* **165**, 1494-507 (1987).
46. Ebanks, R. et al. A single arginine to tryptophan interchange at beta-chain residue 458 of human complement component C4 accounts for the defect in classical pathway C5 convertase activity of allotype C4A6. Implications for the location of a C5 binding site in C4. *J Immunol* **148**, 2803-11 (1992).
47. Law, S. & Dodds, A. C3, C4 and C5: the thioester site. *Biochem Soc Trans* **18**, 1155-9 (1990).
48. Janatova, J. & Tack, B. Fourth component of human complement: studies of an amine-sensitive site comprised of a thiol. component. *Biochemistry* **20**, 2394-402 (1981).
49. Soothil, F. & Harvey, B. Defective opsonization: a common immunity deficiency. *Arch Dis Child* **51**, 91-9 (1976).
50. *Idem.* A defect of the alternative pathway of complement. *Clin Exp Immunol* **27**, 30-3 (1977).
51. Sumiya, M. et al. Molecular basis of opsonic defect in immunodeficient children. *Lancet* **337**(1991).
52. Super, M., Thiel, S., Lu, J., Levinsky, R. & Turner, M. Association of low levels of mannan-binding protein with a common defect in opsonisation. *Lancet* **2**, 1236-9 (1989).
53. Turner, M. Mannose-binding lectin: the pluripotent molecule of the innate immune system. *Immunol Today* **17**, 532-40 (1996).
54. Stahl, P. & Ezekowitz, R. The mannose receptor is a pattern recognition receptor involved in host defense. *Curr Opin Immunol* **10**, 50-5 (1998).
55. Reid, K. & Turner, M. Mammalian lectins in activation and clearance mechanisms involving the complement system. *Springer Sem Immunopathol* **15**, 307-26 (1994).
56. Holmskov, U., Malhotra, R., Sim, R. & Jensenius, J. Collectins: collagenous C-type lectins of the innate immune defense system. *Immunol Today* **15**, 67-74 (1994).
57. Dahl, M. et al. MASP-3 and its association with distinct complexes of the mannan-binding lectin complement activation pathway. *Immunity* **15**, 127-35 (2001).
58. Thiel, S. et al. A second serine protease associated with mannan-binding lectin that activates complement. *Nature* **386**, 506-10 (1997).
59. Sato, T., Endo, Y., Matsushita, M. & Fujita, T. Molecular characterisation of a novel serine protease involved in activation of the complement system by mannose-binding protein. *Int Immunol* **6**, 665-9 (1994).
60. Takada, F., Takayama, Y., Hatsuse, H. & Kawakami, M. A new member of the C1s family of complement proteins found in a bactericidal factor, Ra-reactive factor, in human serum. *Biochem Biophys Res Comm* **196**, 1003-9 (1993).
61. Matsushita, M. & Fujita, T. Activation of the classical complement pathway by mannose-binding protein in association with a novel C1s-like serine protease. *J Exp Med* **176**, 1497-502 (1992).
62. Takahashi, M., Endo, Y., Fujita, T. & Matsushita, M. A truncated form of mannose-binding lectin-associated serine protease (MASP)-2 expressed by alternative

polyadenylation is a component of the lectin complement pathway. *Int Immunol* **11**, 859-63 (1999).

63. Stover, C., Schwaeble, W., Lynch, N., Thiel, S. & Speicher, M. Assignment of the gene encoding mannan-binding-lectin-associated serine protease 2 (MASP2) to human chromosome 1p36.3-p36.2 by *in situ* hybridisation and somatic-cell hybrid analysis. *Cytogenet Cell Genet* **84**, 148-9 (1999).
64. Thiel, S. et al. Interaction of C1q and mannan-binding lectin (MBL) with C1r, C1s, MBL-associated serin proteases 1 and 2, and the MBL-associated protein MAp19. *J Immunol* **165**, 878-87 (2000).
65. Gadjeva, M., Thiel, S. & Jensenius, J. The mannan-binding-lectin pathway of the innate immune response. *Curr Opin Immunol* **13**, 74-8 (2001).
66. Matsushita, M., Thiel, S., Jensenius, J., Terai, I. & Fujita, T. Proteolytic activities of two types of mannose-binding lectin-associated serine protease. *J Immunol* **165**, 2637-42 (2000).
67. Thielens, N. et al. Interaction properties of human mannan-binding lectin (MBL)-associated serine proteases 1 and 2, MBL-associated protein 19 and MBL. *J Immunol* **166**, 5068-77 (2001).
68. Chen, C. & Wallis, R. Stoichiometry of complexes between mannose-binding protein and its associated serine proteases. Defining functional units for complement activation. *J Biol Chem* **276**, 25894-902 (2001).
69. Wallis, R. & Dodd, R. Interaction of mannose-binding protein with associated serine proteases: effects of naturally occurring mutations. *J Biol Chem* **275**, 30962-9 (2000).
70. Matsushita, M. & Fujita, T. Cleavage of the third component of complement (C3) by mannose-binding-protein-associated serine protease (MASP) with subsequent complement activation. *Immunobiology* **194**, 443-8 (1995).
71. Rossi, V. et al. Substrate specificities of recombinant mannan-binding-lectin-associated serine proteases 1 and 2. *J Biol Chem* **276**, 40880-7 (2001).
72. Gotze, O. The alternative pathway of activation. in *The complement system* (eds. Rother, K. & Till, G.) 154 (Springer, Berlin, 1986).
73. Pangburn, M. & Müller-Eberhard, H. The alternative pathway of complement. *Springer Semin Immunopathol* **7**, 163-92 (1984).
74. Lachmann, P. & Hughes-Jones, N. Initiation of complement activation. *Springer Semin Immunopathol* **7**, 143-62 (1984).
75. Pangburn, M. & Muller-Eberhard, H. Relation of putative thioester bond in C3 to activation of the alternative pathway and the binding of C3b to biological targets of complement. *J Exp Med* **152**, 1102-14 (1980).
76. Pangburn, M., Morrison, D., Schreiber, R. & Muller-Eberhard, H. Activation of the alternative pathway: recognition of surface structures of activators by bound C3b. *J Immunol* **124**, 977-82 (1980).
77. Minta, J. & Lepow, I. Studies on the subunit structure of human properdin. *Immunochemistry* **11**, 361-8 (1974).
78. Nolan, K. & Reid, K. Properdin. *Methods Enzymol* **223**, 35-46 (1993).
79. Fearon, D., Daha, M., Weiler, J. & Austen, K. The natural modulation of the amplification phase of complement activation. *Transplant Rev* **32**, 12-25 (1976).
80. Weiler, J., Daha, M., Austen, K. & Fearon, D. Control of the amplification convertase of complement by the plasma protein beta1H. *Proceedings of the National Academy of Sciences of the United States of America* **73**, 3268 (1976).
81. Chakravarti, D., Chakravarti, B., Parra, C. & Muller-Eberhard, H. Structural homology of complement protein C6 with other channel-forming proteins of complement. *Proc Natl Acad Sci USA* **86**, 2799-803 (1989).

82. Morgan, B. Regulation of the complement membrane attack pathway. *Crit Rev Immunol* **19**, 173 - 8 (1999).
83. Thai, C. & Ogata, R. Complement components C5 and C7: recombinant factor I modules of C7 bind to the C345C domain of C5. *J Immunol* **173**, 4547-52 (2004).
84. DiScipio, R., Linton, S. & Rushmere, N. Function of the Factor I Modules (FIMS) of human complement component C6. *J Biol Chem* **274**, 31811-8 (1999).
85. Thai, C. & Ogata, R. Recombinant C345C and Factor I modules of complement components C5 and C7 inhibit C7 incorporation into the complement membrane attack complex. *J Immunol* **174**, 6227-32 (2005).
86. Preissner, K., Podack, E. & Muller-Eberhard, H. The membrane attack complex of complement: relation of C7 to the metastable membrane binding site of the intermediate complex C5b-7. *J Immunol* **135**, 445-51 (1985).
87. Podack, E., Kolb, W. & Muller-Eberhard, H. The C5b-9 complex: subunit composition of the classical and alternative pathway-generated complex. *J Immunol* **116**, 1431-4 (1976).
88. Tschopp, J. & Podack, E. Membranolysis by the ninth component of human complement. *Biochem Biophys Res Comm* **100**, 1409-14 (1981).
89. Bhakdi, S. et al. Relative inefficiency of terminal complement activation. *J Immunol* **141**, 3117-22 (1988).
90. Tamura, N., Shimada, A. & Chang, S. Further evidence for immune cytolysis by antibody and the first eight components of complement. *Immunology* **22**, 131-40 (1972).
91. Scibek, J., Plumb, M. & Sodetz, J. Binding of human complement C8 to C9: role of the N-terminal modules in the C8 alpha subunit. *Biochemistry* **41**, 14546-51 (2002).
92. Dankert, J., Shiver, J. & Esser, A. Ninth component of complement: self-aggregation and interaction with lipids. *Biochemistry* **24**, 2754-62 (1985).
93. Sims, P. Permeability characteristics of complement-damaged membranes: evaluation of the membrane leak generated by the complement proteins C5b-9. *Proc Natl Acad Sci USA* **78**, 1838-42 (1981).
94. Esser, A. Big MAC attack: complement proteins cause leaky patches. *Immunol Today* **12**, 316-20 (1991).
95. Ramm, L., Whitlow, M. & Mayer, M. Transmembrane channel formation by complement: functional analysis of the number of C5b6, C7, C8 and C9 molecules required for a single channel. *Proc Natl Acad Sci USA* **79**, 4751-5 (1982).
96. Benz, R., Schmid, A., Wiedmer, T. & Sims, P. Single channel analysis of the conductance fluctuations induced in lipid bilayer membranes by complement proteins C5b-9. *J Membr Biol* **94**, 37-45 (1986).
97. Wiedmer, T. & Sims, P. Cyanine dye fluorescence used to measure membrane potential changes due to the assembly of complement proteins C5b-9. *J Membr Biol* **84**, 249-58 (1985).
98. Morgan, B., Dankert, J. & Esser, A. Recovery of human neutrophils from complement attack: removal of the membrane attack complex by endocytosis and exocytosis. *J Immunol* **138**, 246-53 (1987).
99. Morgan, B. Complement membrane attack on nucleated cells: resistance, recovery, and non-lethal effects. *Biochem J* **264**, 1-14 (1989).
100. Morgan, B. Effects of the membrane attack complex of complement on nucleated cells. *Curr Top Microbiol Immunol* **178**, 115-40 (1992).
101. Carney, D., Koski, C. & Shin, M. Elimination of terminal complement intermediates from the plasma membrane of nucleated cells: the rate of disappearance differs for cells carring C5b-7 or C5b-8 or a mixture of C5b-8 with a limited number of C5b-9. *J Immunol* **134**, 1804-9 (1985).

102. Carney, D., Hammer, C. & Shin, M. Elimination of terminal complement complexes in the plasma membrane of nucleated cells: influence of extracellular Ca2+ and association with cellular Ca2+. *J Immunol* **137**, 263-70 (1986).
103. Scolding, N. et al. Vesicular removal by oligodendrocytes of membrane attack complexes formed by activated complement. *Nature* **339**, 620-2 (1989).
104. Morgan, B. & Campbell, A. The recovery of human polymorphonuclear leucocytes from sublytic complement attack is mediated by changes in intracellular free calcium. *Biochem J* **231**, 205-8 (1985).
105. Campbell, A. & Morgan, B. Monoclonal antibodies demonstrate protection of polymorphonuclear leukocytes against complement. attack. *Nature* **317**, 164-6 (1985).
106. Morgan, B. Mechanisms of tissue damage by the membrane attack complex of complement. *Comp Inflamm* **6**, 104-11 (1989).
107. Morgan, B. Clinical complmentology: recent progress and future trends. *Eur J Clin Invest* **24**, 219-28 (1994).
108. Kilgore, K. et al. Sublytic concentration of the membrane attack complex of complement induce endothelial interleukin-8 and monocyte chemoattractant protein-1 through nuclear factor-kappaB activation. *Am J Pathol* **150**, 2019-31 (1997).
109. Niculescu, F., Rus, H. & Shin, M. Receptor-independent activation of guanine nucleotide-binding regulatory proteins by terminal complement complexes. *J Biol Chem* **269**, 4417-23 (1994).
110. Niculescu, F., Rus, H., van Biesen, T. & Shin, M. Activation of Ras and mitogen-activated protein kinase pathway by terminal complement complexes is G protein dependent. *J Immunol* **158**, 4405-12 (1997).
111. Niculescu, F., Badea, T. & Rus, H. Sublytic C5b-9 induces proliferation of aortic smooth muscle cells. Role of mitogen activated protein kinase and phophatidylinositol 3-kinase. *Atherosclerosis* **142**, 47-56 (1999).
112. Rus, H., Niculescu, F. & Shin, M. Sublytic complement attack induces cell cycle in oligodendrocytes. *J Immunol* **156**, 4892-900 (1996).
113. Rus, H., Niculescu, F., Badea, T. & Shin, M. Terminal complement complexes induce cell cycle entry in oligodendrocytes through mitogen activated protein kinase pathway. *Immunopharmacol* **38**, 177-87 (1997).
114. McGreal, E. & Gasque, P. Structure-function studies of the receptors for complement C1q. *Biochem Soc Trans* **30**, 1010-4 (2002).
115. Andrews, B., Shadforth, M., Cunningham, P. & Davis, J. Demonstration of a C1q receptor on the surface of human endothelial cells. *J Immunol* **127**, 1075-80 (1981).
116. Arvieux, J., Reboul, A., Bensa, J. & Colomb, M. Characterisation of the C1q receptor on a human macrophage cell line U937. *Biochem J* **218**, 547-55 (1984).
117. Dickler, H. & Kunkel, H. Interaction of aggregated gamma-globulin with B lymphocytes. *J Exp Med* **136**, 191-6 (1972).
118. Ghebrehiwet, B. & Hamburger, M. Purification and partial characterization of a C1q inhibitor from the membranes of human peripheral blood lymphocytes. *J Immunol* **129**, 157-62 (1982).
119. Ghebrehiwet, B., Silvestri, L. & McDevitt. Identification fo the Raji cell membrane-derived C1q inhibitor as a receptor for human C1q: Purification and immunochemical characterization. *J Exp Med* **160**, 1375-89 (1984).
120. Ghebrehiwet, B. Functions associated with the C1q receptor. *Behring Institut Mitteilungen* **84**, 204-15 (1989).
121. Tenner, A. & Cooper, N. Identification of types of cells in human peripheral blood that bind C1q. *J Immunol* **126**, 1174-9 (1981).

122. Guan, E. et al. Phagocytic cell molecules that bind the collagen-like region of C1q. Involvement in the C1q-mediated enhancement of phagocytosis. *J Biol Chem* **266**, 20345-55 (1991).
123. Ghebrehiwet, B., Lim, B., Peerschke, E., Willis, A. & Reid, K. Isolation, cDNA cloning, and overexpression of a 33-kD cell surface glycoprotein that binds to the globular "heads" of C1q. *J Exp Med* **179**, 1809-21 (1994).
124. Krainer, A., Conway, G. & Kozak, D. The essential pre-mRNA slicing factor SF2 influences 5' splice site selection by activating proximal sites. *Cell* **62**, 35-42 (1990).
125. Klickstein, L., Barbashov, S., Liu, T., Jack, R. & Nicholson-Weller, A. Complement receptor type 1 (CR1, CD35) is a receptor for C1q. *Immunity* **7**, 345-55 (1997).
126. Sim, R. & Malhotra, R. Interactions of carbohydrates and lectins with complement. *Biochem Soc Trans* **22**, 106-11 (1994).
127. McGreal, E., Ikewaki, N., Akatsu, H., Morgan, B. & Gasque, P. Human C1qRp is identical with CD93 and the mNI-11 antigen but does not bind C1q. *J Immunol* **168**, 5222-32 (2002).
128. Fonseca, M. et al. C1qR(P), a myeloid cell receptor in blood, is predominantly expressed on endothelial cells in human tissue. *J Leukoc Biol* **70**, 793-800 (2001).
129. Peerschke, E., Reid, K. & Ghebrehiwet, B. Identification of a novel 33 kDa C1q-binding site on human platelets. *J Immunol* **152**, 5896-901 (1994).
130. Eggleton, P. et al. Identification of a gC1q-binding protein (gC1q-R) on the surface of human neutrophils. Subcellular localisation and binding properties in comparison with the cC1q-R. *J Clin Invest* **95**, 1569-78 (1995).
131. Narayanan, A., Lurton, J. & Raghu, G. Distribution of receptors of collagen and globular domains of C1q in human lung fibroblasts. *Am J Respir Cell Mol Biol* **17**, 84-90 (1997).
132. Herwald, H., Dedio, J., Kellner, R., Loos, M. & Mueller-Esterl, W. Isolation and characterization of the kininogen-binding protein p33 from endothelial cells. Identity with the gC1q receptor. *J Biol Chem* **271**, 13040-7 (1996).
133. Peerschke, E. & Ghebrehiwet, B. Platelet membrane receptors for the complement component C1q. *Semin Hematol* **31**, 320-8 (1994).
134. van Den Berg, R. et al. Intracellular localization of the human receptor for the globular domains of C1q. *J Immunol* **158**, 3909-3916 (1997).
135. Dedio, J., Jahnen-Dechent, W., Bachmann, M. & Muller-Esterl, W. The multiligand-binding protein gC1q-R putative C1q receptor is a mitochondria protein. *J Immunol* **160**, 3534-42 (1998).
136. Furlong, S. et al. C3 activation is inhibited by analogs of compstatin but not by serine protease inhibitors or peptidyl alpha-ketoheterocycles. *Immunopharmacology* **48**, 199-212 (2000).
137. Ghiran, I. et al. Complement receptor 1/CD35 is a receptor for mannan-binding lectin. *J Exp Med* **192**, 1797-808 (2000).
138. Fearon, D. & Wong, W. Complement ligand-receptor interactions that mediate biological responses. *Annu Rev Immunol* **1**, 243-71 (1983).
139. Fearon, D. et al. Immunoregulatory functions of complement: structural and functional studies of complement receptor type 1 (CR1; CD35) and type 2 (CR2; CD21). *Prog Clin Biol Res* **297**, 211-20 (1989).
140. Fearon, D. & Carter, R. The CD19/CR2/TAPA-1 complex of B lymphocytes: linking natural to acquired immunity. *Ann Rev Immunol* **13**, 127-49 (1995).
141. Anderson, D., Miller, L., Schmalstieg, F., Rothlein, R. & Springer, T. Contributions of the Mac-1 glycoprotein family to adherence-dependent granulocyte functions: structure-function assessments employing subunit-specific monoclonal antibodies. *J Immunol* **137**, 15-27 (1986).

142. Corbi, A., Kishimoto, T., Miller, L. & Springer, T. The human leukocyte adhesion glycoprotein Mac-1 (complement receptor type 3, CD11b) alpha subunit. Cloning, primary structure, and relation to the integrins, von Willebrand factor and factor B. *J Biol Chem* **263**, 12403-11 (1988).
143. Larson, R. & Springer, T. Structure and function of leukocyte integrins. *Immunol Rev* **114**, 181-217 (1990).
144. Rothlein, R. & Springer, T. Complement receptor type three-dependent degradation of opsonized erythrocytes by mouse macrophages. *J Immunol* **135**, 2668-72 (1985).
145. Ames, R. et al. Molecular cloning and characterization of the human anaphylatoxin C3a receptor. *J Biol Chem* **271**, 20231-4 (1996).
146. Gerard, N. & Gerard, C. The chemotactic receptor for human C5a anaphylatoxin. *Nature* **349**, 614-7 (1991).
147. Ross, S. & Densen, P. Complement deficiency states and infection: Epidemiology, pathogenesis and consequences of neisserial and other infections in an immune deficiency. *Medicine* **63**, 243-73 (1984).
148. Arnaout, M., Spits, H., Terhorst, C., Pitt, J. & Todd, R.I. Deficiency of a leukocyte surface glycoprotein (LFA-1) in two patients with Mo1 deficiency. Effects of cell activation on Mo1/LFA-1 surface expression in normal and deficient leukocytes. *J Clin Invest* **74**, 1291-300 (1984).
149. Fearon, D. & Collins, L. Increased expression of C3b receptors on polymorphonuclear leukocytes induced by chemotactic factors and by purification procedures. *J Immunol* **130**, 370-5 (1983).
150. Campbell, R., Law, S., Reid, K. & Sim, R. Structure, organization, and regulation of the complement genes. *Ann Rev Immunol* **6**, 161-95 (1988).
151. Ahearn, J. & Fearon, D. Structure and function of the complement receptors, CR1 (CD35) and CR2 (CD21). *Adv Immunol* **46**, 183-219 (1989).
152. Janatova, J., Reid, K. & Willis, A. Disulfide bonds are localized within the short consensus repeat units of complement regulatory proteins: C4b-binding protein. *Biochemistry* **28**, 4754-61 (1989).
153. Hourcade, D., Holers, V. & Atkinson, J. The regulators of complement activation (RCA) gene cluster. *Adv Immunol* **45**, 381-416 (1989).
154. Ziccardi, R. A new role for C-1-inhibitor in homeostasis: control of activation of the first component of human complement. *J Immunol* **128**, 2505-8 (1982).
155. Ziccardi, R. Demonstration of the interaction of native C1 with monomeric immunoglobulins and C1 inhibitor. *J Immunol* **134**, 2559-63 (1985).
156. Perkins, S. Hydrodynamic data show that C1- inhibitor of complement forms compact complexes with C1-r and C1-s. *FEBS Letts* **271**, 89-92 (1990).
157. Chesne, S., Villiers, C., Arlaud, G., Lacroix, M. & Columb, M. Fluid-phase interaction of C1 inhibitor (C1 Inh) and the subcomponents C1r and C1s of the first component of complement, C1. *Biochem J* **201**, 61-70 (1982).
158. Ziccardi, R. & Cooper, N. Active disassembly of the first complement component C-1, by C-1 inactivator. *J Immunol* **123**, 788-92 (1979).
159. Sim, R., Arlaud, G. & Colomb, M. C1 inhibitor-dependent dissociation of human complement component C1 bound to immune complexes. *Biochem J* **179**, 449-57 (1979).
160. Tenner, A. & Frank, M. Activator-bound C1 is less susceptible to inactivation by C1 inhibition than is fluid-phase C1. *J Immunol* **137**, 625-30 (1986).
161. Vik, D., Munoz-Canoves, P., Chaplin, D. & Tack, B. Factor H. *Curr Top Microbiol Immunol* **153**, 147-62 (1990).

162. Harrison, R. & Lachmann, P. Novel cleavage products of the third component of human complement. *Mol Immunol* **17**, 219-28 (1980).
163. Seya, T. et al. Human factor H and C4b-binding protein serve as factor I-cofactors both encompassing inactivation of C3b and C4b. *Mol Immunol* **32**, 355-60 (1995).
164. Hessing, M. The interaction between complement component C4b-binding protein and the bitamin K-dependent protein S forms a link between blood coagulation and the complement system. *Biochem J* **277**, 581-92 (1991).
165. Gigli, I., Fujita, T. & Nussenzweig, V. Modulation of the classical pathway C3 convertase by the plasma proteins C4 binding protein and C3b inactivator. *Proc Natl Acad Sci USA* **76**, 6596-600 (1979).
166. Pangburn, M. Differences between the binding sites of the complement regulatory proteins DAF, CR1 and factor H on C3 convertases. *J Immunol* **136**, 2216-21 (1986).
167. Seya, T., Turner, J. & Atkinson, J. Purification and characterisation of a membrane protein (gp45-70) that is a cofactor for cleavage of C3b and C4b. *J Exp Med* **163**, 837-55 (1986).
168. Seya, T. & Atkinson, J. Functional properties of membrane cofactor protein of complement. *Biochem J* **264**, 581-8 (1989).
169. Lublin, D. et al. Molecular cloning and chromosomal localization of human membrane cofactor protein (MCP). Evidence for inclusion in the multigene family of complement-regulatory proteins. *J Exp Med* **168**, 181-94 (1988).
170. McLaughlin, P. et al. Soluble CD46 (membrane cofactor protein, MCP) in human reproductive tract fluids. *J Reprod Immunol* **31**, 209-19 (1996).
171. Seya, T. et al. Purification and functional properties of soluble forms of membrane cofactor protein (CD46) of complement: identification of forms increased in cancer patients' sera. *Int Immunol* **7**, 727-36 (1995).
172. Riley, R., Tannenbaum, P., Abbot, D. & Atkinson, J. Cutting edge: inhibiting measles virus infection but promoting reproduction: an explanation for splicing and tissue-specific expression of CD46. *J Immunol* **169**, 5405-9 (2002).
173. Chowdhury, N. et al. Complement-inhibiting activity of human seminal plasma and semen quality. *Arch Androl* **36**, 109-18 (1996).
174. Feninchel, P. et al. Localization and characterization of the acrosomal antigent recognized by GB24 on human spermatozoa. *Mol Reprod Dev* **27**, 173-8 (1990).
175. Anderson, D., Abbott, A. & Jack, R. The role of complement component C3b and its receptors in sperm-oocyte interaction. *Proc Natl Acad Sci USA* **90**, 10051-5 (1993).
176. Kinoshita, T., Medof, M., Hong, K. & Nussenzweig, V. Membrane-bound C4b interacts endogenously with complement receptor CR1 of human red cells. *J Exp Med* **164**, 1377-88 (1986).
177. Iida, K. & Nussenzweig, V. Complement receptor is an inhibitor of the complement cascade. *J Exp Med* **153**, 1138-50 (1981).
178. Ross, G., Lambris, J., Cain, J. & Newman, S. Generation of three different fragments of bound C3 with purified factor I or serum. I. Requirements for factor H vs CR1 cofactor activity. *J Immunol* **129**, 2051-60 (1982).
179. Medof, M., Iida, K., Mold, C. & Nussenzweig, V. Unique role of the complement receptor CR1 in the degradation of C3b associated with immune complexes. *J Exp Med* **156**, 1739-54 (1982).
180. Medicus, R., Melamed, J. & Arnaout, M. Role of human factor I and C3b receptor in the cleavage of surface-bound C3bi molecules. *Eur J Immunol* **13**, 465-70 (1983).
181. Medof, M. et al. Cloning and characterization of cDNAs encoding the complete sequence of decay-accelerating factor of human complement. *Proc Natl Acad Sci USA* **84**, 2007-11 (1987).

182. Moran, P. & Caras, I. A nonfunctional sequence converted to a signal for glycophosphatidylinositol membrane anchor attachment. *J Cell Biol* **115**, 329-36 (1991).
183. Medof, M., Kinoshita, T. & Nussenzweig, V. Inhibition of complement activation on the surface of cells after incorporation of decay-accelerating factor (DAF) into their membranes. *J Exp Med* **160**, 1558-78 (1984).
184. Fujita, T., Inoue, T., Ogawa, K., Iida, K. & Tamura, N. The mechanism of action of decay-accelerating factor (DAF). DAF inhibits the assembly of C3 convertases by dissociating C2a and Bb. *J Exp Med* **166**, 1221-8 (1987).
185. Nicholson-Weller, A., Burge, J., Fearon, D., Weller, P. & Austen, K. Isolation of a human erythrocyte membrane glycoprotein with decay-accelerating activity for C3 convertases of the complement system. *J Immunol* **129**, 184-9 (1982).
186. Levin, Y., Skidgel, R. & Erdos, E. Isolation and characterization of the subunits of plasma carboxypeptidase N (kininase 1). *Proc Natl Acad Sci USA* **79**, 4618-23 (1982).
187. Matthews, K., Mueller-Ortiz, S. & Wetsel, R. Carboxypeptidase N: a pleiotropic regulator of inflammation. *Mol Immunol* **40**, 785-93 (2004).
188. Plummer, T. & Hurwitz, M. Human plasma carboxypeptidase N. Isolation and characterization. *J Biol Chem* **253**, 3907-11 (1978).
189. Bokisch, V. & Muller-Eberhard, H. Anaphylatoxin inactivator of human plasma: its isolation and characterization as a carboxypeptidase. *J Clin Invest* **49**, 2427-32 (1970).
190. Burgi, B., Brunner, T. & Dahinden, C. The degradation product of the C5a anaphylatoxin C5adesArg retains basophil-activating properties. *Eur J Immunol* **24**, 1583-9 (1994).
191. Nemerow, G., Yamamoto, K. & Lint, T. Restriction of complement-mediated membrane damage by the eigth component of complement: a dual role for C8 in the complement attack sequence. *J Immunol* **123**, 1245-52 (1979).
192. Kolb, W. & Muller-Eberhard, H. The membrane attack complex of complement: isolation and subunit composition of the C5b-9 complex. *J Exp Med* **141**, 724-35 (1975).
193. Podack, E. & Muller-Eberhard, H. Isolation of human S-protein, an inhibitor of the membrane attack complex of complement. *J Biol Chem* **254**, 9808-14 (1979).
194. Barnes, D., Silnutzer, J., See, C. & Shaffer, M. Characterization of human serum spreading factor with monoclonal antibody. *Proc Natl Acad Sci USA* **80**, 1362-6 (1983).
195. Barnes, D. & Silnutzer, J. Isolation of human serum spreading factor. *J Biol Chem* **258**, 12548-52 (1983).
196. Suzuki, S., Oldberg, A., Hayman, E., Pierschbacher, M. & Ruoslahti, E. Complete amino acid sequence of human vitronectin deduced from cDNA. Similarity of cell attachment sites in vitronectin and fibronectin. *EMBO J* **4**, 2519-24 (1985).
197. Jenne, D. & Stanley, K. Molecular cloning of S-protein, a link between complement, coagulation, and cell-substrate adhesion. *EMBO J* **4**, 3153-7 (1985).
198. Hayman, E., Pierschbacher, M., Ohgren, Y. & Ruoslahti, E. Serum spreading factor (vitronectin) is present at the cell surface and in tissues. *Proc Natl Acad Sci USA* **80**, 4003-7 (1983).
199. Podack, E. & Muller-Eberhard, H. Binding of desoxycholate, phophatidylcholine vesicles, lipoprotein, and of the S-protein to complexes of terminal complement components. *J Immunol* **121**, 1025-30 (1978).
200. Podack, E., Preissner, K. & Muller-Eberhard, H. Inhibition of C9 polymerization within the SC5b-9 complex of complement by S-protein. *Acta Pathologica, Microbiologica, et Immunologica Scandinavica Supplement* **284**, 89-96 (1984).
201. Preissner, K., Podack, E. & Muller-Eberhard, H. SC5b-7, SC5b-8, and SC5b-9 complexes of complement: ultrastructure and localization of the S-protein (vitronectin) within the macromolecules. *Eur J Immunol* **19**, 69-75 (1989).

202. Ware, C., Wetsel, R. & Kolb, W. Physicochemical characterization of fluid phase (SC5b-9) and membrane derived (MC5b-9) attack complexes of human complement purified by immunoadsorbent affinity chromatography or selective detergent extraction. *Mol Immunol* **18**, 521-31 (1981).
203. Ware, C. & Kolb, W. Assembly of the functional membrane attack complex of human complement: formation of disulfide-linked C9 dimers. *Proc Natl Acad Sci USA* **78**, 6426-30 (1981).
204. Falk, R. et al. Neoantigen of the polymerized ninth component of complement. Characterization of a monoclonal antibody and immunohistochemical localization in renal disease. *J Clin Invest* **72**, 560-73 (1983).
205. Mollnes, T., Lea, T. & Harboe, M. Detection and quantification of the terminal CSb-9 complex of human complement by a sensitive enzyme-linked immunosorbent assay. *Scand J Immunol* **20**, 157-66 (1984).
206. Tschopp, J., Masson, D., Schafer, S., Peitsch, M. & Preissner, K. The heparin binding domain of S-protein/vitronectin binds to complement components C7, C8 and C9 and perforin from cytolytic T-cells and inhibits their lytic activities. *Biochemistry* **27**, 4103-9 (1988).
207. Hayman, E., Pierschbacher, M., Suzuki, S. & Ruoslahti, E. Vitronectin - a major cell attachment-promoting protein in fetal bovine serum. *Exper Cell Res* **160**, 245-58 (1985).
208. Pierschbacher, M., Hayman, E. & Ruoslahti, E. The cell attachment determinant in fibronectin. *J Cell Biochem* **28**, 115-26 (1985).
209. Gebb, C., Hayman, E., Engvall, E. & Ruoslahti, E. Interaction of vitronectin with collagen. *J Biol Chem* **261**, 16698-703 (1986).
210. Hogasen, K., Mollnes, T., Tschopp, J. & Harboe, M. Quantitation of vitronectin and clusterin. Pitfalls and solutions in enzyme immunoassays for adhesive proteins. *J Immunol Methods* **160**, 107-15 (1993).
211. Tsuruta, J., Wong, K., Fritz, I. & Griswold, M. Structural analysis of sulphated glycoprotein 2 from amino acid sequence. Relationship to clusterin and serum protein 40, 40. *Biochem J* **268**, 571-8 (1990).
212. Murphy, B. et al. SP-40,40 is an inhibitor of C5b-6-initiated haemolysis. *Int Immunol* **1**, 551-4 (1989).
213. Choi, N., Nakano, Y., Tobe, T., Mazda, T. & Tomita, M. Incorporation of SP-40,40 into the soluble membrane attack complex (SMAC, SC5b-9) of complement. *Int Immunol* **2**, 413-7 (1990).
214. Rosenberg, M. & Silkensen, J. Clusterin: physiologic and pathophysiologic considerations. *Int J Biochem Cell Biol* **27**, 633-45 (1995).
215. Silkensen, J., Schwochau, G. & Rosenberg, M. The role of clusterin in tissue injury. *Biochem Cell Biol* **72**, 483-8 (1994).
216. Ahuja, H., Tenniswood, M., Lockshin, R. & Zakeri, Z. Expression of clusterin in cell differentiation and cell death. *Biochem Cell Biol* **72**(1994).
217. Rosenberg, M., Manivel, J., Carone, F. & Kanwar, Y. Genesis of renal cysts is associated with clusterin expression in experimental cystic disease. *J Am Soc Nephrol* **5**, 1669-74 (1995).
218. Jenne, D. et al. Clusterin (complement lysis inhibitor) forms a high density lipoprotein complex with apolipoprotein A-I in human plasma. *J Biol Chem* **266**, 11030-6 (1991).
219. O'Bryan, M. et al. Human seminal clusterin (SP-40,40). Isolation and characterization. *J Clin Invest* **85**, 1477-86 (1990).
220. O'Bryan, M., Murphy, B., Liu, D., Clarke, G. & Baker, H. The use of anticlusterin monoclonal antibodies for the combined assessment of human sperm morphology and acrosome integrity. *Human Reproduction* **9**, 1490-6 (1994).

221. Sugita, Y., Nakano, Y. & Tomita, M. Isolation from human erythrocytes of a new membrane protein which inhibits the formation of complement transmembrane channels. *J Biochem* **104**, 633-7 (1988).
222. Holguin, M., Frederick, L., Bernshaw, N., Wilcox, L. & Parker, C. Isolation and characterization of a membrane protein from normal human erythrocytes that inhibits reactive lysis of the erythroxytes of paroxysmal nocturnal hemoglobinuria. *J Clin Invest* **84**, 7-17 (1989).
223. Okada, N., Harada, R., Fujita, T. & Okada, H. Monoclonal antibodies capable of causing hemolysis of neurmainidase-treated human erythrocytes by homologous complement. *J Immunol* **143**, 2262-6 (1989).
224. Okada, H. et al. 20 kDa homologous restriction factor of complement resembles T cell activating protein. *Biochem Biophys Res Comm* **162**, 1553-9 (1989).
225. Davies, A. et al. CD59, an LY-6-like protein expressed in human lymphoid cells, regulates the action of the complement membrane attack complex on homologous cells. *J Exp Med* **170**, 637-54 (1989).
226. Stefanova, I. et al. Characterization of a broadly expressed human leucocye surface antigen MEM-43 anchored in membrane through phosphatidylinositol. *Mol Immunol* **26**, 153-61 (1989).
227. Nose, M., Katoh, M., Okada, N., Kyogoku, M. & Okada, H. Tissue distribution of HRF20, a novel factor preventing the membrane attack of homologous complement, and its predominant expression on endothelial cells *in vivo*. *Immunology* **70**, 145-9 (1990).
228. Meri, S., Waldmann, H. & Lachmann, P. Distribution of protectin (CD59), a complement membrane attack inhibitor, in normal human tissues. *Lab Invest* **65**, 532-7 (1991).
229. Meri, S. et al. Human protectin (CD59), an 18,000-20,000 MW complement lysis restricting factor, inhibits C5b-8 catalysed insertion of C9 into lipid bilayers. *Immunology* **71**, 1-9 (1990).
230. Rollins, S. & Sims, P. The complement-inhibitory activity of CD59 resides in its capacity to block incorporation of C9 into membrane C5b-9. *J Immunol* **144**, 3478-83 (1990).
231. Ninomiya, H. & Sims, P. The human complement regulatory protein CD59 binds to the alpha-chain of C8 and to the "b" domain of C9. *J Biol Chem* **267**, 13675-80 (1992).
232. Hughes, T., Piddlesden, S., Williams, J., Harrison, R. & Morgan, B. Isolation and characterization of a membrane protein from rat erythrocytes which inhibits lysis by the membrane attack complex of rat complement. *Biochem J* **284**, 169-76 (1992).
233. Powell, M., Marchbank, K., Rushmere, N., van den Berg, C. & Morgan, B. Molecular cloning, chromosomal localization, expression, and functional characterization of the mouse analogue of human CD59. *J Immunol* **158**, 1692-702 (1997).
234. Hinchcliffe, S., Rushmere, N., Hanna, S. & Morgan, B. Molecular cloning and functional characterization of the pig analog of CD59. *J Immunol* **160**, 3924-33 (1998).
235. van den Berg, C. & Morgan, B. Complement-inhibiting activities of human CD59 and analogues from rat, sheep, and pig are not homologously restricted. *J Immunol* **152**, 4095-101 (1994).
236. Rother, R. et al. Inhibition of complement-mediated cytolysis by the terminal complement inhibitor of herpesvirus saimiri. *J Virol* **68**, 730-7 (1994).
237. Fodor, W. et al. Primate terminal complement inhibitor homologues of human CD59. *Immunogenetics* **41**, 51 (1995).
238. Colten, H. & Rosen, F. Complement deficiencies. *Ann Rev Immunol* **10**, 809-34 (1992).
239. Figueroa, J., Andreoni, J. & Densen, P. Complement deficiency states and meningococcal disease. *Immunol Res* **12**, 295-311 (1993).
240. Morgan, B. & Walport, M. Complement deficiencies and disease. *Immunol Today* **12**, 301-6 (1991).

241. Lachmann, P. & Walport, M. in *Autoimmunity and Autoimmune Disease* (ed. J, W.) 149-171 (John Wiley and Sons, 1987).
242. Morgan, B. & Harris, C. The complement system: a brief overview. in *Complement Regulatory Proteins* 1-31 (Academic Press, London, 1999).
243. Dragon-Durey, M. et al. Heterozygous and homozygous factor h deficiencies associated with haemolytic uremic syndrome or membranoproliferative glomerulonephritis: report and genetic analysis of 16 cases. *J Am Soc Nephrol* **15**, 787-95 (2004).
244. Lachmann, P. Inherited complement deficiencies. *Philos Trans R Soc Lond B Biol Sci* **306**, 419-30 (1984).
245. Morgan, B. *Complement: Clinical Aspects and relevance to disease.*, (Academic Press Limited, 1990).
246. Stoiber, H., Speth, C. & Dierich, M. Role of complement in the control of HIV dynamics and pathogenesis. *Vaccine* **21**, S77-82 (2003).
247. Loenen, W., Bruggemann, C. & Wierz, E. Immune evasion by human cytomegalovirus: lessons in immunology and cell biology. *Semin Immunol* **13**, 41-9 (2001).
248. Spiller, O. et al. Complement regulation by Kaposi's sarcoma-associated herpesviurs ORF4 protein. *J Virol* **77**, 592-9 (2003).
249. Spiller, O., Blackbourn, D., Mark, L., Proctor, D. & Blom, A. Functional activity of the complement regulator encoded by Kaposi's sarcoma-associated herpesvirus. *J Biol Chem* **278**, 9283-9 (2003).
250. Blue, C., Spiller, O. & Blackbourn, D. The relevance of complement to virus biology. *Virology* **319**, 176-84 (2004).
251. Morgan, B. & Harris, C. Complement therapeutics; history and current progress. *Mol Immunol* **40**, 159-70 (2003).
252. Louie, S., Park, B. & Yoon, H. Biological response modifiers in the management of rheumatoid arthritis. *Am J Health System Pharm* **60**, 346-55 (2003).
253. Morgan, B. Physiology and pathophysiology of complement: progress and trends. *Critical reviews in Clin Lab Sci* **32**, 265-75 (1995).
254. Brodeur, J., Ruddy, S., Schwartz, L. & Moxley, G. Synovial fluid levels of complement SC5b-9 and fragment Bb are elevated in patients with rheumatoid arthritis. *Arthritis Rheum* **34**, 1531-7 (1991).
255. Mollnes, T. et al. Complement activation in rheumatoid arthritis evaluated by C3dg and the terminal complement complex. *Arthritis Rheum* **29**, 715-21 (1986).
256. Oleesky, D., Daniels, R., Williams, B., Amos, N. & Morgan, B. Terminal complement complexes and C1/C1 inhibitor complexes in rheumatoid arthritis and other arthritic conditions. *Clin Exp Immunol* **84**, 250-5 (1991).
257. Perrin, L., Nydegger, U., Zubler, R., Lambert, P. & Miescher, P. Correlation between levels of breakdown products of C3, C4 and properdin factor B in synovial fluids from patients with rheumatoid arthritis. *Arthritis Rheum* **20**, 647-52 (1977).
258. Kemp, P. et al. Immunohistochemical determination of complement activation in joint tissues of patients with rheumatoid arthritis and osteoarthritis using neo-antigen specific monoclonal antibodies. *J Clin Lab Immunol* **37**, 147-62 (1992).
259. Sanders, M. et al. Membrane attack complex of complement in rheumatoid synovial tissue demonstrated by immunofluorescent microscopy. *J Rheumatol* **13**, 1028-34 (1986).
260. Owens, T. The enigma of multiple sclerosis: inflammation and neurodegeneration cause heterogeneous dysfunction and damage. *Curr Opin Neurol* **16**, 259-65 (2003).
261. Martino, G. et al. Inflammation in multiple sclerosis: the good, the bad and the complex. *Lancet Neurol* **1**, 499-509 (2002).

262. Kirklin, J. The postperfusion syndrome: Inflammation and the damaging effects of cardiopulmonary bypass. in *Cardiopulmonary Bypass: Current Concepts and Controversies* (ed. Tinker, J.) 131 (Saunders, Philadelphia, PA, 1989).
263. Kirklin, J. & Kirklin, J. Cardiopulmonary bypass for cardiac surgery. in *Surgery of the chest* (eds. Sabiston, D.J. & Speicher, F.) 1107-1125 (Saunders, WB, Philadelphia, 1990).
264. Elgebaly, S. et al. Evidence of cardiac inflammation after open heart operations. *Ann Thorac Surg* **57**, 391-6 (1994).
265. Cremer, J. et al. Systemic inflammatory response after cardiac operations. *Ann Thorac Surg* **61**, 1714-20 (1996).
266. Westaby, S. Organ dysfunction after cardiopulmonary bypass. A systemic inflammatory reaction initiated by extracorporeal circuit. *Intensive Care Med* **13**, 89-95 (1987).
267. Kirklin, J. et al. Complement and the damaging effects of cardiopulmonary bypass. *J Thorac Cardiovasc Surg* **86**, 845-57 (1983).
268. Sims, P. & Wiedmer, T. The response of human platelets to activated components of the complement system. *Immunol Today* **12**, 338-42 (1991).
269. Chenoweth, D. et al. Complement activation during cardiopulmonary bypass: evidence for generation of C3a and C5a anaphylatoxins. *N Engl J Med* **304**, 497-503 (1981).
270. Jansen, N. et al. Endotoxin release and tumour necrosis factor formation during cardiopulmonary bypass. *Ann Thorac Surg* **54**, 744-8 (1992).
271. Cavarocchi, N. et al. Oxygen free radical generation during cardiopulmonary bypass: correlation with complement activation. *Circulation* **74**, III130-3 (1986).
272. Fosse, E., Mollnes, T. & Ingvaldsen, B. Complement activation during major operations with or without cardiopulmonary bypass. *J Thorac Cardiovasc Surg* **93**, 860-6 (1987).
273. Steinberg, J., Kapelanski, D., Olson, J. & Weiler, J. Cytokine and complement levels in patients undergoing cardiopulmonary bypass. *J Thorac Cardiovasc Surg* **106**, 1008-16 (1993).
274. Sato, T. et al. The terminal sequence of complement plays an essential role in antibody-mediated renal cell apoptosis. *J Am Soc Nephrol* **10**, 1242-52 (1999).
275. Orren, A. Molecular mechanisms of complement component C6 deficiency; a hypervariable exon 6 region responsible for three of six reported defects. *Clin Exp Immunol* **119**, 255-8 (2000).
276. Ruderman, E. Evaluation and management of psoriatic arthritis: the role of biologic therapy. *J Am Acad Dermatol* **41**, S125-32 (2003).
277. Drosos, A. Methotrexate intolerance in elderly patients with rheumaotid arthritis: what are the alternatives? *Drugs Aging* **20**, 723-36 (2003).
278. Frohman, E., Kramer, P., Dewey, R., Kramer, L. & Frohman, T. Benign paroxysmal positioning vertigo in multiple sclerosis: diagnosis, pathophysiology and therapeutic techniques. *Mult Scler* **9**, 250-5 (2003).
279. Giovannoni, G. Strategies to treat and prevent the development of neutralizing anti-interferon-beta antibodies. *Neurology* **61**, S13-7 (2003).
280. Polman, C. & Uitdehaag, B. New and emerging treatment options for multiple sclerosis. *Lancet Neurol* **2**, 563-6 (2003).
281. Zhang, J. T-cell vaccination for autoimmune diseases: immunologic lessons and clinical experience in multiple sclerosis. *Expert Rev Vaccines* **1**, 285-92 (2002).
282. Opdenakker, G., Nelissen, I. & Van Damme, J. Functional roles and therapeutic targeting of gelatinase B and chemokines in multiple sclerosis. *Lancet Neurol* **2**, 747-56 (2003).
283. Martino, G. Perspectives in gene therapy for MS. *Int MS J* **10**, 84-8 (2003).
284. Blevins, G. & Martin, R. Future immunotherapies in multiple sclerosis. *Semin Neurol* **23**, 147-58 (2003).

285. Flexner, S. & Noguchi, H. Snake venom in relation to hemolysis, bacteriolysis and toxicity. *J Exp Med* **6**, 277-301 (1903).
286. Cochrane, C., Muller-Eberhard, H. & Aikin, B. Depletion of plasma complement in vivo by a protein of cobra venom:its effect on various immunologic reactions. *J Immunol* **105**, 55-69 (1970).
287. Gewurz, H., Clark, D., Cooper, M., Varco, R. & Good, R. Effect of cobra venom-induced inhibition of complement activity on allograft and xenograft rejection reactions. *Transplantation* **5**, 1296-303 (1967).
288. Muller-Eberhard, H. & Fjellstrom, K. Isolation of the anticomplementary protein from cobra venom and its mode of action on C3. *J Immunol* **107**, 1666-72 (1971).
289. Phillips, G. Studies on a hemolytic factor of cobra venom requiring a heat-labile serum factor. *Biochem Biophys Acta* **201**, 364-74 (1970).
290. Maillard, J. & Zarco, R. Decomplementation by a factor extracted from cobra venom. Effect on several immune reactions of the guinea pig and rat. *Ann Inst Pasteur Paris* **114**, 756-74 (1968).
291. Cooper, N. Formation and function of a complex of the C3 proactivator with a protein from cobra venom. *J Exp Med* **137**, 451-60 (1973).
292. von Zbern, I. Effects of venoms of different animal species on the complement system. in *Activators and inhibitors of complement* (ed. RB, S.) 127-**131** (Kluwer, Dordrecht, 1993).
293. Younger, J. et al. Systemic and lung physiological changes in rats after intravascular activation of complement. *J Appl Physiol* **90**, 2289-95 (2001).
294. Holden, C. Flurry over venom. *Science* **207**, 161 (1980).
295. Caldwell, J. Venoms, copper, and zinc in the treatment of arthritis. *Rheum Dis Clin North Am* **25**, 919-28 (1999).
296. Forbes, R., Pinto-Blonde, M. & Guttmann, R. The effect of anticomplementary cobra venom factor on hyperacute rat cardiac allograft rejection. *Lab Invest* **39**, 463-70 (1978).
297. Whittum, J. & Lindquist, R. Mechanisms of cardiac allograft rejection in the inbred rat: the effect of complement depletion by cobra venom factor on hyperacute cardiac allograft rejection. *Transplantation* **24**, 226-8 (1977).
298. van den Bogaerde, J. et al. Induction of long-term survival of hamster heart xenografts in rats. *Transplantation* **52**, 15-20 (1991).
299. Thomas, F., Naff, G., Thomas, J. & Dvorak, K. Prevention of hyperacute kidney rejection of decomplementation using purified cobra venom factor. *J Surg Res* **22**, 189-94 (1977).
300. Maroko, P. et al. Reduction by cobra venom factor of myocardial necrosis after coronary artery occlusion. *J Clin Invest* **61**, 661-70 (1978).
301. Vriesendorp, F., Flynn, R., Pappolla, M. & Koski, C. Complement depletion affects demyelination and inflammation in experimental allergic neuritis. *J Neuroimmunol* **58**, 157-65 (1995).
302. Morariu, M. & Dalmasso, A. Experimental allergic encephalomyelitis in cobra venom factor-treated and C4-deficient guinea pigs. *Ann Neurol* **4**, 427-30 (1978).
303. Pabst, H., Day, N., Gewurz, H. & Good, R. Prevention of experimental allergic encephalomyelitis with cobra venom factor. *Proc Soc Exp Biol Med* **136**, 555-60 (1971).
304. Abrahamson, H. Prevention of experimental allergic encephalomyelitis with cobra venom factor. *J Asthma Res* **8**, 151-2 (1971).
305. Rudofsky, U., Steblay, R. & Pollara, B. Inhibition of experimental autoimmune renal tubulointerstitial disease in guinea pigs by depletion of complement with cobra venom factor. *Clin Immunol Immunopathol* **3**, 396-407 (1975).
306. Salant, D., Belok, S., Madaio, M. & Couser, W. A new role for complement in experimental membranous nephropathy in rats. *J Clin Invest* **66**, 1339-50 (1980).

307. Lennon, V., Seybold, M., Lindstrom, J., Cochrane, C. & Ulevitch, R. Role of complement in the pathogenesis of experimental autoimmune myasthenia gravis. *J Exp Med* **147**, 973-83 (1978).
308. Opal, S., Kessler, C., Roemisch, J. & Knaub, S. Antithrombin, heparin, and heparan sulfate. *Crit Care Med* **30**, S325-31 (2002).
309. Weiler, J., Yurt, R., Fearon, D. & Austen, K. Modulation of the formation of the amplification convertase of complement, C3b, Bb, by native and commercial heparin. *J Exp Med* **147**, 409-21 (1978).
310. Weiler, J. Polyions regulate the alternative amplification pathway of complement. *Immunopharmacology* **6**, 245-55 (1983).
311. Almeda, S., Rosenberg, R. & Bing, D. The binding properties of human complement component C1q. Interaction with mucopolysaccharides. *J Biol Chem* **258**, 785-91 (1983).
312. Hughes-Jones, N. & Gardner, B. The reaction between the complement subcomponent C1q, IgG complexes and polyionic molecules. *Immunology* **34**, 459-63 (1978).
313. Baker, P., Lint, T., McLeod, B., Behrends, C. & Gewurz, H. Studies on the inhibition of C56-induced lysis (reactive lysis). VI. Modulation of C56-induced lysis polyanions and polycations. *J Immunol* **114**, 554-8 (1975).
314. Heyer, E. et al. Heparin-bonded cardiopulmonary bypass circuits reduce cognitive dysfunction. *J Cardiothorac Vasc Anesth* **16**, 37-42 (2002).
315. Harig, F., Feyrer, R., Mahmoud, R., Blum, U. & von der Emde, J. Reducing the post-pump syndrome by using heparin-coated circuits, steroids, or aprotinin. *Thorac Cardiovasc Surg* **47**, 111-8 (1999).
316. Asghar, S. Pharmacological manipulation of complement system. *Pharmacol Rev* **36**, 223-44 (1984).
317. Carobbi, A. et al. Suramin as an anticomplementary agent in xenotransplantation. *Transplant Proc* **24**, 700 (1992).
318. Asghar, S., Dingemans, K., Kammeijer, A., Faber, W. & Abdel Mawla, M. Suppression of complement-mediated vascular injury at Arthus reaction sites by complement inhibitors. *Complement* **3**, 40-8 (1986).
319. Brackertz, D. & Kueppers, F. A one year's follow up of treatment of hereditary angioneurotic edema (HAE) with suramin. *Allergol Immunopathol (Madr)* **2**, 163-8 (1974).
320. Westaby, S. Aprotinin in perspective. *Ann Thorac Surg* **55**, 1033-41 (1993).
321. van Oeveren, W. et al. Effects of aprotinin on hemostatic mechanisms during cardiopulmonary bypass. *Ann Thorac Surg* **44**, 640-5 (1987).
322. Donaldson, V. & Evans, R. A biochemical abnormality in hereditary anioneurotic edema. Absence of serum inhibitor of C1'-esterase. *Am J Med* **35**, 37-44 (1963).
323. Jaffe, C., Atkinson, J., Gelfand, J. & Frank, M. Hereditary angioedema: the use of fresh frozen plasma for prophylaxis in patients undergoing oral surgery. *J Allergy Clin Immunol* **55**, 386-93 (1975).
324. Agostoni, A., Bergamaschini, L., Martignoni, G., Cicardi, M. & Marasini, B. Treatment of acute attacks of hereditary angioedema with C1-inhibitor concentrate. *Ann Allergy* **44**, 299-301 (1980).
325. Caliezi, C. et al. C1-esterase inhibitor: an anti-inflammatory agent and its potential use in the treatment of diseases other than hereditary angiodema. *Pharmacol Rev* **52**, 91-112 (2000).
326. Gadek, J. et al. Replacement therapy in hereditary angiodema. Successful treatment of acute episodes of angiodema with partly purified C1 inhibitor. *N Engl J Med* **302**, 542-6 (1980).
327. Bergamaschini, L. et al. C1 inhibitor concentrate in the therapy of hereditary angiodema. *Allergy* **38**, 81-4 (1983).

328. Agostoni, A. & Cicardi, M. Hereditary and acquired C1-inhibitor deficiency: Biological and clinical characteristics in 235 patients. *Medicine* **71**, 206-15 (1992).
329. Bork, K. & Witzke, G. Long-term prophylaxis with C1-inhibitor (C1 INH) concentrate in patients with recurrent angiodema caused by hereditary and acquired C1-inhibitor deficiency. *J Allergy Clin Immunol* **83**, 677-82 (1989).
330. Waytes, A., Rosen, F. & Frank, M. Treatment of hereditary angiodema with a vapor-heated C1 inhibitor concentrate. *N Engl J Med* **334**, 1630-4 (1996).
331. Kunschak, M. et al. A randomized, controlled trial to study the efficacy and safety of C1 inhibitor concentrate in treating hereditary angioedema. *Transfusion* **38**, 540-9 (1998).
332. Hong, K., Kinoshita, T., Kitajima, H. & Inoue, K. Inhibitory effect of K-76 monocarboxylic acid, an anticomplementary agent, on the C3b inactivator system. *J Immunol* **127**, 104-8 (1981).
333. Miyazaki, W. et al. Effects of K-76 moncarboxylic acid, an anticomplementary agent, on various in vivo immunological reactions and on expeimental glomerulonephritis. *Complement* **1**, 134-46 (1984).
334. Englberger, W. et al. Rosmarinic acid: a new inhibitor of complement C3-convertase with anti-inflammatory activity. *Int J Immunopharmacol* **10**, 729-37 (1988).
335. Sahu, A., Rawal, N. & Pangburn, M. Inhibition of complement by covalent attachment of rosmarinic acid to activated C3b. *Biochem Pharmacol* **57**, 1439-46 (1999).
336. Ling, M. & al, e. A component of the medicinal herb ephedra blocks activation in the classical and alternative pathways of complement. *Clin Exp Immunol* **102**, 582-8 (1995).
337. Hitomi, Y. & Fujii, S. Inhibition of various immunological reactions in vivo by a new synthetic complement inhibitor. *Int Arch Allergy Appl Immunol* **69**, 262-7 (1982).
338. Fujii, S. & Hitomi, Y. New synthetic inhibitors of C1r, C1 esterase, thrombin, plasmin, kallikrein and trypsin. *Biochem Biophys Acta* **661**, 342-5 (1981).
339. Inagi, R. et al. FUT-175 as a potent inhibitor of C5/C3 convertase activity for production of C5a and C3a. *Immunol Lett* **27**, 49-52 (1991).
340. Ino, Y. et al. Effects of FUT-175, a novel synthetic protease inhibitor, on the development of adjuvant arthritis in rats and some biological reactions dependent on complement activation. *Gen Pharmacol* **18**, 513-6 (1987).
341. Miyagawa, S. et al. Prolonging discordant xenograft survival with anticomplement reagents K76COOH and FUT175. *Transplantation* **55**, 709-13 (1993).
342. Blum, M. et al. Complement inhibition by FUT-175 and K76-COOH in a pig-to-human lung xenotransplant model. *Xenotransplantation* **5**, 35-43 (1998).
343. Miyata, T. et al. Effectiveness of nafamostat mesilate on glomerulonephritis in immune-complex diseases. *Lancet* **341**, 1353 (1993).
344. Fujita, Y. et al. Inhibitory effect of FUT-175 on complement activation and its application for glomerulonephritis with hypocomplementemia. *Nippon Jinzo Gakkai Shi* **35**, 393-7 (1993).
345. Ueda, N. et al. Inhibitory effects of newly synthesized active center-directed trypsin-like serine protease inhibitors on the complement system. *Inflamm Res* **49**, 42-6 (2000).
346. Smith, G. Filamentous fusion phage: novel expression vectors that display cloned antigens on the virion surface. *Science* **228**, 1315-7 (1985).
347. Lowman, H. Bacteriophage display and discovery of peptide leads for drug development. *Annu Rev Biophys Biomolecular Structure* **26**, 401-24 (1997).
348. Cwirla, S., Peters, E., Barrett, R. & Dower, W. Peptides on phage: a vast library of peptides for identifying ligands. *Proc Natl Acad Sci USA* **87**, 6378-82 (1990).
349. Devlin, J., Panganiban, L. & Devlin, P. Random peptide libaries: a source of specific protein binding molecules. *Science* **249**, 404-6 (1990).

350. Scott, J. & Smith, G. Searching for peptide ligands with an epitope library. *Science* **249**, 386-90 (1990).
351. Geysen, H., Rodda, S. & Mason, T. A priori delineation of a peptide which mimics a discontinuous antigenic determinant. *Mol Immunol* **23**, 709-15 (1986).
352. Geysen, H., Rodda, S., Mason, T., Tribbick, G. & Schoofs, P. Strategies for epitope analysis using peptide synthesis. *J Immunol Methods* **102**, 259-74 (1987).
353. Rasched, I. & Oberer, E. Ff coliphages: structural and functional relationships. *Microbiol Rev* **50**, 401-27 (1986).
354. Russell, M. Filamentous phage assembly. *Mol Microbiol* **5**, 1607-13 (1991).
355. Roberts, B. et al. Directed evolution of a protein: selection of potent neutrophil elastase inhibitors displayed on M13 fusion phage. *Proc Natl Acad Sci USA* **89**, 2429-33 (1992).
356. Delacourt, C. et al. Protection against acute lung injury by intravenous or intratracheal pretreatment with EPI-HNE-4, a new potent neutrophil elastase inhibitor. *Am J Respir Cell Mol Biol* **26**, 290-7 (2002).
357. Villard, S. et al. Peptide decoys selected by phage display block in vitro and in vivo activity of a human anti-FVIII inhibitor. *Blood* **102**, 949-52 (2003).
358. Somers, V. et al. A panel of candidate tumor antigens in colorectal cancer revealed by the serological selection of a phage displayed cDNA expression library. *J Immunol* **169**, 2772-80 (2002).
359. Lauvrak, V., Brekke, O., Ihle, O. & Lindqvist, B. Identification and characterisation of C1q-binding phage displayed peptides. *Biol Chem* **378**, 1509-19 (1997).
360. Roos, A. et al. Specific inhibition of the classical complement pathway by C1q-binding peptides. *J Immunol* **167**, 7052-9 (2001).
361. Sahu, A., Kay, B. & Lambris, J. Inhibition of human complement by a C3-binding peptide isolated from a phage-displayed random peptide library. *J Immunol* **157**, 884-91 (1996).
362. Nilsson, B. et al. Compstatin inhibits complement and cellular activation in whole blood in two models of extracorporeal circulation. *Blood* **92**, 1661-7 (1998).
363. Fiane, A. et al. Compstatin, a peptide inhibitor of C3, prolongs survival of *ex vivo* perfused xenografts. *Xenotransplantation* **6**, 52-65 (1999).
364. Berger, M. Inflammation in the lung in cystic fibrosis: a vicious cycle that does more harm than good? in *Clinical Reviews in Allergy: Cystic Fibrosis*, Vol. 9 (ed. Gershwin, E.) 119-141 (Humana, Clifton, NJ, 1991).
365. Birrer, P. et al. Protease-antiprotease imbalance in the lungs of children with cystic fibrosis. *Am J Respir Crit Care Med* **150**, 201-13 (1994).
366. Jackson, A., Hill, S., Afford, S. & Stockley, R. Sputum sol-phase proteins and elastase activity in patients with cystic fibrosis. *Eur J Respir Dis* **65**, 114-24 (1984).
367. Wark, P. DX-890 (Dyax). *IDrugs* **5**, 586-9 (2002).
368. Hufton, S. et al. Phage display of cDNA repertoires: the pVI display system and its applications for the selection of immunogenic ligands. *J Immunol Methods* **231**, 39-51 (1999).
369. Hufton, S., Moerkerk, P., de Bruine, A., Arends, J. & Hoogenboom, H. Serological antigen selection of phage displayed colorectal tumour cDNA libraries. *Biochem Soc Trans* **26**, S5 (1998).
370. Sahin, U. et al. Human neoplasms elicit multiple specific immune responses in the autologus host. *Proc Natl Acad Sci USA* **92**, 11810-3 (1995).
371. Farries, T. & Atkinson, J. Separation of self from non-self in the complement system. *Immunol Today* **8**, 212-5 (1987).
372. Weisman, H. et al. Recombinant soluble CR1 suppressed complement activation, inflammation and necrosis associated with reperfusion of ischemic myocardium. *Trans Assoc Am Physicians* **103**, 64-72 (1990a).

373. Weisman, H. et al. Soluble human complement receptor type 1: In vivo inhibitor of complement suppressing post-ischemic myocardial inflammation and necrosis. *Science* **249**, 146-51 (1990b).
374. Homeister, J., Satoh, P., Kilgore, K. & Lucchesi, B. Soluble complement receptor type 1 prevents human complement-mediated damage of the rabbit isolated heart. *J Immunol* **150**, 1055-64 (1993).
375. Shandelya, S. *Circulation* (1993).
376. Smith, E.I. et al. Reduction of myocardial reperfusion injury with human soluble complement receptor type 1 (BRL 55730). *Eur J Pharmacol* **236**, 477-81 (1993).
377. Pemberton, M., Anderson, G., Vetvicka, V., Justus, D. & Ross, G. Microvascular effects of complement blockade with soluble recombinant CR1 on ischemia/reperfusion injury of skeletal muscle. *J Immunol* **150**, 5104-13 (1993).
378. Goodfellow, R., Williams, A., Levin, J., Williams, B. & Morgan, B. Local therapy with soluble complement receptor 1 (sCR1) suppresses inflammation in rat mono-articular arthritis. *Clin Exp Immunol* **110**, 45-52 (1997).
379. Goodfellow, R., Williams, A., Levin, J., Williams, B. & Morgan, B. Soluble complement receptor 1 (sCR1) inhibits the development and progression of rat collagen-induced arthritis. *Clin Exp Immunol* **119**, 210-6 (2000).
380. Rioux, P. TP-10 (AVANT immunotherapeutics). *Curr Opin Investig Drugs* **2**, 364-71 (2001).
381. Zimmerman, J., Dellinger, R., Straube, R. & Levin, J. Phase I trial of the recombinant soluble complement receptor 1 in acute lung injury and acute respiratory distress syndrome. *Crit Care Med* **28**, 3149-54 (2000).
382. Christiansen, D., Milland, J., Thorley, B., McKenzie, I. & Loveland, B. A functional analysis of recombinant soluble CD46 in vivo and a comparison with recombinant soluble forms of CD55 and CD35 in vitro. *Eur J Immunol* **26**, 578-85 (1996).
383. Christiansen, D. & al, e. Engineering of recombinant soluble CD46: an inhibitor of complement activation. *Immunology* **87**, 348-354 (1996).
384. Moran, P. et al. Human recombinant soluble decay accelerating factor inhibits complement activation in vitro and in vivo. *J Immunol* **149**, 1736-43 (1992).
385. Sugita, Y. et al. Recombinant soluble CD59 inhibits reactive haemolysis with complement. *Immunology* **82**, 34-41 (1994).
386. Scesney, S. et al. A soluble deletion mutant of the human complement receptor type 1, which lacks the C4b binding site, is a selective inhibitor of the alternative complement pathway. *Eur J Immunol* **26**, 1729-35 (1996).
387. Rittershaus, C. et al. Recombinant glycoproteins that inhibit complement activation and also bind the selectin adhesion molecules. *J Biol Chem* **274**, 11237-44 (1999).
388. Mulligan, M. et al. Endothelial targeting and enhanced antiinflammatory effects of complement inhibitors possessing sialyl Lewis(x) moieties. *J Immunol* **162**, 4952-9 (1999).
389. Huang, J. et al. Neuronal protection in stroke by an sLex-glycosylated complement inhibitory protein. *Science* **285**, 595-9 (1999).
390. Dodd, I. et al. Overexpression in Escherichia coli, folding, purification and characterisation of the first three short consensus repeat modules of human complement receptor type 1. *Protein Expr Purif* **6**, 727-36 (1995).
391. Smith, R. et al. Cell surface engineering using a complement regulatory molecule modified with a synthetic myristoyl-electrostatic switch derivative. *Molecular Immunology* **35**, 280 (1998).
392. Linton, S. et al. Therapeutic efficacy of a novel membrane-targeted complement regulator in antigen arthritis in the rat. *Arthritis Rheum* **43**, 2590-7 (2000).

393. Dong, J., Pratt, J., Smith, R., Dodd, I. & Sacks, S. Strategies for targeting complement inhibitors in ischemia/reperfusion injury. *Mol Immunol* **36**, 957-63 (1999).
394. Smith, R. et al. *Mol Immunol* **38**, 122 (2001).
395. Smith, R. Targeting anticomplement agents. *Biochem Soc Trans* **30**, 1037-41 (2002).
396. Athanasou, N. et al. The immunohistology of synovial lining cells in normal and in inflammed synovium. *J Pathol* **155**, 133-42 (1988).
397. Palmer, D., Selvendran, Y., Allen, C., Revell, P. & Hogg, N. Features of synovial membrane identified with monoclonal antibodies. *Clin Exp Immunol* **59**, 529-38 (1985).
398. Harris, C., Fraser, D. & Morgan, B. Tailoring anti-complement therapeutics. *Biochem Soc Trans* **30**, 1019-26 (2002).
399. Fraser, D. & al, e. Bacterial expression and membrane targeting of the rat complement regulator Crry: a new model anticomplement therapeutic. *Protein Sci* **11**, 2512-21 (2002).
400. Zhang, H., Yu, J., Bajwa, E., Morrison, S. & Tomlinson, S. Targeting of functional antibody-CD59 fusion proteins to a cell surface. *J Clin Invest* **103**, 55-61 (1999).
401. Zhang, H., Lu, S., Morrison, S. & Tomlinson, S. Targeting of functional antibody-decay-accelerating factor fusion proteins to a cell surface. *J Biol Chem* **276**, 27290-5 (2001).
402. Pugsley, M. Etanercept. Immunex. *Curr Opin Investig Drugs* **2**, 1725 - 31 (2001).
403. Quigg, R. et al. Blockade of antibody-induced glomerulonephritis with Crry-Ig, a soluble murine complement inhibitor. *J Immunol* **160**, 4553-60 (1998).
404. Harris, C., Williams, A., Linton, S. & Morgan, B. Coupling complement regulators to immunoglobulin domains generates effective anti-complement reagents with extended half-life in vivo. *Clin Exp Immunol* **129**, 198-207 (2002).
405. Rehrig, S. et al. Complement inhibitor, complement receptor 1-related gene/protein y-Ig attenuates intestinal damage after the onset of mesenteric ischemia/reperfusion injury in mice. *J Immunol* **167**, 5921-7 (2001).
406. Reff, M. et al. Depletion of B cells in vivo by chimeric mouse human monoclonal antibody to CD20. *Blood* **83**, 435-45 (1994).
407. Anderson, K. et al. Expression of human B cell-associated antigens on leukemias and lymphomas: a model of human B cell differentiation. *Blood* **63**, 1424-33 (1984).
408. Grillo-Lopez, A. Rituximab: an insider's historical perspective. *Semin Oncol* **27**, 9-16 (2000).
409. Miller, R., Oseroff, A., Stratte, P. & Levy, R. Monoclonal antibody therapeutic trials in seven patients with T-cell lymphoma. *Blood* **62**, 988-95 (1983).
410. Sears, H., Herlyn, D., Steplewski, Z. & Koprowski, H. Effects of monoclonal antibody immunotherapy on patients with gastrointestinal adenocarcinoma. *J Biol Response Modifiers* **3**, 138-50 (1984).
411. Khazaeli, M. et al. Phase I trial of multiple large doses of murine monoclonal antibody CO17-1A. II Pharmacokinetics and immune response. *J Natn Cancer Inst* **80**, 937-42 (1988).
412. LoBuglio, A. et al. Mouse/human chimeric monoclonal antibody in man: kinetics and immune response. *Proc Natl Acad Sci USA* **86**, 4220-4 (1989).
413. Moreland, L. et al. Use of chimeric monoclonal anti-CD4 antibody in patients with refractory rheumatoid arthritis. *Arthritis Rheum* **36**, 307-18 (1993).
414. Weiden, P. et al. Rhenium-186-labeled chimeric antibody NR-LU-13: pharmacokinetics, biodistribution and immunogenicity relative to murine analog NR-LU-10. *J Nucl Med* **34**, 2111-9 (1993).
415. Weir, A. et al. Formatting antibody fragments to mediate specific therapeutic functions. *Biochem Soc Trans* **30**, 512-6 (2002).
416. King, D. in *Applications and Engineering of Monoclonal Antibodies* (eds. Taylor & Francis) 65-75 (London, 1998).

417. McLaughlin, P. et al. Rituximab chimeric anti-CD20 monoclonal antibody therapy for relapsed indolent lymphoma: half of patients respond to a four-dose treatment program. *J Clin Oncol* **8**, 2825-33 (1998).
418. Anderson, D., Grillo-Lopez, A., Varns, C., Chambers, K. & Hanna, N. Targeted anti-cancer therapy using rituximab, a chimeric anti CD20 antibody (IDEC-C2B8) in the treatment of non-Hodgkin's B-cell lymphoma. *Biochem Soc Trans* **25**, 705-8 (1997).
419. Clynes, R., Towers, T., Presta, L. & Ravetch, J. Inhibitory Fc receptors modulate in vivo cytotoxicity against tumour targets. *Nat Med* **6**, 443-6 (2000).
420. Maloney, D., Smith, B. & Rose, A. Rituximab: mechanisms of action and resistance. *Semin Oncol* **29**, 2-9 (2002).
421. Coiffier, B. et al. CHOP chemotherapy plus rituximab compared with CHOP alone in elderly patients with diffuse large-B-cell lymphoma. *N Engl J Med* **346**, 235-42 (2002).
422. Avivi, I., Robinson, S. & Goldstone, A. Clinical use of rituximab in haematological malignancies. *Br J Cancer* **89**, 1389-94 (2003).
423. McLaughlin, P., Hagemeister, F. & Grillo-Lopez, A. Rituximab in indolent lymphoma: the single agent pivotal trial. *Semin Oncol* **26**, 79-87 (1999).
424. Shaw, T., Quan, J. & Totoritis, M. B cell therapy for rheumatoid arthritis: the rituximab (anti-CD20) experience. *Ann Rheum Dis* **62**, ii55-9 (2003).
425. Edwards, J., Leandro, M. & Cambridge, G. B-lymphocyte depletion therapy in rheumatoid arthritis and other autoimmune disorders. *Biochem Soc Trans* **30**, 824-8 (2002).
426. Edwards, J. & Cambridge, G. Sustained improvement in rheumatoid arthritis following a protocol designed to deplete B lymphocytes. *Rheumatology (Oxford)* **40**, 205-11 (2001).
427. Edwards, J. et al. Efficacy and safety of rituximab, a B-cell targeted chimeric monoclonal antibody: a randomized, placebo-controlled trial in patients with rheumatoid arthritis. *Arthritis Rheum* **46**, S197 (2002).
428. De Vita, S. et al. Efficacy of selective B cell blockade in the treatment of rheumatoid arthritis. Evidence for a pathogenic role of B cells. *Arthritis Rheum* **46**, 2029-33 (2002).
429. Leandro, M., Edwards, J. & Cambridge, G. Clinical outcome in 22 patients with rheumatoid arthritis treated with B lymphocyte depletion. *Ann Rheum Dis* **61**, 883-8 (2002).
430. Tuscano, J. Successful treatment of infliximab-refractory rheumatoid arthritis with rituximab. *Arthritis Rheum* **46**, 3420, LB11 (2002).
431. Stasi, R., Pagano, A., Stipa, E. & Amadori, S. Rituximab chimeric anti-CD20 monoclonal antibody treatment for adults with chronic idiopathic thrombocytopenic purpura. *Blood* **98**, 952-7 (2001).
432. Zaja, F. et al. Efficacy and safety of rituximab in type II mixed cryoglobulinemia. *Blood* **101**, 3827-34 (2003).
433. Pestronk, A. et al. Treatment of IgM antibody assoicated polyneuropathies using rituximab. *J Neurol Neurosurg Psychiatry* **74**, 485-9 (2003).
434. Lipsky, P. Systemic lupus erythematosus: an autoimmune disease of B cell hyperactivity. *Nat Immunol* **2**, 764-6 (2001).
435. Anolik, J., Campbell, D., Felgar, R. & al, e. B lymphocyte depletion in the treatment of systemic lupus (SLE): phase I/II trial of rituximab (Rituxan(R)) in SLE. *Arthritis Rheum* **46**, S289 (2002).
436. Leandro, M., Edwards, J., Cambridge, G., Ehrenstein, M. & Isenberg, D. An open study of B lymphocyte depletion in systemic lupus erythematosus,. *Arthritis Rheum* **46**, 2673-7 (2002).
437. Treumann, A., Lifely, M., Schneider, P. & Ferguson, M. Primary structure of CD52. *J Biol Chem* **270**, 6088-99 (1995).

438. Gilleece, M. & Dexter, T. Effect of Campath-1H antibody on human haematopoietic progenitors in vitro. *Blood* **82**, 807-12 (1993).
439. Hederer, R. et al. The CD45 tyrosine phosphatase regulates Campath-1H (CD52)-induced TCR-dependent signal transduction in human T cells. *Int Immunol* **12**, 505-16 (2000).
440. Heit, W. et al. Ex vivo T-cell depletion with the monoclonal antibody Campath-1 plus human complement effectively prevents acute graft-versus-host disease in allogeneic bone marrow transplantation. *Br J Haematol* **64**, 479-86 (1986).
441. Dyer, M., Hale, G., Hayhoe, F. & Waldmann, H. Effects of CAMPATH-1 antibodies in vivo in patients with lymphoid malignancies: influence of antibody isotype. *Blood* **73**, 1431-9 (1989).
442. Greenwood, J., Clark, M. & Waldmann, H. Structure motifs involved in human IgG antibody effector functions. *Eur J Immunol* **23**, 1098-104 (1993).
443. Rowan, W., Tite, J., Topley, P. & Brett, S. Cross-linking of the CAMPATH-1 antigen (CD52) mediates growth inhibition in human B- and T-lymphoma cell lines, and subsequent emergence of CD52-deficient cells. *Immunology* **95**, 427-36 (1998).
444. Green, L. et al. Antigen-specific human monoclonal antibodies from mice engineered with human Ig heavy and light chain YACs. *Nat Genet* **7**, 13-21 (1994).
445. Mendez, M. et al. Functional transplant of megabase human immunoglobulin loci recapitulates human antibody responses in mice. *Nat Genet* **15**, 146-56 (1997).
446. Bross, P. et al. Approval summary:gemtuzumab ozogamicin in relapsed acute myeloid leukemia. *Clin Cancer Res* **7**, 1490-6 (2001).
447. Giles, F. Gemtuzumab ozogamicin: promise and challenge in patients with acute myeloid leukaemia. *Expert Rev Anti-cancer Ther* **2**, 630-40 (2000).
448. Wellhausen, S. & Peiper, S. CD33: biochemical and biological characterization and evaluation of clinical relevance. *J Biol Regul Homeost Agents* **16**, 139-43 (2002).
449. Bernstein, I. Monoclonal antibodies to the myeloid stem cells: therapeutic implications of CMA-676, a humanized anti-CD33 antibody calicheamicin conjugate. *Leukemia* **14**, 474-5 (2000).
450. van Der Velden, V. et al. Targeting of the CD33-calicheamicin immunoconjugate Mylotarg (CMA-676) in acute myeloid leukemia: in vivo and in vitro saturation and internalization by leukemic and normal myeloid cells. *Blood* **97**, 3197-204 (2001).
451. Dedon, P., Salzberg, A. & Xu, J. Exclusive production of bistranded DNA damage by calicheamicin. *Biochemistry* **32**, 3617-22 (1993).
452. LaMarr, W., Yu, L., Nicolaou, K. & Dedon, P. Supercoiling affects the accessibility of glutathione to DNA-bound molecules: positive supercoiling inhibits calicheamicin-induced DNA damage. *Proc Natl Acad Sci USA* **95**, 102-7 (1998).
453. Yu, L., Goldberg, I. & Dedon, P. Solution structure of the calicheamicin gamma 1I-DNA complex. *J Mol Biol* **265**, 187-201 (1997).
454. Hinman, L. et al. Preparation and characterization of monoclonal antibody conjugates of the calicheamicins: a novel and potent family of anti-tumor antibiotics. *Cancer Res* **53**, 3336-42 (1993).
455. Hiatt, A., Merlock, R., Mauch, S. & Wrasidlo, W. Regulation of apoptosis in leukemic cells by analogs of dynemicin A. *Bioorg Med Chem* **2**, 315-22 (1994).
456. Salzberg, A. & Dedon, P. DNA bending is a determinant of calicheamicin target recognition. *Biochemistry* **39**, 7605-12 (2000).
457. Amico, D. et al. Differential response of human acute myeloid leukaemia cells to gemtuzumab ozogamicin (Mylotarg(R)) in vitro. Role of Chk1 and Chk2 phosphorylation and caspase 3. *Blood* **101**, 4589-97 (2003).

458. Wurzner, R. et al. Inhibition of terminal complement complex formation and cell lysis by monoclonal antibodies. *Complement Inflamm* **8**, 328-40 (1991).
459. Kroshus, T. et al. Complement inhibition with an anti-C5 monoclonal antibody prevents acute cardiac tissue injury in an *ex vivo* model of pig-to-human xenotransplantation. *Transplantation* **60**, 1194-202 (1995).
460. Rinder, C. et al. Blockade of C5a and C5b-9 generation inhibits leukocyte and platelet activation during extracorporeal circulation. *J Clin Invest* **96**, 1564-72 (1995).
461. Evans, M., Hartman, S., Wolff, D., Rollins, S. & Squinto, S. Rapid expression of an anti-human C5 chimeiric Fab utilizing a vector that replicates in COS and 293 cells. *J Immunol Methods* **184**, 123-38 (1995).
462. Huston, J. et al. Protein engineering of antibody binding sites: Recovery of specific activity in an anti-digoxin single-chain Fv analogue produced in Escherichia coli. *Proc Natl Acad Sci USA* **85**, 5879-83 (1988).
463. Bird, R. et al. Single chain antigen-binding proteins. *Science* **242**, 423-6 (1988).
464. Kortt, A. et al. Recombinant anti-sialidase single-chain variable fragment antibody. Characterization, formation of dimer and higher-molecular-mass multimers and the solution of the crystal structure of the single-chain variable fragment/sialidase complex. *Eur J Biochem* **221**, 151-7 (1994).
465. Pantoliano, W. et al. Conformational stability, folding, and ligand-binding affinity of single-chain Fv immunoglobulin fragments expressed in Escherichia coli. *Biochemistry* **30**, 10117-25 (1991).
466. Zdanov, A. et al. Structure of a single-chain antibody variable domain (Fv) fragment complexed with a carbohydrate antigen at 1.7-A resolution. *Proc Natl Acad Sci USA* **91**, 6423-7 (1994).
467. Yokota, T., Milenic, D., Whitlow, M. & Schlom, J. Rapid tumor penetration of a single-chain Fv and comparison with other immunoglobulin forms. *Cancer Res* **52**, 3402-8 (1992).
468. Evans, M. et al. In vitro and in vivo inhibition of complement activity by a single-chain Fv fragment recognising human C5. *Mol Immunol* **32**, 1183-95 (1995).
469. Thomas, T. et al. Inhibition of complement activity by humanised anti-C5 antibody and single-chain Fv. *Mol Immunol* **33**, 1389-401 (1996).
470. Fitch, J. et al. Pharmacology and biological efficacy of a recombinant, humanised, single-chain antibody C5 complement inhibitor in patients undergoing coronary artery bypass graft surgery with cardiopulmonary bypass. *Circulation* **100**, 2499-506 (1999).
471. Whiss, P. Pexelizumab Alexion. *Curr Opin Investig Drugs* **3**, 870-7 (2002).
472. Hillmen, P. et al. Effect of eculizumab on hemolysis and transfusion requirements in patients with paroxysmal nocturnal hemoglobinuria. *New Engl J Med* **350**, 552-9 (2004).
473. McCafferty, J., Griffiths, A., Winter, G. & Chiswell, D. Phage antibodies: filamentous phage displaying antibody variable domains. *Nature* **348**, 552-4 (1990).
474. Vaughan, T. et al. Human antibodies with sub-nanomolar affinities isolated from large non-immunized phage display library. *Nat Biotechnol* **14**, 309-14 (1996).
475. Osbourn, J., Jermutus, L. & Duncan, A. Current methods for the generation of human antibodies for the treatment of autoimmune diseases. *Drug Discovery Today* **8**, 845-51 (2003).
476. Weinblatt, M. et al. Adalimumab, a fully human anti-tumour necrosis factor alpha monoclonal antibody for the treatment of rheumatoid arthritis in patients taking concomitant methotrexate: the ARMADA trial. *Arthritis Rheum* **48**, 35-45 (2003).
477. Wetsel, R. & Kolb, W. Complement-independent activation of the fifth component (C5) of human complement: limited trypsin digestion resulting in the expression of biologic activity. *J Immunol* **128**, 2209-16 (1982).

478. Vogt, W., Damerau, B., von-Zabern, I., Nolte, R. & Brunahl, D. Non-enzymatic activation of the fifth component of human complement by oxygen radicals. Some properties of the activation product, C5b-like C5. *Mol Immunol* **26**, 1133-42 (1989).
479. Tedesco, F., Rottini, G., Basaglia, M., Roncelli, L. & Patriarca, P. Monoclonal antibodies anti-C8 interfere with the killing of Escherichia coli 0111:B4 by PMN cationic proteins. *Complement* **4**, 230- (1987).
480. Abraha, A. & Luzio, J. Inhibition of the formation of the complement membrane-attack complex by a monoclonal antibody to the complement component C8α subunit. *Biochem J* **264**, 933-6 (1989).
481. Zeitz, H., Zeff, R., Gewurz, H. & Lint, T. Decreased C5b67-inhibitor activity in two families with hereditary functional deficiency of the eigth component of complement. *J Immunol* **130**, 2809-13 (1983).
482. Laemmli, U. Cleavage of structural proteins during the assembly of the head of bacteriophage T4. *Nature* **227**, 680-5 (1970).
483. Morrissey, J. Silver stain for proteins in polyacrylamide gels - a modified procedure with enhanced uniform sensitivity. *Anal Biochem* **117**, 307-10 (1981).
484. Harris, C., Lublin, D. & Morgan, B. Efficient generation of monoclonal antibodies for specific protein domains using recombinant immunoglobulin fusion proteins: pitfalls and solutions. *J Immunol Methods* **268**, 245-58 (2002).
485. van Dixhoorn, M. et al. Characterisation of complement C6 deficiency in a PVG/c rat strain. *Clin Exp Immunol* **109**, 387-96 (1997).
486. Rother, U. & Rother, K. Uber einen angeborenen Komplement-Defekt bei Kaninchen. *Z ImmunoForsch Exp Ther* **121**, 224-9 (1961).
487. Kohler, G. & Milstein, C. Continuous cultures of fused cells secreting antibody of predifined specificity. *Nature* **256**, 495-7 (1975).
488. Harlow, E. & David, L. Chapter 7 Growing hybridomas. in *Antibodies - a laboratory manual* 280 (Cold Spring Harbor Laboratory, Cold Spring Harbor, New York, 1988).
489. Harlow, E. & David, L. Chapter 6 Monoclonal antibodies. in *Antibodies, A laboratory manual* 203, 277 (Cold Spring Harbor, New York, 1988).
490. van den Berg, C. Purification of Complement Components, Regulators, and Receptors by Classical Methods. in *Complement methods and protocols*, Vol. Methods in molecular biology, 150 (ed. Morgan, B.) 15 (Humana Press, 2000).
491. Jonsson, U. et al. Real-time biospecific interaction analysis using surface plasmon resonance and a sensor chip technology. *BioTechniques* **11**, 620-7 (1991).
492. Sjolander, S. & Urbaniczky, C. Integrated fluid handling system for biomolecular interaction analysis. *Anal Chem* **63**, 2338-45 (1991).
493. Harrison, R. & Lachmann, P. Complement technology, Chapter 39. 39.1-39.49.
494. Harrison, R. Purification, assay and characterisation of complement proteins from plasma. 75.1-75.50.
495. Hammer, C., Wirtz, G., Renfer, L., Gresham, H. & Tack, B. Large scale isolation of functionally active components of the human complement system. *J Biol Chem* **256**, 3995-4006 (1981).
496. Podack, E., Kolb, W. & Muller-Eberhard, H. Purification of the sixth and seventh component of human complement without loss of hemolytic activity. *J Immunol* **116**, 263-9 (1976).
497. Handbook, A. *Affinity Chromatography - principles and methods.*
498. Mead, R., Singhrao, S., Neal, J., Lassman, H. & Morgan, B. The membrane attack complex of complement causes severe demyelination associated with acute axonal injury. *J Immunol* **168**, 458-65 (2002).

499. Wurzner, R. et al. Functionally active complement proteins C6 and C7 detected in C6- and C7- deficient individuals. *Clin Exp Immunol* **83**, 430-7 (1991).
500. Wurzner, R. et al. Molecular basis of subtotal complement deficiency: a carboxyterminally truncated but functionally active C6. *J Clin Invest* **95**, 1877-83 (1995).
501. Koski, C., Ramm, L., Hammer, C., Mayer, M. & Shin, M. Cytolysis of nucleated cells by complement: cell death displays multi-hit characteristics. *Proc Natl Acad Sci USA* **80**, 3816-20 (1983).
502. Nielsen, H., Larsen, S. & Vikingsdottir, T. Rate-limiting components and reaction steps in complement-mediated haemolysis. *APMIS* **100**, 1053-60 (1992).
503. Orren, A. et al. Properties of a low molecular weight complement component C6 found in human subjects with subtotal C6 deficiency. *Immunology* **75**, 10-6 (1992).
504. Yu, J., Bradt, B. & Cooper, N. Molecular cloning of the C6A form cDNA of the mouse sixth complement component: functional integrity despite the absence of factor I modules. *Immunogenetics* **51**, 779-87 (2000).
505. Orren, A., Preece, C. & Dowdle, E. Genetically determined molecular weight differences in murine complement component C6. *Eur J Immunol* **15**, 100-3 (1985).
506. Orren, A., Hobart, M., Nash, H. & Lachmann, P. Close linkage between mouse genes determining the two forms of complement component C6 and component C7, and *Cis* action of a *C6* regulatory gene. *Immunogenetics* **21**, 591-9 (1985).
507. Orren, A., Hayakawa, J., Johnson, J., Nash, H. & Hobart, M. Allotypes of mouse complement component C6 in inbred strains and some wild populations. *Immunogenetics* **28**, 153-7 (1988).
508. Leenaerts, P. et al. Hereditary C6 deficiency in a strain of PVG/c rats. *Clin Exp Immunol* **97**, 478-82 (1994).
509. Rother, K. Rabbits deficient in C6. *Prog Allergy* **39**, 192-201 (1986).
510. Ito, W. et al. Influence of the terminal complement-complex on reperfusion injury, no-reflow and arrhythmias: a comparison between C6-competent and C6-deficient rabbits. *Cardiovasc Res* **32**, 294-305 (1996).
511. Ortiz-Ortiz, L. & Weigle, W. Cellular events in the induction of experimental allergic encephalomyelitis in rats. *J Exp Med* **144**, 604-16 (1976).
512. Tran, G. et al. Attenuation of experimental allergic encephalomyelitis in complement component 6-deficient rats is associated with reduced complement C9 deposition, P-selectin expression, and cellular infiltrate in spinal cords. *J Immunol* **168**, 4293-300 (2002).
513. Zhou, W. et al. Predominant role for C5b-9 in renal ischemia/reperfusion injury. *J Clin Invest* **105**, 1363-71 (2000).
514. Tofukuji, M. et al. Anti-C5a monoclonal antibody reduces cardiopulmonary bypass and cardioplegia-induced coronary endothelial dysfunction. *J Thorac Cardiovasc Surg* **116**, 1060-8 (1998).
515. Williams, J. et al. Intestinal reperfusion injury is mediated by IgM and complement. *J Appl Physiol* **86**, 938-42 (1999).
516. Heller, T. et al. Selection of a C5a receptor antagonist from phage libraries attenuating the inflammatory response in immune complex disease and ischemia/reperfusion injury. *J Immunol* **163**, 985-94 (1999).
517. Rollins, S., Matis, L., Springhorn, J., Setter, E. & Wolff, D. Monoclonal antibodies directed against human C5 and C8 block complement-mediated damage of xenogeneic cells and organs. *Transplantation* **60**, 1284-92 (1995).
518. Rinder, C. et al. Selective blockade of membrane attack complex formation during simulated extracorporeal circulation inhibits platelet but not leukocyte activation. *J Thorac Cardiovasc Surg* **118**, 460-6 (1999).

519. Biesecker, G. & Gomez, C. Inhibition of acute passive transfer experimental autoimmune myasthenia gravis with Fab antibody to complement C6. *J Immunol* **142**, 2654-9 (1989).
520. Vakeva, A. et al. Myocardial infarction and apoptosis after myocardial ischemia and reperfusion: role of the terminal complement components and inhibition by anti-C5 therapy. *Circulation* **97**, 2259-67 (1998).
521. Wang, Y., Rollins, S., Madri, J. & Matis, L. Anti-C5 monoclonal antibody therapy prevents collagen-induced arthritis and ameliorates established disease. *Proc Natl Acad Sci USA* **92**, 8955-9 (1995).
522. Wurzner, R., Mewar, D., Fernie, B., Hobart, M. & Lachmann, P. Importance of the third thrombospondin repeat of C6 for terminal complement complex assembly. *Immunology* **85**, 214-9 (1995).
523. Drake, A., Myszka, D. & Klakamp, S. Characterizing high-affinity antigen/antibody complexes by kinetic- and equilibrium-based methods. *Anal Biochem* **328**, 35-43 (2004).
524. Nieba, L., Krebber, A. & Pluckthun, A. Competition BIAcore for measuring true affinities: large differences from values determined from binding kinetics. *Anal Biochem* **234**, 155-65 (1996).
525. Canziani, G., Klakamp, S. & Myszka, D. Kinetic screening of antibodies from crude hybridoma samples using Biacore. *Anal Biochem* **325**, 301-7 (2004).
526. Carnahan, J. et al. Epratuzumab, a humanized monoclonal antibody targeting CD22: characterization of in vitro properties. *Clin Cancer Res* **9**, 3982s-90s (2003).
527. Taremi, S., Prosise, W., Rajan, N., O'Donnell, R. & Le, H. Human interleukin 4 receptor complex: neutralization effect of two monoclonal antibodies. *Biochemistry* **35**, 2322-31 (1996).
528. Choulier, L. et al. Comparative properties of two peptide-antibody interactions as deduced from epitope delineation. *J Immunol Meth* **259**, 77-86 (2002).
529. Liautard, J. et al. Specific inhibition of IL-6 signalling with monoclonal antibodies against the gp130 receptor. *Cytokine* **9**, 233-41 (1997).
530. Bretscher, P. & Cohn, M. A theory of self-nonself discrimination. *Science* **169**, 1042-9 (1970).
531. Baumgarth, N. A two-phase model of B-cell activation. *Immunol Rev* **176**, 171-80 (2000).
532. Nossal, G. Kinetics of antibody formation and regulatory aspects of immunity. *Acta Endocrinol Suppl* **194**, 96-116 (1974).
533. Kinetics Level 1 course notes, B.
534. Dawes, J., James, K., Micklem, L., Pepper, D. & Prowse, C. Monoclonal antibodies directed against human α-thrombin and the thrombin-antithrombin III complex. *Thromb Res* **36**, 397-409 (1984).
535. Baerga-Ortiz, A., Bergqvist, S., Mandell, J. & Komives, E. Two different proteins that compete for binding to thrombin have opposite kinetic and thermodynamic profiles. *Protein Sci* **13**, 166-76 (2004).
536. Millipore. Prosep-G Data Sheet. 1-4.
537. Division, M.B. Affinity Chromatography Media. *User Guide*, 1-12.
538. Ladner, R., Sato, A., Gorzelany, J. & de Souza, M. Phage display-derived peptides as therapeutic alternatives to antibodies. *Drug Discovery Today* **9**, 525-9 (2004).
539. Parmley, S. & Smith, G. Antibody-selectable filamentous fd phage vectors: affinity purification of target genes. *Gene* **73**, 305-18 (1988).
540. Smith, G. & Scott, J. Libraries of peptides and proteins displayed on filamentous phage. *Methods Enzymol* **217**, 228-57 (1993).
541. O'Neil, K. et al. Identification of novel peptide antagonists for GPIIb/IIIa from a conformationally constrained phage peptide library. *Proteins* **14**, 509-15 (1992).

542. Doorbar, J. & Winter, G. Isolation of a peptide antagonist to the thrombin receptor using phage display. *J Mol Biol* **144**, 361-9 (1994).
543. Goodson, R., Doyle, M., Kaufman, S. & Rosenberg, S. High-affinity urokinase receptor antagonists identified with bacteriophage peptide display. *Proc Natl Acad Sci USA* **91**, 7129-33 (1994).
544. Barry, M., Dower, W. & Johnston, S. Toward cell-targeting gene therapy vectors: selection of cell-binding peptides from random peptide-presenting phage libraries. *Nat Med* **2**, 299-305 (1996).
545. Smith, M., Shi, L. & Navre, M. Rapid identification of highly active and selective substrates for stromelysin and matrilysin using bacteriophage peptide display libraries. *J Biol Chem* **270**, 6440-9 (1995).
546. Barbas, S. & Barbas, C. Filamentous phage display. *Fibrinolysis* **8**, 245-52 (1994).
547. Lowman, H., Bass, S., Simpson, N. & Wells, J. Selecting high-affinity binding proteins by monovalent phage display. *Biochemistry* **30**, 10832-8 (1991).
548. Soumillion, P. et al. Selection of beta-lactamase on filamentous bacteriophage by catalytic activity. *J Mol Biol* **237**, 415-22 (1994).
549. Choo, Y. & Klug, A. Designing DNA-binding proteins on the surface of filamentous phage. *Curr Opin Biotechnol* **6**, 431-6 (1995).
550. Cortese, R. et al. Identification of biologically active peptides using random libraries displayed on phage. *Curr Opin Biotechnol* **6**, 73-80 (1995).
551. Felici, F., Castagnoli, L., Musacchio, A., Jappelli, R. & Cesarini, G. Selection of antibody ligands from a large library of oligopeptides expressed on a multivalent exposition vector. *J Mol Biol* **222**, 301-10 (1991).
552. Hong, S. & Boulanger, P. Protein ligands of the human adenovirus type 2 outer capsid identified by biopanning of a phage-displayed peptide library on separate domains of wild-type and mutant penton capsomers. *EMBO J* **14**, 4714-27 (1995).
553. Oldenburg, K., Loganathan, D., Goldstein, I., Schultz, P. & Gallop, M. Peptide ligands for a sugar-binding protein isolated from a random peptide library. *Proc Natl Acad Sci USA* **89**, 5393-7 (1992).
554. Scott, J., Loganathan, D., Easley, R., Gong, X. & Goldstein, I. A family of concanavalin A-binding peptides from a hexapeptide epitope library. *Proc Natl Acad Sci USA* **89**, 5398-402 (1992).
555. Hoess, R., Brinkmann, U., Handel, T. & Pastan, I. Identification of a peptide which binds to the carbohydrate-specific monclonal antibody B3. *Gene* **128**, 43-9 (1993).
556. Davis, A.I. C1 inhibitor and hereditary angioneurotic edema. *Ann Rev Immunol* **6**, 595-628 (1988).
557. Tosi, M. Molecular genetics of C1 inhibitor. *Immunobiology* **199**, 358-65 (1998).
558. Williams, A. & Baird, L. DX-88 and HAE: a developmental perspective. *Transfus Apher Sci* **29**, 255-8 (2003).
559. Rubinstein, D. et al. Receptor for the globular heads of C1q (gC1q-R, p33, hyaluronan-binding protein) is preferentially expressed by adenocarcinoma cells. *Int J Cancer* **110**, 741-50 (2004).
560. Peterson, K., Zhang, W., Keilbaugh, S., Peerschke, E. & Ghebrehiwet, B. The C1q binding membrane proteins cC1q-R and gC1q-R are released from activated cells: subcellular localization and immunochemical characterization. *Clin Immunol Immunopathol* **84**, 17-26 (1997).
561. Ghebrehiwet, B. et al. Evidence that the two C1q binding membrane proteins, gC1q-R and cC1q-R, associate to form a complex. *J Immunol* **159**, 1429-36 (1997).

562. Ghebrehiwet, B., Lim, B.-L., Kumar, R., Feng, X. & Peerschke, E. gC1q-R/p33, a member of a new class of multifunctional and multicompartmental cellular proteins, is involved in inflammation and infection. *Immunol Rev* **180**, 65-77 (2001).
563. Xu, Z., Hirasawa, A., Shinoura, H. & Tsujimoto, G. Interaction of the α_{1B}–adrenergic receptor with gC1q-R, a multifunctional protein. *J Biol Chem* **274**, 2149-54 (1999).
564. Granger, C. et al. Pexelizumab, an anti-C5 complement antibody, as adjunctive therapy to primary percutaneous coronary intervention in acute myocardial infarction - the COMplement inhibition in myocardial infarction treated with angioplasty (COMMA) trial. *Circulation* **208**, 1184-90 (2003).
565. Mahaffey, K. et al. Effect of Pexelizumab, an anti-C5 complement antibody, as adjunctive therapy to fibrinolysis in acute myocardial infarction - The COMPlement inhibition in myocardial infarction treated with thromboLYtics (COMPLY) Trial. *Circulation* **108**, 1176-83 (2003).
566. Marzari, R. et al. The cleavage site of C5 from man and animals as a common target for neutralizing human monoclonal antibodies: *in vitro* and *in vivo* studies. *Eur J Immunol* **32**, 2773-82 (2002).
567. Duncan, A. & Winter, G. The binding site for C1q on IgG. *Nature* **332**, 738-40 (1988).
568. Burton, D. & Woof, J. Human antibody effector function. *Adv Immunol* **51**, 1-84 (1992).
569. Kontermann, R., Wing, M. & Winter, G. Complement recruitment using bispecific diabodies. *Nature Biotechnol* **15**, 629-31 (1997).
570. McLafferty, M., Kent, R., Ladner, R. & Markland, W. M13 bacteriophage displaying disulfide-constrained microproteins. *Gene* **128**, 29-36 (1993).
571. Wood, S. et al. Crystal structure analysis of deamino-oxytocin: conformational flexibility and receptor binding. *Science* **232**, 633-6 (1986).
572. Hoess, R., Mack, A., Walton, H. & Reilly, T. Identification of a structural epitope by using a peptide library displayed on filamentous bacteriophage. *J Immunol* **153**, 724-9 (1994).
573. Luzzago, A., Felici, F., Tramontano, A., Pessi, A. & Cortese, R. Mimicking of discontinuous epitopes by phage-displayed peptides, I. Epitope mapping of human H ferritin using a phage library of constrained peptides. *Gene* **128**, 51-7 (1993).
574. Manual, N.E.B.I.I. Ph.D.-C7C™ Phage Display Peptide Library Kit: Instruction Manual.
575. Peters, E., Schatz, P., Johnson, S. & Dower, W. Membrane insertion defects caused by positive charges in the early mature region of protein pIII of filamentous phage fd can be corrected by prlA suppressors. *J Bacteriol* **176**, 4296-305 (1994).
576. Altschul, S. et al. Gapped BLAST and PSI-BLAST: a new generation of protein database search programs. *Nucleic Acids Res* **25**, 3389-402 (1997).
577. Koivunen, E., Gay, D. & Ruoslahti, E. Selection of peptides binding to the $\alpha_5\beta_1$ integrin from phage display library. *J Biol Chem* **268**, 20205-10 (1993).
578. Koivunen, E., Wang, B. & Ruoslahti, E. Isolation of a highly specific ligand for the $\alpha 5\beta 1$ integrin from a phage display library. *J Cell Biol* **124**, 373-80 (1994).
579. Haviland, D., Haviland, J., Fleischer, D., Hunt, A. & Wetsel, R. Complete cDNA sequence of human complement pro-C5. Evidence of truncated transcripts derived from a single copy gene. *J Immunol* **146**, 362-68 (1991).
580. Wetsel, R. et al. Molecular analysis of human complement component C5: localization of the structural gene to chromosome 9. *Biochemistry* **27**, 1474-82 (1988).
581. Lundwall, A. et al. Isolation and sequence analysis of a cDNA clone encoding the fifth complement component. *J Biol Chem* **260**, 2108-12 (1985).
582. Fernandez, H. & Hugli, T. Primary structural analysis of the polypeptide protion of human C5a anaphylatoxin. Polypeptide sequence determination and assignment of the oligosaccharide attachment site in C5a. *J Biol Chem* **253**, 6955-64 (1978).

583. Bohnsack, J., Mollison, K., Buko, A., Ashworth, J. & Hill, H. Group B streptococci inactivate complement component C5a by enzymic cleavage at the C-terminus. *Biochem J* **273**, 635-40 (1991).
584. Zuiderweg, E., Mollison, K., Henkin, J. & Carter, G. Sequence-specific assignments in the 1H NMR spectrum of the human inflammatory protein C5a. *Biochemistry* **27**, 3568-80 (1988).
585. Zuiderweg, E., Nettesheim, D., Mollison, K. & Carter, G. Tertiary structure of human complement component C5a in solution from nuclear magnetic resonance data. *Biochemistry* **28**, 172-85 (1989).
586. Zhang, X., Boyar, W., Galakatox, N. & Gonnella, N. Solution structure of a unique C5a semi-synthetic antagonist: implications in receptor binding. *Protein Sci* **6**, 65-72 (1997).
587. Zhang, X., Boyar, W., Toth, M., Wennogle, L. & Gonnella, N. Structural definition of the C5a C terminus by two-dimensional nuclear magnetic resonance spectroscopy. *Proteins* **28**, 261-7 (1997).
588. Haefliger, J., Tschopp, J., Vial, N. & Jenne, D. Complete primary structure and functional characterization of the sixth component of the human complement system. Identification of the C5b-binding domain in complement C6. *J Biol Chem* **264**, 18041-51 (1989).
589. DiScipio, R. & Hugli, T. The molecular architecture of human complement component C6. *J Biol Chem* **264**, 16197-206 (1989).
590. Hobart, M., Fernie, B. & DiScipio, R. Structure of the human C6 gene. *Biochemistry* **32**, 6198-205 (1993).
591. Lengweiler, S., Schaller, J., DiScipio, R. & Rickli, E. Elucidation of the disulfide-bonding pattern in the factor I modules of the sixth component (C6) of human complement. *Biochim Biophys Acta* **1342**, 13-18 (1997).
592. Dewald, G., Nothen, M. & Cichon, S. Polymorphism of huma complement component C6: an amino acid substitution (Glu/Ala) within the second thrombospondin repeat differentiates between the two common allotypes C6 A and C6 B. *Biochem Biophys Res Comm* **194**, 458-64 (1993).
593. Hofsteenge, J., Blommers, M., Hess, D., Furmanek, A. & Miroshnichenko, O. The four terminal components of the complement system are C-mannosylated on multiple tryptophan residues. *J Biol Chem* **274**, 32786-94 (1999).
594. DiScipio, R., Chakravarti, D., Muller-Eberhard, H. & Fey, G. The structure of human complement component C7 and the C5b-7 complex. *J Biol Chem* **263**, 549-60 (1988).
595. Hobart, M., Fernie, B. & DiScipio, R. Structure of the human C7 gene and comparison with the C6, C8A, C8B, and C9 genes. *J Immunol* **154**, 5188-94 (1995).
596. Bunkenborg, J., Pilch, B., Podtelejnikov, A. & Wisniewski, J. Screening for N-glycosylated proteins by liquid chromatography mass spectrometry. *Proteomics* **4**, 454-65 (2004).
597. Fernie, B. et al. Molecular bases of combined subtotal deficiencies of C6 and C7: their effects in combination with other C6 and C7 deficiencies. *J Immunol* **157**, 3648-57 (1996).
598. Fernie, B., Orren, A., Sheehan, G., Schleisinger, M. & Hobart, M. Molecular bases of C7 deficiency: three different defects. *J Immunol* **159**, 1019-26 (1997).
599. Fernie, B. & Hobart, M. Complement C7 deficiency: seven further molecular defects and their associated marker haplotypes. *Hum Genet* **103**, 513-9 (1998).
600. DiScipio, R. Formation and structure of the C5b-7 complex of the lytic pathway of complement. *J Biol Chem* **267**, 17087-94 (1992).
601. Szardenings, M. Phage display of random peptide libraries: applications, limits and potential. *J Recept Signal Transduct Res* **23**, 307-49 (2003).
602. Clement, G. et al. Peptabodies as tools to test ligands isolated from phage-displayed peptide libraries. *J Immunol Methods* **276**, 135-41 (2003).

603. Kay, B. et al. An M13 phage library displaying random 38-amino acid peptides as a source of novel sequences with affinity to select targets. *Gene* **128**, 59-65 (1993).
604. Kay, B. Mapping protein-protein interactions with biologically expressed random peptide libraries. *Persp Drug Discovery Design* **2**, 251 (1995).
605. Paparella, D., Yau, T. & Young, E. Cardiopulmonary bypass induced inflammation: pathophysiology and treatment. An update. *Eur J Cardiothorac Surg* **21**, 232-44 (2002).
606. Takabayashi, T. et al. A new biologic role for C3 and C3a desArg: regulation of TNF-α and IL-1β synthesis. *J Immunol* **156**, 3455-60 (1996).
607. Fischer, W., Jagels, M. & Hugli, T. Regulation of IL-6 synthesis in human peripheral blood mononuclear cells by C3a and C3a(desArg). *J Immunol* **162**, 453-9 (1999).
608. Christman, J., Lancaster, L. & Blackwell, T. Nuclear factor κ B: a pivotal role in the systemic inflammatory response syndrome and new target for therapy. *Intensive Care Med* **24**, 1131-8 (1998).
609. Ilton, M. et al. Differential expression of neutrophil adhesion molecules during coronary artery surgery with cardiopulmonary bypass. *J Thorac Cardiovasc Surg* **118**, 930-7 (1999).
610. Jordan, J., Zhao, Z.-Q. & Vinten-Johansen, J. The role of neutrophils in myocardial ischemia-reperfusion injury. *Cardiovasc Res* **43**, 860-78 (1999).
611. Andersen, L. et al. Presence of circulating endotoxins during cardiac operations. *J Thorac Cardiovasc Surg* **93**, 115-9 (1987).
612. Rocke, D., Gaffin, S., Wells, M., Koen, Y. & Brock-Utine, J. Endotoxemia associated with cardiopulmonary bypass. *J Thorac Cardiovasc Surg* **93**, 832-7 (1987).
613. Kharazmi, A. et al. Endotoxemia and enhanced generation of oxygen radicals by neutrophils from patients undergoing cardiopulmonary bypass. *J Thorac Cardiovasc Surg* **98**, 381-5 (1989).
614. Nilsson, L., Kulander, L., Nystrom, S. & Eriksson, O. Endotoxins in cardiopulmonary bypass. *J Thorac Cardiovasc Surg* **100**, 777-80 (1990).
615. Braue, A. The role of the gut in the development of multiple organ dysfunction in cardiothoracic patients. *Ann Thorac Surg* **55**, 822-39 (1993).
616. Ohri, S. et al. Cardiopulmonary bypass impairs small intestinal transport and increases gut permeability. *Ann Thorac Surg* **55**, 1080-6 (1993).
617. Andersen, L., Landow, L., Baek, L., Jansen, E. & Baker, S. Association between gastric intramucosal pH and splanchnic endotoxin, antibody to endotoxin, and tumor necrosis factor-α concentrations in patients undergoing cardiopulmonary bypass. *Crit Care Med* **21**, 210-7 (1993).
618. Sinclair, D., Haslam, P., Quinlan, G., Pepper, J. & Evans, T. The effect of cardiopulmonary bypass on intestinal and pulmonary endothelial permeability. *Chest* **108**, 718-24 (1995).
619. Riddington, D. et al. Intestinal permeability, gastric intramucosal pH and systemic endotoxemia in patients undergoing cardiopulmonary bypass. *JAMA* **275**, 1007-12 (1996).
620. Jirik, F. et al. Bacterial lipopolysaccharide and inflammatory mediators augment IL-6 secretion by human endothelial cells. *J Immunol* **142**, 144-7 (1989).
621. Giroir, B. Mediators of septic shock: new approaches for interrupting the endogenous inflammatory cascade. *Crit Care Med* **21**, 780-9 (1993).
622. Ruvulo, G. et al. Nitric oxide formation during cardiopulmonary bypass. *Ann Thorac Surg* **57**, 1055-7 (1994).
623. Tsujino, M. et al. Induction of nitric oxide synthase gene by interleukin-1β in cultured rat cardiocytes. *Circulation* **90**, 375-83 (1994).

624. Ungureanu-Longrois, D. et al. Induction of nitric oxide synthase activity by cytokines in ventricular myocytes is necessary but not sufficient to decrease contractile repsonsiveness to beta-adrenergic agonists. *Circ Res* **77**, 494-502 (1995).
625. Shindo, T. et al. Nitric oxide synthesis in cardiac myocytes and fibroblasts by inflammatory cytokines. *Cardiovasc Res* **29**, 813-9 (1995).
626. Sato, H. et al. Basal nitric oxide expresses endogenous cardioprotection during reperfusion by inhibition of neutrophil-mediated damage after surgical revascularization. *J Thorac Cardiovasc Surg* **11**, 399-409 (1997).
627. Engelman, D. et al. Constitutive nitric oxide release is impaired after ischemia and reperfusion. *J Thorac Cardiovasc Surg* **110**, 1047-53 (1995).
628. Hall, R., Smith, M. & Rocker, G. The systemic inflammatory response to cardiopulmonary bypass: pathophysiological, therapeutic and pharmacological considerations. *Anesth Analg* **85**, 766-82 (1997).
629. Teoh, K., Bradley, C., Gauldie, J. & Burrows, H. Steroid inhibition of cytokine-mediated vasodilation after warm heart surgery. *Circulation* **92**, II-347-53 (1995).
630. Kawamura, T., Inada, K., Nara, N., Wakusawa, R. & Endo, S. Influence of methylprednisolone on cytokine balance during cardiac surgery. *Crit Care Med* **27**, 545-8 (1999).
631. Wan, S. et al. Does steroid pretreatment increase endotoxin release during clinical cardiopulmonary bypass? *J Thorac Cardiovasc Surg* **117**, 1004-8 (1999).
632. Hill, G., Alonson, A., Thiele, G. & Robbins, R. Glucocorticoids blunt neutrophil CD11b surface glycoprotein upregulation during cardiopulmonary bypass in humans. *Anesth Analg* **79**, 23-7 (1994).
633. Joyce, D., Steer, J. & Abraham, L. Glucocorticoid modulation of human monocyte/macrophage function: control of TNF-alpha secretion. *Inflamm Res* **46**, 447-51 (1997).
634. Steer, J., Kroeger, K., Abraham, L. & Joyce, D. Glucocorticoids suppress TNF-α expression by human monocytic THP-1 cells by suppressing transactivation through adjacent NF-κB and c-Jun/ATF-2 binding sites in the promoter. *J Biol Chem* **275**, 18432-40 (2000).
635. Katsuyama, K. et al. Differential inhibitory actions by glucocorticoid and aspirin on cytokine-induced nitric oxide production in vascular smooth muscle cells. *Endocrinology* **140**, 2183-90 (1999).
636. Levi, M. et al. Pharmacological strategies to decrease excessive blood loss in cardiac surgery: a meta-analysis of clinically relevant endpoints. *Lancet* **354**, 1940-7 (1999).
637. Kim, H. et al. Chloro-methyl ketones block induction of nitric oxide synthase in murine macrophages by preventing activation of nuclear factor-kappa B. *J Immunol* **154**, 4741-8 (1995).
638. Schini-Kert, V., Boese, M., Fisslthaler, B. & Mulsch, A. N-alpha-tosyl-L-lysine chloromethylketone prevents expression of iNOS in vascular smooth muscle by blocking activation of NF-kappa B. *Arterioscler Thromb Vasc Biol* **17**, 672-9 (1997).
639. Lentsch, A. et al. Inhibition of NF-kappaB activation and augmentation of IkappaBeta by secretory leukocyte protease inhibitor during lung inflammation. *Am J Pathol* **154**, 239-47 (1999).
640. Defraigne, J., Pincemail, J., Larbuisson, R., Blaffart, F. & Limet, R. Cytokine release and neutrophil activation are not prevented by heparin-coated circuits and aprotinin administration. *Ann Thorac Surg* **69**, 1084-91 (2000).
641. Gu, Y. et al. Heparin-coated circuits reduce the inflammatory response to cardiopulmonary bypass. *Ann Thorac Surg* **55**, 917-22 (1993).

642. Videm, V. et al. Heparin-coated cardiopulmonary bypass equipment. I Biocompatibility markers and development of complications in high-risk population. *J Thorac Cardiovasc Surg* **117**, 794-802 (1999).
643. Wan, S. et al. Heparin-coated circuits reduce myocardial injury in heart or heart-lung transplantation: a prospective, randomized trials. *Ann Thorac Surg* **68**, 1230-5 (1999).
644. te Velthuis, H. et al. Heparin coating of extracorporeal circuits inhibits contact activation during cardiac operations. *J Thorac Cardiovasc Surg* **114**, 117-22 (1997).
645. Moen, O. et al. Attenuation of changes in leukocyte surface markers and complement activation with heparin-coated cardiopulmonary bypass. *Ann Thorac Surg* **63**, 105-11 (1997).
646. Videm, V. et al. Heparin-coated cardiopulmonary bypass equipment. II Mechanism for reduced complement activation in vivo. *J Thorac Cardiovasc Surg* **117**, 803-9 (1999).
647. Ranucci, M. et al. Heparin-coated circuits for high risk patients: a multi-center, prospective, randomized trial. *Ann Thorac Surg* **67**, 994-1000 (1999).
648. Moen, O. et al. Disparity in blood activation by two different heparin-coated extracorporeal bypass circuits: a randomized, masked clinical trial. *J Thorac Cardiovasc Surg* **112**, 472-483 (1995).
649. Naik, S., Knight, A. & Elliot, M. A prospective randomized study of a modified technique of ultrafiltration during pediatric open-heart surgery. *Circulation* **84**, III-422-31 (1991).
650. Grunefelder, J. et al. Modified ultrafiltration lowers adhesion molecules and cytokine levels after cardiopulmonary bypass without clinical relevance in adults. *Eur J Cardiothorac Surg* **17**, 77-83 (2000).
651. Journois, D. et al. Hemofiltration in pediatric cardiac surgery. *Anesthesiology* **81**, 1181-9 (1994).
652. Moncada, S. & Higgs, A. Mechanisms of disease: the L-arginin-nitric oxide pathway. *N Engl J Med* **329**, 2002-12 (1993).
653. Orime, Y. et al. Cytokine and endothelial damage in pulsatile and nonpulsatile cardiopulmonary bypass. *Artificial Organs* **23**, 508-12 (1999).
654. Watarida, S. et al. A clinical study on the effects of pulsatile cardiopulmonary bypass on the blood endotoxin levels. *J Thorac Cardiovasc Surg* **108**, 620-5 (1994).
655. Taggart, D. et al. Endotoxemia, complement and white blood cells activation in cardiac surgery: a randomized trial of laxatives and pulsatile perfusion. *Ann Thorac Surg* **57**, 376-82 (1994).
656. Regraqui, I. et al. The effects of cardiopulmonary bypass temperature on neuropsychologic outcome after coronary artery operations: a prospective randomized trial. *J Thorac Cardiovasc Surg* **112**, 1036-45 (1996).
657. Nandate, K. et al. Cerebrovascular cytokine response during coronary artery bypass surgery: specific production of Interleukin-8 and its attenuation by hypothermic cardiopulmonary bypass. *Anesth Analg* **89**, 823-8 (1999).
658. Boldt, J., Osmer, C., Linke, L., Gorlach, G. & Hempelmann, G. Hypothermic versus normothermic cardiopulmonary bypass: influence on circulating adhesion molecules. *J Cardiothorac Vasc Anesth* **10**, 342-7 (1996).
659. Birdi, I., Caputo, M., Underwood, M., Bryan, A. & Angelini, G. The effects of cardiopulmonary bypass temperature on inflammatory response following cardiopulmonary. *Eur J Cardiothorac Surg* **16**, 540-5 (1999).
660. Ohata, T. et al. Role of nitric oxide in a temperature dependent regulation of systemic vascular resistance in cardiopulmonary bypass. *Eur J Cardiothorac Surg* **18**, 342-7 (2000).
661. Investigators, T.W.H. Randomised trial of normothermic versus hypothermic coronary bypass surgery. *Lancet* **343**, 559-63 (1994).

662. Menasche, P. et al. Does normothermia during cardiopulmonary bypass increase neutrophil-endothelium interactions? *Circulation* **90**, II-275-9 (1994).
663. Menasche, P. et al. Influence of temperature on neutrophil trafficking during clinical cardiopulmonary bypass. *Circulation* **92**, II-334-40 (1995).
664. Le Deist, F. et al. Hypothermica during cardiopulmonary bypass delays but does not prevent neutrophil-endothelial cell adhesion. A clinical study. *Circulation* **92**, II-345-8 (1995).
665. Gong, J. et al. Tubing loops as a model for cardiopulmonary bypass circuits: both the biomaterial and the blood-gas phase interfaces induce complement activation in an in vitro model. *J Clin Immunol* **16**, 222-9 (1996).
666. Larsson, R. et al. Inhibition of complement activation by soluble recombinant CR1 under conditions resembling those in a cardiopulmonary circuit: reduced up-regulation of CD11b and complete abrogation of binding of PMNs to the biomaterial surface. *Immunopharmacology* **38**, 119-27 (1997).
667. Hugo, F., Kramer, S. & Bhakdi, S. Sensitive ELISA for quantitating the terminal membrane C5b-9 and fluid-phase sC5b-9 complex of human complement. *J Immunol Methods* **99**, 243-51 (1987).
668. Lazar, H., Bao, Y., Gaudiani, J., Rivers, S. & Marsh, H.J. Total Complement Inhibition: An effective strategy to limit ischemic injury during coronary revascularization on cardiopulmonary bypass. *Circulation* **100**, 1438-42 (1999).
669. Gupta-Bansal, R., Parent, J. & Brunden, K. Inhibition of complement alternative pathway function with anti-properdin monoclonal antibodies. *Mol Immunol* **37**, 191-201 (2000).
670. Sugita, Y. & Masuho, Y. CD59: its role in complement regulation and potential for therapeutic use. *Immunotechnology* **1**, 157-68 (1995).
671. Rushmere, N., Tomlinson, S. & Morgan, B. *Immunology* **90**, 640-6 (1997).
672. Vakeva, A., Jauhiainen, M., Ehnholm, C., Lehto, T. & Meri, S. High-density lipoproteins can act as carriers of glycophosphoinositol lipid-anchored CD59 in plasma. *Immunology* **82**, 28-33 (1994).
673. Fraser, D. et al. Generation of a recombinant, membrane-targeted form of the complement regulator CD59. *J Biol Chem* **278**, 48921-7 (2003).
674. Schwartzman, S., Fleischmann, R. & Morgan, G.J. Do anti-TNF agents have equal efficacy in patients with rheumatoid arthritis? *Arthritis Rheum* **6**, S3-11 (2004).
675. Moreland, L. Drugs that block tumour necrosis factor: experience in patients with rheumatoid arthritis. *Pharmacoeconomics* **22**, 39-53 (2004).
676. Kaplan, M. Eculizumab (Alexion). *Curr Opin Investig Drugs* **3**, 1017-23 (2002).
677. Inal, J. Schistosoma TOR (trispanning orphan receptor), a novel, antigenic surface receptor of the blood-dwelling, Schistosoma parasite. *Biochim Biophys Acta* **1445**, 283-98 (1999).
678. Inal, J. & Sim, R. A Schistosoma protein, Sh-TOR is a novel inhibitor of complement which binds human C2. *FEBS Lett* **470**, 131-4 (2000).
679. Parizade, M., Arnon, R., Lachmann, P. & Fishelson, Z. Functional and antigenic similarities between a 94 kD protein of Schistosoma mansoni (SCIP-1) and human CD59. *J Exp Med* **179**, 1625-36 (1994).
680. Inal, J. & Schifferli, J. Complement C2 receptor inhibitor trispanning and the β-chain of C4 share a binding site for complement C2. *J Immunol* **168**, 5213-21 (2002).
681. Oh, K., Kweon, M., Rhee, K., Lee, K. & Sung, H. Inhibition of complement activation by recombinant Sh-CRIT-ed1 analogues. *Immunology* **110**, 73-9 (2003).
682. Akesson, P., Sjoholm, A. & Bjorck, L. Protein SIC, a novel extracellular protein of Streptococcus pyogenes interfering with complement function. *J Biol Chem* **271**, 1081-8 (1996).

683. Fernie-King, B. et al. Streptoccocal inhibitor of complement (SIC) inhibits the membrane attack complex by preventing uptake of C567 onto cell membranes. *Immunology* **103**, 390-8 (2001).